

VLADISLAV AKHMATOV

Analysis of dynamic behaviour of electric power systems with large amount of wind power

Ph.D. Thesis

ELECTRIC POWER ENGINEERING, ØRSTED-DTU,
TECHNICAL UNIVERSITY OF DENMARK

NESA A/S

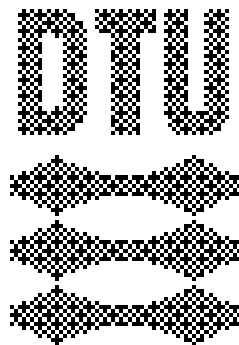
INFORMATICS AND MATHEMATICAL MODELLING,
TECHNICAL UNIVERSITY OF DENMARK

APRIL 2003

Analysis of dynamic behaviour of electric power systems with large amount of wind power

Vladislav Akhmatov

Submitted to Electric Power Engineering, Ørsted-DTU,
Technical University of Denmark
in partial fulfilment of the requirements
for the degree of Doctor of Philosophy and
the Danish Industrial Ph.D. degree



Electric Power Engineering, Ørsted-DTU
Technical University of Denmark
Kgs. Lyngby, Denmark
April 2003

Analysis of dynamic behaviour of electric power systems with large amount of wind power

Vladislav Akhmatov

© Vladislav Akhmatov, 1999-2003.

Electric Power Engineering, Ørsted-DTU,
Technical University of Denmark.

ISBN Softbound	87-91184-18-5
ISBN CD-ROM	87-91184-19-3

This work has been accomplished within the framework of the Danish Industrial Ph.D. programme under the Academy of Technical sciences, and is partly funded by the Danish power company NES A/S. The project has been carried out as a co-operation between NES A, Electric Power Engineering, Ørsted-DTU and Informatics and Mathematical Modelling, Technical University of Denmark. April 2003.

Preface

This dissertation has been submitted to Ørsted-DTU, Section of Electric Power Engineering, Technical University of Denmark (DTU) in partial fulfilment of the requirements for the degree of Doctor of Philosophy and the Danish Industrial Research / Ph.D. degree. The project has been carried out within the areas of Electric Power Engineering and Grid-connection of Wind Power. The issue of Grid-connection of Wind Power is very timely because the amount of wind power in electric power systems increases rapidly world-wide.

The project has been carried out in a co-operation between the Danish power distribution company NESA A/S, Ørsted-DTU, Section of Electric Power Engineering, DTU and Department of Informatics and Mathematical Modelling (IMM), DTU. The project has been carried out from November 1999 to April 2003. The public presentation of this dissertation found place on November 18th, 2003, at Technical University of Denmark. This final version of the thesis has been completed at December 2003.

The project was interrupted from July 2000 to December 2000 due to the practical investigations on short-term voltage stability of the eastern Danish power system with grid-connection of the large offshore wind farm at Rødsand /Nysted. This break was by the request of the company NESA and the author participated in this practical work for Consulting Dept. of the company NESA.

Acknowledgements

This Industrial Ph.D. project was funded by the company NESA and the Danish Academy of Technical Sciences, grant EF-823. The project has enrolled the above-mentioned organisations and also a number of participants from the Danish industry.

The author is thankful to the supervisors Ass. Prof. Arne Hejde Nielsen, Ørsted-DTU, Dr. Hans Knudsen, The Danish Energy Authority, Dr. Jørgen Nygaard Nielsen, NESA A/S, Dr. Niels Kjølstad Poulsen, IMM, retired Prof. J. Kaas Pedersen, Ørsted-DTU, and Dr.tech. Martin P. Bendsøe, a member of the Danish Academy of Technical Sciences, for their direction and support throughout the project.

The author is also thankful to Jarle Eek, Vestas Wind Systems, Björn Andresen, Gamesa Wind Engineering (formerly with Vestas Wind Systems), Jan Thisted, Bonus Energy, Niels Raben and Martin Heyman Donovan, Energi-E2 (formerly with Wind Energy Centre, SEAS), Erik Jørgensen, Hansen-Henneberg Copenhagen A/S, Kent Hansen Søbrink, ELTRA, Dr. Tonny W. Rasmussen, Ørsted-DTU, Stig Øye, Department of Energy Technology, DTU, and many others, who have followed and contributed to this project.

Vladislav Akhmatov,
Kgs. Lyngby, Denmark

Resume

The Industrial Ph.D. project “Analysis of dynamic behaviour of electric power systems with large amount of wind power” has been started by the Danish power distribution company NESA because wind power penetration into the Danish power grid has rapidly increased. The project was started ultimo 1999, e.g. four year before commissioning of the large offshore wind farm at Rødsand /Nysted should take place in eastern Denmark. The project should build-up the know-how about (i) representation of existing wind turbine concepts in the dynamic simulation tools, (ii) grid-connection of a large amount of wind power and (iii) maintaining of short-term (transient) voltage stability.

The main goal of this project has been to answer the following question: what would happen in the power grid with a large amount of wind power when a three-phase, short-circuit fault has occurred in the transmission power network? The project has been a pioneering work in the area of dynamic modelling of wind turbines in electric power supply.

At the project start, the fixed-speed wind turbines equipped with conventional asynchronous generators were the most common wind turbine concept in Denmark. During the last three years, the wind turbines equipped with frequency converters and power electronics have become represented in a number of large wind turbine sites in Denmark and abroad. At the project start, the existing dynamic simulation tools did not contain models of wind turbines of sufficient complexity and accuracy to be used in investigations of short-term voltage stability. Therefore this project has focused on representation of the four main concepts in dynamic simulation tools:

- 1) Fixed-speed wind turbines equipped with no-load compensated induction generators, which is the so-called Danish concept. Those can be either fixed-pitch or with blade-angle control.
- 2) Pitch-controlled wind turbines equipped with doubly-outage induction generators and variable rotor resistance control.
- 3) Variable-speed, pitch-controlled wind turbines equipped with doubly-fed induction generators and partial-load frequency converters.
- 4) Variable-speed, pitch-controlled wind turbines equipped with direct-driven, multi-pole synchronous generators and frequency converters. Here, the model is described in case of permanent magnet generators.

The dynamic wind turbine models of all the four wind turbine concepts have been applied to investigate transient voltage stability and suggest uninterrupted operation (ride-through) features. The main investigations have been carried out with use of the model of a large (offshore) wind farm consisting of eighty wind turbines. Especially, it has focused on the Danish concept since this has still been the most common concept in Denmark.

Consequences of incorporation of a large amount of wind power and local combined heat-power units have been investigated with use of a detailed and sufficiently realistic model of a large power network. Here, it has been distinguished between (i) local sites feeding into the local distribution networks and (ii) large wind farms connected to the transmission power networks and assigned to the technical specifications of the transmission system operator. Considerations of representing the

local generation units and their protection have been explained. The investigations have been carried out with respect to the following issues.

- 1) When the wind turbines in the large wind farms have been (i) fixed-speed active-stall controlled and equipped with induction generators or (ii) variable-speed pitch-controlled and equipped with doubly-fed induction generators and partial-load frequency converters.
- 2) Access of the connection point of the large wind farm to (i) a strong power network or (ii) a weak power network.

Accessing a connection point in a strong power network has been found favourable to maintain (i) short-term voltage stability and (ii) uninterrupted operation of the large wind farms. Operation of the large wind farms, especially the frequency converters of variable-speed wind turbines, could be affected by weak power grids and dynamic behaviour of local generation units at transient events.

Resumé på dansk

Det danske elselkab NESA har startet erhvervsforskerprojektet "Analysis of dynamic behaviour of electric power systems with large amount of wind power" fordi mængden af nettilsluttet vindkraft i det danske elsystem voksede meget støt. Derved var der behov for videnopbygning. Erhvervsforskerprojektet var startet ultimo 1999, altså fire år før nettilslutningen af den store havvindmøllepark ved Rødsand skulle finde sted. Erhvervsforskerprojektet skulle bidrage til at opbygge know-how omkring (i) repræsentation af eksisterende vindmøllekoncepter i dynamiske simuleringsværktøjer, (ii) nettilslutning af store mængder vindkraft og (iii) transient spændingsstabilitet af elsystemer.

Projektets primære mål var at besvare følgende spørgsmål: hvad der ville ske i elsystemet med en stor mængde vindkraft i tilfælde af en trefaset kortslutningsfejl i transmissionssystemet. Projektet betragtes som et stykke banedrydende arbejde i dynamiske modeller af vindmøller i elforsyningen.

Ved projektets start var vindmøller med fast omløbstal udstyret med konventionelle asynkrongeneratorer den mest udbredte koncept i Danmark. I løbet af sidste tre år kom der et teknologihop. Vindmøller med variabelt omløbstal udstyret med konverterer og effektelektronik blev placeret i store vindmølleparker i Danmark og udlandet. Vindmøllemodeller af tilstrækkelig detalierungsgrad og nøjagtighed var ikke en del af de eksisterende simuleringsværktøjer anvendt til spændingsstabilitetsundersøgelser. Derfor fokuserede erhvervsforskerprojektet på modelopbygning af de fire vindmøllekoncepter i dynamiske simuleringsværktøjer:

- 1) Vindmøller med fast omløbstal udstyret med tomgangskompenserede asynkrongeneratorer. Dette er kendt som den danske koncept. Vindmøllerne kan være stall-regulerede eller med bladvinkelregulering.
- 2) Pitch-regulerede vindmøller med dobbelt-viklede asynkrongeneratorer og variabel rotormodstand.

- 3) Pitch-regulerede vindmøller med variabelt omløbstal udstyret med dobbelt-tilsluttede asynkrongeneratorer med partialeffekt-frekvensomformere.
- 4) Pitch-regulerede vindmøller med variabelt omløbstal udstyret med frekvensomformerstyrede multipole synkrongeneratorer med fuld effekt. I det her tilfælde er modellen beskrevet for permanentmagnetgeneratorer.

De dynamiske vindmøllemodeller af alle de fire koncepter var anvendt i undersøgelser af spændingsstabilitet og muligheder for drift uden udkoblinger under netforstyrrelser. Hovedundersøgelserne var afviklet ved anvendelse af modellen af en stor vindmøllepark med 80 vindmøller. Specielt var der fokuseret på den danske koncept fordi dette var den mest udbredte type vindmøller i Danmark.

Konsekvenser af nettilslutningen af store mængder af vindkraft og decentrale lokal-kraftvarmeanlæg var undersøgt ved anvendelsen af en tilstrækkelig detaljeret og realistisk elnetmodel. I undersøgelserne var der skelnet mellem (i) decentrale anlæg og parker nettilsluttet lokale distributionssystemer og (ii) store vindmølleparker, som er nettilsluttet transmissionssystemet og underlagt tilslutningsbetingelserne formuleret af den systemansvarlige. Forudsætninger for repræsentation af decentrale anlæg og deres beskyttelse var forklaret og taget i betragtning. Undersøgelserne var med henblik på det følgende.

- 1) Når vindmøllerne i de store parker var (i) fastomløbstals, active-stall regulerede og udstyret med asynkrongeneratorer eller (ii) variabeltomløbstals, pitch-regulerede og udstyret med dobbelt-tilsluttede asynkrongeneratorer med partialeffekt-frekvensomformere.
- 2) Når de store parker var tilsluttet (i) et stift elsystem eller (ii) et svagt elsystem.

Adgang til tilslutningspunktet i et stift elsystem var fundet meget favorabelt for spændingsstabilitet, samt for drift af vindmølleparker uden udkoblinger under netfejl. Når tilsluttet et svagt elsystem med decentrale anlæg, forstyrrelser af uafbrudt drift af store vindmølleparker og specielt uafbrudt drift af frekvensomformere af vindmøller med variabelt omløbstal ville være størst.

Table of Contents

Preface	i
Acknowledgements	ii
Resume	iii
Resumé på dansk	iv
Table of Contents	1
1. Introduction	7
1.1. Motivation and problem formulation	8
1.2. Wind turbine concepts	9
1.3. Modelling issues	13
1.3.1. Dynamic wind turbine models	13
1.3.2. Dynamic simulation tool	17
1.4. Outline of this presentation	19
2. Mechanical system of a wind turbine	21
2.1. Aerodynamic model of a wind turbine	24
2.1.1. Static representation	24
2.1.2. Dynamic inflow phenomena at pitching	26
2.1.3. Representation in voltage stability investigations	28
2.2. Shaft system representation	30
2.2.1. Identification of shaft system parameters	31
2.2.2. Explanation of soft coupling	34
2.2.3. Application area of two-mass model	35
2.2.3.1. Fixed-speed wind turbines	36
2.2.3.2. Variable-speed wind turbines	37
2.3. Neglecting tower representation	38
2.4. AEC of wind turbine rotor	41
2.5. Short resume	43
3. Generic blade-angle control	45
4. Induction generators of fixed-speed wind turbines	49
4.1. Balanced transient events	50
4.2. Unbalanced transient events	51
4.3. Significance of generator rotor inertia	52
4.4. Significance of shaft representation	53
4.5. Aerodynamic wind turbine model – Coupling by speed	55

4.6. Protective relay modelling	56
5. Modelling of large wind farms	57
5.1. Aggregated model of a large wind farm – An example	58
5.2. Reduced equivalents of large wind farms	58
5.3. Effect of absent mutual interaction on reduction of wind farm model	62
6. Voltage stability of large wind farms with fixed-speed wind turbines	65
6.1. Electric torque versus speed characteristic	65
6.2. Static stability limit of induction generators	67
6.3. Dynamic stability limit of induction generators	67
6.4. Dynamic stability limit of wind turbines	69
6.5. Shaft relaxation process	70
6.6. Consequence of dynamic stability limit	72
6.7. Simulation case with large wind farm	72
6.8. Voltage instability when no arrangements	74
6.9. Use of dynamic reactive compensation	75
6.10. Generator parameters versus voltage stability	80
6.11. Enforcing mechanical construction	80
6.12. Blade-angle control acting at grid faults	83
6.12.1. Blade-angle control – Use of alternative signals	84
6.12.2. Blade-angle control – Ordering of power reduction	86
6.13. Mixed wind farm	87
6.14. Robustness of voltage control principles	89
6.14.1. Failure of dynamic reactive compensation	89
6.14.2. Failure of blade-angle control	89
6.15. Protective relay system	91
6.16. Resume	93
7. Large wind farms with doubly-outage induction generators and variable rotor resistance	95
7.1. Generic control scheme	96
7.2. Influence of control system parameters on voltage stability	98
7.3. Mixed wind farm	99
7.4. Considerations on protective relay system	101
7.5. Resume	102
8. Variable-speed wind turbines – Operation and modelling considerations	103
8.1. Range of rotational speed	106
8.2. Generic versus optimised pitch	107
8.3. Generator concepts of variable-speed wind turbines	110

9. Variable-speed wind turbines equipped with PMG	111
9.1. Generator model	113
9.2. Mechanical system representation	115
9.3. Frequency converter system and its control	116
9.3.1. Control system of generator-side converter	118
9.3.2. Control system of grid-side converter	119
9.3.3. Additional reactive power control	120
9.3.4. Coupling between the two VSC	120
9.3.5. Tuning of frequency converter control	121
9.4. Protective system of converter and generator	122
9.4.1. Evaluation of converter blocking in simulations	123
9.4.2. Generator protection at faults	123
9.5. Uninterrupted operation at transient events	124
9.5.1. Uninterrupted operation of converter	124
9.5.2. Feature with blocking and re-starting of converter	127
9.5.2.1. Blocking of generator-side converter	128
9.5.2.2. Control co-ordination	129
9.5.2.3. Re-start of converter	129
9.5.2.4. Simulation example	129
9.6. On mutual interaction between wind turbines	131
9.7. Resume	133
10. Variable-speed wind turbines equipped with DFIG	135
10.1. DFIG modelling in steady-state	137
10.1.1. Initialisation of generator model	138
10.1.2. Initialisation of converter model	140
10.1.3. Verification of DFIG model initialisation	141
10.2. Transient DFIG model	143
10.2.1. State equations of DFIG	143
10.2.2. Shaft system model	146
10.2.3. Converter system model	146
10.2.3.1. Rotor converter model	146
10.2.3.2. Modelling of DC-link and grid-side converter	147
10.2.3.3. Optional control of reactive power and voltage	148
10.2.3.4. Why do not neglect grid-side converter	149
10.2.4. Protective system and converter blocking	151
10.2.5. Interface to simulation tool and network model	154
10.2.6. Numeric stability of model	155
10.3. Notification of problems	156
10.4. Uninterrupted operation feature of wind turbines	158
10.4.1. Case of strong power networks	159
10.4.2. Case of weak power networks	159

10.4.3. Blocking and re-start sequences of rotor converter	160
10.4.4. Value of external rotor resistance	162
10.4.5. Reactive power control co-ordination	163
10.4.6. Example with uninterrupted operation of wind turbines	164
10.5. On mutual interaction between wind turbines	166
10.6. Resume	166
11. Power system analysis with large amount of wind power	169
11.1. Model of large power system	171
11.1.1. Modelling of large power plant units	172
11.1.2. Modelling of large consumption centres	173
11.1.3. Modelling of local CHP units	174
11.1.4. Representation of local wind turbine sites	174
11.1.5. Representation of large wind farms	175
11.2. Assumptions on power system operation	176
11.3. Operation of local generation units at grid disturbances	177
11.3.1. Considerations of small power loss	177
11.3.2. On risk of mutual oscillations between local wind turbine sites	179
11.3.3. Evaluation of disconnection and power loss	182
11.3.4. Preventing grid from possible risk of over-voltage	185
11.3.5. Resume	186
11.4. Access to strong power grid	187
11.4.1. Large wind farm with fixed-speed wind turbines	188
11.4.1.1. Use of power ramp	189
11.4.1.2. Case of strong power system	191
11.4.2. Large wind farm with variable-speed wind turbines	192
11.4.2.1. Incorporation into weak power systems	194
11.4.2.2. Fast converter re-start in weak power networks?	195
11.4.2.3. Damping of speed fluctuations	198
11.4.3. Character of dynamic reactive compensation	200
11.4.4. Co-incidents of events - worst case	201
12. Conclusion	203
12.1. Conclusion to modelling part	203
12.1.1. On generator modelling	203
12.1.2. On shaft system modelling	204
12.1.3. On aerodynamic rotor and blade-angle control modelling	205
12.1.4. On converter modelling	205
12.1.5. On model validation	207
12.2. Conclusion to part with power system studies	207
12.2.1. Reduced wind farm equivalents	207

12.2.2. Voltage stability considerations – Fixed-speed wind turbines in large wind farms	207
12.2.3. Voltage stability considerations – Variable-speed wind turbines in large wind farms	209
12.2.4. Voltage stability considerations – Local sites	210
12.2.5. On mutual interaction between wind turbines	211
12.3. Practical application of results	212
Literature	213
Further readings	219
Appendix 2.A. Excitation of wind turbine construction at grid disturbances	225
Appendix 4.A. Per Unit system of wind turbine model	227
Appendix 4.B. Validation of wind turbine model from measurements	229
4.B.1. A case of full-scale validation: Tripping – re-connection of a wind turbine	229
4.B.1.1. Experiment	231
4.B.1.2. Computational work	233
4.B.1.2.1. Assumptions on model of fixed-speed wind turbines	234
4.B.1.2.2. Induction generator model	234
4.B.1.2.3. Shaft system model236
4.B.1.3. Wind turbine model validation	236
4.B.1.3.1. Network model and initialisation	236
4.B.1.3.2. Simulations with two-mass model	237
4.B.1.3.3. Simulations with lumped-mass model	239
4.B.1.3.4. Simulations with third-order generator model	239
4.B.1.3.5. Discrepancies	241
4.B.1.3.6. Results of validating work	242
4.B.2. Induction generator model validation	243
Appendix 6.A. Induction generator parameters vs. transient voltage stability	247
A special issue: Application of high-temperature superconducting components with wind farms	249
SI.1. Background	249
SI.2. Wind farm model	249
SI.3. Simplified model of superconducting fault current limiter	250
SI.4. Physical approach of HTS components251
SI.4.1. Current- and temperature- dependence of line current	251
SI.4.2. Temperature- and cooling model	252

IS.4.3. Transient approach of line current	253
SI.5. Formulation of practical problems on stability	254
SI.5.1. Case of HTS cables	254
SI.5.2. Application of SCFL	256
IS.6. Resume	258
IS.7. Acknowledgements and credits	259
About author	261
List of equations (PDF only)	
List of figures (PDF only)	
List of tables (PDF only)	

1. Introduction

Incorporation of wind power into electric power systems goes faster than it has been predicted. At the end of 2002, it has been 2,888 MW grid-connected wind power in Denmark with 2,315 MW in the western part and 573 MW in the eastern part of the country (Eltra, 2003). This should cover more than 20 % of electric power consumption (in average) in the country. The world largest offshore wind farm (in figures of the year 2002) is taken in operation at Horns Rev, Western Denmark. The wind farm consists of eighty 2 MW variable-speed wind turbines from the Danish manufacturer Vestas Wind Systems. This wind farm is connected to the transmission power network of the transmission system operator Eltra.

This project is followed by the large offshore wind farm at Rødsand in eastern Denmark, in the year 2003. The Rødsand (also called Nysted) wind farm is with seventy-two 2.3 MW fixed-speed wind turbines from the Danish manufacturer Bonus Energy. The wind farm is connected to the transmission power network of the transmission system operator Elkraft System. Other large offshore projects are under consideration in Denmark. Large penetration of wind power may affect operation of the Danish power system (Jensen, 2002).

A number of projects with incorporation of large offshore wind farms into electric power networks are announced in our neighbouring countries. In Germany, commissioning of 10,000 MW wind power in selected offshore sites in Northern and Baltic Seas is announced. It will take place in the years 2004 to 2010. In Sweden, around 3,800 MW wind power will be commissioned in offshore sites in Baltic Sea during the same period (Ackermann et al, 2001(a)). This will be with use of variable-speed or fixed-speed wind turbines. Such large projects in our neighbouring countries will probably affect operation of the Danish power system as well.

Large penetration of wind power into electric power networks will reduce amount of electric power supply from conventional power plants (Akhmatov et al, 2000(a)). It is necessary to know the consequences of dynamic interaction between large wind farms and electrical power systems before grid-incorporation of the wind farms will take place. The electric power supply undergoes changing from a well-known and developed technology built-up around conventional power plants and their control to a partly unknown technology – wind power.

The first step is already done. The Danish transmission system operators have formulated the Specifications for grid-connection of large wind farms to transmission power networks (Eltra, 2000). Presently, similar technical specifications have been formulated in many countries. We are also talking about harmonisation of such specifications within the UCTE area. The specifications contain a set of technical requirements which the wind turbines must comply before the permission to grid-connection of the wind farm to the transmission power network will be given (Radtke, 2002).

The majority of the wind turbines in Denmark is, however, in local sites and connected to local distribution networks. Those wind turbines are not assigned to the specifications formulated by the transmission system operators¹. Those wind turbines produce so much electric power as the wind blows. Those wind turbines are not assigned to requirements for contribution to reactive power and

¹ Recently, the Danish transmission system operators work on the specifications for connection of wind turbines to the grids with the voltages below 100 kV. But these requirements will only be for new installations.

voltage control (Ackermann et al, 2001(b)). But their total power capacity is so large that it can be expected that those wind turbines may affect operation of the power system significantly.

Drastic increase of amount of grid-connected wind power has occurred during last few years. The same tendency will be expected in the years to come. Therefore it focuses on maintaining of stability and safety of operation of electric power networks with large amount of grid-connected wind power (Akhmatov et al, 2000(b)) and also on economical aspects of technical solutions with grid-incorporation of wind power.

1.1. Motivation and problem formulation

The industrial Ph.D. project “Analysis of dynamic behaviour of electric power systems with large amount of grid-connected wind power” is started in November 1999 and finished in April 2003. The public presentation of the Ph.D. project has been on November 18th, 2003.

The project is funded by the electric power company NESA, Copenhagen, Denmark, which has the exclusive rights on the results and the model codes produced in this project, and the Danish Academy of Technical Sciences. The project has enrolled the following participants.

- 1) Planning Dept., NESA.
- 2) Electric Power Engineering Group, Ørsted-DTU, Technical University of Denmark.
- 3) Dept. of Informatics and Mathematical Modelling, Technical University of Denmark.

Furthermore, a number of companies and organisations have kindly contributed to this project by their know-how and data. Those are the Danish wind turbine manufacturers Vestas Wind Systems and Bonus Energy, the Danish power distribution company SEAS, the Danish transmission system operator Eltra and many other.

When incorporation of large amount of wind power into electric power systems takes place, a number of technical problems will be met and need solutions. In this project, it focuses mainly on what will happen if the electric power network with large amount of grid-connected wind power is subjected to a three-phased, short-circuit fault. This topic relates to maintaining of transient voltage stability of electric power systems with large amount of wind power. Previous investigations (Bruntt et al, 1999) have concluded that a short-circuit fault in the transmission power network could possibly start voltage collapse in the power system with large amount of grid-connected wind power.

The content of this work could be separated into two sub-parts.

- 1) Developing of dynamic wind turbine models and their implementation into existing simulation tools applied to investigations of transient voltage stability. This will produce a toolbox with the dynamic models of the existing wind turbine concepts. At this stage, the complexity of the dynamic wind turbine models is defined. The models are implemented in the chosen simulation tool. Further preparation of the models for commercial applications shall take place at NESA.

- 2) Application of the dynamic wind turbine models in investigations of transient voltage stability and consequences of a short-circuit fault for operation of the wind turbines and the electric power system. It will also contain definitions of general patterns and criteria, which can be applicable to improve transient voltage stability and definition what we need to do to reach compliance with the specifications of the transmission system operators (Eltra, 2000).

This project, started in the year 1999, has been a *pioneering work* with modelling of wind turbines. At the start of the project, the dynamic simulation tools did not contain dynamic wind turbine models of sufficient complexity. During the last two years, the suppliers of the dynamic simulation tools developed and implemented dynamic wind turbine models. Presently, the main simulation tools such as PSS/E (PTI), SimPow (ABB), PowerFactory (DigSilent) contain standardised models of electricity-producing wind turbines – the toolboxes being a part of the simulation tools.

No-doubt, that the around twenty publications made during this Ph.D. project, with explanation of the modelling details, have contributed to faster developing of dynamic wind turbine models in existing dynamic simulation tools.

As can be understood from the title of this project, it focuses mainly on *interaction between the wind turbines and the electric power system*, e.g. item 2. The dynamic wind turbine models are the tools applied in this work. The dynamic wind turbine models will be explained at the level, which is sufficient to understand their complexity details and relevant for the purpose of this work. Validation of the dynamic wind turbine models will be given when possible. Pointers to technical literature and works of other authors will also be given, where more details about representation of given components and parts of the wind turbine construction can be found.

1.2. Wind turbine concepts

Electricity-producing wind turbines can be distinguished according to their operation and control principles. The wind turbines can be, then:

- 1) (i) fixed-speed, operating within a narrow range of the rotational speed slightly above the synchronous speed, or (ii) variable-speed wind turbines, operating within a large range of rotational speed both below and above the synchronous speed. In variable-speed wind turbines, the rotational speed is optimised according to incoming wind for getting more power.
- 2) (i) fixed-pitch wind turbines where the global pitch angle does not change dynamically or (ii) variable-pitch, e.g. with blade-angle control. In wind turbines with blade-angle control, the power output is optimised by adjusting the global pitch angle according to incoming wind.
- 3) Wind turbines equipped with (i) no-load compensated induction generators with shorted rotor circuits, (ii) doubly-fed induction generators controlled by partial-load frequency converters, or (iii) multi-pole synchronous generators and full-load frequency converters.
- 4) (i) directly-connected to ac-grids or (ii) connected to ac-grids through frequency converters.
- 5) Possibly, more characterisation criteria can be found.

Although a number of distinguishes, there are common details characterising the existing wind turbine concepts and their interaction with the power grid. This allows classification and systematisation, which is a necessary step to produce generic, but sufficiently realistic, models of electricity-producing wind turbines to investigate transient voltage stability. In this work, the following wind turbine concepts will be discussed.

- 1) The so-called Danish concept, which is characterised by (i) the three-bladed turbine, (ii) the shaft system with the low-speed (LS) and the high-speed (HS) shafts and the gearbox in between and (iii) the no-load compensated² induction generator. This concept represents fixed-speed wind turbines with or without blade-angle control.
- 2) The wind turbines equipped with induction generator with variable rotor resistance. The mechanical construction is similar to the Danish concept, but the rotor circuit of the induction generator is not shorted, but through the slip-rings connected to the converter. The converter operation corresponds to adding an external rotor resistance in series with the rotor circuit.
- 3) Variable-speed, pitch-controlled wind turbines equipped with doubly-fed induction generators (DFIG). The induction generator is grid-connected at the stator terminals and also at the rotor mains via the partial-load frequency converter.
- 4) Variable-speed, pitch-controlled wind turbines equipped with synchronous generators. In this work, this concept is limited to a multi-pole permanent magnet generator (PMG), connected to an ac-grid through the full-load frequency converter.

The above-mentioned concepts are illustrated in **Fig. 1.1**. The wind turbines of the Danish concept can be stall-controlled, e.g. fixed-pitch, or equipped with active-stall blade angle control. Also, fixed-speed wind turbines can be pitch-controlled, but it is uncommon. The manufacturers NEG-Micon, Bonus Energy and Nordex are the world-largest which produce the fixed-speed wind turbines equipped with induction generators with the rated power around 2 MW. The majority of the wind turbines of this concept and various rated power are incorporated into the Danish power grid, which is why the term “the Danish concept”.

Those are collected into relatively small wind turbine sites (groups) of the rated power capacities from few MW up to 30 MW and connected commonly to local distribution networks. The offshore wind farm of 40 MW rated power and consisting of twenty fixed-speed active-stall wind turbines equipped with induction generators is taken in operation in the year 2001 at Middelgrund, Copenhagen, Denmark. The wind farm is connected to the local distribution network of Copenhagen on-shore. The wind turbines are from the Danish manufacturer Bonus Energy.

² Induction generators can be either no-load compensated or full-compensated. No-load compensation is found in older fixed-speed wind turbines, whereas newer and larger wind turbines are with full-compensated induction generators. Full-compensation is with use of capacitor banks. Information about compensation can be received from the wind turbine manufacturer. In Denmark, the wind turbines connected to the grid after 1996 may be considered as full-compensated. Information about compensation failures can be useful, but is not available for this project.

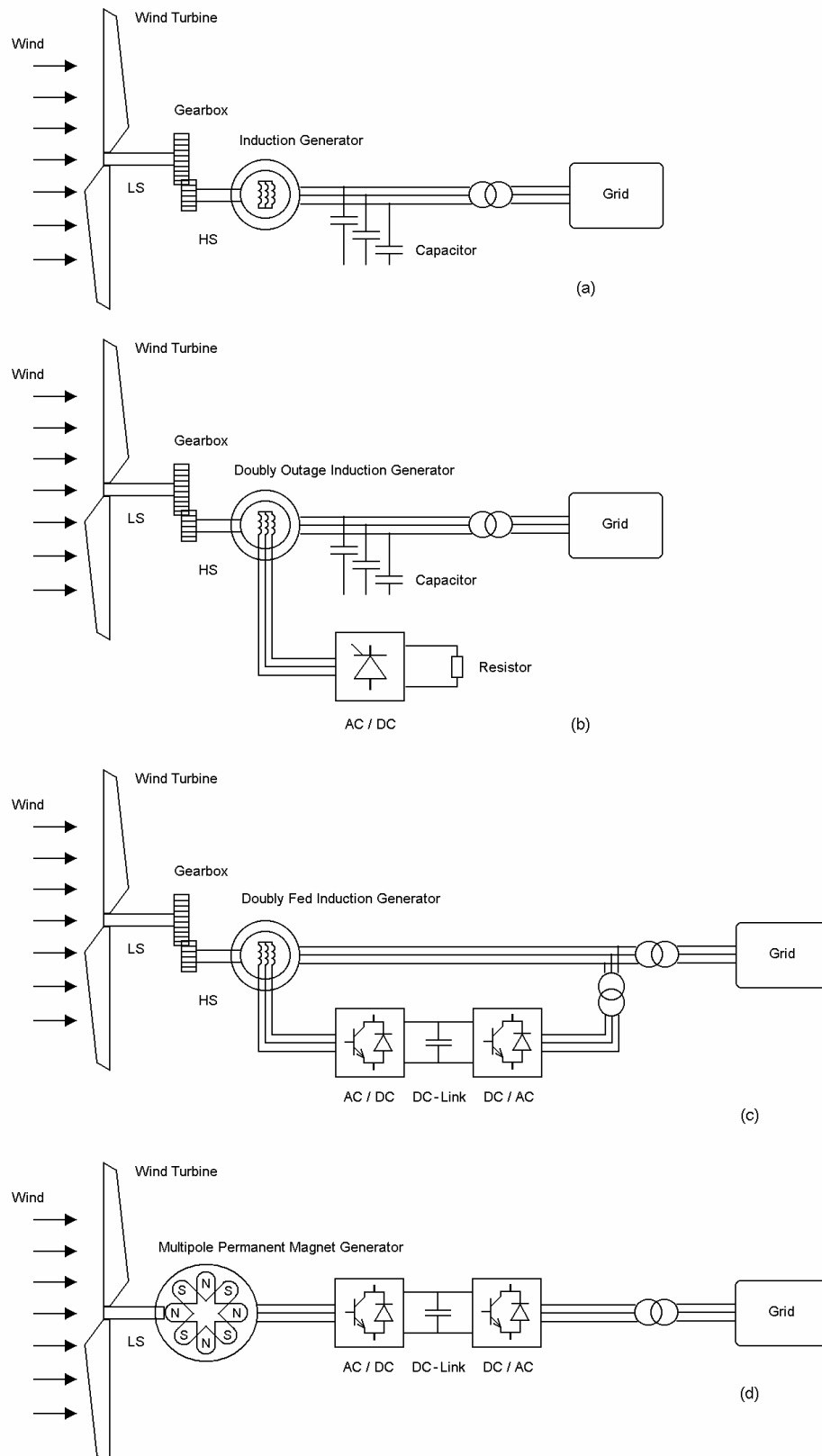


Fig. 1.1. Concepts of electricity-producing wind turbines covered in this work: **(a)** – the fixed-speed wind turbine equipped with a no-load compensated induction generator, **(b)** – the partly variable-speed wind turbine equipped with a doubly outage induction generator with variable rotor resistance, **(c)** – the variable-speed wind turbine equipped with a doubly fed induction generator controlled by the back-to-back converter, **(d)** – the variable-speed wind turbine equipped with a permanent magnet synchronous generator grid-connected through the frequency converter.

Also, this concept is promising for large-scale offshore applications. The offshore wind farm of 150 MW rated power and consisting of seventy-two wind turbines of the same concept is commissioned in the year 2003. The wind turbines are again from the manufacturer Bonus Energy. This wind farm is located at Rødsand south to the Danish island of Lolland, just south to the main island of Zealand. Through a 20 km cable, the wind farm is ac-connected to the transmission network on-land. The Rødsand offshore wind farm shall comply with the Danish specifications for connecting of large wind farms to transmission networks.

The wind turbines equipped with doubly-outage induction generators with variable rotor resistance can be associated with the OptiSlip® wind turbines produced by the Danish manufacturer Vestas Wind Systems. The converter controls dynamically the external resistance within a given range, which is why the term “variable rotor resistance”. The wind turbines are pitch-controlled. The power capacity of the wind turbines of this concept is up to 1.8 MW. Presence of external rotor resistance, which is dynamically controlled, results in a wider range of rotational speeds, but still within few percents above the synchronous speed.

In the variable-speed wind turbines equipped with DFIG, the power is supplied from the stator to the power grid and supplied to or absorbed from the grid via the rotor circuit. In this concept, the rotor circuit is connected to the power grid through the partial-load frequency converter. The generator is excited through the rotor circuit by the rotor converter and can operate reactive-neutral with the power grid. Additionally, reactive power can be controlled with use of the grid-side converter. However, the grid-side converter is normally reactive-neutral.

The converter control can be organised so that the DFIG will exchange a less amount of reactive power with the grid for voltage control in undisturbed operation situations. The mechanical system of these wind turbines is similar to the fixed-speed concept. The purpose of the variable-speed feature is optimisation of the power gain by adjusting the rotational speed. The rotational speed of the turbine can be in the range of 10 to 25 rev./min., which is why the concept is termed “variable-speed”. The variable-speed wind turbines are commonly pitch-controlled for better power output optimisation. The largest manufacturers of this concept are Vestas Wind Systems, G.E. Wind, NEG-Micon, Nordex, Gamesa Eólica, Tacke and many others. In figures of 2002, the largest commercial wind turbine equipped with DFIG is 3.2 MW wind turbine from G.E. Wind. As reported in press, the manufacturer NEG-Micon has erected an experimental wind turbine of 4.2 MW equipped with DFIG in the year 2003.

This concept seems to be promising for large-scale offshore wind farms. The offshore wind farm at Horns Rev in Western Denmark, been taken in operation in the year 2002, is with eighty 2 MW variable-speed wind turbines equipped with DFIG. The wind turbines are from the Danish manufacturer Vestas Wind Systems. The wind farm shall comply with the Danish specifications (Jensen, 2002).

The German manufacturer Enercon is the largest supplier of the variable-speed wind turbines equipped with the multi-pole, synchronous generators that are connected to ac-grids through frequency converters. The range of rotational speed is similar to the concept with DFIG. The concept is characterised by absence of the gearbox and by the ring-generator of a relatively large diameter. The synchronous generators are electrically-excited. The synchronous generator, when direct driven by the wind turbine, generates the electric frequency equal to the mechanical

frequency of the turbine multiplied by the number of pole-pairs of the generator. The power from the generator is supplied through the frequency converter to the power grid with a fixed electric frequency (50 Hz in Europe). The grid-side converter can operate reactive-neutral, but, principally, it can also be used to control reactive power and voltage in the grid. The electricity-producing wind turbines of this concept are pitch-controlled.

The largest commercial wind turbine from the manufacturer Enercon is of 1.8 MW, but a prototype of 4.5 MW rated power, denoted E112, is taken in operation in Germany in the year 2002. The generator diameter is about 8 m and the blade length is 52 m (Enercon, 2002).

About 75% of the wind turbines produced by Enercon are for the German market and this concept is not entirely represented in Danish sites yet.

In this work, the author took contact to the Danish company Multipolgenerator Aps worked on the concept of the converter-controlled, multi-pole, permanent magnet generator (PMG) for wind energy converters. The collaboration was for modelling of this wind turbine concept. In the wind turbine concept with PMG, the rotor maintaining the permanent magnets provides excitation of the generator; the rotor is directly connected to the LS shaft of the turbine rotor. The stator of the generator supplies the electric power to the grid through the frequency converter.

Presently, the manufacturer Lagerwey Windmaster produces the wind turbines equipped with PMG, LW72. The rated power is 2 MW, the rotor diameter is 72 m and the rated generator voltage is 4 kV. The PMG is from the Swedish generator manufacturer ABB.

Let us resume the introductory section with focus on wind turbine modelling details. First, the turbine rotor is a common part in all the concepts. Second, the concepts with the induction generators, the variable rotor-resistance and the DFIG have similar representations of the shaft systems which are the two-shaft system with a gearbox in-between. This is not the case in the wind turbines with direct-driven PMG. Third, the frequency converters are seen in the concept with DFIG as well as with PMG, but the control strategies of the converters in these two concepts can be different. Fourth, the generator concepts seem to be different all the wind turbine concepts. Notify, however, that the three first concepts are with induction generators by different applications and only the fourth concept, e.g. with PMG, contains multi-pole, synchronous generators.

This discussion can be useful for modelling issues focused on (i) functionality of the wind turbine components and (ii) their importance for investigations of transient voltage stability.

1.3. Modelling issues

First, the complexity of the simulation models of electricity-producing wind turbines must comply with physics of these energy conversion systems. Second, the model complexity depends on the target of the investigations where the models shall be used. Further, the models shall be in agreement with the interface of the simulation tool, which corresponds to the implementation process. Choice of the simulation tool depends on the target of the investigations.

1.3.1. Dynamic wind turbine models

The target is investigations of (i) transient voltage stability of large power systems with relation to incorporation of a large amount of wind power and (ii) interaction between the wind turbines and

the power network. Basically, the electricity-producing wind turbines shall be treated as complex electromechanical systems (Akhmatov et al., 2000(a)) with representation of (i) electrical components such as generators, frequency converters and their control systems and (ii) mechanical parts of the construction such shaft systems, turbine rotors and their control. The wind turbine models should not be over-simplified.

On the other hand, representation of a given component of the wind turbine construction shall have a purpose and an explanation with relation to the target of the investigations, but not only because this component is present in the construction. Over-detailed models will be more difficult to describe and explain, slow simulations and produce several unnecessary outputs; this may also confuse interpretation of the results.

In other words, the model complexity and the purpose of the investigations shall be in agreement with each other. With relation to modelling of the wind power incorporated into the eastern Danish power grid, we distinguish between two groups of the electricity-producing wind turbines.

- 1) The first group of approximately 400 MW rated power capacity is grid-connected to the local distribution networks. When subjected to a grid fault, the protective relay systems of the wind turbines register an abnormal operation and give order to trip when at least one of the monitored parameters has exceeded its respective relay settings. The majority of these wind turbines are of the Danish concept.
- 2) The second group relates to the large offshore wind farm of 150 MW rated power that is assigned to the Danish specifications. The large offshore wind farm is ac-connected to the transmission network. According to the Danish specifications, (i) the voltage shall be re-established after the grid fault and (ii) no subsequent disconnection of the offshore wind farms will be accepted in case of (n-1).
- 3) Possibly, a similar pattern with diversity of the wind turbine operation will be seen in other power systems.

The total duration of the dynamic behaviours to be investigated is up to 10 seconds. In simulations, the power grid will be subjected to a three-phased³ short circuit fault of a given duration, typically in the range of 100 ms or so. When the fault is cleared, the voltage through the power system shall be re-established within the predefined range, which means that neither under- nor over-voltage will be accepted.

³ Discussion: the most frequent short-circuit faults in transmission power grids are single-phase-to-ground faults. Also, phase-to-phase faults and two-phase-to-ground faults are more frequent in the transmission power grids than three-phase faults. First of all, three-phase faults are much more serious events with respect to maintaining transient voltage stability than other types of faults. When voltage recovers after a three-phase fault, this will presumably also recover after other types of faults. Secondly, only balanced, three-phase events are possible to compute in the simulation tool PSS/E, which is used in this project. Third, consequences of single- and two-phase faults can be investigated in PSS/E when applying a three-phased fault with a suitable residual voltage in the faulted node. In case of a single-phase short-circuit fault, the positive-sequence voltage in the faulted node drops to around 0.75 to 0.80 PU; this is an approximation.

With respect to the decentralised wind turbine sites connected to the local distribution networks, it is rather not to say whether they will be tripped by the given grid fault. The protective relay systems monitor the terminal voltage, the machine current, the grid frequency, the rotational speed etc. and order the wind turbines to trip. This occurs at registering of abnormal operation in the electric power system (Akhmatov, 2002(a)).

Although presence of the formal specifications (Eltra, 2000), it must be kept in mind that the wind turbines within the large offshore wind farms are equipped with protective relays and, hence, can trip. The target of the investigations is therefore to find technical solutions where the voltage recovers and the parameters monitored by the protective relays do not exceed their settings. Exceeding the protective relay settings in simulations indicates that the wind farm will possibly trip. Tripping of the large wind farm can occur even in situations where the voltage recovered in simulations. In this case, the technical solution will not be acceptable.

According to the discussion above, the following requirements can be formulated to the dynamic wind turbine models to be used in investigations of transient voltage stability.

- 1) The dynamic wind turbine models must predict sufficiently accurate values of the electric power, the reactive power and the voltage profile. This is the definitive requirement independent from considerations about relaying.
- 2) The models must predict sufficiently accurate values, which are monitored by the protective relay system. These are both the electric values (voltage, machine current, grid frequency, etc.) and the mechanical values (the generator rotor speed, for example).
- 3) In case of the variable-speed wind turbines with converter-controlled generators, which are DFIG and PMG, the converter representation is extremely important. It is because these wind turbines are often tripped at the converter blocking (Akhmatov, 2002(a)). In other words, the transient behaviour of the generator and the converter describes the wind turbine operation during the transient events.
- 4) The model to be used for local wind turbine sites shall be equipped with a supplementary model that disconnects the compensating capacitor, the generator, the converter and order stop of the wind turbine⁴. Use of the supplementary relay models is probably not always necessary in case of large offshore wind farms, because exceeding the protective relay settings will indicate that the solution is unacceptable.
- 5) Accuracy of the relay model and the relay setting data are important.
- 6) After tripping, the wind turbines are waiting for re-establishing of normal grid operation. After 15 min. or so when the normal grid operation is re-established, the wind turbines start

⁴ Discussion: notify that either the wind turbine stop or disabling of the state calculations can be important to include. When a wind turbine is tripped in simulations, the electric torque is zero, but the mechanical torque is not. This may affect numerical stability of the model due to the movement equation and, in some cases, crash the simulation. The standardised models in PSS/E are with disabling the states of islanded generators to prevent such situations, whereas PowerFactory does not have this, which is why the user must provide a routine to prevent over-speeding of disconnected generators. On the other hand, standardised models in PSS/E do not seem to be suitable to investigate such islanded operation of generators, but this is possible in PowerFactory.

re-connection. As seen, this behaviour is not of interest for investigations of transient voltage stability. Consequently, there are no specific demands to the models on the generator computations when disconnection has occurred.

From this viewpoint, the requirements to the models to be used for representation of the wind turbines in large offshore wind farms as well as in local sites connected to the local distribution networks seem to be similar. This is, however, not a complete picture. The models to be used for representation of the wind farms assigned to the grid-connection specifications can be more complex than the models for local sites. For example,

- 1) The model of the variable-speed wind turbine with the converter-controlled generator in a local sites shall contain representation of the converter protection featuring the converter blocking and the generator trip at the grid fault. The model of the wind turbine of the same concept to be used for simulation of the large offshore wind farm shall additionally contain representation of the uninterrupted wind turbine operation feature with the converter re-start.
- 2) Additionally, the large offshore wind farms shall comply with several specific requirements, which are not present in case of local wind turbine sites⁵. According to the Danish specifications, the large offshore wind farms shall be able to reduce their electric power production from an arbitrary level to less than 20 % of the rated power in less than 2 seconds by an external signal given from the system to the wind farm. This technical specification implies that the wind turbine model shall be with a sufficiently accurate representation of the blade-angle control applied for this technical feature. This may also require representation of the mechanical system model and aerodynamics of the turbine rotor.

The block diagram of the dynamic wind turbine model, which is applied to investigate transient voltage stability, is shown in **Fig. 1.2**. The model contains the blocks with representation of the basic wind turbine components.

- 1) The aerodynamic model of the turbine rotor. The incoming wind, V , is considered stationary because the duration of the investigations is short.
- 2) The shaft system model, representing possible torsional oscillations in the shaft system.
- 3) The electric generator model. It is a transient model.
- 4) The blade-angle control and the servo model, if it is a variable-pitch wind turbine.
- 5) The converter and its control, if the wind turbine generator is converter-controlled.
- 6) The protective relay system model, where it is necessary.

This general representation is according to the description of the wind turbine concepts given in **Section 1.2**. This relates also to the requirements formulated for the dynamic wind turbine model for investigations of transient voltage stability. The blocks and the couplings of the dynamic wind turbine model will be explained for each wind turbine concept in the following presentation. Unnecessary blocks can be omitted.

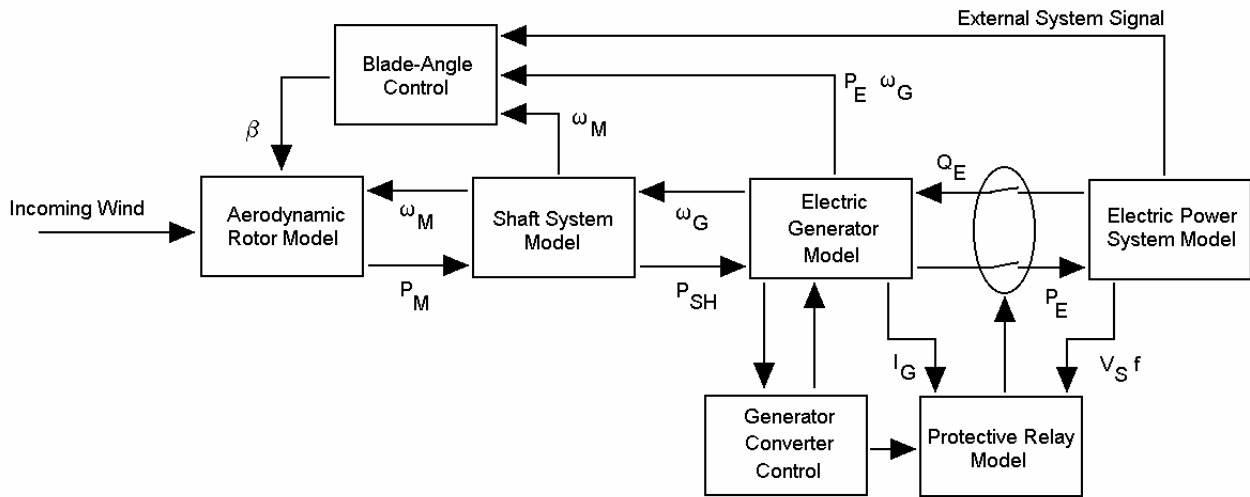


Fig. 1.2. Dynamic wind turbine model to be applied in investigations of transient voltage stability. The model is general for all the wind turbine concepts described in this work. Here P_M , P_{SH} and P_E are the mechanical power, the generator rotor shaft power and the electric power, respectively, Q_E is the reactive power, I_G is the machine current, V_S is the terminal voltage, f is the grid frequency, ω_G and ω_M are the generator rotor speed and the turbine rotor speed, respectively, and β denotes the pitch angle.

1.3.2. Dynamic simulation tool

Now, the wind turbine models shall be implemented in an existing, suitable simulation tool. The voltage stability investigations shall be executed on large power system models with representation of the transmission network, the power plant units and their control and the large offshore wind farm feeding into the transmission network. Representation of the local distribution networks with consumption centres and decentralised generation such as wind turbine sites and combined heat-power (CHP) units feeding into the local distribution networks can also be needed. Among a number of possible tools, the simulation tool Power System Simulator for Engineers (PSS/E) from the supplier Power Technologies, Inc., (PTI), New York, U.S.A. is chosen for this work.

The simulation tool PSS/E contains documented and verified models of synchronous generators, which are used in conventional power plants, the excitation control, the governors, the power system stabilisers (PSS) of different concepts and other models. The tool PSS/E contains the dynamic models for representation of consumption centres at fluctuating voltage and grid-frequency. The tool allows implementation of user-written models, which is an important issue for the modelling work. The tool allows simulations with the power grids of arbitrary configurations and complexities and with an arbitrary number of generation units. It is useful for detailed representation of many local wind turbine sites and CHP.

The tool PSS/E has a number of considerations, which are similar to considerations of any other dynamic simulation tool. This might be kept in mind because these considerations can introduce restrictions on user-written modelling of electricity-producing wind turbines.

⁵ Remember our note in **Section 1**.

- 1) The simulation tool PSS/E is the fundamental-frequency simulation tool, which implies that the legal range of frequency deviation is typically within a range of $\pm 10\%$ about the rated frequency (50 Hz in Europe). The higher harmonics of the fundamental frequency are not modelled using the tool PSS/E. The standardised models of the tool and their assumptions, the network equivalent models and, hence, the network solutions are found on this assumption.
- 2) It operates with positive-sequence equivalents of the electric power systems, which requires symmetrical three-phase networks. The generators are modelled by their positive-sequence equivalents as well.
- 3) By the mentioned above, balanced events in the power grid can only be modelled, where the condition dealing with symmetrical three-phase network representations is not broken. An example of a balanced fault can be a three-phase short-circuit fault subjected to all the three phases of the faulted node or of the faulted line at the same time.
- 4) Unbalanced events are simulated as balanced events, according to the interface of PSS/E. An example on this is given in the following items.
- 5) During execution of dynamic simulations, the network solution at any time, t , is found by computation of the load-flow network solution at any time-step. When explained in simplified terms, it is achieved using the algorithm producing the vector of the currents going into the network at the power system nodes, $[I]$, using the node admittance matrix, $[[Y]]$, multiplied by the vector of the node voltages to ground, $[V]$. By this way, the fundamental-frequency transients in the network solution are omitted. This routine makes it possible to compute unbalanced events in the tool PSS/E without breaking the assumption of symmetrical three-phased networks. A line tripping or a short-circuit fault are represented with re-writing of the node admittance matrix, $[[Y]]$.
- 6) Tripping of a three-phase line is an unbalanced disturbance because opening of the each of the three phases occurs at the currents passing zero in the respective phases. Obviously the fundamental-frequency transients, expressed by the dc-offset in the line current, are eliminated at such unbalanced disturbances. According to the algorithm of the tool PSS/E, the three-phase line is simply tripped as all the three phases are switched off at the same time, e.g. symmetrically, but with neglected transients of the current.
- 7) Notice that the dc-offset in the line currents are also neglected at balanced faults such as a three-phase short circuit fault, although the dc-offset will be in the physical current. This consideration can be explained by the fact that this simplification does not influence on the voltage profile in the entire power grid, but allows a relatively large time step. This speeds up the computational process of the network solution significantly. That is an advantage for simulation of large power systems.
- 8) Electrical machines are commonly given by the machine voltage sources, E_{MACH} , behind its step-up transformer and the dynamic impedance, Z_{MACH} . In PSS/E, this common representation is replaced by the Norton-equivalents and the electric machines contribute to the network solution by the vector of machine currents, $[I_{\text{MACH}}]$, injected to the power system at the machine nodes. The algorithm applied to the network solution introduces the restrictions on the interface between the machine models and the entire network model.

Those restrictions are that the fundamental-frequency transients, e.g. the dc-offset in the machine current, $[I_{MACH}]$, shall be omitted. The standardised models of synchronous generators are by this consideration (Kundur, 1994). This is suitable purposing power stability investigations carried out on models of the power systems dominated by conventional power plants equipped with synchronous generators (Kundur, 1994).

These considerations introduce a number of restrictions on the user-written models that are the dynamic wind turbine models, in this case. It must be kept in mind when interfacing the user-written models to the simulation tool.

1.4. Outline of this presentation

According to the introductory section, this project is a multi-task work. This presentation will contain elements of (i) electric machinery theory, (ii) shaft system representation, (iii) aerodynamic relations and control features, (iv) converter system modelling and control, (v) interaction between wind turbines and electric power systems, (vi) transient voltage stability, (vii) modelling of large wind farms and power systems etc. Description of this multi-task work will be well-structured.

Description of the modelling work will be started with presentation of the mechanical construction of the wind turbine and evaluation which parts of the construction shall be included in the dynamic wind turbine model. The complexity of the mechanical construction representation will be discussed with relation to application of the dynamic wind turbine model in investigations of transient voltage stability. This description is given in **Section 2**.

In **Section 3**, the blade-angle control will be given with its generic control system. Here, it is both for pitch and active-stall control. The description given in **Sections 2** and **3** shall be common for all the wind turbine concepts.

Description of the dynamic wind turbine models of different concepts can be organised by different ways. Generally, electricity-producing wind turbines can be separated into two groups.

- 1) Fixed-speed wind turbines equipped with induction generators excited from the power grid. In this group, the Danish concept and the wind turbines with variable rotor resistance are present. The main problem with respect to maintaining voltage stability will be a risk of fatal over-speeding of the wind turbines at the grid faults (Akhmatov et al, 2000(b)). There is also a functional similarity between these two concepts.
- 2) Variable-speed wind turbines with converter-controlled generators, which are DFIG or PMG. The generators are excited by the converters, but not from the power grid. Over-speeding is not any fatal problem of this concept in means of maintaining transient voltage stability. In these two concepts, the challenge is to organise the converter control providing uninterrupted operation of the wind turbines and protection of power electronics (the converters) at the grid disturbances (Akhmatov, 2002(a)). There is also a functional similarity between these two concepts in terms of power output optimisation by the variable-speed operation.

Here, it is chosen to organise this description in terms of interaction between the wind turbines of the given concept and the electric power system. This choice is also made with respect to presentation of the investigation results. The description begins with the Danish concept. When the aerodynamic rotor model and the shaft system are both already discussed, it will focus on modelling of induction generators at different kinds of disturbances, balanced versus unbalanced. Furthermore, interacting between the shaft system and the induction generator is taken into account. This is treated in **Section 4**.

Aggregated modelling of large wind farms with fixed-speed wind turbines is given in **Section 5**. Here, it is explained under which conditions the large wind farm with many wind turbines can be represented by a single-machine equivalent, e.g. one wind turbine model with re-scaled power capacity, in investigations of transient voltage stability.

Section 6 deals with (i) maintaining transient voltage stability, (ii) discussing possible mutual interaction within and (iii) suggestions to improve transient voltage stability of large wind farms with fixed-speed wind turbines. In other words, **Sections 4, 5 and 6** cover the fixed-speed concept only. This focus is because the majority of the wind turbines incorporated into the Danish power system are of this concept.

Pitch controlled wind turbines equipped with doubly-outage induction generators with variable rotor-resistance are described in **Section 7**. The converter control is given with a generic scheme. Again, interaction between the large wind farm and the electric power network is investigated.

Variable-speed wind turbine concepts are described in **Sections 8, 9 and 10**. The task of power output optimisation and possible restrictions of variable-speed operation are outlined in **Section 8**. Dynamic interaction between the large wind farm and the electric power system is described in case of (i) PMG and full-load frequency converters in **Section 9**, and (ii) DFIG and partial-load frequency converters in **Section 10**. Also here, it focuses on whether there is any risk of mutual interaction between many wind turbines and their frequency converters at the grid faults.

Finally, experiences with modelling of the electricity-producing wind turbines of different concepts will be used in demonstrating examples on investigation of transient voltage stability of large power networks. Such networks may contain (i) a large number of local wind turbine sites and CHP units, (ii) a number of power plants, (iii) large consumption centres and also (iv) a large wind farm, assigned to the specifications of the transmission system operator (Eltra, 2000). Here, it will be illustrated that such stability investigations shall be executed at sufficiently realistic considerations. Access to a strong power grid will also be discussed. The results are of interest because a number of parameters will influence on the outcome of such investigations. This work is presented in **Section 11**.

Conclusion is given in **Section 12**. This presentation will also include a less number of specific topics, which are collected in **Appendices**.

2. Mechanical system of a wind turbine

A sketch of the mechanical construction of a wind turbine is given in **Fig. 2.1**. This representation interprets the aeroelastic code (AEC) of the wind turbine. Some kinds of oscillations and vibrations can be excited in the mechanical construction of the wind turbine, when subjected to a grid fault, (Akhmatov, 2003(d)). In general, studying such oscillations and vibrations excited in the construction of the wind turbine should be treated with use of the AEC.

However, it does not seem to be necessarily to represent all kinds of such oscillation phenomena in the dynamic model of electricity-producing wind turbines applied to investigate transient voltage stability of power grids. Complexity of the mechanical representation shall be in agreement with the target of investigations. From this viewpoint, the complexity details of the mechanical construction should be reduced to following.

- 1) Aerodynamics of the rotating wind turbine. This will give a coupling between the speed deviation and the mechanical power produced by the wind turbine, at a constant wind. Also, this gives a coupling between the pitch angle and the mechanical power of the turbine.
- 2) Representation of the wind turbine shaft system. This is to represent interaction between the mechanical and the electrical parameters of the wind turbine.
- 3) Model of the blade-angle control system by pitch or active-stall. This is to simulate variable-pitch wind turbines and explained in **Section 3**.

Other phenomena in the mechanical construction will not influence on the outcome of investigations of transient voltage stability with the main target to resume if voltage recovers after a short-circuit fault in the power grid. The duration of such grid stability investigations is up to 10 seconds. Among such phenomena relating to excitation of the wind turbine construction, which are disregarded in the dynamic wind turbine model, are the following.

- 1) Turbulence in incoming wind. This means natural fluctuations around the mean value of wind speed. The time period of such fluctuations is in a range of seconds.
- 2) Long-term wind fluctuations. This means variations of the mean wind speed with the time period of minutes or longer. Incoming wind speed is assumed stationary when treating investigations of transient voltage stability.
- 3) Neither mechanical oscillations in the wind turbine blades nor oscillations in the tower influence on maintaining of transient voltage stability.

The considerations given in items 1 and 2 are by “a common sense”. There is no factual documentation to confirm or to reject the argumentation given in these items. The consideration in item 3 relates to use of the lumped model of the wind turbine rotor. On this assumption, the wind turbine rotor is represented by its lumped inertia constant and the blades are considered stiff. Furthermore, the tower is considered stiff, instead of use of the AEC with a flexible tower model.

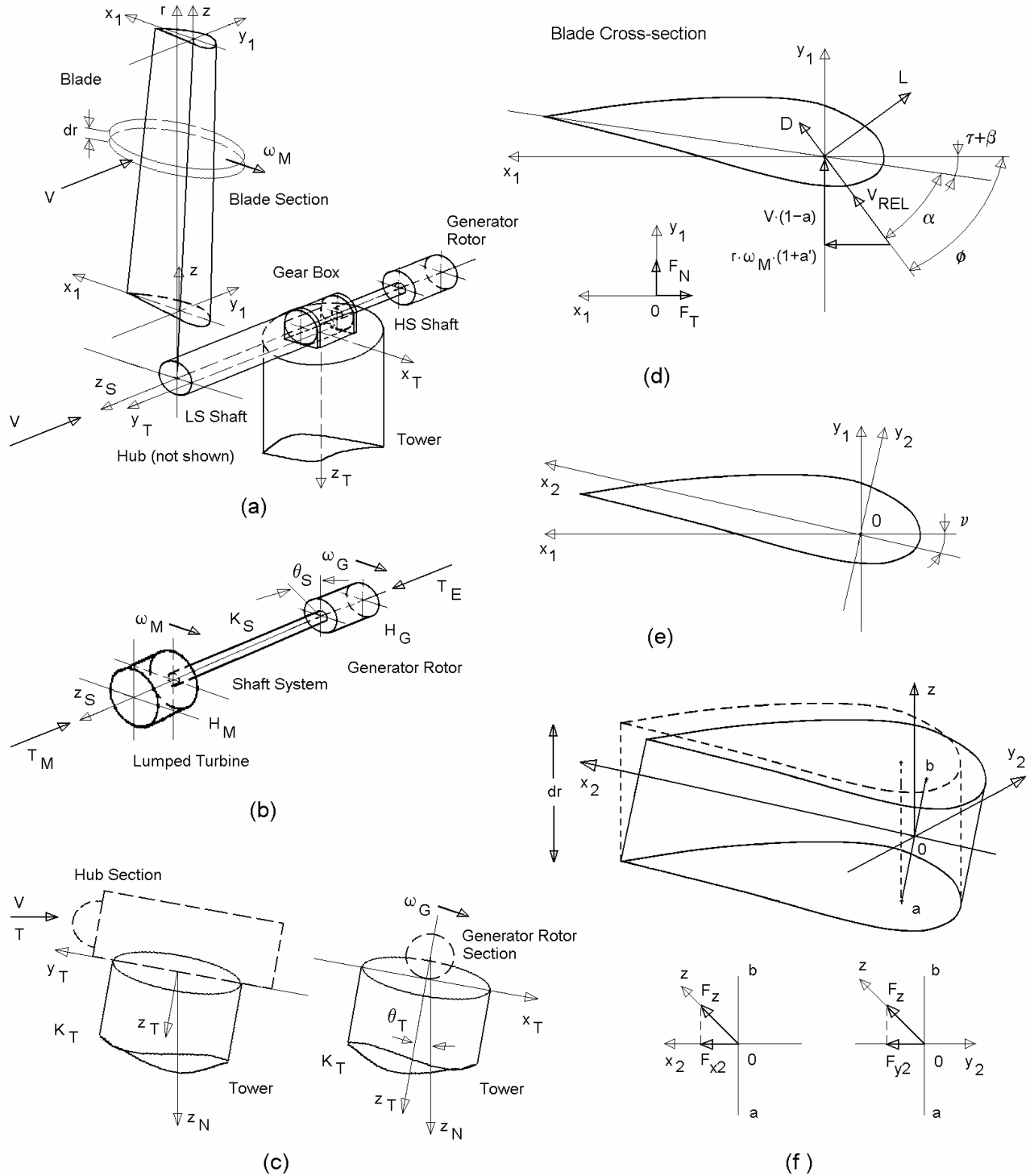


Fig. 2.1. Mechanical construction model in terms of AEC: **(a)** – components of the wind turbine construction, **(b)** – shaft system model, **(c)** – tower, **(d)** – use of BEM method on the blade cross-section, **(e)** – introducing the principal axis, **(f)** – deformations and computation of centrifugal forces. Reported in (Akhmatov, 2003(d)).

The above-mentioned phenomena will rather relate to flicker investigations than to investigations of transient voltage stability in the power grid. These phenomena can, however, be taken into account in investigations of long-term voltage stability in extremely weak power systems with many wind turbines in terms of small-signal stability. Our investigations have shown that the problem with possible risk of long-term voltage instability initialised by small-signal disturbances

from the wind turbines, which is flicker, does not exist in the power system of Eastern Denmark (Knudsen and Akhmatov, 2001). This is why concerns about maintaining of long-term voltage stability and wind turbine models used for such investigations are not described in this report.

On the other hand, electricity-producing wind turbines shall be understood as self-bearing mechanical constructions. The power capacities and the geometrical sizes of modern wind turbines increase rapidly⁶. The wind turbines in the large offshore wind farms shall comply with technical specifications formulated by the transmission system operator (Eltra, 2000). The power ramp⁷ required in the Danish specifications can be an example on concerns about a possible risk of excitation of the mechanical construction.

- 1) Excitation of the mechanical construction is expressed by insufficiently damped oscillations of different parts of the construction. It may lead to that different parts of the mechanical construction oscillate against each other with an increasing magnitude. Such insufficiently damped mutual oscillations may occur in the wind turbine blades, the tower and the shaft.
- 2) It is thinkable that excitation of the mechanical construction can be initialised by a fault in the power grid. No documentation confirming or rejecting this concern is found, except an example in our simulations (Akhmatov, 2003(d)).
- 3) It is thinkable that excitation of the mechanical construction can be started by a specific control algorithm applied to the wind turbines in specific operational situations. An example on this can be the power ramp with use of the blade-angle control ordered at a grid fault. It is primarily in situations where some of the parameters of the control system are insufficiently tuned.
- 4) When excitation is started, the wind turbines will possibly be tripped and stopped by the protective system monitoring mechanical vibrations in the wind turbine construction. This leads to power loss and demands of immediate power reserves. This outcome will be unexpected if the stability investigations have predicted voltage recovery at the grid fault and no other problems relating to operation of the wind turbines are found with use of models with simplified representation of the wind turbine construction.
- 5) Another problem relating to understanding of the wind turbine as a self-bearing mechanical construction is their life-time. The control algorithms suggested for wind turbines for any purpose, including improving of transient voltage stability, may not lead to shortening of the guaranteed (expected) life-time of the wind turbines. With use of the wind turbine model with the AEC in a less number of simulations, such excitation problems can be indicated and,

⁶ The largest commercial wind turbines today are between 2.0 to 3.2 MW of rated power and with the rotor diameter of 80 to 90 m. RePower Systems AG and the Danish manufacturer LM Glasfiber have announced the rotor blade with the rotor diameter of 125 m to be used in the Repower 5M variable-speed, pitch-controlled wind turbines of 5 MW of rated power, by press release "REpower and LM Glasfiber develop a rotor blade for a 5-megawatt plant" of 17th August 2002.

⁷ Ordered power reduction from an arbitrary operational point to less than 20 % of the rated power in less than 2 seconds.

probably, eliminated (Akhmatov, 2003(d)). This work is responsibility of the manufacturer and shall take place before commissioning of the large wind farm.

Notice that the wind turbine model with the AEC is quite large and demands significantly more data of the blade geometry and its elasticity than simply the turbine rotor inertia. It is not necessary to carry out investigations of transient voltage stability with use of such complex models. The wind turbine model with use of the AEC can, however, be understood as an investment. The wind turbine model with use of the AEC could be applied in a less number of simulations to be sure that the control algorithms, suggested for the wind turbines and for the power system, neither start excitation nor reduce the expected life-time of the wind turbines.

The majority of the simulation cases, described in this report, are made with use of the simplified model where the rotating turbine is considered lumped. The wind turbine model with the AEC has only been applied in few simulations. This work is done to eliminate possible discussions about risk of fatal excitation of the mechanical construction of the wind turbines and a risk of reducing their life-time. This topic is shortly described in **Appendix 2.A**.

2.1. Aerodynamic model of a wind turbine

An aerodynamic model of the wind turbines will be the common part of the dynamic models of the electricity-producing wind turbines independently from the concept. This representation is necessary because it gives a coupling between the rotational speed and the mechanical torque produced by the wind turbine rotor.

In variable-pitch concepts, this also gives a coupling between the pitch angle and the mechanical power of the turbine rotor.

2.1.1. Static representation

In equilibrium, the mechanical torque supplied from the wind turbine rotor to the LS shaft, T_M , and the thrust, T , can be computed with the Blade Element Momentum (BEM) method (Freris, 1990, Sørensen and Kock, 1995). The blades are separated into a number of sections along each blade. The blade geometrical and aerodynamic properties are given for each section as functions of the local radius, r , from the hub to the blade tip, $r = R$. Each blade section is of the thickness dr as shown in **Fig. 2.1.a**. The axes x_1 and z define the plane of rotation.

The cross-sectional airfoil element of the blade section at the local radius, r , is shown in **Fig. 2.1.d**. The cross-sectional element defines the blade element at radius r in (x_1, y_1) -plane. The local velocity, $V_{REL}(r)$, being relative to the rotating blade, is given by superimposing the axial velocity $V(1-a)$ and the rotational velocity $r\omega_M(1+a')$ at the rotor plane. The undisturbed wind speed is V and the tangential velocity of the rotating blade section is $r\omega_M$. The induced velocities in the rotor plane are $-aV$ and $+a'r\omega_M$, with the respective factors a and a' . These are induced by the vortex system of the wind turbine. The local angle of attack is defined by the following relation (Sørensen and Kock, 1995).

$$\alpha = \phi - (\tau + \beta) \quad (2.1)$$

The angle

$$\phi = \tan^{-1} \left(\frac{V(1-a)}{r\omega_M(1+a')} \right) \quad (2.2)$$

is the angle between the relative velocity, $V_{REL}(r)$, and the rotor plane, the local twist is τ and the pitch angle is β . In case of fixed-pitch wind turbines that are practically the same as stall-controlled wind turbines β is constant.

The lift force, L , and the drag force, D , are defined by the following relations.

$$L = \frac{1}{2} \rho_{AIR} V_{REL}^2 c C_L, \quad D = \frac{1}{2} \rho_{AIR} V_{REL}^2 c C_D, \quad (2.3)$$

where ρ_{AIR} is the air density, being 1.225 kg/m³ for the standardised air, c is the chord of the blade section and C_L and C_D are the lift and the drag coefficients, respectively.

The normal, F_N , and the tangential, F_T , forces being parallel to the axes y_1 and x_1 , respectively, and acting onto the blade given section are found by inspection of the sketch in **Fig. 2.1.d**.

$$F_N = L \cos(\phi) + D \sin(\phi), \quad F_T = L \sin(\phi) - D \cos(\phi). \quad (2.4)$$

In case of stall-controlled wind turbines, this description is resumed by definition of the thrust, T , the mechanical torque, T_M , the mechanical power, P_M , and the power coefficient, C_P , of the wind turbine (Sørensen and Kock, 1995; Younsi et al., 2001).

$$\begin{aligned} T &= B \int_0^R F_N(r) dr, \\ P_M &= \omega_M T_M, \quad T_M = B \int_0^R r F_T(r) dr, \\ C_P &= \frac{P_M}{P_V}, \quad P_V = \frac{1}{2} \rho_{AIR} V^3 \pi R^2. \end{aligned} \quad (2.5)$$

and B denotes the number of blades which are three for the given concept, P_V is the wind power available in the swept wind turbine rotor area πR^2 .

Notify that the power coefficient of any wind turbine cannot exceed its theoretical upper limit $C_P^{MAX} = 16/27 \approx 0.59$. This value is the so-called Betz limit and reached for steady-state operation of wind turbines (Pretlove and Mayer, 1994; Walker and Jenkins, 1997; Hansen 2000).

Commonly, the curve of power coefficient, C_P , versus tip-speed-ratio, $\lambda = \frac{\omega_M R}{V}$, is given by the wind turbine manufacturer. This curve will give a sufficiently detailed representation of aerodynamics of stall-controlled wind turbines to be used in investigations of transient voltage stability. So long as the incoming wind speed, V , is stationary and the turbine speed, ω_M , does not change too fast and too much, the wind turbine operation is only characterised by small deviations from equilibrium. This is a fair consideration to investigate transient voltage stability. At this

consideration, the representation of the wind turbine aerodynamics by the C_P - λ -curve is sufficiently accurate. The mechanical power is, then, defined as

$$P_M = \frac{1}{2} \rho_{AIR} V^3 \pi R^2 C_P(\lambda). \quad (2.6)$$

In the majority of investigations of transient voltage stability, the pitch- and the active-stall controlled wind turbines are modelled using the C_P - λ - β -curves. This can be understood as a number of C_P - λ -curves of the given wind turbine at different values of the pitch angle, β . Each operational point at the given C_P - λ -curve at the given pitch angle, β , represents equilibrium. Representation of the wind turbine aerodynamics in terms of the C_P - λ - β -curves is, in other words, based on the consideration that the wind turbine is in equilibrium at any time of operation. The mechanical power, P_M , is defined by **Eq. (2.6)**, but with use of $C_P(\lambda, \beta)$.

2.1.2. Dynamic inflow phenomena at pitching

The consideration of reaching equilibrium at any time of operation is the same as to say that the wind profile distribution, formed around the wind turbine rotor, is able to change immediately at changes of the pitch angle, β . In other words, it is considered that the wind turbine would transit from a present state of equilibrium to another state of equilibrium without any delay, but by a step. This consideration will, however, be in disagreement with physics of the wind turbine (Øye, 1986; Snel and Schepers, 1992).

This transition process between the two states of equilibrium is continuous, but not immediate. The transition process is defined by dynamic inflow phenomena (Øye, 1986). Dynamic inflow phenomena manifest themselves by the overshoots occurring in the mechanical torque of the turbine rotor at pitching. First time, it was observed by Øye (1986) on pitch-controlled, medium-sized wind turbines in Denmark. Later, the same behaviour was observed from measurements on the 2 MW pitch-controlled wind turbine equipped with an induction generator. The results of this experiment are published by Snel and Schepers (1992) and again by Snel and Schepers (editors, 1995). In the experiments published by Snel and Schepers (1992), the 2 MW wind turbine is subjected to a “step” of the pitch angle. This “pitch-step” is achieved by a sudden change in the pitch reference. The pitch angle is then adjusted by the pitch servo with the servo time constant $T_{SERVO} = 0.25$ s and at the pitch rate limits of 7.2 °/s.

The measured curve of the mechanical torque corresponding to the study case II.4 from (Snel and Schepers, editors, 1995) is shown in **Fig. 2.2**. This study case II.4 is similar to the main study case from (Snel and Schepers, 1992). Case II.4 corresponds to the operational point at the wind speed of 8.7 m/s and the initial pitch angle of 0°. At the time $t = 1$ s, the pitch reference was set to +3.7 °, and at the time $t = 30$ s, the pitch reference was set to 0 ° again. As seen, the measured torque is with notable overshoots at pitching.

The overshoots in the mechanical torque at pitching cannot be explained in terms of the static BEM-method. For representation of the overshoots in the mechanical torque at pitching, the static BEM-method shall be revised. This can be achieved with introduction of the characteristic time constants of the transition process (Øye, 1986). The characteristic time constants are in the order of $2R/V$ and $c/(\omega_M R)$ (Snel and Schepers, editors, 1995). Revision of the BEM-method is by the

engineering model suggested by Øye (1986). In the Øye model, dynamic inflow phenomena are implemented by introducing the lags in the induced velocities.

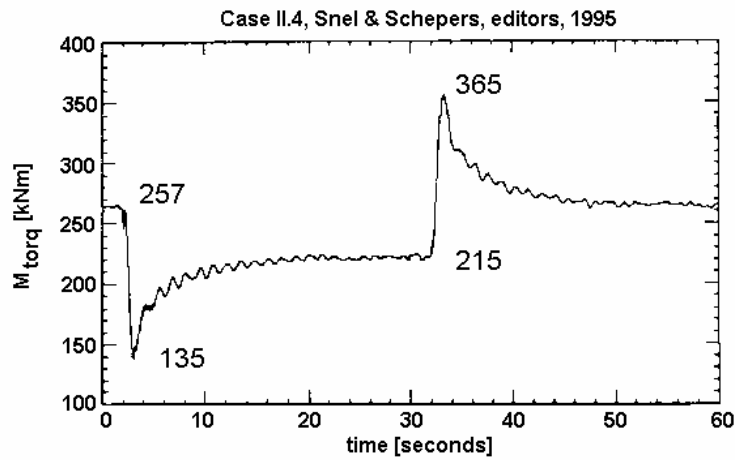


Fig. 2.2. Measured mechanical torque of the wind turbine at a pitch change, reported in (Snel and Schepers, editors, 1995).

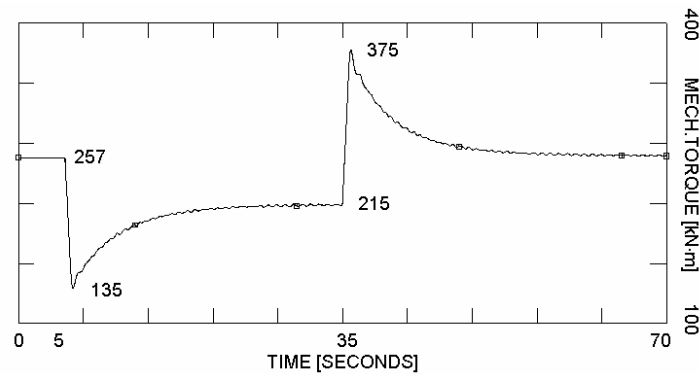


Fig. 2.3. Computed mechanical torque, T_M , of the wind turbine as response to a pitch change, reported in (Akhmatov, 2003(d)).

The model of the wind turbine with representation of dynamic inflow phenomena by the Øye model is implemented in the simulation tool PSS/E as an user-written model. The wind turbine data are found in (Snel and Schepers, editors, 1995). These data are for the wind turbine from the experiment of the study case II.4. The model of induction generators is given in **Section 4**.

The simulated mechanical torque of the wind turbine, corresponding to the study case II.4 from (Snel and Schepers, editors, 1995), is shown in **Fig. 2.3**. The measured and the simulated curves are in very good agreement. The following shall be noticed. Oscillations in the measured torque of the wind turbine, shown in **Fig. 2.3**, are caused by oscillations in the wind turbine construction. Similar oscillations are seen in the simulated behaviour in **Fig. 2.3**. It is reached with use of the AEC of the turbine rotor described in **Section 2.4**.

2.1.3. Representation in voltage stability investigations

Influence of the unsteady inflow phenomena on the wind turbine behaviour is illustrated in **Fig. 2.4** by the simulated curves of the wind turbine controlled by pitch, respectively, by active-stall. The curves are modelled with use of model with unsteady inflow phenomena – the Øye model and with use of the C_P - λ - β -curves, e.g. at the considerations of equilibrium.

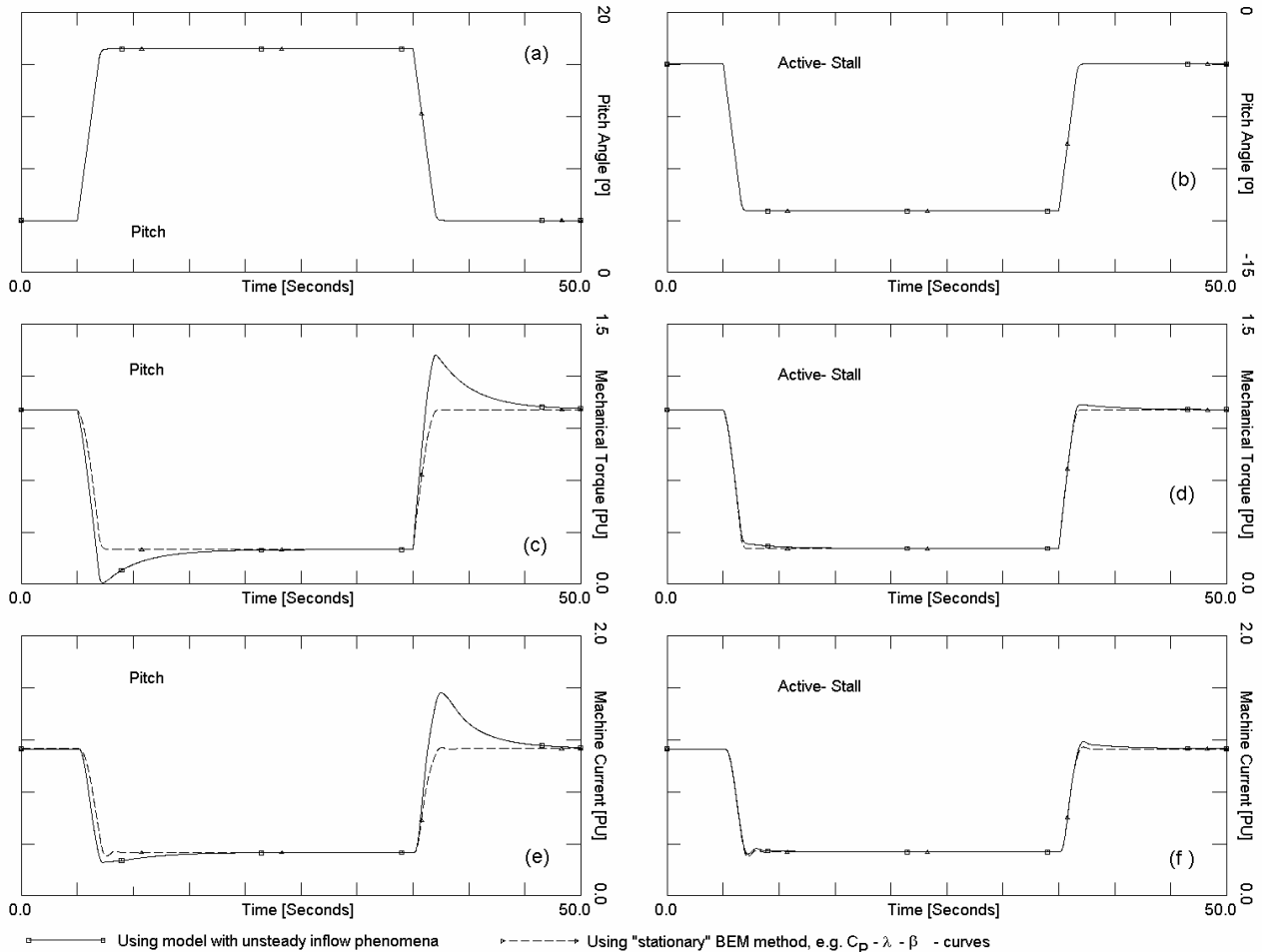


Fig. 2.4. Simulated curves using model with unsteady inflow phenomena versus model by BEM-method in case of pitch- and active-stall- controls: (a) and (b) – pitch angle in case of pitch with the maximal pitch rate of 8 °/s, respectively, active-stall with the maximal pitch rate of 5 °/s, (c) and (d) – mechanical torque of the turbine, (e) and (f) – the machine current as illustration of the consequences of the aerodynamic model chosen with respect to the electric values of the induction generator.

The model with unsteady inflow phenomena includes more computations than the model with use of the C_P - λ - β -curves. The simulating case shall give an indication (i) where the model with unsteady inflow phenomena shall be applied and (ii) where it is sufficiently to use the C_P - λ - β -curves. The simulating case is chosen according to the Danish specifications, e.g. with the power ramp. Here the wind turbine being initially at rated operation is ordered to the 20 % level of the

rated power and, after a while, returns to the rated operational point. The case is with the 2 MW wind turbine (equipped with an induction generator) with the rotor diameter of 61 m.

As can be seen, it is only a marginal difference between the behaviours modelled with unsteady inflow phenomena versus with the C_P - λ - β -curves at the active-stall control mode. This is because the blades are pitched across to the incoming wind. At this control mode the wind profile around the turbine rotor does not change significantly.

At pitch control mode, a significant discrepancy is seen due to the overshoot in the mechanical torque, T_M . This overshoot is caused by unsteady inflow phenomena. At the pitch control mode, the blades are pitched away from the incoming wind. This leads to a relatively significant change of the wind profile formed around the rotating turbine. Consequently, the unsteady inflow phenomena play a part. Presence of overshoots in the mechanical torque of the wind turbine rotor, T_M , at pitching is validated against measurements.

So far, the following can be resumed according to the complexity details of the aerodynamic model of wind turbines in investigations of transient voltage stability.

- 1) Aerodynamics of stall- and active-stall controlled wind turbines can always be modelled with use of the C_P - λ -curves and the C_P - λ - β -curves⁸, respectively. It is because pitching here does not produce any significant overshoot.
- 2) It will be preferred to represent the pitch-controlled wind turbines by the aerodynamic model with dynamic inflow phenomena. It is because of the overshoot in the mechanical torque at (relatively fast) pitching. The simplified model with the C_P - λ - β -curves does not produce such overshoots.
- 3) The behaviours shown in **Fig. 2.4** with the overshoots in the mechanical torque, T_M , at pitching are computed at the rated operational point, e.g. at the wind speed of 15 m/s, and for the wind turbine with the rotor diameter of 61 m. From the characteristic time constants of the transition process, it can be concluded that the overshoots will be ever stronger at a low wind speed and at larger diameters of the wind turbine rotors. Notify that the rotor diameters of modern wind turbines are approaching 90 m.
- 4) Pitch-controlled wind turbines can be represented by the models with the C_P - λ - β -curves in cases where accuracy of the mechanical torque computation is not critical for the results of the investigations.

Only at sufficiently slow pitching, the overshoots are almost eliminated and the wind turbine model with use of C_P - λ - β -curves can be applied in any cases without discussion. As seen in **Fig. 2.5**, this is at the pitch rates in the range of 2 °/s for the given wind turbine.

Why is it important to keep in mind the overshoots in the mechanical torque at pitching? It is because this indicates that the rate of the pitch control is restricted for reducing overshoots in the torque applied to the LS shaft of the wind turbine.

Secondly, the overshoot will be transferred to electrical and mechanical parameters of the wind turbine and its generator. In case of fixed-speed wind turbines equipped with induction generators,

⁸ Remember our assumption of stationary wind.

the overshoot in the mechanical torque, T_M , leads to a similar behaviour in the generator current, the electric power and the reactive consumption and also the terminal voltage. In case of variable-speed wind turbines, where operational point of the generator is controlled by the converter, the overshoot in the mechanical torque results in fluctuations of the rotational speed. This leads to excitation of torsional oscillations in the shaft system and so it affects the gearbox (in case of wind turbines equipped with doubly-fed induction generators).

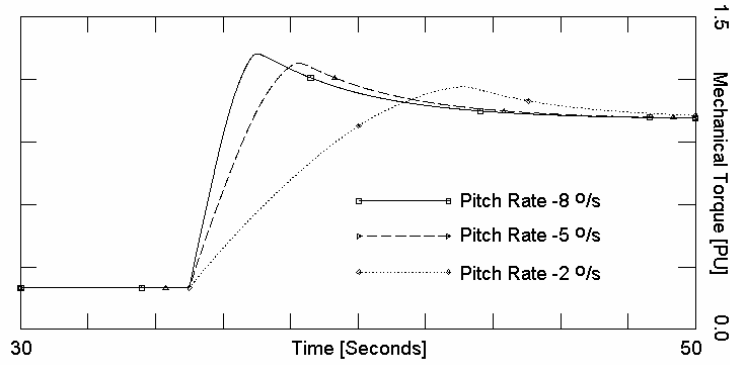


Fig. 2.5. Mechanical torque of the pitch-controlled wind turbine at ordered power increase from 20 % of the rated up to the rated power, simulated at different pitch rate limitations.

These restrictions of pitch control shall be kept in mind when the C_P - λ - β -curves are applied for representation of pitch-controlled wind turbines in any kind of investigations.

Similarly, there will be restrictions on the rate of active-stall control. However, such restrictions are caused by a stronger sensitivity of the mechanical torque, T_M , with respect to the blade-angle position, β .

2.2. Shaft system representation⁹

At the start of this industrial Ph.D. project, representation of the shaft system in the dynamic wind turbine model used in investigations of transient voltage stability was neglected. The mechanical construction of the wind turbines was simply modelled as a lumped-mass system with the lumped inertia constant of the turbine rotor and the generator rotor.

$$H_L = H_M + H_G, \quad (2.7)$$

where H_L denotes the lumped inertia constant and H_G and H_M are the inertia constant of the generator rotor, respectively, of the wind turbine rotor. The movement equation of the wind turbine applied in investigations of transient voltage stability was given by the lumped-mass model (Akhmatov et al., 2000(c)).

$$2H_L \frac{d\omega_L}{dt} = T_M - T_E - D_L \omega_L, \quad (2.8)$$

⁹ In this Section, the per unit system is applied, see **Appendix 4.A**.

where ω_L is the rotational speed of the lumped mechanical system and $\omega_L = \omega_G = \omega_M$, ω_G is the generator rotor speed. T_E denotes the electric torque of the (induction) generator and D_L is the damping of the lumped system.

One of significant results of this industrial Ph.D. project is demonstration of electromechanical interaction between the shaft systems of fixed-speed wind turbines¹⁰ and the electric power grid. This interaction plays a part in investigations of transient voltage stability. The electromechanical interaction is seen as torsional oscillations, primarily, in the shaft systems equipped with gearboxes. The electromechanical interaction is expressed by fluctuations of the voltage, the machine current, the generator rotor speed and other electrical and mechanical parameters of the (fixed-speed) wind turbines. The natural frequency of these fluctuations is equal to the shaft torsional mode.

For representation of electromechanical interaction in investigations of transient voltage stability, the movement equations are given by the two-mass model. The two-mass model represent the torsional twist, θ_s , about the axis Z_s , shown in **Fig. 2.1.b**. It is given by (Akhmatov et al, 2002(b)):

$$\begin{cases} 2H_M \frac{d\omega_M}{dt} = T_M - K_s \theta_s - D_M \omega_M , \\ 2H_G \frac{d\omega_G}{dt} = K_s \theta_s - T_E - D_G \omega_G , \\ \frac{d\theta_s}{dt} = \omega_0 (\omega_M - \omega_G) , \end{cases} \quad (2.9)$$

where K_s is the shaft stiffness, D_M and D_G are the damping coefficients of the turbine rotor and the generator rotor, respectively, and ω_0 denotes the electric system speed¹¹.

2.2.1. Identification of shaft system parameters

Possible torsional oscillations of a significant magnitude in the shaft systems of (fixed-speed) wind turbines have been indicated in earlier experiments (Pedersen et al, 2000). Pedersen et al (2000) have described the results of an experiment where the Danish wind farm at Rejsby Hede was in isolated operation (tripping of the wind farm from the entire power grid) during around one second. Later, the results of this experiment are used for evaluation of the shaft system parameters (Akhmatov et al, 2003(a)) and also for identification of the electromechanical interaction as well as for explanation of its nature (Pedersen et al, 2003).

In the following, it is demonstrated how the mechanical parameters of the shaft system can be evaluated from measurements of the electric frequency at isolated operation of the wind turbines.

¹⁰ The electromechanical interaction between the wind turbine shafts and the power grid with relation to transient voltage stability is firstly described in our work (Akhmatov and Knudsen, 1999) and (Akhmatov et al, 2000(a)). At that time, the fixed-speed wind turbines equipped with induction generators and the shaft systems with gearboxes were the dominating wind turbine concept.

¹¹ In some situations, also the shaft damping should be included in the shaft system equations. This damping represents basically thermal losses caused by torsion in the shaft material. Its value can be received from the wind turbine manufacturer.

This demonstration is from (Akhmatov et al, 2003(a)). The parameters of the shaft system, which are validated, are with relation to the two-mass model by **Eqs. (2.9)**. It is the turbine rotor inertia constant, H_M , the generator rotor inertia constant, H_G , and the shaft stiffness, K_S .

The Rejsby Hede wind farm consists of forty medium-sized, fixed-speed, stall-controlled wind turbines. The rated power of each wind turbine is 600 kW. The experiment was carried out when the wind speed was approx. 10 m/s and the wind farm was approx. 80% reactive compensated.

After tripping of the wind farm, the fluctuating behaviour of the electric frequency was observed. This fluctuating behaviour is shown in **Fig. 2.6**.

Analysis of the measured frequency curve is given by the following. Re-writing the lumped system movement equation (2.8) it is reached.

$$\omega_L \frac{d\omega_L}{dt} = \frac{P_M}{2(H_M + H_G)}, \quad (2.10)$$

where the electric torque, T_E , is zero at tripping.

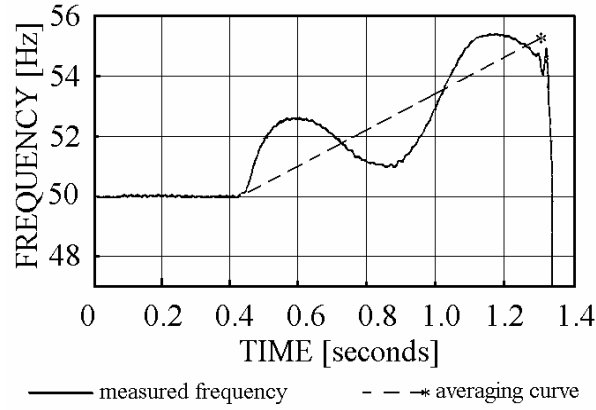


Fig. 2.6. Electric frequency of the Rejsby Hede wind farm measured at tripping experiment. Reported in (Pedersen. et al, 2000).

Integrating **Eq. (2.10)** from the time of tripping, $t = t_0$, and the speed $\omega_L(t_0) = 1 + s(t_0)$, where $s(t_0)$ is the initial generator rotor slip, to the time $t = t_0 + \Delta t$ and the speed $\omega_L(t_0) + \Delta\omega_L(t_0 + \Delta t)$, the increase in the lumped system speed is found.

$$\Delta\omega_L = \frac{\int_{t_0}^{t_0+\Delta t} P_M(\tau) d\tau}{2\omega_L(t_0) \cdot (H_M + H_G)}. \quad (2.11)$$

Applying **Eq. (2.11)**, the turbine rotor inertia constant is defined.

$$H_M = \frac{\int_{t_0}^{t_0+\Delta t} P_M(\tau) d\tau}{2 \cdot \omega_L(t_0) \cdot \Delta\omega_L} - H_G \approx \frac{1/2 \cdot (P_M(t_0) + P_M(t_0 + \Delta t)) \cdot \Delta t}{2 \cdot \Delta f} - H_G. \quad (2.12)$$

Here Δf is the change of the electric frequency, which is proportional to the change in the lumped speed, $\Delta\omega_L$. Increase of the mechanical power of the wind turbine during the isolated operation,

$P_M(t_0 + \Delta t) > P_M(t_0)$, is caused by coupling between the mechanical power, P_M , and the rotational speed, ω_M . It is estimated from the slope of the C_P - λ -curve of the given wind turbine.

The generator inertia constant is considered $H_G = 0.5$ s, according to (Akhmatov and Knudsen, 1999). From the average curve of the electric frequency shown in **Fig. 2.6**, the following parameters are set $\Delta t = 0.85$ s, $\Delta f = 0.1$ PU. The average mechanical power $\frac{1}{2} \cdot (P_M(t_0) + P_M(t_0 + \Delta t))$ is evaluated to 0.70 PU. Applying **Eq. (2.12)**, the turbine rotor inertia constant is found $H_M = 2.5$ s.

The oscillating behaviour of the electric frequency cannot be explained in terms of the lumped-mass model. Using the two-mass model, **Eqs. (2.9)**, the movement equation of the tripped wind turbine with respect to the shaft twist is derived.

$$\frac{d^2}{dt^2} \theta_s + \frac{\omega_0 K_s}{2} \cdot \frac{H_M + H_G}{H_M H_G} \cdot \theta_s = 0. \quad (2.13)$$

The oscillating behaviour of the electric frequency, $f(t)$, is treated as a homogenous solution of this movement equation. From **Eq. (2.13)** the shaft torsional mode, f_T , is found, according to:

$$\frac{d^2}{dt^2} \theta_s + (2\pi f_T)^2 \cdot \theta_s = 0. \quad (2.14)$$

The shaft stiffness, K_s , is defined with use of **Eqs. (2.13)** and **(2.14)**.

$$K_s = \frac{8\pi^2 f_T^2}{\omega_0} \cdot \frac{H_M H_G}{H_M + H_G}. \quad (2.15)$$

The period of the electric frequency oscillations is 0.6 s. The natural frequency is, therefore, $f_T = 1.7$ Hz. This is the shaft torsional mode (Pedersen et al., 2003). Applying **Eq. (2.15)** and the data of H_G , H_M and f_T , the shaft stiffness is found $K_s = 0.30$ PU/el.rad.

For validation, the tripping experiment is simulated in case of one wind turbine with the same parameters of the shaft system as found from the experiment. The simulating case is at the same operational conditions (10 m/s wind and 80% reactive compensated). The simulated behaviour of the electric frequency is shown in **Fig. 2.7**. The extrema of the measured and the simulated curves of the electric frequency are compared in **Table 2.1**. As can be seen, the measured and the simulated behaviours are in very good agreement.

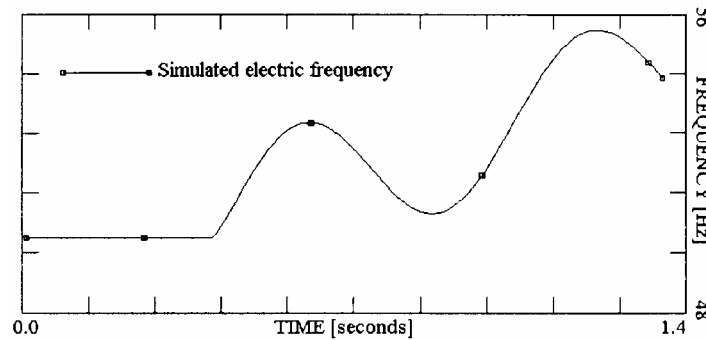


Fig. 2.7. Simulated behaviour of electric frequency at tripping experiment.

The results of the islanding experiment at the Rejsby Hede wind farm and its validation presented by Pedersen et al (2003) indicate that the effective shaft stiffness of the wind turbines can be significantly lower than the shaft stiffness of the conventional power plant units (Hinrichsen and Nolan, 1982). It explains why the wind turbine shafts are often denoted as soft shafts (Akhmatov et al, 2000(a)). For comparison, the stiff shafts of conventional power plant units are in the range of 30 to 50 PU/el.rad. (Hinrichsen and Nolan, 1982; Kundur, 1994).

Value	Measured	Simulated
First Maximum	53.0 Hz	53.0 Hz
First Minimum	51.0 Hz	50.6 Hz
Second Maximum	55.5 Hz	55.7 Hz
Period	0.6 s	0.6 s
Eigenfrequency	1.7 Hz	1.7 Hz

Table 2.1. Comparison between measured and simulated behaviours of electric frequency at tripping experiment.

Second, the inertia constant of the turbine rotor, which consists of three large and heavy blades, is only around few seconds. These results are important with respect to the electromechanical interaction between (fixed-speed) wind turbines and electric power grids.

2.2.2. Explanation of soft coupling

In terms of the two-mass model, **Eqs. (2.9)**, the wind turbine is treated as a complex electromechanical system. Here the turbine rotor and the generator rotor are coupled through the shaft system. The two-mass model is characterised by presence of the two rotating masses. The first rotating mass is for the turbine rotor and the second one is the generator rotor.

The two-mass model indicates also that the shaft system of the wind turbine shall be understood as the two-speed system. It is because of the significant difference between the mechanical speed of the turbine rotor and the electric system speed. The turbine rotor speed, ω_M , can be in the range of up to 25 rev./min.¹² The electric system speed at the generator terminals, ω_0 , is fixed to the rated electric frequency and 3000 rev./min.¹³

The exception can only be in case of the generators connected to the power grid through the full-load frequency converters. In this case, the electric system speed is given by the electric frequency generated by the voltage-source converter at rated operation.

Conveniently, the movement equations of the two-mass model **(2.9)** are written with respect to one rotational speed reference. This implies that all the parameters applied in the movement equations are derived with respect to the chosen speed reference. It is kept in mind that the shaft system modelled by **Eqs. (2.9)** shall be applied as a part of the wind turbine model for investigations of transient voltage stability and coupled with the (standardised) models of

¹² In case of modern, medium-sized wind turbines with the rated power around 1 MW. Larger wind turbines have slower turbine rotors, as usual.

¹³ This value is commonly given as the rated electric frequency that is 50 Hz in Europe.

generators. This is why it is natural to transform the mechanical parameters of the shaft system to the units with respect to the electric system speed (Akhmatov et al, 2000(a)). The meaning of this transformation is termed by Hinrichsen and Nolan (1982) as the shaft system parameters viewed from the generator terminals. It can simply be understood as a transformation between mechanical and electrical radians. In other words, all the mechanical parameters applied in the movement equations are computed with respect to the electrical radians.

The shaft system of the wind turbine is with the gearbox with the gear ratio N_{ME} . The (induction) generator of the wind turbine is with a (less) number of pole-pairs N_{EE} . The transformation of the parameters from the mechanical to the electrical values leads to that the inertia constant of the turbine rotor, H_M , and the shaft stiffness, K_S , are reduced by the ratio $(N_{ME}N_{EE})^2$, according to (Akhmatov et al, 2000(a)). The inertia constant of the generator rotor, H_G , is reduced by the ratio $(N_{EE})^2$.

In other words, a significant difference between the rotational speed of the turbine rotor and the electric system speed, when measured in SI-units, causes the dynamic behaviour indicating the soft coupling between the turbine rotors and the generator rotors – the so-called soft shafts of wind turbines. The dynamic behaviour of the electric parameters of the generators applied in wind turbines relating to the soft shafts is registered in measurements. Notify that the dynamic behaviour, which characterises the torsional oscillations of the soft shafts, is firstly observed in case of and relates mostly to the fixed-speed wind turbines where the shaft systems are with gearboxes (Pedersen et al, 2003). It is because the gear ratio of these wind turbines, N_{ME} , is sufficiently large.

However, a similar oscillating behaviour can also be registered in case of (variable-speed) wind turbines equipped with direct-driven multipole generators. Such oscillations are reported by Westlake et al (1996). Excitation of the torsional oscillations in the shaft, which transform to electric parameter fluctuations of notable magnitudes, is due to sufficiently many pole-pairs, N_{EE} , of the generator. In the investigations reported by Westlake et al (1996), the direct-driven synchronous generator was with 83 pole-pairs.

2.2.3. Application area of two-mass model

Compared to the lumped-mass model, the two-mass model is with a more complex representation of the shaft system and requires more data. It is necessary to evaluate where the two-mass model must be applied in investigations of transient voltage stability and where the lumped-mass model still can be used.

The torsional oscillations of the soft shafts relate to internal swings in the mechanical constructions of wind turbines. Such oscillations can rather be a responsibility area of the wind turbine manufacturers than of the transmission system operators. Since the shaft representation by the two-mass model is applied as a part of the dynamic wind turbine in investigations of transient voltage stability, this is caused by significant interaction between the shaft torsional oscillations and the electric parameters of the wind turbine generator and the power grid (Akhmatov et al, 2000(b)).

This interaction is not certain in case of any wind turbine concepts, but corresponds to a major group of wind turbines. In the majority of situations, the shaft systems shall be represented by the

two-mass model. There will also be fewer situations where the shaft systems can be represented by the lumped-mass model.

2.2.3.1. Fixed-speed wind turbines

In case of fixed-speed wind turbines equipped with induction generators, it is a strong coupling between the generator rotor speed and the electric parameters of the induction generators (Knudsen and Akhmatov, 1999). Oscillations in the shaft system excited by the grid disturbances will lead to fluctuations of the generator rotor speed and also to fluctuations of the electric parameters of the induction generators (Akhmatov et al, 2000(b)). As explained in (Akhmatov et al, 2000(b)), the phenomenon of accumulating and designating of the potential energy in the twisted wind turbine shafts is extremely important.

At normal operation, the wind turbine shafts are pre-twisted and accumulate an amount of the potential energy, W_s .

$$W_s = \frac{1}{2} K_s \theta_s^2 = \frac{1}{2} K_s \left(\frac{T_M}{K_s} \right)^2 = \frac{1}{2} \frac{T_M^2}{K_s}, \quad (2.16)$$

where the value of the twist, θ_s , is given at normal operation, e.g. the initial value. At a short circuit fault, the voltage, V_s , and so the electric torque, T_E , are reduced. Therefore, the pre-twisted shafts start relaxation, e.g. decreasing of the shaft twist. At relaxation, the potential energy of the shaft is transferred to the kinetic energy of the generator rotor. This results in ever more acceleration of the generator rotor (Akhmatov et al, 2000(b)). More acceleration of the induction generators will lead to more reactive absorption and slower voltage recovery after the fault.

The induction generators are characterised by a strong coupling between the generator rotor slip and the electric and the reactive power of the generators. Oscillations of the generator rotor slip will cause fluctuations of the electric power. The natural frequency of the electric and the reactive power fluctuations is the torsional shaft mode (Hinrichsen and Nolan, 1982; Akhmatov et al, 2000(a)). Therefore, the fluctuations of the voltage with the same natural frequency will also be seen (Akhmatov and Knudsen, 1999). In other words, (i) the voltage fluctuations and (ii) its slower recovery after the grid fault are the outcome of the transient mechanical behaviour of the twisted shafts of wind turbines equipped with induction generators.

By this argumentation, the shaft systems of fixed-speed wind turbines shall be represented by the two-mass model in situations where the shaft stiffness is sufficiently low. The stiffness of the shaft system depends, however, of several factors. Those are the material, the thickness and the length of the shaft as well as the gear ratio, $N_{ME} \cdot N_{EE}$, (Akhmatov and Knudsen, 1999). Different wind turbines from different wind turbine manufacturers will be characterised by the shaft systems of different stiffness. The term “sufficiently low” implies that the decision about use of the two-mass model relates to the value of the shaft stiffness and so to the potential energy accumulated in the shaft system.

If the shaft systems of the wind turbines are sufficiently stiff, ideally at $K_s \rightarrow \infty$, the lumped-mass model will be used. It becomes obvious because the potential energy accumulated in the shafts is reciprocal of the shaft stiffness. The ideally stiff shafts do not accumulate potential energy

because they cannot twist. Second, the lumped-mass model by **Eqs. (2.8)** can be reached from the two-mass model by **Eqs. (2.9)** by inserting of $K_S \rightarrow \infty$ (Akhmatov et al, 2003(a)).

Akhmatov and Knudsen (2002) reported that already in case of the shaft stiffness $K_S = 3.0$ PU/el.rad. there are neither significant fluctuations in the generator rotor speed nor the voltage. The shaft torsional oscillations are seen as ripples of very small magnitude in the voltage behaviour. This behaviour does not influence on transient voltage stability. It can be suggested that the value of $K_S = 3.0$ PU/el.rad. is the boundary, defined by experience, for use of the two-mass model.

Resuming this discussion, the two-mass model shall be applied in case of fixed-speed wind turbines equipped with induction generators because of a strong coupling between the mechanical and the electrical parameters of the induction generators. However, when the shaft stiffness is around or above 3.0 PU/el.rad, the lumped-mass model can be applied.

In the majority of situations, the shaft coupling is soft, which is why use of the two-mass model is common for representation of fixed-speed wind turbines in investigations of transient voltage stability. The subject on the shaft modelling and conditions of acceleration of the induction generators at the grid faults will be discussed in **Sections 4–6**.

2.2.3.2. Variable-speed wind turbines

Variable-speed wind turbines are equipped with generators controlled by the converters. The converter control is organised with independent control of the electric and the reactive power (Yamamoto and Motoyoshi, 1991). The soft shafts can still be present in the wind turbine construction and cause (i) more acceleration of the generator rotors and (ii) oscillations of the generator rotor speed.

Independent control of the electric and the reactive power by the converters implies, however, that the fluctuating behaviour of the generator rotor speed and the dynamic behaviour of the voltage are de-coupled. Ever significant fluctuations of the generator rotor speed have no significant influence on the voltage behaviour (Akhmatov, 2002(b)). This implies that presence of the soft shafts of variable-speed wind turbines has no relation to maintaining of transient voltage stability at the grid faults. This argumentation is common to use the lumped-mass model by **Eqs. (2.8)** for representation of the shaft systems of variable-speed wind turbines in voltage stability investigations.

Use of the two-mass model for the shaft system representation can, however, be an advantage, because of a possible risk of excitation of the (soft) shaft systems of variable-speed wind turbines. This excitation can be started by the grid disturbances (Akhmatov, 2002(b)). When the torsional oscillations of the shaft systems are insufficiently damped (by the control systems), the wind turbines can be disconnected and stopped. This outcome relates not only to internal oscillations of the wind turbine construction, but also to results of voltage stability investigations. It is because incorporation of immediate power reserves will be demanded by the power system controllers in case of sudden disconnection risk of many wind turbines.

Furthermore, use of the two-mass model of the soft shafts of variable-speed wind turbines can be suggested according to the following argumentation. The electric power fluctuations of variable-

speed wind turbines will follow the oscillations of the generator rotor speed (Akhmatov, 2002(b)). The natural frequency of these fluctuations is the shaft torsional mode.

$$f_T = \frac{1}{2\pi} \sqrt{\frac{\omega_0 K_s (H_M + H_G)}{2H_M H_G}}. \quad (2.17)$$

Normally it is in the range of one to few Hz. It is relatively close to the natural frequencies of large power plants with synchronous generators. It is thinkable that there can be a risk of mutual oscillations between the large power plants and the wind farms with variable-speed wind turbines, if damping of the wind turbines or the power plants is insufficient. Presently, no information confirming or rejecting this statement is found in literature.

When the converter is applied to damp such shaft oscillations (Akhmatov, 2002(b)), this is by sending a signal to increase the power at increasing generator rotor speed and to reduce the power at reducing speed. This is achieved by controlling the rotor current. Then, the rotor current follows the behaviour of the generator rotor speed in this control mode. Excessive speed fluctuations may cause excessive rotor current reaching the trip limit of the converter.

The concerns about the shaft torsional oscillations are relevant when the shaft stiffness is sufficiently low. The two-mass model shall be applied in case of relatively soft shafts. In case of stiff shafts, with the shaft stiffness around or above 3.0 PU/el.rad., the lumped-mass model will be preferred in investigations of transient voltage stability. This is by the same argumentation as in case of fixed-speed wind turbines.

In case of wind turbines equipped with DFIG, the shaft systems are with gearboxes with a large gear ratio, as usual. It is because the stators of the DFIG are connected to the power grid, which demands a transformation from a low speed of the turbine rotor to the electric grid frequency (50 Hz in Europe) at the stator terminals of the DFIG. The shaft systems of this wind turbine concept are sufficiently soft (Akhmatov, 2002(b)) and shall be represented by the two-mass model. Modelling details of wind turbines equipped with DFIG are in **Sections 10.2.2** and **11.4.2.3**.

In case of wind turbines equipped with multi-pole generators connected to the power grid through the frequency converters, there is no certain answer. Use of the shaft model will depend on a number of factors including the number of pole-pairs of the generator, as explained in **Section 9.2**.

2.3. Neglecting of tower representation

Periodic oscillations of the towers of fixed-speed wind turbines are reported by Thiringer and Dahlberg (2001) from measurements of flicker. This result indicates a coupling between the side-wise tower oscillations and the induction generator slip. Oscillations of the tower, illustrated in **Fig. 2.1.c**, can be excited by the following mechanisms.

- 1) By dynamic variations of aerodynamic forces, for instance, variations of the thrust, T . These forces act along the axis y_T . It is obvious that the oscillations along the axis y_T cannot produce fluctuations of the generator rotor speed or of the electric parameters of the generator.

- 2) By the forces coming from the moment difference and acting along the axis x_T . These oscillations introduce a displacement of the generator rotor angle with respect to the stator position. Therefore these side-wise oscillations may influence on the generator speed.
- 3) It is kept in mind that the tower bending may occur by such a way that the aerodynamic forces may cause the tower bending along the both axis x_T and y_T (Thomsen, 2002).

At normal operation, the moment difference mentioned in item 2 is the following.

$$\Delta T = T_M - T_{HS} = (N_{ME} - 1)T_{HS}, \quad T_{HS} = N_{EE}T_E, \quad (2.18)$$

where T_{HS} is the mechanical torque applied to the high-speed shaft (HS). This moment difference contributes to the side-wise tower bending along the axis x_T . As can be seen, the tower oscillations along the axis x_T can be excited by the fluctuations of the wind turbine torque, T_M , as well as by transient behaviour of the electric torque, T_E , at the grid faults.

Generally, the tower oscillations can be computed using the AEC. In such computations, the tower is represented as a beam (Chaviaropoulos, 1996). Using the well-known relations of the beam theory (Gere and Timoshenko, 1997), the elastic oscillations of the wind turbine tower can be computed. The tower oscillations are commonly neglected in the wind turbine model applied in investigations of transient voltage stability. This neglecting is by the following argumentation.

- 1) The main target of this work is voltage stability investigations. The tower oscillations do not influence on maintaining of transient voltage stability.
- 2) The magnitude of the tower oscillations is relatively small. In (Thomsen, 2002) it is observed that side-wise tower oscillations can be around few cm for the 60 m tower. Possible influence of the tower oscillations on the generator speed deviation is considered insignificant. See also next item for more details.
- 3) The tower stiffness, K_T , is large. In the quantities of the electric system speed its value shall only be reduced by the number of pole-pairs squared, which is $(N_{EE})^2$. When the number of the pole-pairs, N_{EE} , is much smaller than the ratio of the gearbox, N_{ME} , then the shaft stiffness, K_S , will be much smaller than the tower stiffness, K_T . Therefore, the potential energy accumulated

in the tower, $W_T = \frac{1}{2} \frac{\Delta T^2}{K_T} \approx \frac{1}{2} \frac{T_M^2}{K_T}$, is significantly smaller than the potential energy accumulated in the pre-twisted shaft W_S . This implies that the most significant contribution to more acceleration of the (induction) generator rotor comes from the shaft relaxation rather than from the tower relaxation at the grid faults. It is why the tower oscillations have no significant influence on the generator speed deviation¹⁴.

¹⁴ Discussion: notice that this argumentation is for the fixed-speed wind turbines equipped with induction generators. In this concept the gear ratio of the shaft is significantly larger than the number of the pole-pairs of the induction generator. In case of the wind turbine concept with direct-driven multi-pole generators, e.g. no gearboxes, this argumentation is not certain. Also in this case, the towers can be considered stiff in investigations of transient voltage stability because their influence on the generator rotor speed is insufficient. The tower oscillations can be damped by well-tuned converters of the multi-pole generators. This discussion relates rather to design of wind turbines than to investigations of transient voltage stability. Tuning of the converters is responsibility of the wind turbine manufacturer.

Formally, representation of any tower oscillations excited by the electric torque will result in disagreement with the (standardised) generator models derived under assumption of the stood-still stator. The standardised models of the induction and the synchronous generators are derived with use of the Park transformation. In terms of the Park transformation, the phase quantities such as the three-phased voltages, the three-phased currents and the three-phased fluxes are transformed into their respective phasors in the (D,Q) -quantities. The three-phased voltage will be, for instance, given by its phasor (the vector) with a magnitude and a phase angle. The basic consideration of the Park transformation is that the stator is stationary, while the rotor rotates. The consideration of the stationary stators is very common. Ever it is not always mentioned in literature on theory of electric machinery.

This consideration has a sense from a historical point of view. It is because the electric machines applied in large power plants and in factories are fixed to ground. When considering the electricity-producing wind turbines, the generators are placed on tops of slightly oscillating towers and so the generator stators move with the tower tops. It implies that the consideration of the stationary stators is broken and the transformation shall be revised.

Minus friction in the rotating parts and the electric losses in the generator windings, all the power from the rotating rotor is transferred to the electric power and supplied from the stationary stator mains to the grid. This is expressed by the power balance equation $2H_G(d\omega_G/dt) = (P_M - P_E - \text{losses})/\omega_G$ and fulfilled in case of stationary stators. If the stator moves, when following the tower oscillations, then the extra contribution from this movement shall be added to the power balance equation.

The (D,Q) -reference frame of the transformation is commonly used according to the following. The D -axis follows the rotor angular position and the Q -axis is displaced by $\pi/2$ with respect to the D -axis. The angle of the transformation, θ , is the angle between the rotating D -axis and the selected phase in the stationary stator. When the tower moves along x_T -axis, this leads to a change of the angular position of the stator and corresponds to a displacement of the angle of the transformation, θ . This implies that the transformation matrix, where the angle θ is applied, shall be revised. The angle of transformation, θ , is in el.rad. A transformation between mechanical and electrical values will be required for the angle θ (the number of pole pairs, N_{EE}).

The standardised Park transformation will be replaced by a revised transformation with an oscillating stator angular position. It is reflected in the value of the angle of transformation, and, further, with respect to the power balance. This revision will give a coupling between the generator (electrical) and the tower (mechanical) dynamic behaviours at the grid disturbances. When this coupling is absent in the model, further computations with oscillating towers seem to be inaccurate.

It will be more convenient to neglect possible tower oscillations excited at the grid faults rather than develop a revised transformation of the generator equations. This neglecting is fair because possible interaction between the wind turbine towers and the power grids does not influence on maintaining of transient voltage stability. This subject can be, however, of interest for the wind turbine manufacturers and design of the control systems of wind turbines. It is why this detailed discussion is given in here.

This topic has been described in (Akhmatov, 2003(d)).

2.4. AEC of wind turbine rotor

When treating the wind turbine rotor as a self-bearing construction, the model in terms of AEC shall be applied. This can be reached by adding the description of the elastic deformations of the wind turbine blades to the aerodynamic model with unsteady inflow phenomena. The wind turbine blades are subjected to severe forces. These forces are gravity, aerodynamic forces and inertial forces (Younsi et al., 2001; Hansen, 2000). It causes deformations and dynamic oscillations of the blades when forces and loads vary dynamically.

In this Section it is discussed what oscillations of the blades can be excited by the grid disturbances and how to represent these oscillations in the wind turbine model. The gravity results in the periodic deformations of the blades. The contribution from the wind turbulence to the thrust results in stochastic oscillations (Hansen, 2000). Such contributions will always be seen in the dynamic behaviours of the blades, at normal operation of the power grid as well as at the grid faults. This is why such contributions are excluded from this description.

The difference of the blade behaviour between at normal operation of the power grid and at the grid faults will be seen from the contributions of the aerodynamic forces, F_N and F_T , and from the inertial forces. This is why these contributions must be included in the AEC to be used in investigations dealing with the grid faults. The deformations of the wind turbine blades caused by the forces applied onto the blades are computed using the well-known relations of the beam theory (Gere and Timoshenko, 1997; Hansen and Bindner, 1999).

It is, however, kept in mind that bending about one of the rectangular axes, for instance bending about the axis x_1 , will lead to bending about the other axis, in this example about the axis y_1 (Hansen, 2000). To eliminate this difficulty, it is necessary to introduce the rectangular system of the principal axes (x_2, y_2) in each blade section. The first principal axis, x_2 , is displaced from the axis x_1 by the angle ν . The angle ν is dependent on the local blade radius, r , e.g. it varies through the blade length (Hansen, 2000). The principal axes are defined so that bending about one of the principal axis, (e.g. bending about the first principal axis x_2) leads to that the beam only bends about this axis, but not about the other principal axis (in this case about the second principal axis y_2). The principal axes are shown in **Fig. 2.1.e** and all the computations of deformations are treated in the principal axes.

By projecting of the aerodynamic forces, F_N and F_T , onto the principal axes (x_2, y_2) for each blade section and with use of the beam theory, the deflections w_X and w_Y along the principal axes x_2 , respectively, y_2 are found. Acting of the aerodynamic forces results in that the blades of the rotating wind turbine are bend behind the plane of rotation (x_1, z) and forward with the direction of the rotation, $-x_1$. This is illustrated in **Fig. 2.1.a**.

The numerical result, with respect to the computed deflections w_X and w_Y , is not accurate yet. It is because the blades are also subjected to the inertial forces (Younsi et al., 2001). First, the effect of the centrifugal force, F_Z , onto the deflected blade must be included. The centrifugal force acting

along the span-wise axis z is computed as $F_Z = \int_z^R dF_Z = \int_z^R r \omega_M^2 m(r) dr$ where $m(r)$ denotes the mass

distribution along the blade radius (Hansen, 2000). When projecting the centrifugal forces onto the

principal axes (x_2, y_2) , it is seen that these forces reduce the deflections w_X and w_Y along the respective axes x_2 and y_2 . It is shown in **Fig. 2.1.f**.

Second, the inertial force $dF = r \frac{d\omega_M}{dt} m(r) dr$, acting at acceleration or deceleration of the rotating wind turbine, is taken into account. This force is acting along the axis x_1 , (equal to zero in stationary operation, e.g. with ω_M is constant) and projected onto the principal axes, analogously to the description above.

At changing operational conditions, for instance when the blade angle is changed to another position, the forces and the deflections will undergo dynamic changes as well. This process is described by the systems of swing equations (Younsi et al, 2001; Ekelund, 1998, Johansen, 1999), which are set up for each blade section of the thickness dr at the radius r .

$$\begin{cases} M(r) \cdot \frac{d^2 w_X(t)}{dt^2} + C_X(r) \cdot \frac{dw_X(t)}{dt} + K_X(r) \cdot w_X(t) = \sum F_X \left(t, w_X, w_Y, \frac{dw_X}{dt}, \frac{dw_Y}{dt} \right) \\ M(r) \cdot \frac{d^2 w_Y(t)}{dt^2} + C_Y(r) \cdot \frac{dw_Y(t)}{dt} + K_Y(r) \cdot w_Y(t) = \sum F_Y \left(t, w_X, w_Y, \frac{dw_X}{dt}, \frac{dw_Y}{dt} \right) \end{cases} \quad (2.19)$$

Here the mass of the blade section of the thickness dr is $M(r) = \int_{r1}^{r2} m(r) \cdot dr$. The damping coefficients of the blade section are $C_X(r)$ and $C_Y(r)$ in the respective directions x_2 and y_2 . Those are set to zero in this investigation. The stiffness coefficients of the blade section are $K_X(r)$ and $K_Y(r)$ in the respective directions x_2 and y_2 . The forces applied onto the blade section and projected onto the principal axis x_2 and y_2 are denoted as the sums of F_X and F_Y . These forces are (i) the aerodynamic forces, F_N and F_T , and (ii) the inertial forces in projections on the respective (x_2, y_2) -axes.

The time derivatives of the blade deflections $\frac{dw_X}{dt}$ and $\frac{dw_Y}{dt}$ are projected onto the axes x_1 and y_1 and, then, added to the rotational velocity and to the axial velocity, respectively, which are the respective components of the relative velocity, $V_{REL}(r)$. This operation introduces the feed-back by the disturbed wind field. It is applied to calculate the forces acting on the blades, the thrust, T , and the mechanical torque, T_M . This operation is taken into account when interpreting **Eqs. (2.1) –(2.4)** in terms of the AEC.

Notice that the wind turbine blades experience torsion as well. The twist of the blades can be computed by similar technique, but it is omitted in this case. It is because the blades of the given wind turbine (and also in general) are much stiffer with respect to torsion than with respect to deflection.

The wind turbine model by the AEC is only used in few simulating cases with investigations of possible risk of the mechanical construction excitation of grid-connected wind turbines at the grid faults. These investigations relate to the control feature with the ordered power ramp, described in **Section 6.12**. Simulation examples are included in **Appendix 2.A**.

2.5. Short resume

Although complexity of the mechanical construction of electricity-producing wind turbine, only the shaft representation plays a part in investigations of transient voltage stability. Here, the shaft system shall be given with the two-mass model, **Eqs. (2.9)**, when the shaft stiffness is below 3.0 PU/el.rad. Otherwise, the shaft system representation can be neglected and the inertias of the turbine rotor and the generator rotor are lumped together – the lumped-mass model, **Eq. (2.8)**.

Aerodynamics of the rotor is modelled with use of C_P - λ - β curves, **Eq. (2.6)**. It is except of situations where the overshoots in the mechanical torque are significant (fast pitching) for the target of investigations.

When the size of modern wind turbines increases drastically, it can be expected that more kinds of mechanical modes may affect the behaviours of electrical parameters and possibly the transient voltage stability (Akhmatov, 2003(d)). Here, a possible candidate can be interaction between the wind turbine blades and the power system (low-frequency oscillations). Also, the overshoots in the mechanical torque at fast pitching become stronger-represented at increasing length of the wind turbine blades.

3. Generic blade-angle control

In short, purpose of the blade-angle control can be explained by the following.

- 1) Optimisation of the power output of the wind turbines. The target is to produce so much electric power as possible at the given wind. This feature is, however, used at light wind, e.g. at the wind speed below the rated wind.
- 2) Preventing the mechanical power to exceed the rated power at strong wind, e.g. at the wind speed above the rated wind. This feature relates to restriction of the mechanical power by the rated power produced by the wind turbine. It also serves protection of the mechanical construction of the wind turbine against overloads and risks of damages, when reducing the thrust, T , at strong wind (Hansen, 2000; Akhmatov, 2002(a)).

Items 1 and 2 relate to application of wind turbines in relatively small sites and undisturbed operation of power grids. The large offshore wind farms to be constructed in Denmark and connected to the transmission power networks are assigned to the Danish specifications (Eltra, 2000). According to these specifications (Eltra, 2000), the large wind farms shall be able to reduce their power production to the level below 20 % from any arbitrary operational point in less than 2 s. This controllability is thought to control electric power supply from the wind farm and prevent against possible over-generation in situations with strong wind and low consumption. It can be reached using the blade angle control.

The blade angle control can also be used for stabilisation of the large wind farms at grid faults. Therefore this control principle shall be taken into account in investigations of transient voltage stability and represented in the dynamic wind turbine model.

The blade angle control of wind turbines can be organised by two different ways.

- 1) Pitch-control where the mechanical power, P_M , is reduced when the global pitch angle, β , increases. This principle is mostly applied in variable-speed wind turbines. Fixed-speed wind turbines can also be equipped with pitch control as well, but not commonly.
- 2) Active-stall-control where the mechanical power, P_M , is reduced when the global pitch angle, β , decreases. This control principle is commonly applied in fixed-speed wind turbines.

In the pitch-controlled wind turbines, the angle of attack, α , decreases when the global pitch angle increases. As seen in **Fig. 2.1.d**, the blade nose is moved against the incoming wind, V , at increasing pitch β . This is why the lift force, L , decreases as well. This mechanism explains reduction of the mechanical power of the wind turbine.

In case of active-stall control, the angle of attack, α , increases at decreasing pitch, β . The blade section is moved across the incoming wind, V , as can be seen in **Fig. 2.1.d**. The stall occurs, reducing the lift force, L , and the drag force, D , increases, which leads to reduction of the produced mechanical power, P_M .

The model contains initialisation and dynamic simulation of the blade angle control system. Under initialisation, the initial value of the blade angle, β , and its reference, β_{REF} , are found. As

seen from the general description of the idea of the blade angle control, the initial blade angle at light wind is the optimised value, β_{OPT} . The optimised value, β_{OPT} , can be defined using the BEM method from the incoming wind, V . It is reached by the optimisation algorithm of the power gain of the wind turbine, P_M , in the range of wind speeds below than the rated wind. This is, however, not the target of this work to discuss the power optimisation in details. It is mentioned that this optimisation leads to improving of the power gain in the range of very few percents. The optimisation is available at light wind and the optimised pitch angle, β_{OPT} , is in the range of very few degrees around zero¹⁵.

Information about exact value of the initial optimised blade angle does not seem to be important for investigations of transient voltage stability. It is because the investigations are, as usual, executed under the consideration of the rated operational conditions, e.g. at strong wind. In generic modelling (Akhmatov, 2002(a)), it is agreed to set β_{OPT} to zero in the range of wind speeds below the rated. This gives the initial value of the blade angle, β , and the initial reference blade angle, β_{REF} , at light wind.

The initial blade angle, β , and its reference, β_{REF} , at rated operational point, e.g. at strong wind, can be found with use of the BEM method. It is by the algorithm applied for maintaining of the rated power-supply (the rated electric power with inclusion of losses in the generator and the shaft system). The curves of the initial blade angle versus the incoming wind are given in **Fig. 3.1**. The curves are computed with the BEM method for the given 2 MW wind turbine. The values of β at strong wind are, obviously, not optimised values. The mechanical power versus wind curves are given in the same figure.

The (dynamic) control system of the blade angle control is organised by a generic scheme where the blade angle position, β , is controlled by the value X . The generic control scheme in case of pitch control with additional comments for active-stall control is given in **Fig. 3.2**. The controlling value, X , can be:

- 1) An electric value. For instance, the electric power, P_E , as described in (Hinrichsen, 1984; Akhmatov, 2001).
- 2) A mechanical value. For instance, the generator rotor speed, ω_G , as described in (Akhmatov, 2002(a); Akhmatov et al, 2003(a)).
- 3) A combination of electrical and mechanical values, according to (Akhmatov et al, 2003(a)).

The controlling value, X , is compared to its reference, X_{REF} . The error signal, X_{ERR} , is then sent to the proportional-differential (PD) controller that is optional and applied for a better sensitivity, and, then, to the proportional-integral (PI) controller producing the reference value of the pitch angle, β_{REF} . This is termed the regular control system and applied at normal operation (Akhmatov, 2001).

¹⁵ This subject will be illustrated by an example in case of variable-speed wind turbines in **Section 8.2**.

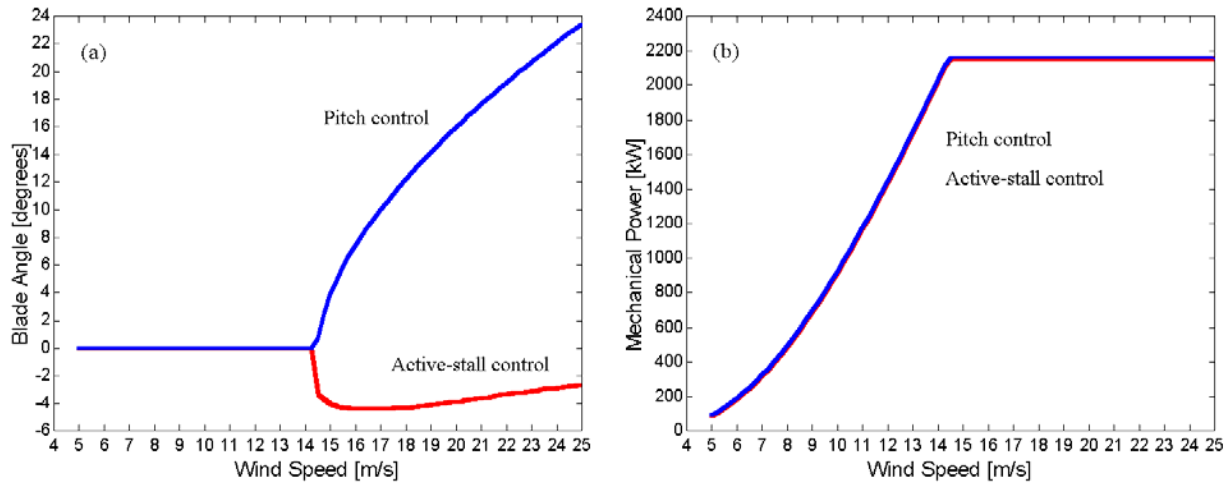


Fig. 3.1. Curves computed by BEM-method¹⁶ using assumptions of the generic blade angle control: (a) – stationary blade angle versus wind in pitch and active-stall modes, (b) – mechanical power versus wind in pitch and active-stall modes, identical in terms of the generic model. Note that the mechanical power is kept at the rated value by the blade angle control in strong wind.

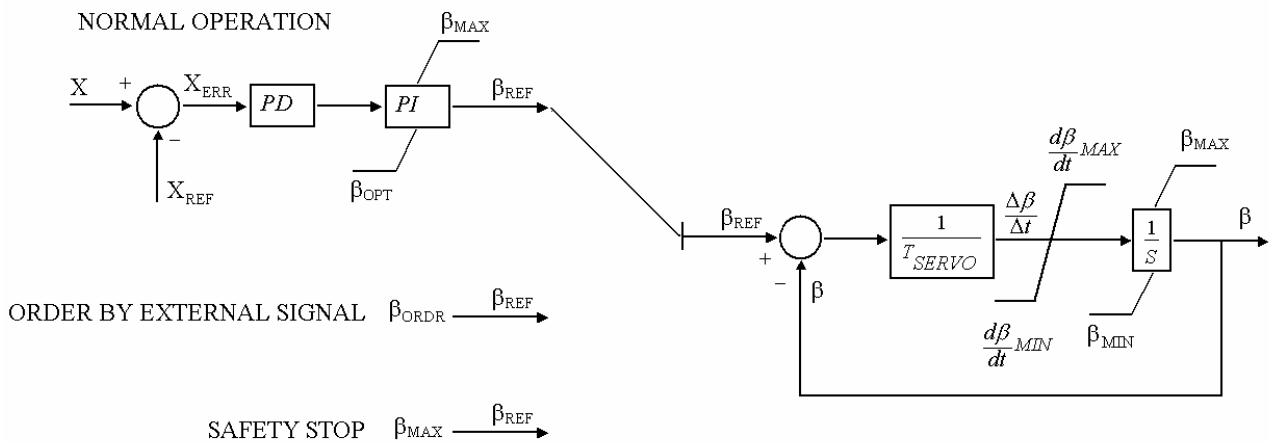


Fig. 3.2. Generic control scheme of the blade angle control – case of the pitch angle control. Active-stall control will be achieved by change of the upper limit of the PI-controller to β_{OPT} , the lower limit of the PI-controller to β_{MIN} and the reference value at the safety stop mode to β_{MIN} .

The reference value, β_{REF} , is in the range depending on the control mode.

- 1) It is between the optimised value, β_{OPT} , and the maximal pitch value, $\beta_{MAX} = 90^\circ$, in case of pitch-controlled wind turbines.
- 2) It is between the minimal value, β_{MIN} , and the optimised value, β_{OPT} , in case of active-stall control.

¹⁶ For illustration, the both control modes are computed for the same 2 MW fixed-speed, pitch-controlled wind turbine. The wind turbine data are found in (Snel and Schepers, editors, 1995).

The restrictions on the reference value, β_{REF} , shall be kept in mind.

- 1) In case of pitch-controlled wind turbines, the (dynamic) reference value, β_{REF} , may not be below the optimised value, β_{OPT} . Otherwise, there is a risk that the control system goes to the active-stall control domain.
- 2) In case of active-stall control, the (dynamic) reference value, β_{REF} , may not increase the optimised value, β_{OPT} . Otherwise, there is a risk that the control system will go to the pitch control domain.

When modelling the variable-pitch wind turbines in small sites, the description of the regular control system is sufficient. For representation of large offshore wind farms assigned to the Danish specifications (Eltra, 2000), the generic model of the blade angle control is extended with the feature of the power ramp. The power ramp implies the power reduction of the wind farm by the order from the external system.

When the order to reduce the power production is given, the regular control system is disabled. The reference value is then set to the value $\beta_{REF} = \beta_{ORDR}$, which corresponds to the level of the power production ordered by the external system. It can be the level of 20 % of the rated power, according to the Danish specifications, but not always. The value of β_{ORDR} can be computed knowing the incoming wind and the rotational speed (Akhmatov et al, 2003(a)). The wind farm operates with reduced power production so long as the order is given. When this order is cancelled, the regular control system is reset and restarted (Akhmatov et al, 2003(a)).

Additionally, the feature of safety stop (Snel and Schepers, editors, 1995) is implemented. When safety stop is ordered, the regular control system is disabled. The reference value is set to $\beta_{REF} = \beta_{STOP}$ where $\beta_{STOP} = \beta_{MAX}$ in case of pitch control and $\beta_{STOP} = \beta_{MIN}$ in case of active-stall control. The order to stop cannot be cancelled.

Further, the reference value, β_{REF} , is compared to the actual pitch angle, β . The error signal, e.g. the difference between the pitch and its reference, is corrected by the pitch servo. The first order servo model is applied (Kundur, 1994). Notice that the second-order servo models can be found in other investigations (Hansen and Bindner, 1999).

For the purpose of getting a realistic response of the generic control systems, for the pitch as well as for the active-stall controls, a number of delay mechanisms are implemented into the control system models (Akhmatov, 2002(a)). These delays represent, basically, sampling and filters damping natural frequencies in the wind turbine construction (Leith and Leithead, 1997; Akhmatov, 2002(a)).

Notice that the models of the blade angle controls may additionally include the blocks representing compensation for the non-linear aerodynamics of the wind turbine (Leithead et al, 1992; Leith and Leithead, 1997). The generic model to be used in power stability investigations does not include this representation.

4. Induction generators of fixed-speed wind turbines

Description of modelling details of wind turbine induction generators, which is given in (Akhmatov and Knudsen, 1999), is followed in this Section. It is kept in mind that the model of induction generators shall be applied in investigations of transient voltage stability. The model of induction generators is a part of the dynamic model of fixed-speed wind turbines. The model equations of induction generators are (Kundur, 1994):

$$\begin{cases} V_{DS} = R_S I_{DS} - \omega_s \psi_{QS} + \frac{d\psi_{DS}}{dt}, \\ V_{QS} = R_S I_{QS} + \omega_s \psi_{DS} + \frac{d\psi_{QS}}{dt}, \\ V_{DR} = R_R I_{DR} - s \omega_s \psi_{QR} + \frac{d\psi_{DR}}{dt}, \\ V_{QR} = R_R I_{QR} + s \omega_s \psi_{DR} + \frac{d\psi_{QR}}{dt}, \\ T_E = \psi_{DS} I_{QS} - \psi_{QS} I_{DS}. \end{cases} \quad (4.1)$$

The model equations (4.1) are in the per unit (P.U.) system¹⁷ and $V_S = (V_{DS}, V_{QS})$ is the terminal voltage, $I_S = (I_{DS}, I_{QS})$ is the stator current, $\psi_S = (\psi_{DS}, \psi_{QS})$ is the stator flux. The rotor voltage, $V_R = (V_{DR}, V_{QR})$, is zero because the rotor circuit is shorted, $I_R = (I_{DR}, I_{QR})$ is the current and $\psi_R = (\psi_{DR}, \psi_{QR})$ is the flux of the rotor in the stator quantities. The value s is the slip, which is negative of the generator rotor speed deviation, $\Delta\omega_G$, and ω_s is the synchronous speed. The value T_E denotes the electric torque. This is the fifth-order model (with addition of the movement equation of the generator rotor) with representation of the fundamental-frequency transients of the stator current¹⁸. These fundamental-frequency transients in stator are given by the time derivatives:

$$\frac{d\psi_S}{dt} = \left(\frac{d\psi_{DS}}{dt}, \frac{d\psi_{QS}}{dt} \right), \quad (4.2.a)$$

and produce the dc-offset in the machine current at balanced transient events in the power network.

In voltage stability investigations, the common third-order model of induction generators is often applied (Kundur, 1994). The third-order model is derived from the model equations (4.1) by omitting the fundamental-frequency transients in stator,

$$\frac{d\psi_S}{dt} = \left(\frac{d\psi_{DS}}{dt}, \frac{d\psi_{QS}}{dt} \right) = (0, 0). \quad (4.2.b)$$

¹⁷ The per unit system is given in **Appendix 4.A**. The equations (4.1) are with respect to the synchronously rotating reference frame.

¹⁸ Discussion: the equation system is given for a single-cage induction generator. When the induction generator is double-cage, the equation system should be extended with two more state equations and so it becomes the seventh-order model. Commonly, the induction generators applied in wind turbines are single-cage.

The simulation tool PSS/E contains the standardised model of induction generators, CIMTR3, which is the common third-order model. The model equations of the common third-order model of induction generators can be found in several books and publications (Kundur, 1994; Thiringer and Luomi, 2001; Feijóo et al., 2000).

4.1. Balanced transient events

Investigations of transient voltage stability are often executed with respect to a three-phased, short-circuit fault in the transmission power network (Kundur, 1994; Bruntt et al., 1999). It is a *balanced* transient event occurring at the same time in all the three phases of the faulted line or the faulted node. In that case, voltage is characterised by a sudden and significant drop.

The simulated response of the induction generator to a short circuit fault is shown in **Fig. 4.1**. The generator is at rated operation, 2 MW¹⁹. The simulations are with use of the third- and the fifth-order models, respectively. The fifth-order model is implemented as an user-written model into the simulation tool PSS/E during this project. As can be seen, it will be a notable discrepancy between the behaviours simulated with use of these two models.

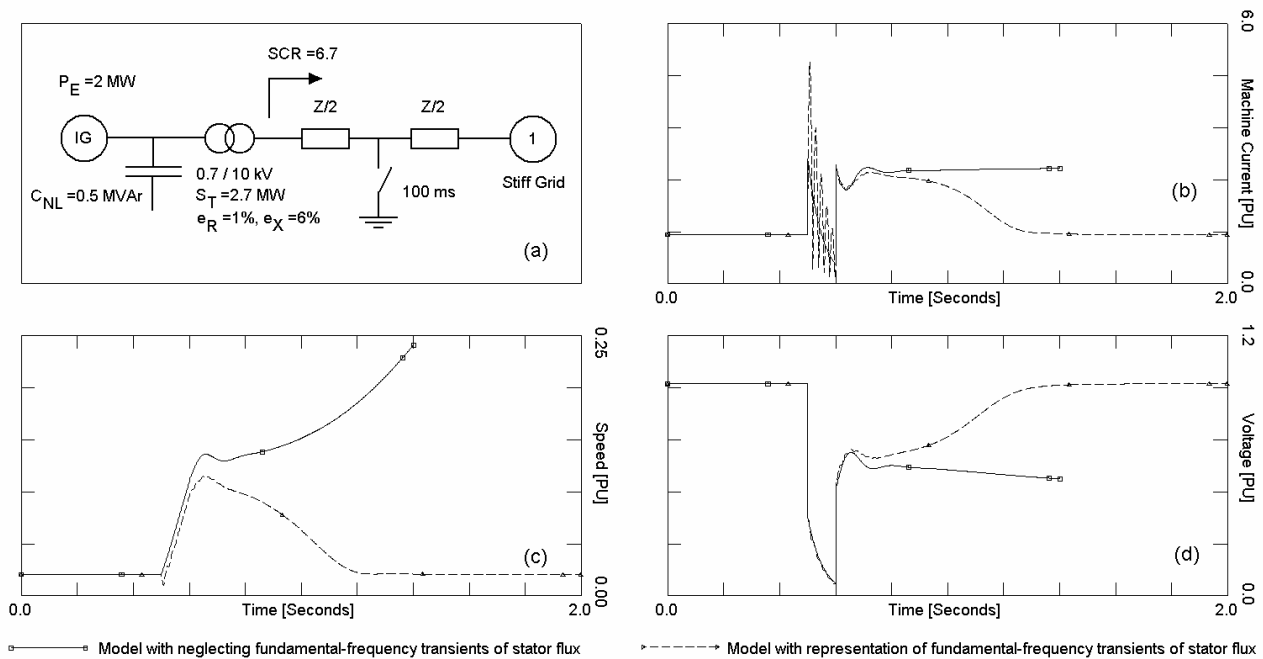


Fig. 4.1. Model-dependent outcome: (a) – network model. Use of the model with neglecting fundamental-frequency transients of stator flux results in (b) – insufficiently low machine current at the fault due to neglecting of transients, (c) –over-pessimistic acceleration of the generator rotor, (d) – risk of voltage instability. Short circuit ratio (SCR) is chosen as $(1000 \text{ MVA})/(150 \text{ MVA}) = 6.7$ and the generator rotor inertia $H_G = 0.5 \text{ s}$.

First, the discrepancy is seen in the behaviour of the machine current. The third-order model predicts the current behaviour without the fundamental-frequency transients. The current magnitude predicted by the third-order model is therefore lower than in case of the fifth-order

¹⁹ Generator data are given in **Appendix 4.A**.

model. The value of the machine current magnitude is important for evaluation of response of the wind turbine protective system²⁰.

The machine current magnitude is one of the monitored parameters. Exceeding the legal range of the machine current, e.g. exceeding the relay settings with respect to the machine current, will cause tripping of the wind turbine. In investigations of transient voltage stability tripping of wind turbines corresponds to power loss and demands of immediate power reserves.

Second, neglecting of the fundamental-frequency transients in stator leads to discrepancy in the braking torque of the induction generator, T_E . Consequently, it leads to discrepancy in the generator rotor speed, ω_G . When applying the common third-order model, the speed, ω_G , increases immediately when the short-circuit fault is subjected. When using the fifth-order model, the generator rotor speed decreases shortly after the fault is subjected – it produces a notch in the speed curve. This short notch is the natural behaviour of generators at a short circuit fault (Akhmatov and Knudsen, 1999).

In case of induction generators, this notch in the generator rotor speed is an important behaviour. It is because of a strong coupling between the electric parameters of induction generators and the slip. For example, the reactive power absorption depends on the generator rotor slip, which also influences on the voltage behaviour after the short-circuit fault. The larger acceleration of the generator rotor during the transient event is computed, the large reactive absorption of the generator will be predicted. Therefore, the third-order model will predict a more pessimistic voltage profile after the transient fault than in case of the fifth-order model of induction generators. This behaviour is explained in (Akhmatov and Knudsen, 1999).

In other words, neglecting of the fundamental-frequency transients in stator leads to over-pessimistic voltage profile at a balanced short-circuit fault (Akhmatov and Knudsen, 1999). For reaching sufficient accuracy the fifth-order model of induction generators shall be applied in investigations of transient voltage stability with incorporation of large amount of wind power.

4.2. Unbalanced transient events

An example on unbalanced transient events can be a line tripping. Disconnection of a three-phased line occurs when the phase-current passes zero in the respective phases, but not at the same time in all the three phases. Therefore, it is an *unbalanced* event. When the phased-current is disrupted at zero passing, the dc-offset in the phased-current is eliminated. Consequently, the fundamental-frequency transients in the stator current magnitude are also eliminated when the induction generator is subjected to an unbalanced three-phased fault (Pedersen et al., 2003).

²⁰ Discussion: the induction generator current behaviour is computed when the saturation is omitted in the model equations. In (Sørensen et al., 2003) it is demonstrated that this phenomenon may increase the current transient by 10 % (in the first peak period of 20 ms duration) when the fault occurs close to the generator terminals. Notify that inclusion of the saturation in the model equations requires more data and computation time, but not necessarily gives a significant contribution to the induction generator current transients. The most significant contribution to the current transients comes from inclusion of the fundamental-frequency transients in the stator current.

This can be reached with use of the common third-order model of induction generators (Pedersen et al, 2003). It is noticed that the fault clearance by tripping of the faulted line is an unbalanced transient event, which is why the fundamental-frequency transients in the machine current are eliminated, see **Fig. 4.1.b**.

Often, balanced and unbalanced transient events will be represented within one and the same sample²¹. Representation of induction generators in such investigations can be reached by accurate implementation of the model into the dynamic simulation tool. The user-written model of induction generators implemented in the tool PSS/E is validated against the results of the standardised model of Matlab/Simulink²².

4.3. Significance of generator rotor inertia

When having an accurate model of induction generators with correct representation of the fundamental-frequency transients in stator, the next step is to estimate the significance of the phenomenon. This work is made by Akhmatov and Knudsen (1999) with use of a simplified network equivalent.

The network equivalent represents the power network of the Elkraft area, eastern Denmark. The equivalent is with 10 nodes and 4 generators. An induction generator, representing a wind farm, is connected to the remote end of the system, parallel to an (equivalent) unit equipped with a synchronous generator. The total power capacity is 1400 MVA. The short circuit capacity of the network is approx. 4000 MVA. The inertia constant, H_G , of the induction generator rotor is 0.5 s. It corresponds to a typical inertia of an induction generator rotor (alone). As found in (Knudsen and Akhmatov, 1999), it is a notable discrepancy in the voltage behaviour between the third- and the fifth-order models when the power capacity of the induction generator is increased (and the power capacity of the synchronous generator is reduced by the same value). It is illustrated in **Fig. 4.2**.

In the most cases, the rotating system consists of more than just the generator rotor. Furthermore, the initial, model-dependent difference in the rotor speed is the main reason of that the fundamental-frequency transients in stator cause a model-dependent difference in the voltage response. Therefore, the model-dependent differences are expected to be less distinct when the inertia becomes larger, and the initial speed difference thereby becomes smaller.

Therefore, the above test is repeated in (Akhmatov and Knudsen, 1999) with increased values of H_G , thus decreasing the speed change caused by the initial transient torque. The rated power of the induction generator is kept 500 MW. For comparison, a typical inertia constant of the wind turbine rotor is in the range around 2.5 s. When including the generator rotor, the total lumped inertia is around 3 s. The results are shown in **Fig. 4.3**. As can be seen, the voltage curves start to converge when the lumped inertia constant, H_G , reaches approx. 1 s and is almost fully converged when H_G is around 3 s. This means that in applications where the lumped inertia constant of the induction generator is relatively large, the common third-order model will produce almost correct results. It is

²¹ Read about the experiment with tripping and re-closing of a wind turbine in **Appendix 4.B**. This experiment is also used for validation of the model of fixed-speed wind turbines equipped with induction generators.

²² Validation is given in **Appendix 4.B**.

only when the inertia becomes rather low – 1 s or less – that it is necessary to use the fifth-order model.

This conclusion is, however, based on the assumption of the rotating masses consisting of one lumped mass. It is noticed that the shaft systems of fixed-speed wind turbines are relatively soft. This influences on the dynamic behaviours of the shaft torque and the generator rotor speed at disturbances.

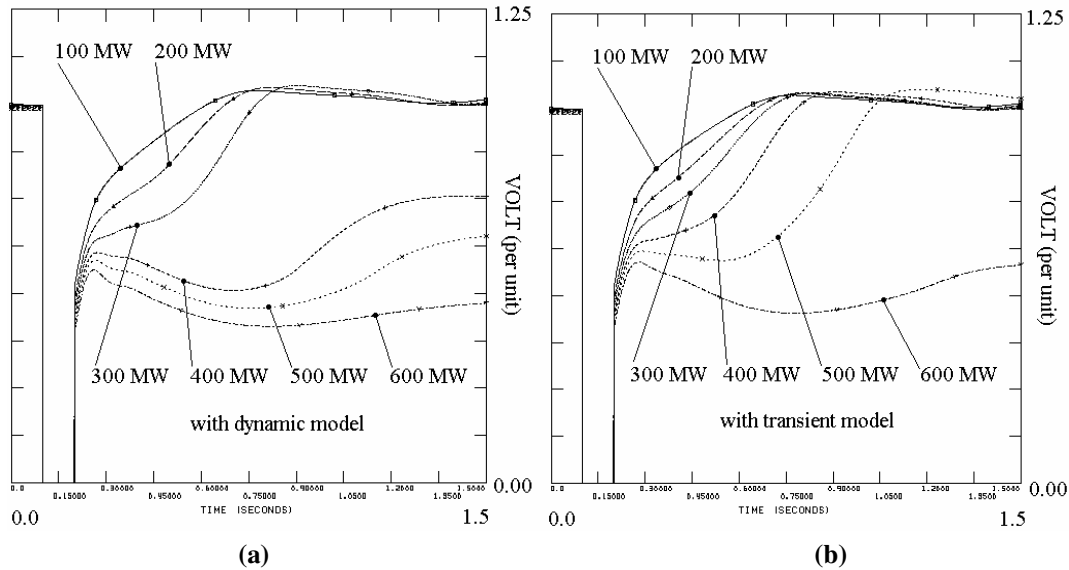


Fig. 4.2. Comparison between model-dependent outcomes with light induction generator rotor: (a) – third-order model, (b) – fifth-order model. Reported in (Knudsen and Akhmatov, 1999).

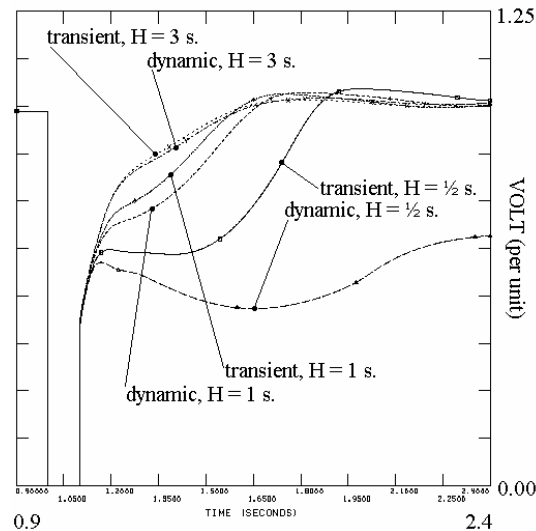


Fig. 4.3. Model comparison - with varying inertia constants. Reported in (Akhmatov and Knudsen, 1999).

4.4. Significance of shaft representation

The fixed-speed wind turbines are characterised by relatively soft shafts connecting light generator rotors with heavy turbine rotors. It is represented with the two-mass model of the wind turbine

shafts. Since the generator rotor itself is light, then it might still go through large speed variations at transient events occurring in the AC network. It is even though the wind turbine itself maybe is not accelerated very much. The acceleration of the generator rotor will be even larger. It is because it will be accelerated not only with the mechanical power from the wind turbine, but also from the tension in the shaft – the tension which is released when the air-gap torque is either reduced or lost due to the transient disturbance in the power network. This subject is explained in **Section 2.2**.

In order to get a full impression of the importance of respectively the fundamental-frequency transients in stator and of the shaft model, 4 comparative simulations are performed in (Akhmatov and Knudsen, 1999). Again the network equivalent of the Elkraft area is applied (Akhmatov and Knudsen, 1999), and the transient event is a 100 ms short circuit fault. However, in this case the rating of the induction generator is 900 MW, and the parallel unit is only 400 MVA. This change is made in (Akhmatov and Knudsen, 1999) in order to have a situation where the differences in the simulation results between the various models are large. Four different models of induction generators of fixed-speed wind turbines are used.

- 1) The third-order (dynamic) model with the two-mass shaft model.
- 2) The fifth-order (transient) model with the two-mass shaft model.
- 3) The third-order model with the lumped mass model.
- 4) The fifth-order model with the lumped mass model.

The simulation results are shown in **Fig. 4.4**. As can be seen the results for the items 3 and 4 (with lumped mass model) are almost identical, as could be expected from the results described in **Section 4.3**.

The results for the cases 1 and 2 (with the two-mass model of the shaft) are however remarkable. First, the curves produced with use of the two-mass model differ very much from the curves obtained with the lumped mass model. Second, the two curves obtained with the two-mass model and different generator models are also notably different from each other than in case of the lumped mass model. It is noticed that worst result will be for the case 1 – the third-order generator model with the two-mass shaft model. This shows that including of the two-mass shaft model will result in a smaller stability margin than what would have been obtained with use of the lumped mass model.

It is also noticed that use of the fifth-order (transient) model together with the two-mass shaft model (case 2) improves the stability margin since the voltages are generally higher and less oscillatory than with the third-order (dynamic) model with the two-mass shaft representation (case 1). But the stability margin is still less than for the lumped mass models, that being either the third-order (case 3) or the fifth-order (case 4) generator model.

The oscillation in the terminal voltage of the induction generator is caused by the mechanical oscillation of the small generator rotor against the larger inertia of the wind turbine rotor. The presence of these oscillations in the AC voltages means that the mechanical shaft oscillation may excite other modes of oscillation in the rest of the AC system; e.g. power oscillations which normally have low frequencies. At first it may seem surprising that the impact of the shaft system is so significant. However, this becomes clear due to the fact that the shaft systems of fixed-speed

wind turbines are relatively soft. A strong interaction between the shaft oscillations and the electric parameters fluctuations of fixed-speed wind turbines is confirmed by the experimental work, see **Appendix 4.B**.

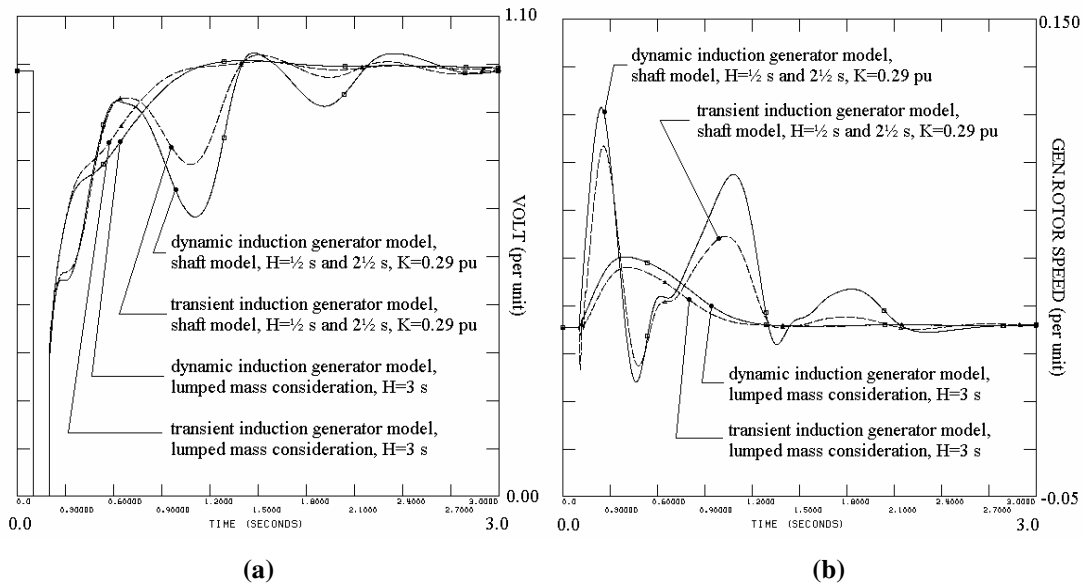


Fig. 4.4. Comparison between models of induction generators of fixed-speed wind turbines: (a) – voltage, (b) – generator rotor speed. Reported in (Akhmatov and Knudsen, 1999).

Consequently, representation of the shaft systems with the two-mass model reduces the stability margin, but this is partly counteracted by the fact that the fifth-order transient model increases the stability margin of induction generators. These results clearly show that the models of induction generators of fixed-speed wind turbines shall have both a two-mass representation of the shaft and of the fundamental-frequency transients in stator. It is in order to generate reliable simulation results in dynamic simulation programs (Akhmatov and Knudsen, 1999). When it is not possible to obtain reliable data of the shaft system, then it is probably better to apply “typical” data rather than to resort to the lumped mass model (Akhmatov and Knudsen, 1999).

4.5. Aerodynamic wind turbine model – Coupling by speed

For completion of the dynamic model of fixed-speed wind turbines, the aerodynamic model of the rotating turbine and its blade-angle control system shall be represented. The aerodynamic model produces the coupling between the rotational speed, ω_M , and the mechanical torque of the wind turbine, T_M . This coupling is achieved with use of the static representation with C_P - λ -curves or with use of the dynamic model with unsteady inflow phenomena. Recommendations about complexity details of the aerodynamic models are given in **Section 2.1**.

The model of the blade-angle control is implemented by a generic way, as it is explained in **Section 3**.

4.6. Protective relay modelling

The protective system of wind turbines monitors several parameters and orders disconnection of the wind turbines at registering of abnormal operation in the power grid. The monitored parameters can be the terminal voltage, the grid frequency, the machine current, the rotational speed etc. These data can be received from the wind turbine manufacturer.

When no better data are available, the Danish recommendations KR-111 can be applied to set the common protective relay system in simulations. Notice that these recommendations describe rather protection of the power network from the voltage and the frequency deviations which are caused by the wind turbines themselves, but not the protection of the wind turbines at transient events in the power network. By the experience of the author, the wind turbine protective relay settings may be much manufacturer-dependent even for the wind turbines of the same rated power capacities.

Ordering to disconnection of the wind turbine is given when at least one of the monitored parameters exceeds its respective relay settings. Importance of representation of the protective relays is demonstrated in **Sections 6.15** and **11.3** in case of fixed-speed wind turbines.

5. Modelling of large wind farms

In investigations of transient voltage stability, the large wind farms can be represented with use of one of the following models.

- 1) Aggregated models with representation of (i) each wind turbine in the farm, (ii) its no-load capacitor, (iii) the transformer connecting the wind turbine generator to the internal network of the wind farm and (iv) with sufficiently detailed representation of the internal network. For this purpose, the wind farm containing eighty wind turbines will be represented with eighty wind turbine models.
- 2) Reduced models where the wind farm containing a larger number of the wind turbines is given by a re-scaled equivalent, e.g. one wind turbine model representing a group of the wind turbines. This reduced representation can be applied at specific conditions.

Modelling details of the large (offshore) wind farms depend on the purpose of the investigations. With relation to investigations of transient voltage stability, it can be as listed below.

- 1) Investigation of the mutual interaction between several electricity-producing wind turbines within a large wind farm.
- 2) Response of the wind turbines to a fault occurring in the internal network of the wind farm.
- 3) Investigation of the collective response of the wind farm to a short-circuit fault occurring in the entire power system.
- 4) Voltage stability investigations of the power grid with incorporation of the large wind farm and its dynamic reactive compensation.

The purpose in item 1 relates to investigation of whether there is a possible risk of self-excitation of the large wind farm with a large number of the wind turbines having identical or different parameters and subjected to given control features. The term of self-excitation relates, in this context, to mutual, uncontrollable oscillations between the wind turbines excited by a disturbance.

Item 2 may relate to investigation of relay settings and estimation of power loss due to trip of a number of the wind turbines as the result of the fault occurring in the wind farm internal network or in the entire power grid. The wind turbines can be at different operational points and, in general, with different parameters and relay settings. Furthermore, (i) investigation of the control features of the wind turbines when operating at different operational points, (ii) test by simulations and (iii) implementation of the control features into individual wind turbines of the farm can also be actual. In both cases, the detailed, aggregated model of the wind farm and its internal network is required.

In cases with investigations of (i) collective response of the wind farm, item 3, and (ii) power stability investigations on incorporation of the large wind farm into the power grid, item 4, the reduced models can be successfully applied. Use the reduced model of the large offshore wind farm (for instance, use of the re-scaled equivalent by one wind turbine model) instead of the aggregated wind farm model (with eighty wind turbine models) will normally be preferred in

investigations with incorporation of the dynamic compensation unit (on-land). This is obvious due to reduction of the complexity of simulations and according to the purpose of the investigation.

The reduced wind farm models give the response of the wind turbines within the wind farm as the integrated whole. This response is without distinguishing between specific operational conditions or details of the specific wind turbines within the given wind farm. Therefore, reduction to the re-scaled equivalents shall be achieved with sufficient accuracy. Reduction to the re-scaled equivalents will always contain an element of inaccuracy, e.g. some phenomena are neglected.

On the other hand, it is possible to formulate a number of quantitative considerations for accuracy estimation of the reduced models to be applied instead of very detailed aggregated models. In the following, aggregated modelling and considerations about reduced wind farm representations are briefly discussed.

5.1. Aggregated model of a large wind farm – An example

An aggregated model of the large offshore wind farm consisting of eighty wind turbines of 2 MW rated power is set up and implemented into the simulation tool PSS/E (Akhmatov et al., 2003(a)). Each wind turbine within the wind farm is represented by the model of the fixed-speed, active-stall controlled wind turbines equipped with no-load compensated induction generators, according to description of **Section 4**.

Through their 0.7 / 30 kV transformers, the wind turbines are connected to the wind farm internal network. The internal network is organised by eight rows, or sections, with ten electricity-producing wind turbines in each section. Within the rows, the wind turbines are connected through the 30 kV sea-cable sections. The distance between two neighbouring wind turbines in the same section is 500 m and the distance between two neighbouring sections is 850 m. The sea-cable sections are through the 30 kV sea-cables connected to the offshore platform with the 30 / 30 / 132 kV tertiary transformer. Then, through the 132 kV sea- and underground- cable the wind farm is connected to the connection point in the transmission system on-land. An ac-connection of the offshore wind farm to the transmission network is chosen. **Fig. 5.1** gives the sketch of the wind farm model.

According to the Danish specifications, the large offshore wind farms shall be reactive-neutral with the power grid at the connection point. This implies that the reactive power exchange between the wind farm and the power grid must be around zero independently from the operational point of the wind farm. This requires that a number of capacitors and reactors shall be incorporated at the connection point or at the offshore platform.

The aggregated model allows simulations of the wind farm under consideration of an irregular wind distribution. Such a consideration is realistic because the wind turbines are shadowing each other for incoming wind. Second, the area of the farm is 4.5 x 6 km squared, which is why it is natural to expect an irregular wind distribution over such a large area.

5.2. Reduced equivalents of large wind farms

Consider a wind farm with eighty electricity-producing wind turbines by the Danish concept. The wind turbines are with identical electrical, e.g. the generator data, and mechanical, e.g. the shaft

system data etc., parameters. The wind turbines are marked by a pair of indexes (i,j) where the first index refers to the section within the wind farm and goes from 1 to N and the second index refers to the wind turbine number in the given section and goes from 1 to M . With relation to the given large wind farm, the indexes are $i = [1,N] = [1,8]$ and $j = [1,M] = [1,10]$.

Combining the large wind farm into a reduced equivalent, a number of conditions shall be fulfilled. These conditions are firstly derived in our work (Akhmatov and Knudsen, 2002) and given by the following. The power capacity of the reduced equivalent, $S_{\Sigma,\Sigma}$, shall be equal to the sum of the power capacities of the individual wind turbines, $S_{I,J}$. This condition is expressed by

$$S_{\Sigma,\Sigma} = \sum_{I=1}^N \sum_{J=1}^M S_{I,J} , \quad (5.1)$$

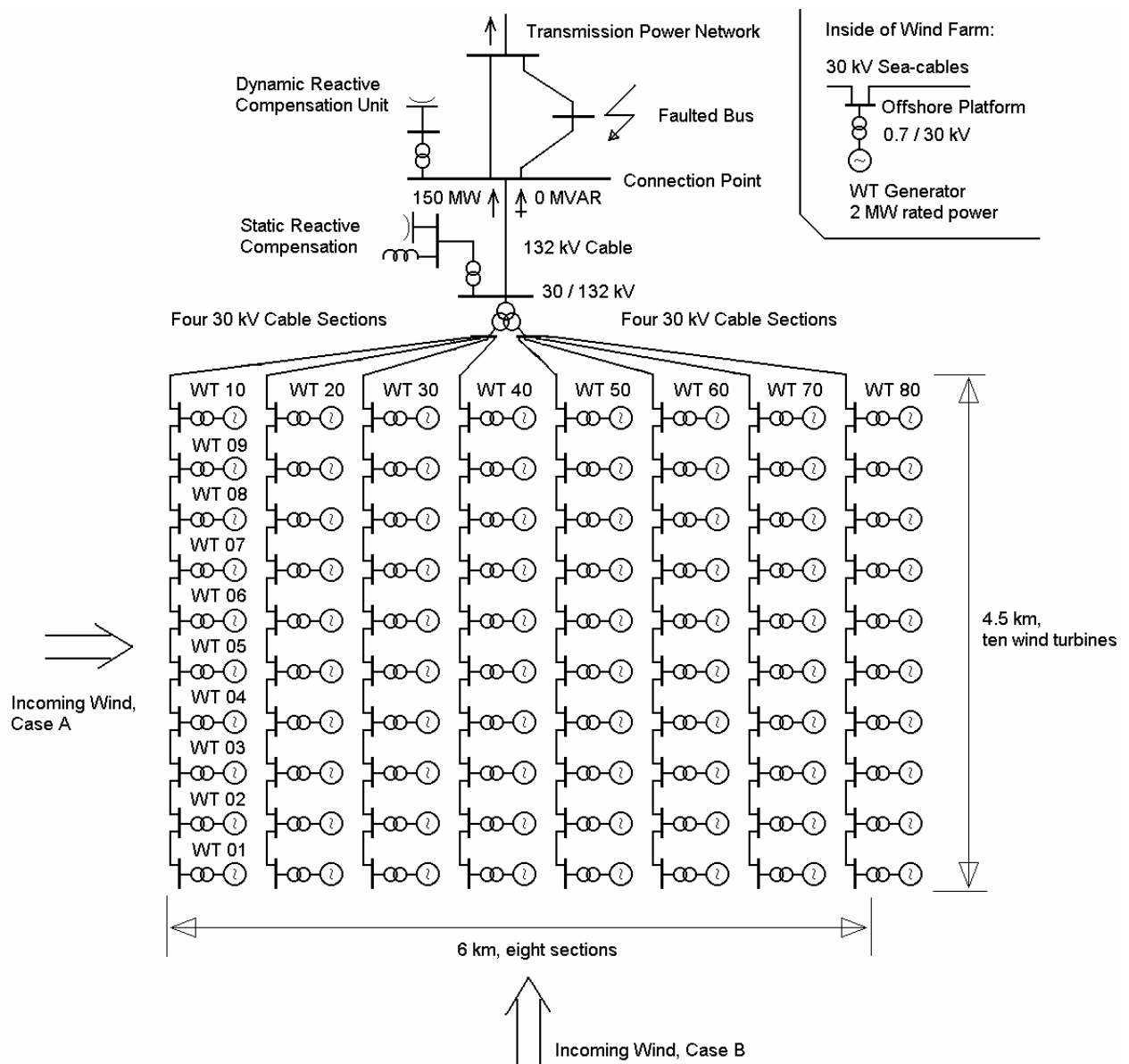


Fig. 5.1. Aggregated model of large offshore wind farm with eighty wind turbines of 2 MW rated power. Layout of the wind farm is reported in (Akhmatov et al, 2003(a)).

This is always fulfilled because the condition implies that the wind farm power capacity, S , is the sum of the power capacities of the wind turbines within the farm.

The power supplied by the reduced equivalent to the grid, $P_{\Sigma,\Sigma}$, shall be equal to the sum of the power supplied by the individual wind turbines, $P_{I,J}$. This is expressed by the following condition.

$$P_{\Sigma,\Sigma} = \sum_{I=1}^N \sum_{J=1}^M P_{I,J} , \quad (5.2)$$

This condition is always fulfilled as well because the condition means that the power supplied by the wind farm, P , is the sum of the power supplied by the wind turbines within the farm.

Further, the dynamics of the induction generators of the wind turbines are given by the slopes of the P - Q -characteristics of the induction generators. The following condition shall be fulfilled.

$$\frac{dQ}{dP}_{\Sigma,\Sigma} = \sum_{I=1}^N \sum_{J=1}^M \frac{dQ_{I,J}}{dP_{I,J}} , \quad (5.3)$$

where $dQ_{I,J}/dP_{I,J}$ is the slope of the P - Q -characteristic of the induction generator of the wind turbine indexed (i,j) , and $dQ/dP_{\Sigma,\Sigma}$ denotes the slope of the P - Q -characteristic of the reduced equivalent of the wind farm. Taking into account that the P - Q -characteristic of the induction generator is approximately a parabola with zero-slope at no-load operation

$$Q = Q_{NL} + aP^2 . \quad (5.4)$$

Here, Q_{NL} is the reactive absorption at no-load and a is the coefficient. As can be seen, **Eqs. (5.2)** and **(5.3)** express the same condition, which is linear.

Since the induction generators are no-load compensated, the reactive absorption of the wind turbines seen from the grid becomes proportional to the electric power squared, see **Eq. (5.4)**. At different operational points of the individual wind turbines, this should give the discrepancy in the initial (steady-state) operational points of the aggregated model versus the reduced equivalent. This discrepancy is, however, not important due to the technical requirement dealing with that the large (offshore) wind farm is reactive neutral in the connection point. Therefore the aggregated model of the large wind farm as well as the reduced equivalent, viewed from the entire power grid, will, practically said, be initialised to the same point with respect to reactive power exchange with the grid (that is zero).

If the wind turbines could be represented by the induction generators driven by the lumped-mass mechanical systems, the aggregated models of the large wind farms to be used in investigations of power system stability could easily be reduced to single-machine equivalents. It is due to **Eqs. (5.1)** - **(5.3)** would always be fulfilled. This would be achieved independently from the operational points of the individual wind turbines within the farm.

However, the wind turbine shafts are relatively soft. This does to mean that the pre-twisted shaft systems accumulate non-negligible amount of potential energy. At the grid faults, the pre-twisted shafts start relaxation, which leads to more acceleration of the generator rotors and influences on the voltage behaviour. This mechanism is described in **Section 2.2**. The potential energy accumulated in the pre-twisted shaft of the wind turbine is given by **Eq. (2.16)**. Hence, the potential energy

accumulated in the pre-twisted shafts of all the wind turbines within the farm, W_S , is by the following relation.

$$W_S = \sum_{I=1}^N \sum_{J=1}^M W_{I,J} = \frac{1}{2K_S} M \cdot N \cdot \langle T_M^2 \rangle, \quad (5.5)$$

where $W_{I,J}$ is the potential energy accumulated in the pre-twisted shaft the wind turbine indexed (i,j) and $\langle X \rangle$ denotes the average value of X .

In case of the single-machine equivalent, the potential energy, $W_{\Sigma,\Sigma}$, will be expressed by the following²³.

$$W_{\Sigma,\Sigma} = \frac{T_{\Sigma,\Sigma}^2}{K_S} = \frac{1}{2K_S} M \cdot N \cdot \langle T_M \rangle^2. \quad (5.6)$$

Here, $T_{\Sigma,\Sigma}$ is the mechanical torque predicted by the reduced equivalent. Comparing **Eqs. (5.5)** and **(5.6)**, it is seen that these two expressions predict the same result for identical values of the mechanical torque of all the wind turbines within the farm. In other words, the reduced equivalent can be used to represent the group of wind turbines working at the same operational points.

The reduced, single-machine equivalents representing large (offshore) wind farms can be applied on the following assumptions (Akhmatov and Knudsen, 2002).

- 1) When investigating the worst case with respect to maintaining voltage stability, the wind farm is considered to be at rated operation, so all the wind turbines within the farm are at rated operational points. The wind farm can be modelled as a single-machine equivalent. The wind farm, for example of eighty wind turbines, is given by the re-scaled wind turbine with the rated power capacity of the whole farm and at rated operation.
- 2) When all the wind turbines within the wind farm are at the same, but not necessarily, rated operational points.
- 3) When the differences between the operational points of the individual wind turbines are not too large, the single-machine equivalent can possibly predict sufficiently accurate results with respect to collective response of the wind farm to a grid disturbance.

When the wind distribution over the wind farm area is irregular, but follows a pattern, the multi-machine equivalent can be applied instead. This means that the whole wind farm is represented by a less number of re-scaled wind turbines. Each equivalent of the multi-machine equivalent is built-up about a group of the wind turbines with the same operational points. Such a situation is illustrated by the following examples.

Consider that the incoming wind is as illustrated by Case A in **Fig. 5.1**. The wind turbines in section 1 shadow the wind turbines in section 2, which shadow again the wind turbines in section 3 of the farm etc. The wind turbines located in the same section operate at the same wind conditions and so at the same operational points. With this wind distribution pattern, the wind farm can be

²³ **Eqs (5.5)** and **(5.6)** are derived from the following, respectively.

$$W_S = \sum_{I=1}^N (\sum_{J=1}^M (W_{I,J})) = 1/(2K_S) \sum_{I=1}^N (\sum_{J=1}^M (T_{I,J}^2)) = \langle N M T_M^2 \rangle / (2K_S) = N M \langle T_M^2 \rangle / (2K_S).$$

$$W_{\Sigma,\Sigma} = 1/(2K_S) T_{\Sigma,\Sigma}^2 = 1/(2K_S) \sum_{I=1}^N (\sum_{J=1}^M (T_{I,J}))^2 = \langle N M T_M \rangle^2 / (2N M K_S) = N M \langle T_M \rangle^2 / (2K_S).$$

separated into eight groups – by the eight sections consisting each of ten wind turbines. Here, each group can be represented by its single-machine equivalent. Hence, the whole wind farm is given by the multi-machine equivalent consisting of eight single-machine equivalents denoted $WT_{I,\Sigma}$. This equivalent is sketched in **Fig. 5.2**.

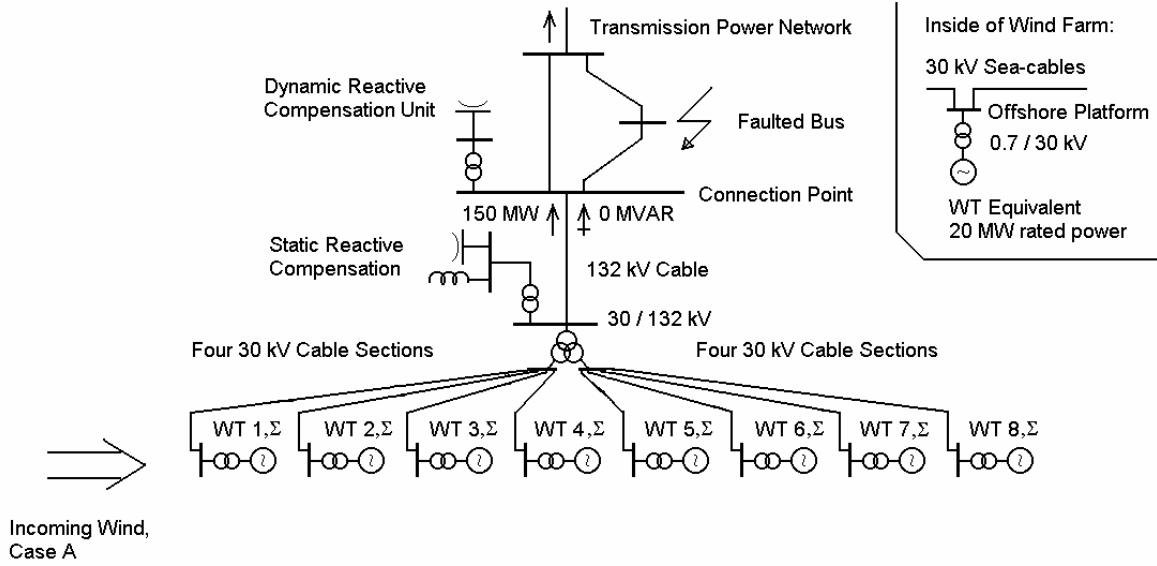


Fig. 5.2. Large offshore wind farm with eighty wind turbines of 2 MW rated power represented as a reduced equivalent.

The rated power capacity of each single-machine equivalent is $S_{I,\Sigma} = \sum_{J=1}^M S_{I,J}$, the electric power supplied is $P_{I,\Sigma} = \sum_{J=1}^M P_{I,J}$ etc. Those are reached with summation by the machine index $J=[1,M]$ in each section $I=[1,N]$.

Now the incoming wind is as illustrated by Case B in **Fig. 5.1**. Using similar argumentation as above, the wind farm can be represented by the multi-machine equivalent consisting of ten single-machine equivalents, $WT_{\Sigma,J}$, with the rated power capacities $S_{\Sigma,J} = \sum_{I=1}^N S_{I,J}$, the electric powers supplied $P_{\Sigma,J} = \sum_{I=1}^N P_{I,J}$ etc. Those are reached with summation by the section index $I=[1,N]$ for each wind turbine group $J=[1,M]$. The sketch of this equivalent is given in **Fig. 5.3**.

5.3. Effect of absent mutual interaction on reduction of wind farm model

It must be stressed on that the discussion above is carried for the large wind farms consisting of the wind turbines with identical data parameters. Those are the machine impedance, the inertia constants and the shaft stiffness. This requirement deals with that the wind turbines within the large wind farm shall produce a coherent response to a grid fault. The term “coherent response” implies

that the oscillating behaviours of electrical and mechanical parameters of the wind turbines within the farm are “in-phase”-response.

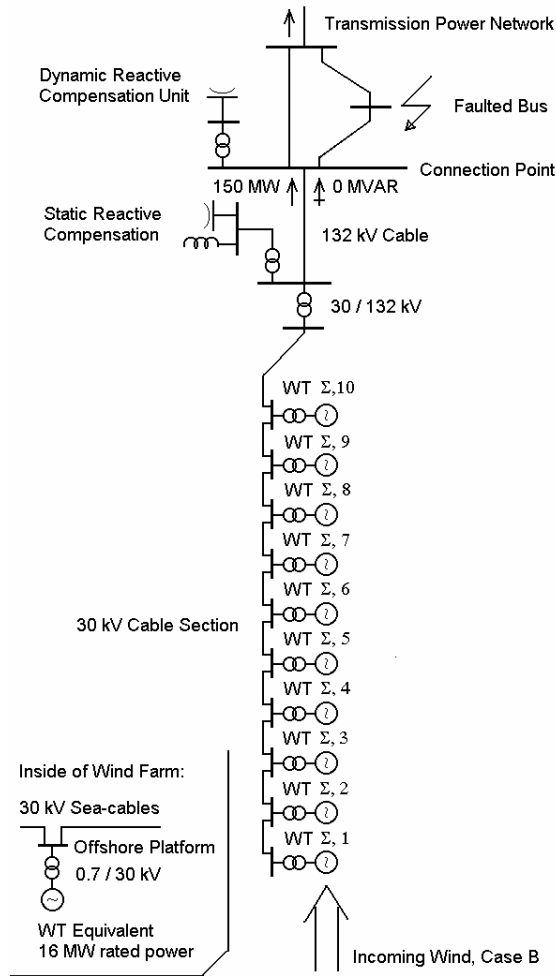


Fig. 5.3. Large offshore wind farm with eighty wind turbines of 2 MW rated power represented as a reduced equivalent.

This consideration is fulfilled in case of the wind turbines equipped with induction generators and also other generator concepts at properly tuned control systems. Here, correctness of this statement is assumed without discussion, but it will be demonstrated by simulations in the following Sections.

In case of induction generators, there is no synchronising torque. Practically said, there is, no mutual interaction between the generators through the electric network²⁴. The shafts of the different wind turbines within the large wind farm relax independently from each other when subjected to the grid fault – therefore the wind turbines at the same operational points can simply be added and represented by a reduced equivalent. The coherent response is seen due to the following reasons.

- 1) The wind turbine data are identical which is why the natural frequencies are identical as well, see **Eq. (2.17)**.
- 2) The short circuit impedance viewed from the terminals of the different wind turbines within the large wind farm is, practically said, of the same value.
- 3) Absent mutual interaction, see **Section 6**²⁵, which is why no mutual oscillations between the wind turbines within the large wind farm will be seen.

On the other hand, absent mutual interaction may introduce restrictions on use of reduced equivalents. Such restrictions will be present in case of wind turbines with different electrical and/or mechanical data. Consider that the wind farm consists of two kinds of wind turbines equipped with the shafts with the stiffness K_{S1} , respectively, K_{S2} . The wind turbines are with no-load compensated induction generators and other data are identical. Applying **Eq. (5.5)** and assuming that the wind farm is with equal number of each kind of the wind turbines and all the

²⁴ Neglecting a feedback through the voltage fluctuations in case of flicker and small-signal stability.

²⁵ Absence of mutual interaction will be demonstrated by simulations given in Section 5, where general stability requirements of the large wind farms are discussed.

wind turbines are at the same operational points, the potential energy accumulated in the shafts will be²⁶

$$W_S = \sum_{I=1}^N \sum_{J=1}^M W_{I,J} = \frac{K_{S1} + K_{S2}}{4K_{S1}K_{S2}} NM \langle T^2 \rangle. \quad (5.7)$$

However, it may not be concluded that the large wind farm can be represented by the single-machine equivalent with the shaft stiffness $K_S = \frac{2K_{S1}K_{S2}}{K_{S1} + K_{S2}}$. It is because such a reduced

representation would require a coupling, e.g. mutual interaction, between the wind turbines within the farm. However, mutual interaction is not present in case of wind turbines equipped with induction generators. The response of the wind farm to the grid fault will be seen as two independent oscillations with two different natural frequencies by **Eq. (2.17)**. In these terms, the wind farm can be represented by the two-machine equivalent by grouping the wind turbines with the shaft stiffness K_{S1} and K_{S2} into their respective single-machine equivalents.

The following is notified when *the worst case* with respect to maintaining of transient voltage stability shall be investigated. When the parameters of the wind turbines are not exactly identical, but close to each other, then the single-machine equivalent may still be applied. With relation to the discussion above, the shaft stiffness of the single-machine equivalent should be, then, chosen as the *lowest* among the given values of the shaft stiffness or as found from **Eq. (5.7)**.

²⁶ $W_S = \sum_{I=1, N} (\sum_{J=1, M} (W_{I,J})) = \sum_{I=1, N/2} (\sum_{J=1, M} (T_{I,J}^2 / K_{S1})) + \sum_{I=1, N/2} (\sum_{J=1, M} (T_{I,J}^2 / K_{S2})) = (1/K_{S1} + 1/K_{S2}) \cdot \sum_{I=1, N/2} (\sum_{J=1, M} (T_{I,J}^2))$
 $= (1/K_{S1} + 1/K_{S2}) \cdot N/2 M \langle T^2 \rangle = (K_{S1} + K_{S2}) / (2K_{S1}K_{S2}) NM \langle T^2 \rangle.$

6. Voltage stability of large wind farms with fixed-speed wind turbines

In this Section, it will be demonstrated how the parameters and the controllability of fixed-speed wind turbines influence on transient voltage stability. The relation between transient voltage stability and the parameters and the controllability of fixed-speed wind turbines will be explained in terms of *dynamic stability limit* of grid-connected induction generators. This important issue is firstly discussed in our work (Akhmatov et al, 2000(c)) and later confirmed by other investigations, for example (Holdsworth et al, 2001).

6.1. Electric torque versus speed characteristic

The static characteristic of the electric torque versus the generator rotor speed of induction generators is given by the well-known relation (Kundur, 1994).

$$T_E(\omega_G) = \frac{V_S^2}{\omega_G} \cdot \frac{R_T(\omega_G)}{R_T^2(\omega_G) + X_T^2(\omega_G)}. \quad (6.1)$$

The machine impedance viewed from the terminals into the induction generator is by the following expressions.

$$\begin{aligned} Z_T &= R_T + jX_T, \\ R_T(\omega_G) &= R_S + \frac{\frac{R_R}{\omega_G - 1} \cdot X_M^2}{\left(\frac{R_R}{\omega_G - 1}\right)^2 + (X_M + X_R)^2}, \\ X_T(\omega_G) &= X_S + \frac{X_M \cdot \left(\left(\frac{R_R}{\omega_G - 1}\right)^2 + X_R(X_M + X_R)\right)}{\left(\frac{R_R}{\omega_G - 1}\right)^2 + (X_M + X_R)^2}. \end{aligned} \quad (6.2)$$

Here R_S and R_R are the resistances of stator and rotor, respectively, and X_S , X_M and X_R are the reactances of stator, magnetising and rotor, respectively, and all the values are in the stator quantities. The value $(1 - \omega_G)$ gives the slip that is negative for a generator-operation mode.

It is noticed that the electric torque, T_E , is the function of the terminal voltage squared. A number of the electric torque versus speed curves are shown in **Fig. 6.1**. The curves are at different terminal voltages, V_S , kept independent from the generator rotor speed. The electric torque versus speed curves of the induction generators can be received from the manufacturer. Such curves are typically plotted for the rated terminal voltage $V_S = 1.00$ PU, which may correspond to the grid with an infinite short circuit capacity, $S_{SC} \rightarrow \infty$.

When connected to the grid, the electric torque versus speed curves are influenced by a number of factors relating to the power grid (Akhmatov et al, 2000(c)). First, the initial value of the terminal voltage is not necessarily exact 1.00 PU. Second, the terminal voltage becomes dependent

on the generator rotor speed. The reactive absorption of the induction generator, Q_E , is given by the relation.

$$Q_E = V_s^2 \frac{X_T(\omega_G)}{R_T^2(\omega_G) + X_T^2(\omega_G)}. \quad (6.3)$$

The reactive power supplied to the terminals by the no-load capacitor is defined as:

$$Q_{NL} = X_{NL} V_s^2, \quad (6.4)$$

with the impedance of the no-load capacitor X_{NL} . At increasing speed, the reactive absorption of the induction generator increases as well and the terminal voltage decays, according to the relation²⁷.

$$\frac{\Delta V_s}{V_s} \sim \frac{-\Delta Q_E + \Delta Q_{NL}}{S_{SC}}. \quad (6.5)$$

Here $(-\Delta Q_E + \Delta Q_{NL})$ denotes the reactive power flow to the connection node of the induction generator. Dependence of the terminal voltage on the generator rotor speed, $V_s(\omega_G)$, shall be taken into account when computing the electric torque versus speed curves of the grid-connected induction generators, **Eq. (6.1)**. This is illustrated by the thick solid curve in **Fig. 6.1**, which is plotted in case of the power grid given in **Fig 4.1.a**.

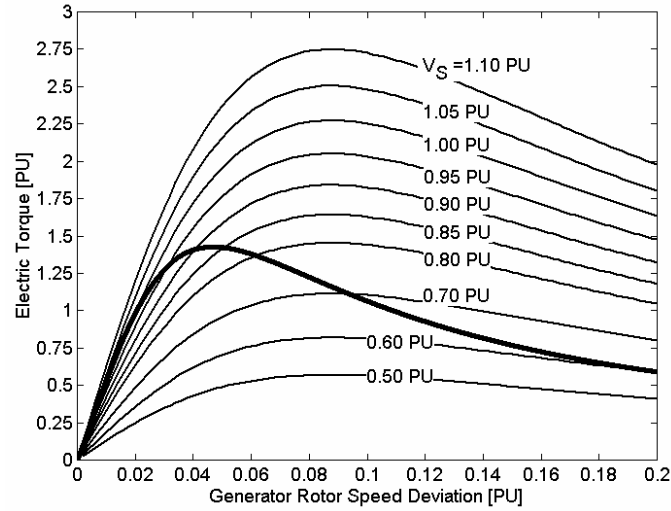


Fig. 6.1. The electric torque versus generator rotor speed curves computed at constant terminal voltages (thin solid) and of the grid-connected generator with fluctuating voltage (**thick solid**) in case of relatively strong power grid.

By inspection of the electric torque versus speed curves, it is noticed:

- 1) The kip-speed and the kip-torque are both reduced, when compared to the respective values of the curve plotted at the rated terminal voltage $V_s = 1.00$ PU.
- 2) At the generator rotor speed above the kip-speed, the electric torque decays significantly faster than in case of the electric torque computed at the rated terminal voltage.
- 3) The above-mentioned tendencies are stronger when the power grid is weaker.

At the present stage, it is kept in mind that the electric torque versus speed curves of the same induction generator will show different behaviours. This means reaching different values of (i) the kip-speed, (ii) the kip-torque and (iii) the decay rate of the electric torque at the speeds above the kip-value, when grid-connected to different power grids.

6.2. Static stability limit of induction generators

The electric torque versus speed characteristic of the induction generator grid-connected to the network shown in **Fig. 3.1.a** is plotted in **Fig. 6.2.a**. First, it focuses only on the induction generator stability, e.g. the shaft torsion is omitted. The mechanical torque, T_M , is accelerating and the electric torque, T_E , is decelerating. The electric torque versus speed characteristic is given by **Eq. (5.1)** and the mechanical torque is defined by the following relation.

$$T_M = \frac{P_M}{\omega_G} . \quad (6.6)$$

Fig. 6.2.a gives the mechanical torque versus speed curves for three operational situations which are (i) the rated operation (100 %), (ii) 75 % of the rated operation and (iii) 50 % of the rated operation. Each operational situation defines two different operational conditions of the induction generator with respect to maintaining stability. When the induction generator is, for instance, at the rated operation, the steady-state operation is only possible in the two operational points marked (1) and (2) in **Fig. 6.2.a**. In these two operational points, the accelerating torque, T_M , and the decelerating torque, T_E , are equal. When considering which torque is accelerating, respectively, decelerating, it is obvious that only the operational point (1) is stable. As can be seen, all the possible steady-state operational points must be in the range from the synchronous speed, e.g. zero speed deviation, to the kip-speed, ω_K .

In case of the induction generator operating at 50 % of the rated power, similar considerations are made. The operational points, where the decelerating, T_E , and the accelerating torque, T_M , are equal, are marked (3), when operating below the kip-speed, respectively, (4), when the speed is above the kip-speed. All the possible steady-state operational points are again in the speed range below the kip-speed, ω_K . In other words, the kip-speed, ω_K , defines the *static stability limit* of the induction generator, independently from the initial operational point. The kip- operational point is marked (K) on the electric torque versus speed curve in **Fig. 6.2.a**. Exceeding the kip-speed should result in fatal over-speeding and voltage instability.

The content of this Section is rather basic knowledge. However, the curves in **Fig. 6.2.a** show something more.

6.3. Dynamic stability limit of induction generators

Consider that the induction generator accelerates due to the grid fault. The fault can be a short-circuit fault preventing the generator from feeding the electric power, P_E , into the grid.

²⁷ $\Delta V_S/V_S = (R_{LINE}P_{LINE} + X_{LINE}Q_{LINE})/S_{SC} = (R_{LINE}(P_E - P_{LOSS}) + X_{LINE}(Q_{NL} - Q_E - Q_{LOSS}))/S_{SC}$.

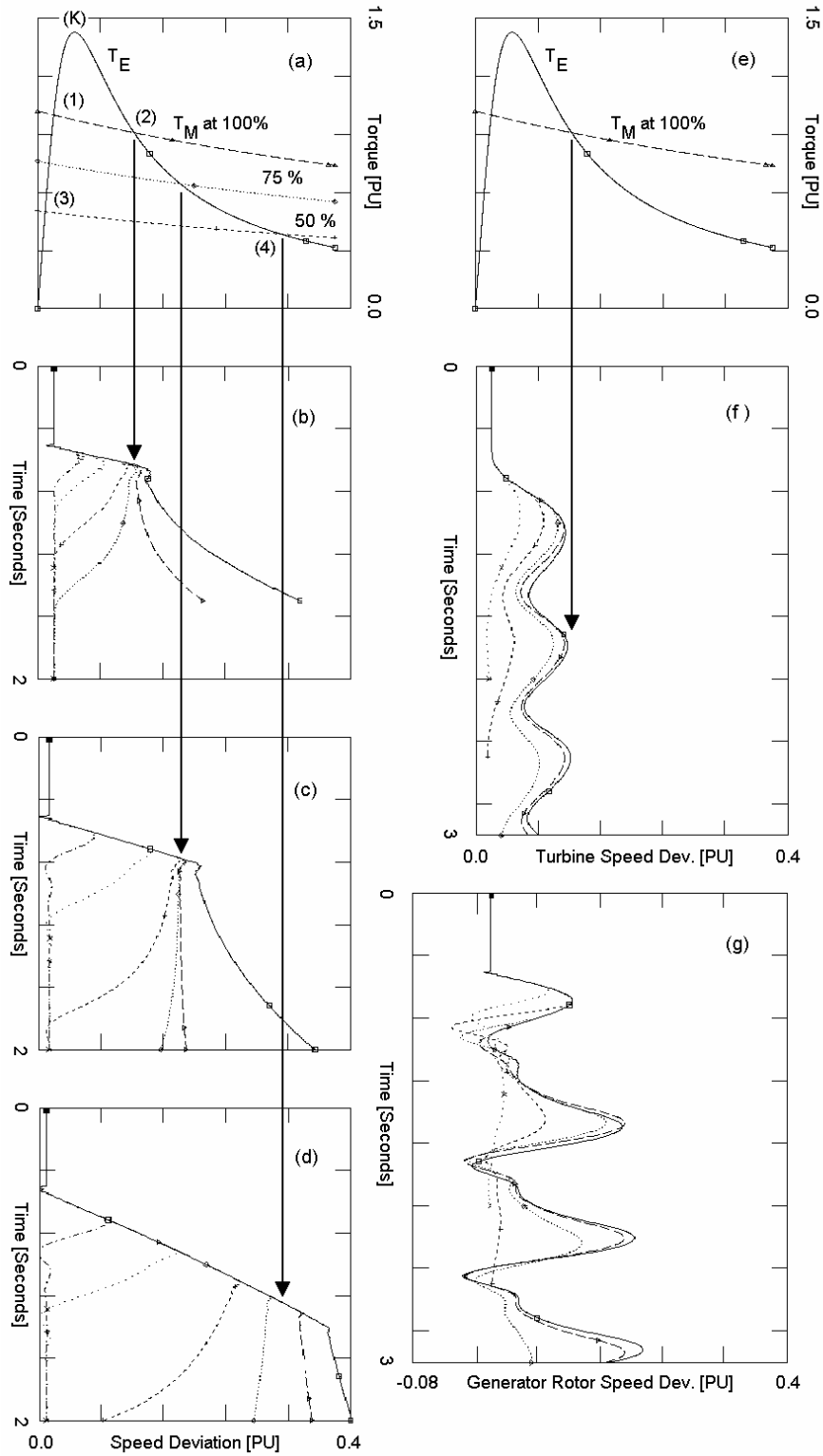


Fig. 6.2. Dynamic stability limit definition: (a) – curves of electric and mechanical torque versus speed of an induction generator at different operational conditions, (b) – generator rotor speed of an induction generator subjected to the grid fault at rated operation with $P_E = 2$ MW and $H_G = 0.5$ s, (c) – the same at 75 % of rated operation, (d) – the same at 50 % of rated operation. Dynamic stability limit in case of wind turbines: (e) – curves of electric and mechanical torque versus speed of at rated operation, (f) – wind turbine speed at the grid fault with $P_E = 2$ MW, $H_G = 0.5$ s, $H_M = 2.5$ s, $K_S = 0.3$ PU/el.rad., (g) – generator rotor speed at the same conditions.

Over-speeding of the induction generator is described by the movement equation re-written in the following form.

$$2H_G \frac{d\omega_G}{dt} = T_M - T_E . \quad (6.8)$$

When the grid fault is cleared, the induction generator will only be able to return to its regular operational point if the generator rotor speed, ω_G , does not exceed the so-called critical value of the speed, ω_{CR} . From **Eq. (6.8)**, it is obvious that the critical speed, ω_{CR} , is given by the relation.

$$T_M = T_E \Rightarrow \omega_{CR} , \quad \omega_{CR} \geq \omega_K . \quad (6.9)$$

Consequently, the critical speed, ω_{CR} , is defined by the cross-point between the curves of the decelerating torque, $T_E(\omega_G)$, and the accelerating torque, $T_M(\omega_G)$. The induction generator, when over-speeded at the grid fault, will return to its regular operational point so long as the decelerating torque, T_E , exceeds the accelerating torque, T_M . If the critical speed, ω_{CR} , is exceeded, the induction generator continues acceleration out of control. In that case, disconnection and use of emergency brake will be necessary.

By inspection of the torque curves in **Fig. 6.2.a**, it is found that the induction generator can be accelerated above the kip-speed without fatal over-speeding. The critical speed will be given by the operational point (2) in case of the rated operation before the fault occurrence. In case of 50 % of the rated operation, the critical speed is given by the operational point (4).

In other words, the critical speed of the induction generator depends of its operational point at pre-fault. The induction generators will show more stable behaviour at the grid faults at lower operational points in means of that the generators may accept more over-speeding and still remain stability. This is shown by simulations in **Fig. 6.2.b-d**. The induction generator maintains stable operation so long as the critical speed, dependent on the initial operational point, is not exceeded.

This result is in agreement with the basic knowledge that the worst case with respect to maintaining voltage stability corresponds to when the grid-connected induction generators are at the rated operation. The induction generators show quite more stable behaviour when below the rated operation. This cannot be explained in terms of the static stability limit definition.

The static stability of induction generators in terms of exceeding the kip-speed, ω_K , which is commonly applied, is insufficient for understanding of transient behaviours in electric power systems with large amount of power supply by the grid-connected induction generators.

The value of the critical speed, ω_{CR} , is firstly introduced in our work and called *the dynamic stability limit* of grid-connected induction generators (Akhmatov et al, 2000(c)). This definition is an useful tool when features on voltage stability improvement shall be found.

6.4. Dynamic stability limit of wind turbines

Now the dynamic stability limit shall be adapted to the electricity-producing wind turbines that are the two-speed systems. For this purpose, the lumped-mass equivalent of the two-mass system is required. The lumped-mass equivalent is seen as the mechanical system following the movement of the two-mass system as the integrated whole (Akhmatov et al, 2000(b)). The movement equation of the lumped-mass equivalent is derived from the two-mass system **Eqs. (2.9)**.

$$2(H_M + H_G) \frac{d\omega_L}{dt} = T_M - T_E, \quad \omega_L = \frac{H_G \omega_G + H_M \omega_M}{H_G + H_M}, \quad (6.10)$$

with the lumped inertia constant $(H_M + H_G)$ and the speed of the lumped-mass equivalent ω_L .

Often, the turbine inertia constant, H_M , is much larger than the inertia constant of the generator rotor, H_G . Therefore the lumped-equivalent speed can be reduced to the turbine speed.

$$\omega_L \approx \omega_M. \quad (6.11)$$

This implies that the critical speed, ω_{CR} , which defines the dynamic stability limit of the grid-connected wind turbines, might be viewed with respect to the turbine speed, ω_M , rather than with respect to the generator rotor speed, ω_G . This correction corresponds to adapting the dynamic stability limit definition, originally derived for the grid-connected induction generators, to case of wind turbines.

The simulations shown in **Fig. 6.2.e-g** illustrate this. As can be seen, the generator rotor speed, ω_G , may exceed the critical speed, ω_{CR} , without any consequences for fatal over-speeding and so with respect to maintaining of transient voltage stability. Fatal over-speeding and, hence, voltage instability occur first when the wind turbine speed, ω_M , approaches the critical speed, ω_{CR} .

It is noticed that instability occurs at *the second swing* of the turbine speed, ω_M , but not at the first swing just after the fault clearance. This example illustrates a clear difference between the over-speeding mechanism of the wind turbines, which are the two-mass systems, and over-speeding of the induction generators.

In other words, it is, shortly after the fault clearance, rather not say whether the fault will lead to fatal over-speeding of the wind turbine. The fatal over-speeding will first manifest itself at the second swing in the behaviours of (i) generator rotor speed, ω_G , (ii) turbine speed, ω_M , (iii) terminal voltage, V_S , etc. This mechanism relates to the shaft relaxation process.

6.5. Shaft relaxation process

Over-speeding of the wind turbines cannot be described in terms of the dynamic stability limit definition alone. It is because the other mechanism contributing to more acceleration of the drivers also plays a part. This is the shaft relaxation process. Influence of this mechanism on the wind turbine over-speeding and maintaining voltage stability is first explained in our work (Akhmatov et al, 2000(b)).

The potential energy accumulated by the pre-twisted shaft with the stiffness K_S is

$$W_S = \frac{1}{2} K_S \theta_S^2 = \frac{1}{2} \frac{T_M^2}{K_S}, \quad (6.12)$$

considering θ_S to be the initial twist of the shaft. The kinetic energy of the rotating two-mass system, at pre-fault conditions, is given by the relation.

$$E = H_M \omega_M^2 + H_G \omega_G^2, \quad (6.13)$$

where ω_M and ω_G denote the initial values of the turbine speed and the generator rotor speed, respectively. When applying the energy conservation before and after the grid fault,

$$(W + E)_{BEFORE} = (W + E)_{AFTER} , \quad (6.14)$$

the following assumptions are made additionally (Akhmatov et al, 2000(b)).

- 1) An almost complete relaxation of the shaft during the fault, which implies that the shaft twist is reduced to zero.
- 2) The inertia of the turbine is much larger than the generator rotor inertia. When the grid fault is short enough, so the turbine speed does not reach to be affected during the faulting time.
- 3) Only the light generator rotor will be affected at the grid fault of a short duration, so its speed is increased by $\Delta\omega_G$.

The energy conservation **Eq. (6.14)** leads to the following.

$$H_M \omega_M^2 + H_G \omega_G^2 + \frac{1}{2} K_S \theta_S^2 = H_M \omega_M^2 + H_G (\omega_G + \Delta\omega_G)^2 + 0. \quad (6.15)$$

Combining **Eqs. (6.12)** and **(6.15)**, the increase of the generator rotor speed by the shaft relaxation process can be expressed by the relation.

$$\Delta\omega_G \sim \frac{T_M^2}{H_G K_S}. \quad (6.16)$$

This relation²⁸ demonstrates that the shaft relaxation contributes to more acceleration of the generator rotor at the grid faults. The lower shaft stiffness is, the larger acceleration of the generator rotor is expected at the grid fault.

The speed of the induction generator rotor with the inertia constant $H_G = 0.5$ s and the generator rotor speed and the turbine speed of the wind turbine with $H_G = 0.5$ s, $H_M = 2.5$ s and $K_S = 0.3$ PU/el.rad., computed in **Section 4**, are plotted in the same scale in **Fig. 6.3**. As seen, the assumption of unchanged turbine speed, ω_M , during the fault of a short duration is fair. The generator rotor is more accelerated in case of the wind turbine than in case of the induction generator alone. It is due to the shaft relaxation process during the fault in case of the wind turbine. This mechanism is not present in case of the induction generator (the lumped-mass) only.

This mechanism contributes to more acceleration of the wind turbine as the integrated whole as well that is important when investigating power system stability.

Importance of the shaft relaxation mechanism for the over-speeding process (and so for transient voltage stability) has first been explained in our work (Akhmatov et al, 2000(b)). Later, the same explanation is given by (Salman and Teo, 2003).

²⁸ This relation is not exact, but sufficient for showing that more acceleration depends on the shaft stiffness. For a correct computation, the losses mechanisms shall be included.

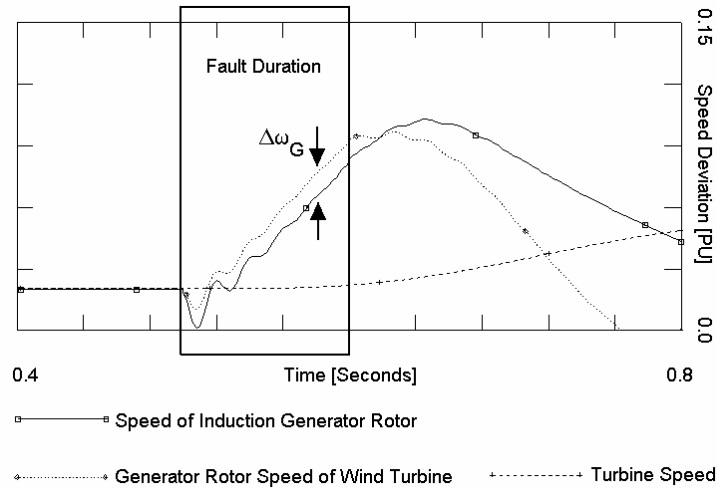


Fig. 6.3. More acceleration of the generator due to the shaft relaxation process in wind turbines.

6.6. Consequence of dynamic stability limit

Instability of grid-connected induction generators as well as the wind turbines equipped with such generators relates unambiguously to risk of fatal over-speeding at the grid faults. Definition of the dynamic stability limit can be applied to suggest technical requirements and arrangements applied onto (i) the power grid, (ii) the wind turbine construction and (iii) their controllability for improving voltage stability.

Prevention of fatal over-speeding can be in any cases reached by increasing the critical speed, ω_{CR} , at the given operational point. Such technical requirements are explained in the following.

6.7. Simulation case with large wind farm

For improving transient voltage stability, the technical requirements can be applied on the grid side as well as on the wind farm side of the system. Such requirements are demonstrated by simulations. The model of the large offshore wind farm with eighty 2 MW fixed-speed, active-stall-controlled wind turbines equipped with no-load compensated induction generators is applied. The wind farm model is described in **Section 5.1**.

This wind turbine concept is chosen because the wind technology in offshore sites must be robust, developed and known from previous practical applications. The wind turbine concept with induction generators has been in operation in on-land sites in Denmark during many years. Therefore it is considered that this concept is also suitable for offshore applications. The Rødsand /Nysted offshore wind farm which has been constructed in eastern Denmark in the year 2003 consists of the fixed-speed, active-stall wind turbines from the Danish manufacturer Bonus Energy.

The wind distribution over the wind farm area is considered irregular and leads to the power production pattern as shown in **Fig. 6.4**. The irregular wind distribution over the wind farm area is assumed because the wind turbines are shadowing each other for incoming wind. The efficiency of the wind farm is 93% at the given wind distribution and the wind farm supplies approximately 150 MW to the power grid at the connection point. In normal operation, the wind farm is reactive neutral with the power grid, according to the Danish specifications (Eltra, 2000).

voltage instability is the result of the short-circuit fault with the following over-speeding of the wind turbines.

According to the Danish specifications, subsequent disconnection of large offshore wind farms is not acceptable. This shall be achieved by two arrangements.

- 1) Ensuring voltage recovery after the grid fault (Akhmatov et al, 2003(a)).
- 2) Adjusting relay settings so unnecessary trip is avoided (Akhmatov et al, 2001).

First, all the simulations are made under *consideration* that the relay settings are so that no subsequent disconnection occurs. Adjusting relay settings will be, then, treated in **Section 6.15**.

6.8. Voltage instability when no arrangements

The blade-angle control is originally developed and applied for power output optimisation by incoming wind. The power grid stability requirements are not necessarily taken into account. An example on this feature is when the control signal to the blade angle control is the electric power, $X = P_E$, and the reference signal is the reference power, $X_{REF} = P_{REF}$, which is defined in accordance to incoming wind, V , (Hinrichsen, 1984; Akhmatov, 2001).

When a short circuit fault occurs in the external network, the voltage, V_S , and so the electric power, P_E , supplied by the induction generator are reduced. The regular control system of active-stall will, presumably, interpret this as lack of electric power and try to increase or maintain the mechanical power (keeping β_{REF} at β_{OPT} if in optimised position already or tracking β_{REF} to β_{OPT}). This action, with keeping the reference angle and so keeping the pitch angle, β , at its value before the grid fault occurrence, corresponds to fixed-pitch operation (stall-controlled wind turbines). Furthermore, tracking the reference angle, β_{REF} , and the actual pitch angle, β , to the optimised position, β_{OPT} , can lead to even larger acceleration of the wind turbines (Akhmatov, 2001). This is thinkable when operating at the wind above the rated wind.

From this viewpoint, it is considered that active-stall wind turbines can simply be represented as stall-controlled wind turbines in investigations of transient voltage stability.

As the basis case with respect to data of the offshore wind turbines, the rotor winding resistance is $R_R = 0.020$ PU, the generator inertia is $H_G = 0.5$ s, the turbine inertia is $H_M = 2.5$ s, and the shaft stiffness is $K_S = 0.3$ PU/el.rad²⁹. If no dynamic reactive compensation is applied, the grid fault will result in voltage instability, see **Fig. 6.5**.

So long as the wind turbines are grid-connected, the fluctuations of the generator rotor speed, the terminal voltage and other parameters registered at the different wind turbines in the wind farm are “in-phase”, but not against each other. This is denoted as the coherent response. The natural frequency of the fluctuations is the shaft torsion mode.

²⁹ Not-mentioned data are as in **Appendix 4.A**.

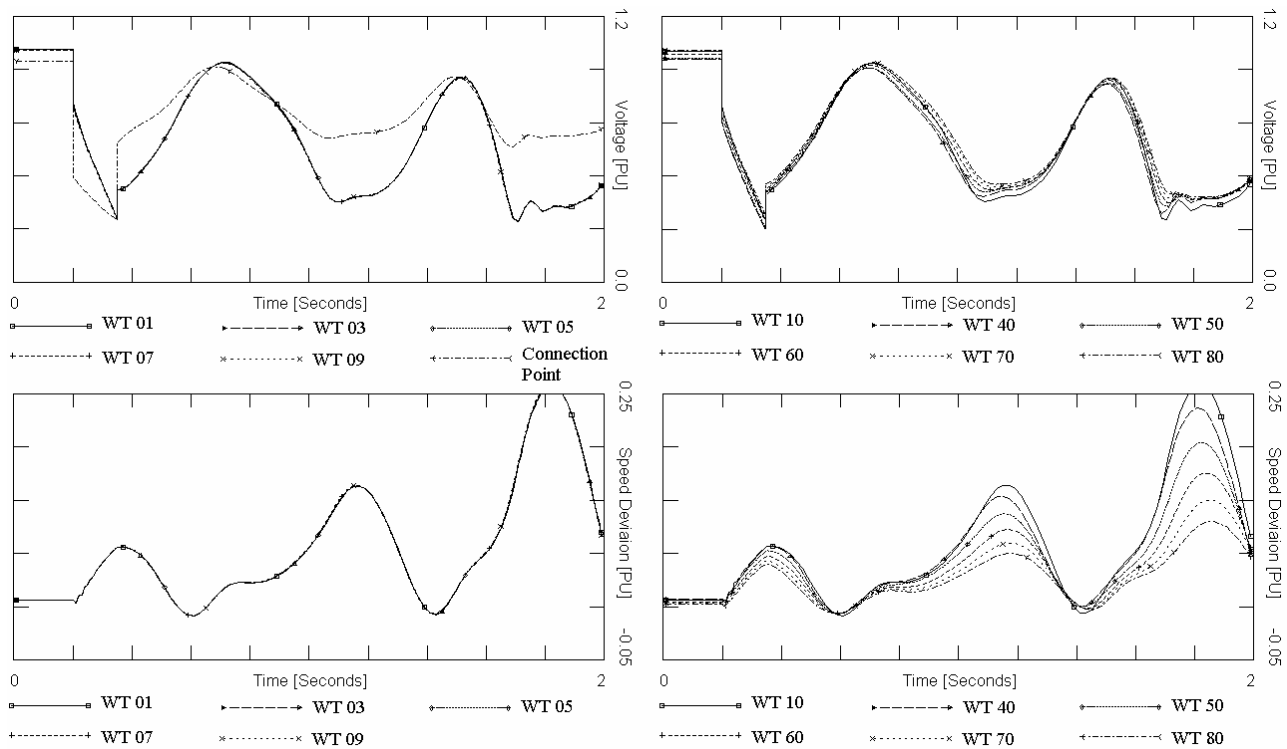


Fig. 6.5. Coherent response of wind farm to the grid fault – fatal over-speeding and voltage instability in case of no arrangements. Reported in (Akhmatov et al, 2003)

Notice that voltage instability will probably not reach to develop to voltage collapse. The wind turbines are with they protective relays, which will disconnect the wind farm at registering of uncontrollable voltage decay. After this subsequent trip, the voltage re-establishes, but immediate power reserves of approximately 150 MW will be required. Voltage collapse does not occur, but disconnection of the large wind farm implies that the solution chosen does not comply with the Specifications of the TSO (Eltra, 2000).

6.9. Use of dynamic reactive compensation

Dynamic reactive compensation of the large wind farm can be organised in several ways. This depends on (i) the factual demands of reactive compensation for voltage re-establishing, (ii) controllability of the equipment and (iii) the cost. When the success criterion is to get the voltage re-establishing within the pre-defined range, e.g. avoid uncontrollable voltage decays as well as over-voltages in the grid, the dynamic reactive compensation can be capacitive or inductive. So long as no disconnection of the wind turbines occurs and the grid-connected induction generators absorb reactive power during voltage re-establishing process, the dynamic reactive compensation should be capacitive. The following equipment can be chosen.

- 1) Synchronous condenser (SC), which is a synchronous machine running without a prime mover or a mechanical load (Taylor, 1994; Kundur, 1994). The reactive power output of this device is controlled by the field excitation and using a voltage regulator, the SC can

automatically adjust the reactive power exchange with the grid to maintain constant terminal voltage.

- 2) Static var compensator (SVC), which is a number of shunt-connected capacitors generating and reactors absorbing reactive power and whose outputs are co-ordinated (Taylor, 1994; Noroozian et al, 2000; Barocio and Messina, 2003). The term “static” indicates that the device contains no moving or rotating components.
- 3) Statcom, which is the voltage source converter controlled by the power electronics with IGBT-switches (Søbrink et al, 1998). In some publications, this unit can also be termed as a static synchronous compensator (Noroozian et al, 2000).

Depending on the factual demands to reactive power controllability, the compensation units can be organised with continuous control, discrete control or as a combination of those both (Kundur, 1994; Akhmatov and Nielsen, 2001). SC and Statcoms are continuous control units. SC are characterised by relatively high running and maintenance cost because of presence of the rotating and moving parts (Taylor, 1994), whilst Statcoms are relatively expensive feature, but with lower running cost. Reactive power control with SVC can be organised in several ways, which influences on the feature cost as well.

- 1) As a continuous reactive power control unit using thyristor-controlled reactors, which is a relatively expensive feature.
- 2) As a discrete control unit with a number of thyristor- or mechanically switched capacitors and reactors, which is a relatively cheap feature.
- 3) As a combination of discrete and continuous units, where the cost of the feature is optimised knowing the factual demands of the reactive power demands from power stability investigations.
- 4) In a practical solution, a number of already exciting shunt-capacitors and reactors in the near power grid can be ordered to switch on or off by the control system of the SVC for expanding its controllability and reducing the cost of the project.
- 5) The running cost of SVC is lower than the running cost of SC, but the continuously controlled SVC can be a more expensive feature than SC (Taylor, 1994).

In this Section, the demands of reactive power control for voltage re-establishing in the large wind farm is examined. The results are explained in the following cases.

- 1) When the SVC unit is applied. The SVC is with continuous reactive power control.
- 2) A less number of computations are made with use of the Statcom model³⁰.
- 3) When the SC is applied. The excitation control of the SC is given by the schemes applied at the two Danish power plant units that are ASV1 and ASV3, respectively. This is made for

³⁰ The models of SVC and Statcom are both implemented as user-written models into the simulation tool PSS/E at NESA in co-operation with the manufacturer ABB. From this viewpoint, those models are exact, but not generic. This work is originally documented in (Noroozian et al, 2000) and documentation is omitted here.

comparison between different control systems of SC. The models of ASV1 and ASV3, the generator data, the excitation control schemes and their respective data are kindly given by the company NESA for this project.

This investigation is reduced to estimation of the factual demands of dynamic reactive power compensation in case of the wind farm with the default data set and fixed-pitch. The cost optimisation in terms of replacing a part of continuous reactive power control by discrete components is not the target of this investigation, although this feature shall be kept in mind in practical solutions.

It is found that for voltage re-establishing after the short-circuit fault, it will be necessary to apply a continuous SVC unit of 100 MVar. Use of an SVC unit with a less capacity results in uncontrollable voltage decay or in insufficiently damped voltage oscillations, indicating voltage instability and will result in disconnection of the wind farm. The simulated curves of the voltage and the generator rotor speed are given in **Fig. 6.6** and **Fig. 6.7**.

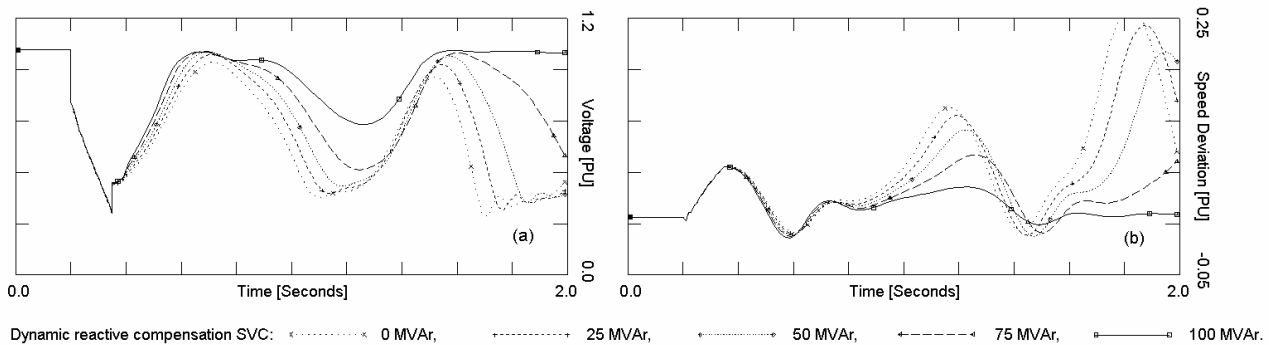


Fig. 6.6. Amount of dynamic reactive compensation with SVC versus voltage recovery: (a) – terminal voltage of the wind turbine WT 01, (b) – generator rotor speed of WT 01.

In this investigation, it is found that the SC to be used for voltage re-establishing after the grid fault shall be in the same range of power capacity as found in case of the SVC. This indicates that the SC and the SVC have similar controllability with respect to voltage control at the grid faults (Akhmatov et al, 2001), although a number of differences in their voltage control principles.

Notice that the voltage drop at the terminals of and the acceleration of the wind turbine generators during the grid fault are lower when using the SC. It is because the SC, contrarily to the SVC, supplies a significant amount of reactive power during the fault. The SC can generate voltage at its terminals – the ability knowing from operation of synchronous generators.

The SVC is, however, only able to control the voltage which is not too low. When voltage is too low, the SVC reaches its boost limit and so operation of the SVC can be compared to operation of a shunt capacitor with $Q_C = X_C V_S^2$ (Taylor, 1994). Normally, the capacitors of SVC will be protected against discharging at insufficiently low voltage.

The voltage profile depends on the control scheme of the SC and its data, which is illustrated in **Fig. 6.8**. As can be seen, the voltage recovers faster in case of the control scheme of ASV1 than in case of ASV3. The explanation is that the control system ASV1 reacts faster on changes of the

terminal voltage than the control system ASV3. This result demonstrates that the voltage behaviour depends on the power capacity of dynamic reactive compensation as well as on the control system.

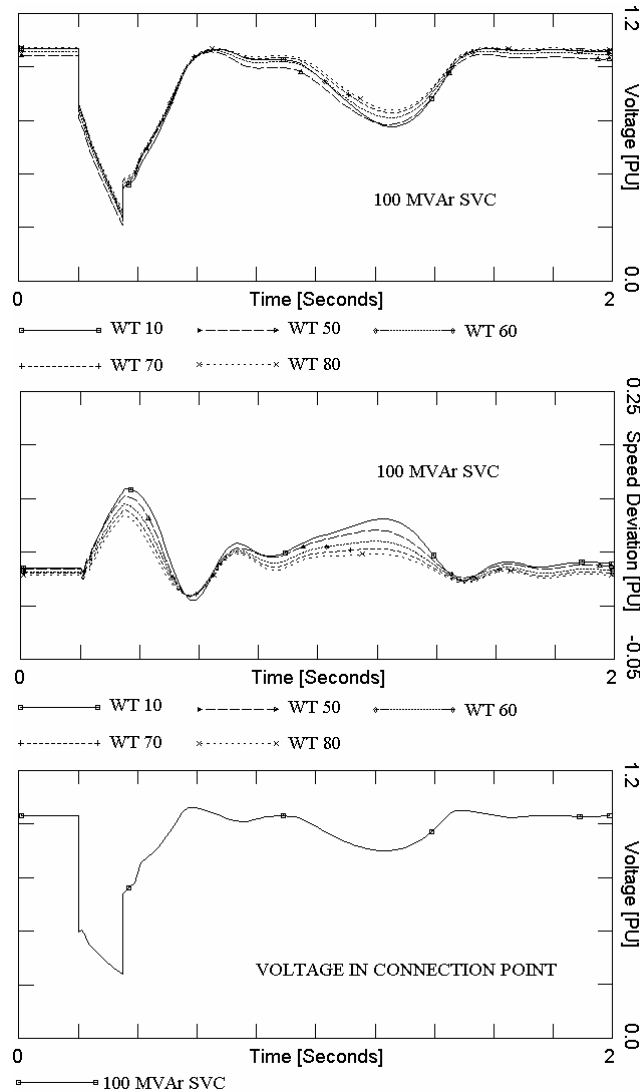


Fig. 6.7. Voltage and generator speed coherent fluctuating behaviours. When the SVC unit of 100 MVar is used, the voltage is re-established. Reported in (Akhmatov et al, 2003).

Finally, using the Statcom in place of the SVC or the SC, an unit with a lower power capacity can be applied to maintain transient voltage stability. It is found that the voltage recovers when the power capacity of the Statcom is in the range of 75 MVar. However the Statcom is the most expensive feature among the discussed above. Reduction of the reactive power demands is not sufficiently significant. Presumably, choosing the Statcom of a lower power capacity instead of the SVC unit will not bring significant benefits in this case. The running cost of the SVC and the Statcom are considered similar due to the both kind of equipment is without rotating or moving parts (Taylor, 1994).

Relatively higher running and maintenance cost of the SC comparing to case of the SVC shall be kept in mind. Resuming that the SVC and the SC units to be incorporated are of similar power capacities, the SVC unit will probably be chosen for maintaining of transient voltage stability of the

large wind farm. The investigations will be continued using the SVC unit as dynamic reactive compensation feature, and its rated capacity is 100 MVar in case of the wind farm with the default data.

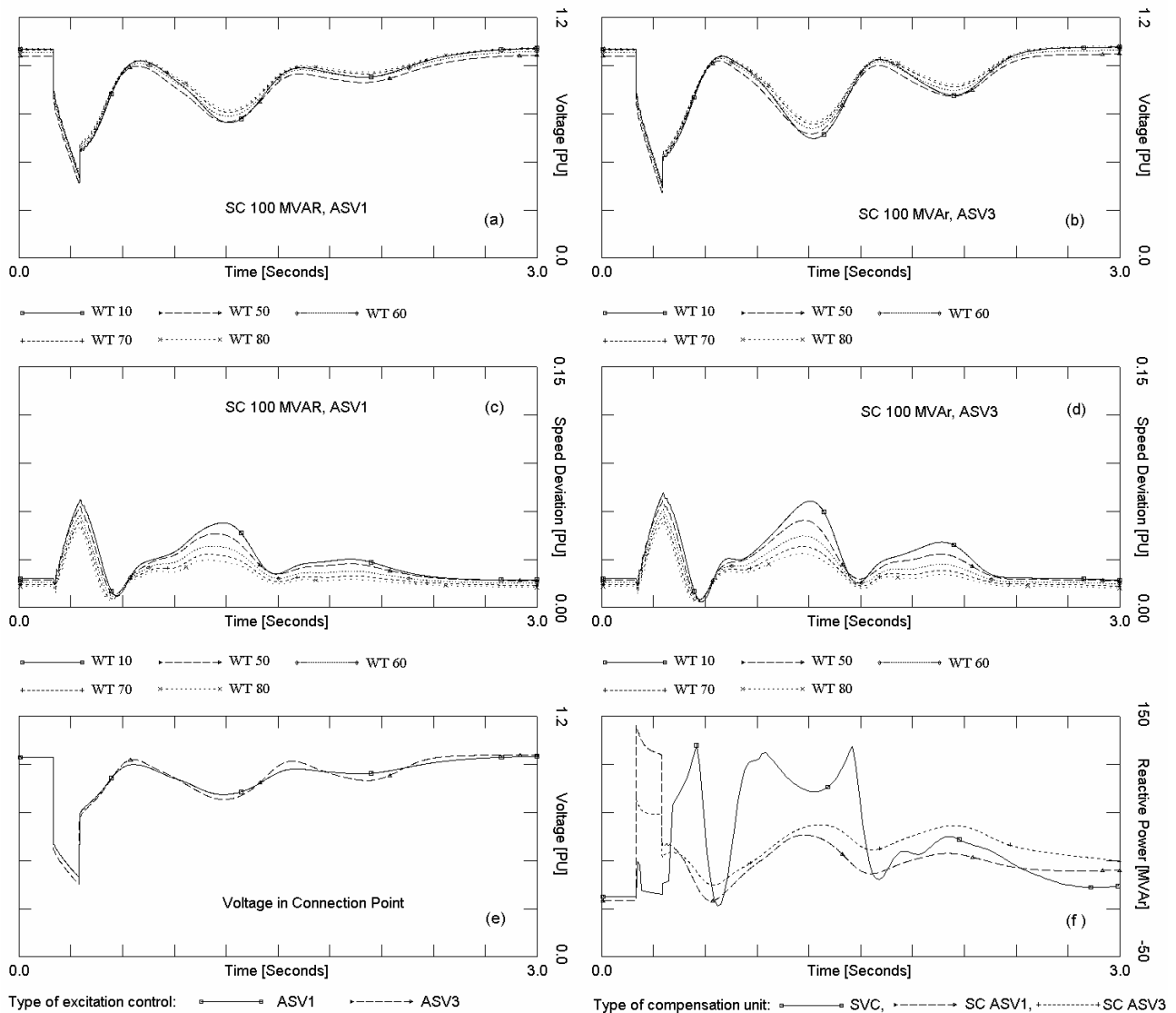


Fig. 6.8. Use of SC for dynamic reactive compensation of the large wind farm: (a), (b) – voltages of selected wind turbines in the farm using the excitation control ASV1, respectively, ASV3, (c), (d) – generator rotor speeds of selected wind turbines using the excitation control ASV1, respectively, ASV3, (e) – voltage in connection point using the excitation control ASV1, respectively, ASV3, (f) – reactive power supplied to the grid from the compensation unit.

Although the wind turbine generators have different initial operational points, the wind turbines show a coherent response at the failure event in the external network. This is because the fluctuations of the voltages and the speeds of the different wind turbines in the farm are “in-phase”. This conclusion is identical to the conclusion found in the previous Section. It is also noticed that use of dynamic reactive compensation units with their control systems does not lead to excitation or operation destabilisation of the large wind farm. Even in case of grid disturbances, no mutual oscillations between the wind turbines or between the wind turbines and the dynamic reactive compensation units are seen.

6.10. Generator parameters versus voltage stability

In terms of dynamic stability limit, use of dynamic reactive compensation means “lifting-up” the electric torque versus speed characteristic in the speed range above the rated speed. This can be understood when considering that the electric torque versus speed characteristic of the induction generator, shown in **Fig. 6.1**, will follow the curve computed for $V_s = 1.0$ PU in the speed range above the kip-speed. This leads to expanding of the critical speed value, ω_{CR} , and hence to improving of transient voltage stability.

Behaviour of the electric torque versus speed characteristic depends on the induction generator parameters such as the stator resistance, the stator reactance, the magnetising reactance, the rotor resistance and the rotor reactance. As demonstrated in (Akhmatov et al, 2000(c)), expanding of the critical speed value can be reached by choosing the parameters of the induction generator according to the following.

- 1) The values of the stator resistance, R_s , the stator reactance, X_s , the magnetising reactance, X_M and the rotor reactance, X_R , are reduced.
- 2) The value of the rotor resistance, R_R , is increased.

This conclusion can simply be reached using **Eqs. (6.1)** and **(6.2)** for the electric torque versus speed characteristic of the induction generator with varying generator parameters. Expanding the critical speed will *always* lead to improving voltage stability (Akhmatov et al, 2000(c)). In this presentation, this is demonstrated by simulations with an increased value of the rotor resistance, R_R . Expanding of the critical speed of the wind turbine at increasing the rotor resistance, R_R , is graphically illustrated in **Fig. 6.9**. Increasing the rotor resistance by the ratio of 2, as in the given example, leads to significant expanding of the critical speed, ω_{CR} . Consequently, the demands of dynamic reactive compensation may be reduced significantly (Akhmatov et al, 2003(a)).

When the rotor resistance is $R_R = 2 \cdot R_{R0} = 0.040$ PU, it will only be necessary to incorporate the SVC unit of 25 MVar instead of 100 MVar (found in simulation case with the default rotor resistance of $R_{R0} = 0.02$ PU). Selected simulation curves with the 25 MVar SVC unit are shown in **Fig. 6.10**. The demands of dynamic reactive compensation are reduced significantly. On the other hand, this solution leads to increasing the power losses in the rotor circuit, according to $P_R = R_R I_R^2$, when the power system is also in normal (undisturbed) operation.

Influence of the induction generator parameters on the voltage profile after a short circuit fault is illustrated by examples collected in **Appendix 6.A**.

6.11. Enforcing mechanical construction

A common opinion is that the higher inertia of the rotating system is, the more stable operation is expected in the power system in post-fault operational situations. In terms of the dynamic stability limit given in **Section 6.4**, the inertia does not influence on the wind turbine critical speed. Consequently, two wind turbines with identical generator data and only different inertias H_{M1} and H_{M2} , where $H_{M1} > H_{M2}$, have the same critical speed values $\omega_{CR1} = \omega_{CR2}$.

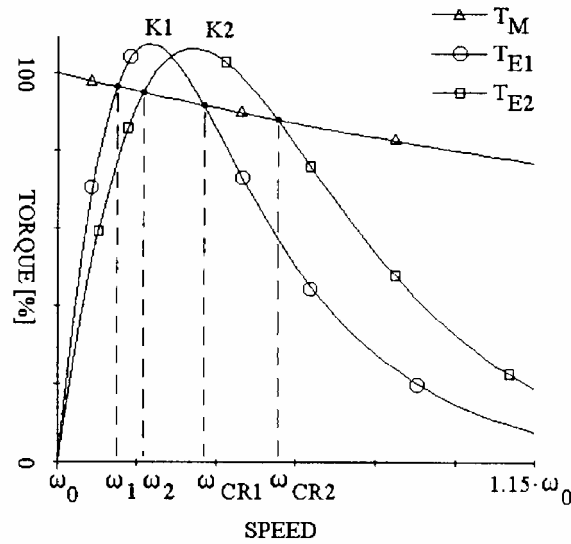


Fig. 6.9. Dynamic stability improvement by increasing the value of the rotor resistance, R_R . The curve marking is T_M – the mechanical torque, T_{E1} – the electric torque with $R_R = R_{R0}$, and T_{E2} – the electric torque with $R_R = 2 \cdot R_{R0}$. When $R_R = R_{R0}$, the wind turbine can operate within the speed range from its initial speed, ω_1 , to the critical speed, ω_{CR1} , without loss of stability. When the rotor resistance is $2 R_{R0}$, the stable operation range is expanded to be from the initial speed, ω_2 , to the critical speed, ω_{CR2} . $K1$ and $K2$ are marking the kip-torque of these wind turbine generators, respectively. Reported in (Akhmatov et al, 2003(a)).

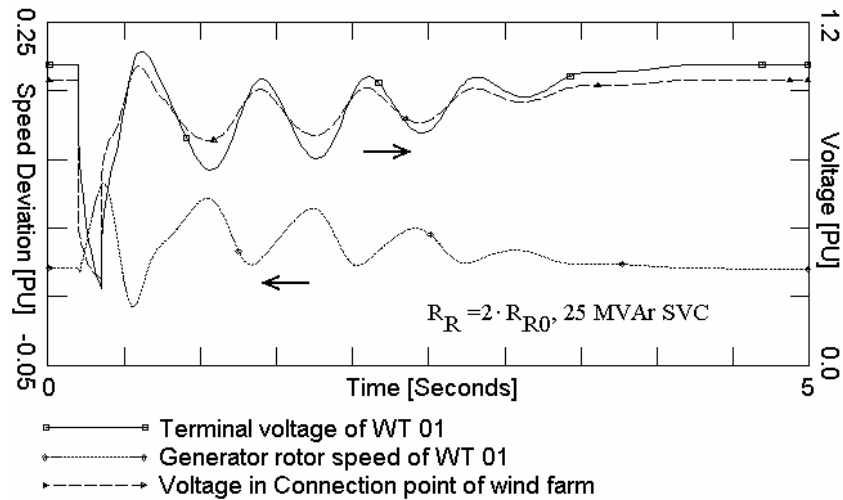


Fig. 6.10. Voltage and generator rotor speed in case with increased value of the rotor resistance. Reported in (Akhmatov et al, 2003(a)).

Due to different inertia values, the wind turbines will accelerate differently at the transient event. Thus, these two wind turbines will have the different values of the critical failure times. The critical failure time, t_{CR} , is defined as the time of the grid fault where the wind turbine still maintains stable operation after the fault is cleared.

Obviously, the heaviest wind turbine has the largest critical failure time $t_{CR1} > t_{CR2}$. Because of this, the heavy wind turbines show more stable behaviour compared to light wind turbines, so long as the failure time is not too long. In practical situations, the failure time is relatively short and the

heavy wind turbines will be preferred with respect to maintaining transient voltage stability (Akhmatov et al, 2000(c)).

Wind turbines are equipped with the shaft systems where the effective shaft stiffness, K_S , is relatively low when viewed from the generator terminals (Hinrichsen and Nolan, 1982). In normal operation, there will be accumulated an amount of potential energy in the pre-twisted shafts (Akhmatov et al, 2000(b)). According to the description of **Section 6.5**, the lower shaft stiffness is, the more potential energy is accumulated in the pre-twisted shafts. At the short circuit fault, the shafts are relaxing and the potential energy is disengaged into the generator rotor kinetic energy. This process results in more intense acceleration of the generator rotor.

The contribution from the shaft systems to more acceleration of the generator rotor is opposite-proportional to the shaft stiffness, K_S . Consequently, increase of the shaft stiffness, K_S , leads to reduction of the wind turbine over-speeding at grid faults and so improvement of transient voltage stability. This is illustrated in **Fig. 6.11**. This conclusion is reached in accordance to the dynamic stability limit, when setting mechanism of transient voltage instability relates to fatal over-speeding of wind turbines.

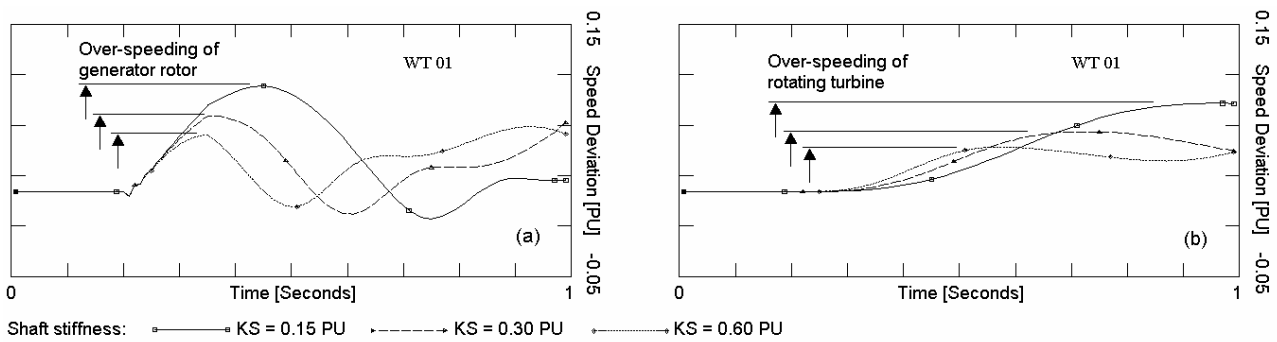


Fig. 6.11. Wind turbine over-speeding at a short circuit fault, $H_M=2.5$ s, $H_G=0.50$ s, and varying shaft stiffness K_S : (a) – generator rotor speed, (b) – turbine speed. No dynamic reactive compensation is used. Reported in (Akhmatov et al, 2003(a)).

Mechanical construction parameters		Dynamic reactive compensation, MVar
H_M , s	K_S , PU/el.rad	
2.5	0.30	100 (default case, Section 5.9)
2.5	0.15	125
2.5	0.60	50
4.5	0.30	50

Table 6.1. Demands of dynamic reactive compensation (SVC) versus wind turbine mechanical parameters, $H_G=0.50$ s. Reported in (Akhmatov et al, 2003(a)).

The simulation results dealing with dynamic reactive compensation demands at varying parameters of the wind turbine mechanical construction, H_M and K_S , are collected in **Table 6.1**. Enforcement of the wind turbine mechanical construction has a significant positive effect on improvement of transient voltage stability.

6.12. Blade-angle control acting at grid faults

In terms of the dynamic stability limit, transient voltage stability of the grids with wind turbines can be improved by a temporary reduction of the wind turbine mechanical power during and shortly after the fault (Akhmatov, 2001). The idea behind this principle is illustrated by **Fig. 6.12**.

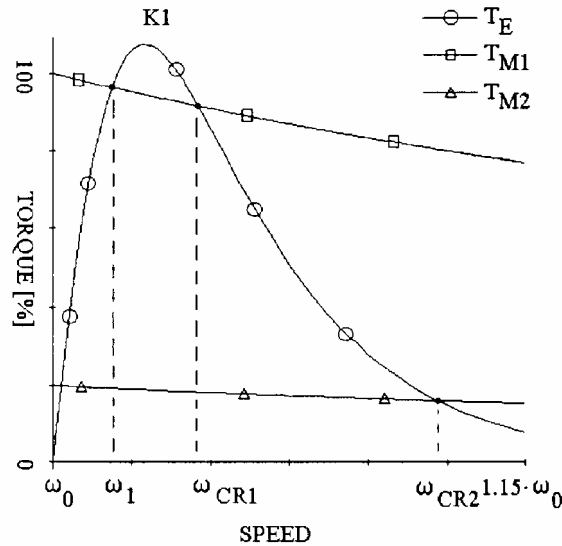


Fig. 6.12. Dynamic stability improvement by mechanical power reduction during and shortly after the grid fault. The curve marking is T_E – the electric torque, T_{M1} – the mechanical torque at rated (100%) operation, and T_{M2} – the mechanical torque at 20% operation. When the wind turbine is at the rated operation, its dynamic stability limit is given by the critical speed, ω_{CR1} . When the wind turbine is ordered to reduce its mechanical power, its dynamic stability limit is expanded to the critical speed, ω_{CR2} . Reduction of the mechanical torque leads to less acceleration of the wind turbines and works as protection against over-speeding as well. $K1$ is marking the kip-torque of the wind turbine induction generator. Reported in (Akhmatov et al, 2003(a)).

Reduction of the mechanical power of the wind turbine can be achieved by the blade-angle control. The generic blade-angle control system is discussed in **Section 3**. The modern wind turbines for large offshore wind farms are already equipped with blade-angle control. The fixed-speed wind turbines with induction generators are equipped with active-stall control (rather than with pitch control). This investigation focuses on use of active-stall control, whereas the results of (Akhmatov, 2001) are reached with use of pitch control.

It is kept in mind that the idea behind active-stall control is the power output optimisation in relation to incoming wind. The regular control system of active-stall applies the electric power, $X = P_E$, as the input signal. As explained in **Section 6.8**, the regular control system of active-stall cannot always be used to improve transient voltage stability. This is because the active-stall wind turbines will operate as fixed-pitch wind turbines during the grid fault. Several modifications of the control system of active-stall should be necessary to achieve the goal of improving transient voltage stability. Such modifications can be the following (Akhmatov et al, 2003(a)).

- 1) Use of alternative input signals, X , to the regular control system.

- 2) Temporary disabling of the regular control system and changing to another control strategy.

6.12.1. Blade angle control – Use of alternative signals

First, it focuses on application of alternative input signals to the (regular) active-stall control system. Among such signals can be the generator rotor speed, because the voltage instability relates to over-speeding of the wind turbines. Second, the signals relating to the electric power grid can also be applicable.

When the generator rotor speed, ω_G , is used as the input signal to the blade angle control system, it can be necessary to add a proportional-differential (PD) controller to the regular control system, see **Fig. 3.2**. This is for getting a better sensitivity of the error signal, $X_{ERR} = \omega_{ERR}$, (Akhmatov et al, 2003(a)), because the generator rotor speed of fixed-speed wind turbines may only vary in the range of few percents. The simulation results with this control feature are given in **Fig. 6.13**.

The other feature is with use of the input signals with relation to the power grid. These signals may contain the terminal voltage, V_S , or the voltage measured at the connection point of the wind farm (Akhmatov et al, 2003(a)). In the power grid, there are always natural voltage fluctuations, for instance, flicker. The blade-angle control system shall be selective. It may not be affected by such voltage fluctuations at normal (undisturbed) operation. For this purpose, the dead-band around the nominal voltage $V_S = 1.0$ PU with V_{DMIN} and V_{DMAX} is used (Akhmatov et al, 2003(a)). The values of V_{DMIN} and V_{DMAX} are set to -0.10 PU and 0.10 PU, respectively, in this investigation.

On the other hand, the voltage is not the value which can be applied to optimise the power output. Therefore, more complex input signals to the blade-angle control system should be applied. The reference signal should be $X_{REF} = P_{REF}$, whereas the controlling signal is $X = P_E / V_S^2$. This feature is suggested due to the following considerations.

- 1) Optimisation of the wind turbine power will be reached at normal operation (remember the dead-band in the measured voltage signal).
- 2) When the voltage is below V_{DMIN} , this indicates that the power grid can be at abnormal operation and the wind turbines shall reduce their mechanical power to stabilise the wind farm.
- 3) The voltage in the denominator, V_S , is in square because the electric power, P_E , is proportional to the terminal voltage squared, **Eqs. (6.1)** and **(6.2)**. In this way, the reference signal, X_{REF} , is compensated for the voltage drop during the short circuit fault.

This feature seems to be closer to the commonly used, where the reference signal is $X_{REF} = P_{REF}$. The exception will only be that the voltage – the value with relation to the power grid – is included in the input signal of the blade-angle control system. The simulation results with use of the additional voltage signal producing the input signal are shown in **Fig. 6.14**.

As can be seen, the voltage is re-established without use of dynamic reactive compensation. This is because the controllability of the active-stall control is sufficient to maintain transient voltage stability, in this case. An accurate tuning of the active-stall control system is essential. With the parameters of the active-stall control system used in these investigations, no mutual

interaction between the wind turbines is seen and the collective response of the wind turbines to the grid fault is coherent.

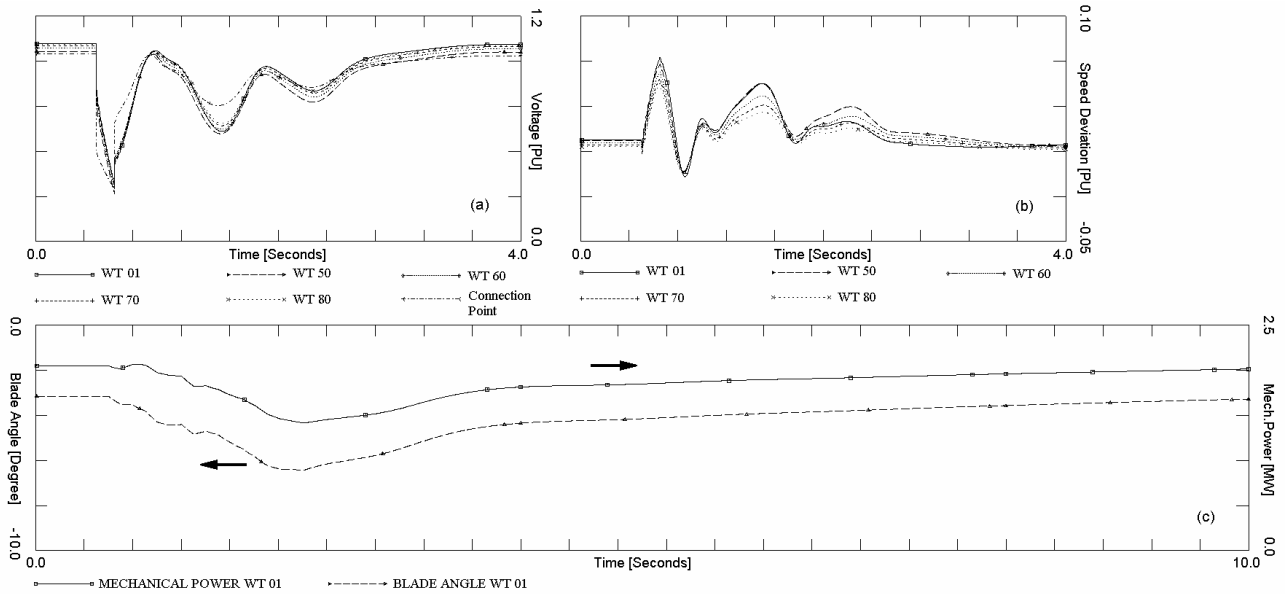


Fig. 6.13. Voltage re-establishing after a short circuit fault in the wind farm with active-stall wind turbines controlled by the generator rotor speed: (a) – terminal voltage of selected wind turbines and in connection point, (b) – generator rotor speed of selected wind turbines, (c) – mechanical torque and the blade angle of the wind turbine WT 01. No dynamic reactive compensation is used. Reported in (Akhmatov et al, 2003(a)).

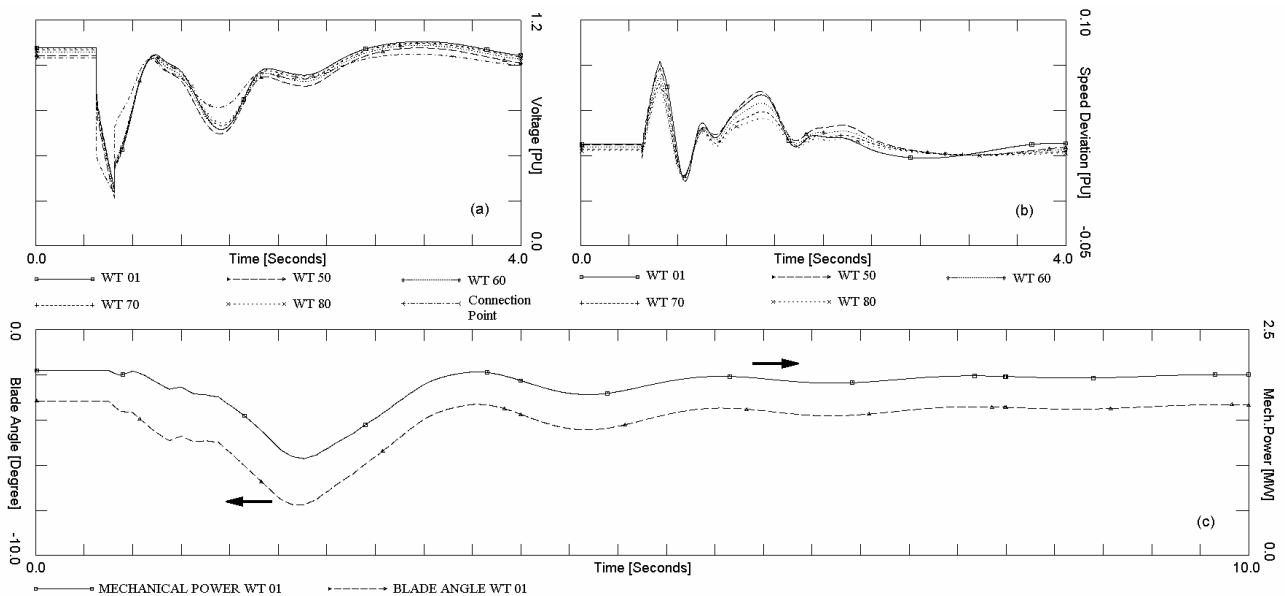


Fig. 6.14. Voltage re-establishing after a short circuit fault in the wind farm with active-stall wind turbines controlled by the signal containing terminal voltage: (a) – terminal voltage of selected wind turbines and in connection point, (b) – generator rotor speed of selected wind turbines, (c) – mechanical torque and the blade angle of the wind turbine WT 01. No dynamic reactive compensation is used. Reported in (Akhmatov et al, 2003(a)).

6.12.2. Blade angle control – Ordering of power reduction ³¹

According to the Danish specifications (Eltra, 2000), the large offshore wind turbines can be ordered to reduce their power supply from an arbitrary operational point to the operational point of less than 20 % of the rated power in less than 2 s. This technical feature can be used to stabilise the large offshore wind farm at the grid fault (Eltra, 2000; Akhmatov, 2001). The order is given by an external signal from the power system. This external signal can be given, for example, when monitoring the voltage in the grid or in the connection point of the wind farm and registering a large voltage drop (Akhmatov et al, 2003(a)).

A delay, which is set to 200 ms in this investigation, is introduced from the moment of the fault occurrence to the moment when the external signal is given to the wind farm. Before the external signal is given and after the order is cancelled, the regular control system of active-stall, is applied. Here the reference value, β_{REF} , is defined from the error signal, $X_{ERR} = P_{ERR} = (P_{REF} - P_E)$.

During the order, this regular control system is switched off and the reference value, β_{REF} , is set to the pre-defined value, β_{ORDR} , according to explanation of **Section 3**. The value of this reference value, $\beta_{REF} = \beta_{ORDR}$, corresponds to the 20 % level of the rated power at (i) the given wind (estimated) and (ii) the rotational speed. Such reference values can be pre-calculated. After the order is cancelled, the regular control system of the blade angle control will re-establish to perform the power optimisation. Duration of the operation with a reduced power may be of few seconds, which is why the power loss due to this control strategy is small and can be neglected.

The simulation results with use of the ordered power reduction at the grid fault are shown in **Fig. 6.15**. The voltage is re-established without use of dynamic reactive compensation. Markings on the curves of the mechanical power, P_M , and the blade-angle, β , denote:

- 1) The moment of the short circuit fault occurrence.
- 2) The moment when the external signal to the wind farm is given. Here the ordered power reduction is started.
- 3) The moment when the order is cancelled and the regular active-stall control system has re-started, using $X_{REF} = P_{REF}$ and $X = P_E$.
- 4) Tracking the blade angle to the new optimised position for reaching the reference power $P_E = P_{REF}$. It is because the lines accessing the faulted node are tripped and so the power grid is recovered to a new operational point.

After the fault is cleared, the wind farm operation is re-established, which is seen from the curves of the electric power given in **Fig. 6.15**. A similar technical solution with reduction of the

³¹ The Danish transmission system operator ELTRA has informed the author that Mr. Poul Degn, a retired associate of ELTRA, considered that the power ramp could perhaps be useful to stabilise the wind farm at grid disturbances. Poul Degn's considerations have been expressed in the Danish Specifications published by ELTRA in 1999 (Eltra, 2000, Part 5.1) and the work of Poul Degn has been dated 1997 (Intern report No. 20806 of ELTRA). The credits to Poul Degn's work are given. The author has not been familiar with work of Poul Degn, but used the Specifications (Eltra, 2000) as the roles given by the transmission system operator to find acceptable solutions to maintain short-term voltage stability.

wind turbine power at the grid fault for the wind farm stabilisation is chosen to be applied at the Danish offshore wind farm at Rødsand / Nysted constructed in the year 2003.

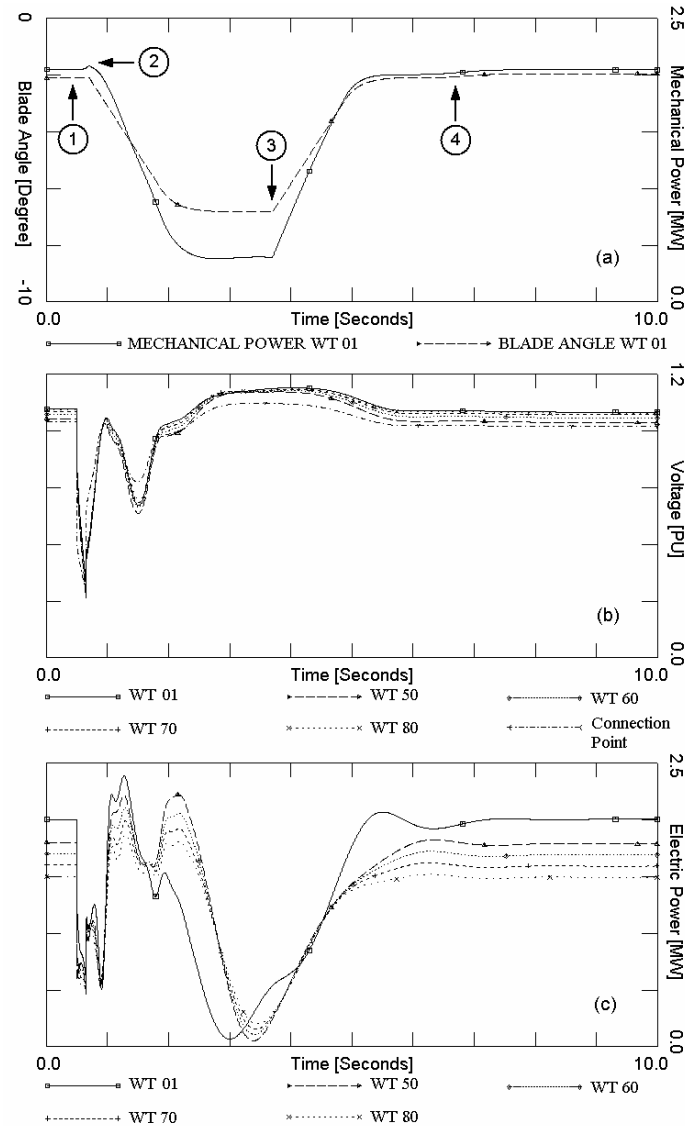


Fig. 6.15. Voltage re-establishing after the grid fault in case where the wind farm is ordered to power reduction by the external signal: (a) – blade angle and mechanical power of the wind turbine WT 01, (b) – terminal voltage of selected wind turbines, (c) – electric power of selected wind turbines. Reported in (Akhmatov et al, 2003(a)).

6.13. Mixed wind farm

The commonly asked question is what will happen if a large wind farm or a group of wind turbines have different mechanical parameters: this question relates to a possible risk of mutual oscillations between the wind turbines with different mechanical parameters at grid disturbances. When the wind turbine mechanical parameters are different, the natural frequencies – the shaft torsional modes – will also be different.

Since the wind turbines are equipped with induction generators, there is no synchronising torque and therefore no significant electric coupling between the generators (Akhmatov et al, 2003(a)). At the first moment, the wind turbines start responding to the grid fault with their natural frequencies.

In absence of synchronising torque, the fluctuations of the electric and the mechanical parameters coming with different frequencies will eliminate each other (Akhmatov et al., 2003(a)). The resulting dynamic behaviour will be smoother than in case of the wind turbines with identical data.

In the following simulation example, the wind turbines in the sections 1, 3, 6 and 8 are with the shaft stiffness $K_S = 0.15$ PU/el.rad., and in the sections 2, 4, 5 and 7 are with $K_S = 0.60$ PU/el.rad. The wind farm is compensated with the SVC unit of 50 MVar, see **Table 6.1**. The simulated curves are given in **Fig. 6.16**. The results demonstrate that use of the wind turbines with different mechanical parameters – the shaft stiffness – within the same wind farm may reduce the voltage oscillations in the connection point as well as at the terminals of the individual wind turbines.

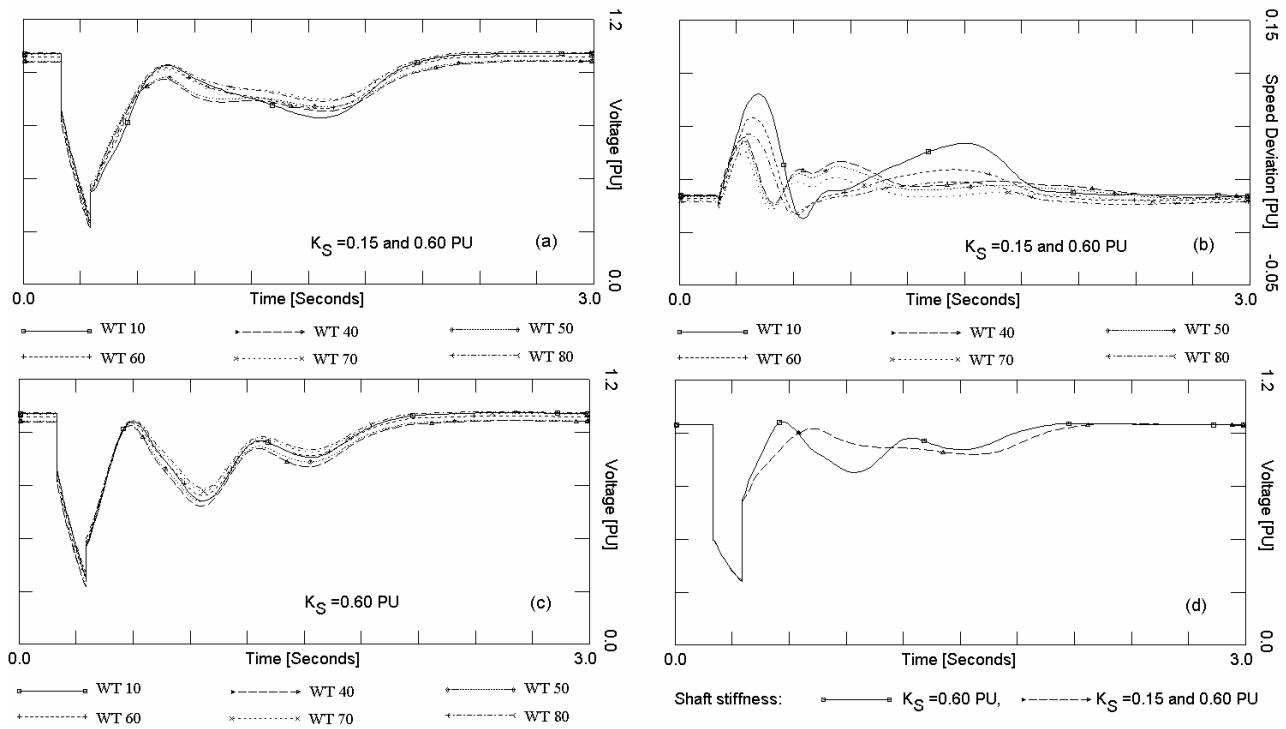


Fig. 6.16. Mixed wind farm with two groups of wind turbines with $K_S = 0.15$ PU/el.rad., respectively, $K_S = 0.60$ PU/el.rad.: (a) – terminal voltage of selected wind turbines in the mixed wind farm, (b) – generator rotor speed of selected wind turbines in the mixed wind farm, (c) – terminal voltage of selected wind turbines in the wind farm with the wind turbines with identical parameters, $K_S = 0.60$ PU/el.rad., (d) – voltage in connection point of the mixed wind farm compared to in case of the wind farm with the wind turbines with identical parameters.

The simulations on the mixed wind farm are also made with different conditions such as:

- 1) The other combinations of the mechanical parameters, for instance, with $K_S = 0.15$ PU/el.rad. and $K_S = 0.30$ PU/el.rad. within the same wind farm.
- 2) The mixed wind farm with wind turbines with active-stall control acting at the grid faults.

In all the simulations, reduction of the voltage oscillations is seen. Incorporation of the mixed wind farm does not necessarily lead to more demands of dynamic reactive compensation.

It may be preferred to mix the wind turbines with different mechanical parameters within the same large wind farm. It is because this feature contributes to damp the fluctuating behaviours that are seen in the electric and the mechanical behaviours of the wind turbines (with the same mechanical parameters).

6.14. Robustness of voltage control principles

In practical operational situations, control equipment failures may occur contemporarily with or be even caused by disturbances in the power system. Such failures can be experienced in the dynamic reactive compensation units or in the blade-angle control systems of the individual wind turbines. Such failures of the control systems may not lead to fatal outcome with respect to maintaining transient voltage stability (Akhmatov et al, 2003(a)). Robustness of the control principles will, in these terms, relate to how large part of the applied control systems may fail still to maintain transient voltage stability.

6.14.1. Failure of dynamic reactive compensation

When the offshore wind turbines have no control acting at short circuit faults, then maintaining of transient voltage stability depends only on robustness of the dynamic reactive compensation units. The dynamic reactive compensation shall contain a number of reserve units, e.g. larger installed capacity than found in investigations of transient voltage stability (Akhmatov et al, 2003(a)).

Capacity of the dynamic reactive compensation of 100 MVar, found in **Section 6.9**, is only the minimal demand. This capacity does not include reserves. At a short circuit fault, failure of some units within these 100 MVar of dynamic reactive compensation will probably result in voltage instability³². Voltage instability will occur if no reserve units of the same capacity, as the failed, are available.

Demands of the reserves can be less than or in the same range as the minimal amount of dynamic reactive compensation. In the given example, this will correspond to 100 MVar as minimal demands plus up to 100 MVar as reserves.

6.14.2. Failure of blade-angle control

When the offshore wind turbines are with the blade-angle control acting at disturbances in the power system, then maintaining of transient voltage stability depends on reliability of the wind turbine control systems. In this case, it is reliability of active-stall control.

In practical operational situations, the active-stall control systems of a less number of wind turbines may fail at a short circuit fault in the power network. This implies that the wind turbines with the failed control systems do not reduce the mechanical power at the fault in the grid. Here,

³² Voltage instability does not necessarily will result in voltage collapse. The wind turbines in a large wind farm are with their protective relays. When the voltage decays, the wind farm will disconnect, which eliminates the cause of the voltage decay. This will however imply that the solution chosen does not comply with the Specifications of the TSO (Eltra, 2000).

failure of the active-stall control corresponds to that the given wind turbine operates as a fixed-pitch wind turbine (Akhmatov et al, 2003(a)).

In these investigations, it is found that the power grid will still maintain transient voltage stability when the blade-angle control fails in up to 25% of the active-stall wind turbines in the offshore wind farm. This number depends, generally, on several factors. Such factor are the strength of the power grid, the kind of the fault, the wind turbine data etc. (Akhmatov et al, 2003(a)).

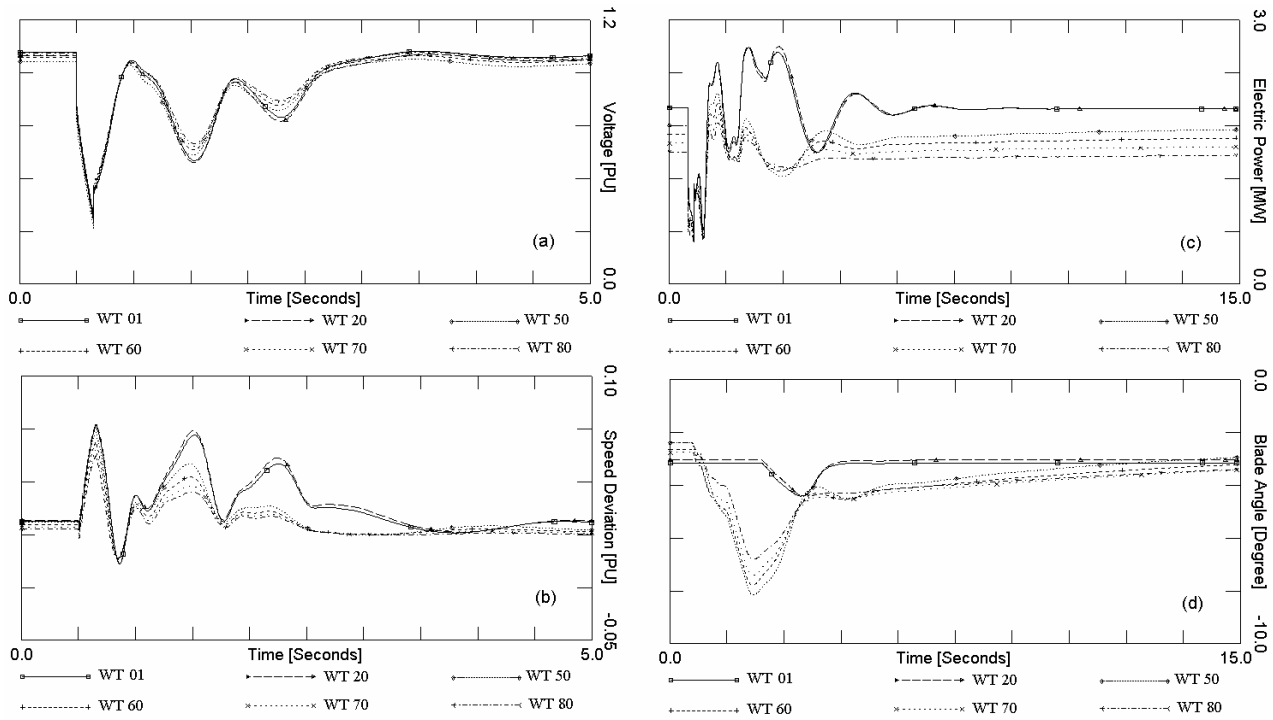


Fig. 6.17. Wind farm operation at a short circuit fault with blade angle control failed in twenty wind turbines. Dynamic behaviours of (a) – terminal voltage of selected wind turbines, (b) – generator rotor speed, (c) – electric power and (d) – blade angle of the same wind turbines. No dynamic reactive compensation is used. These curves shall be compared with the curves in Fig. 6.14. Reported in (Akhmatov et al, 2003).

Robustness of this control principle is illustrated with simulations. The blade angle is controlled with use of the signals $X_{REF} = P_{REF}$ and $X = P_E / V_S^2$, e.g. with inclusion of the voltage, V_S , into the controlling signal, X . It is considered that control systems are failed in twenty wind turbines, WT 01 to WT 20, – the wind turbines in the farm sections 1 and 2. When failed, the control systems of these twenty wind turbines are with $X = P_E$.

Simulation results are shown in Fig. 6.17. As can be seen, the voltage still recovers, but slower when comparing to the case where the active-stall control of all the wind turbines acts at the grid fault. Another observation is that the speed and the power of the wind turbines with failed blade angle control fluctuate more than in case of the wind turbines with acting blade-angle control systems.

6.15. Protective relay system

Although the formal technical specifications, where subsequent tripping of the large offshore wind farms is not acceptable, presence of the protective relay systems of the wind turbines implies that tripping can occur. Uninterrupted operation of the large wind farms at the grid faults shall additionally be ensured by adjusting of the relay settings. This is a part of the solution with compliance to the specifications of the transmission system operators (Eltra, 2000) to maintain transient voltage stability.

The protective relay systems monitor the terminal voltage, the machine current, the grid frequency, the rotational speed and other parameters. Disconnection of the induction generators and their capacitors and stop of the wind turbines will be ordered at registering of abnormal operation. The wind turbines can be tripped by under- and over-voltages, over-currents, speed- and frequency- deviations etc. (Akhmatov et al, 2001). The relay model is set-up with representation of the relay reset mechanisms, measuring delays and the delay from the moment where the trip is ordered to the moment where the wind turbine trips.

Now the relay model is enabled. First, the relay settings are as in case of the wind turbines in decentralised sites on-land. These typical relay settings are found in the Danish recommendations KR-111 and among a number of wind turbines from different Danish manufacturers. The data received from the manufacturers are confidential and not included in this report.

The simulations results are collected in **Table 6.2**. The outcome of the grid disturbance is represented by the terminal voltage of selected wind turbines and the behaviour of the electric power supplied by the wind farm to the grid. The simulation cases, represented in **Table 6.2**, are at different arrangements applied for maintaining of transient voltage stability.

- 1) No arrangements, as in **Section 6.8**.
- 2) Incorporation of 100 MVar SVC, as in **Section 6.9**.
- 3) Incorporation of 100 MVA SC with the excitation control of ASV1, see **Section 6.9**.
- 4) Incorporation of 300 MVA SC with the excitation control of ASV3.
- 5) Use of ordered power reduction by the blade-angle control, as in **Section 6.12.2**.

As can be seen, *any risk of voltage collapse is not present. The main problem can be power loss due to wind turbine tripping at the grid fault.* The investigation shows that the relay settings for over-current and for under-voltage shall be adjusted to the values shown in **Table 6.3**. The adjusted relay settings, which are suggested for over-current and under-voltage, are not critical because such adjustments will not cause damages of induction generators. Such adjustments of the relay settings can be suggested from investigations of short-term voltage stability. This (including practical realisation) shall be responsibility of the wind turbine manufacturer.

When the relay settings are adjusted, unnecessary disconnection of many wind turbines will be avoided. In this case, the results of investigations of transient voltage stability become analogous to the results described in **Sections 6.8 – 6.12**. Notice that the relay setting adjustments, which are suggested in the given case, will not necessarily be applicable in every other situations. In other situations (other wind farms and other power systems), other relay settings should be suggested.

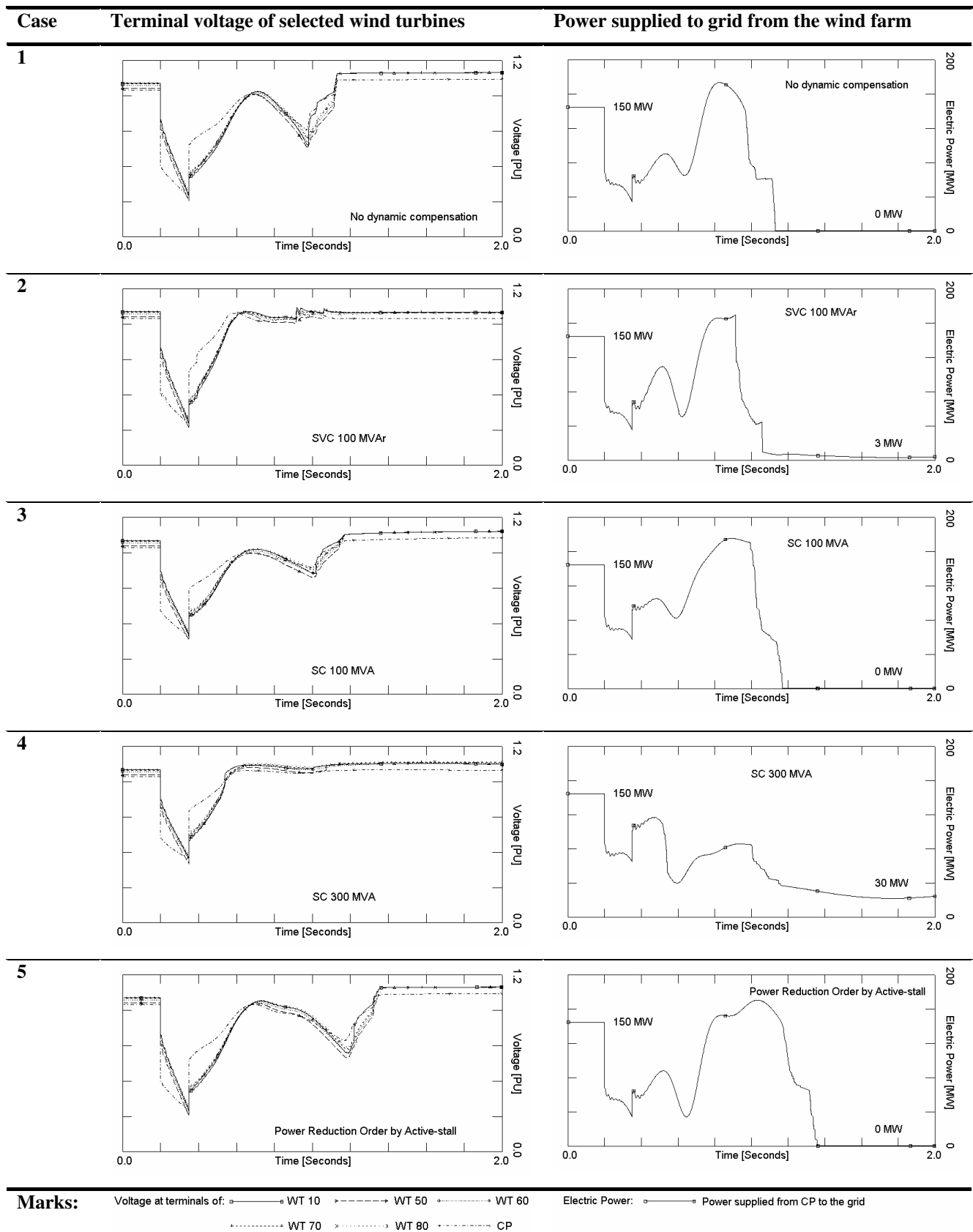


Table 6.2. Simulations with enabled relay model where the relay settings as in case of decentralised wind turbine sites, which is typical for on-land sites in Denmark. Large power loss is the main problem rather than voltage collapse.

Changed relay settings	Limit, PU	Max. time
Over-current	3.0	20 ms
Under-voltage	0.7	0.5 s

Table 6.3. Change of protective relay settings for the large offshore wind farm.

When the finale solution with respect to maintain transient voltage stability and uninterrupted operation of the large (offshore) wind farm is chosen, it can be recommended to execute simulations with use of the relay settings suggested for the wind farm. Such simulations can be executed at the end of investigations and with the controlling features chosen to maintain transient voltage stability. When the controlling feature itself shall be clarified, the simulations can be executed with disabled relay models – this corresponds to **Sections 6.8 –6.12**. In this case, indication of voltage instability should be interpreted as a risk of disconnection of the wind farm and power loss. Outage of the wind farm implies that the solution does not comply with the Specifications of the TSO.

The simulated curves of the monitored parameters such as the terminal voltage, the machine current, the grid frequency etc. with disabled relay model can be applied to adjust the relay settings in practical applications. This is possible when the simulation results predicted by the wind turbine model are sufficiently accurate.

6.16. Resume

In case of fixed-speed wind turbines equipped with no-load compensated induction generators, the main cause of voltage instability is over-speeding of the wind turbines at the grid faults. Fatal over-speeding and so voltage instability can be, in the first place, prevented with use of dynamic reactive compensation. Such dynamic compensation units can be SVC, SC or Statcom.

Fatal over-speeding can also be reduced by choosing of the wind turbine construction parameters by an appropriate way. Furthermore, fatal over-speeding can be prevented with use of the controllability of the blade-angle control acting at the grid faults.

The protective relay settings shall be chosen to avoid unnecessary trip of large wind farms. This does not seem to be any problem in case of fixed-speed wind turbines equipped with induction generators. It is because the adjusted relay settings are not of the character that may cause damages of the wind turbine generators.

Notice that voltage instability in the simulation cases does not necessarily means that voltage collapse occurs. Let us keep in mind that the wind turbines are with their protective relays and therefore can trip, although the Specifications formulated by the TSO. When uncontrollable decay of voltage is registered, the wind turbines will trip, indeed. Then, voltage instability predicted from the simulations should be interpreted as a possible risk of subsequent disconnection of the large wind farm rather than a risk of voltage collapse. In case of a subsequent disconnection, the solution chosen for the wind farm does not comply with the TSO's specifications.

7. Large wind farms with doubly-outage induction generators and variable rotor resistance

In case of the wind turbines equipped with doubly-outage induction generators with variable rotor resistance, the rotor converter operation corresponds to introducing of an external resistance, R_{EXT} , in series with the rotor circuit. The value of the external rotor resistance, R_{EXT} , is dynamically controlled by the rotor converter (Akhmatov et al, 2003(a)). This explains why this control feature is denoted variable rotor resistance (VRR).

Basically, this control feature is primarily developed to reduce flicker where the power fluctuations are dissipated in the external rotor resistance. The Danish manufacturer Vestas Wind Systems produces the OptiSlip® wind turbines. Those are the pitch-controlled wind turbines equipped with the doubly-outage induction generators with VRR. It is demonstrated that when using the generic control system of the variable rotor resistance, R_{EXT} , controlled by the rotor current, I_R , the flicker level can be reduced from approximately 10 % of electric power fluctuations about its average level to less than 1 % (Akhmatov, 1999). This control feature can be very useful to improve the power and voltage quality in the power systems with a large amount of wind power.

The control feature of VRR can also be useful for improving transient voltage stability (when the power grid is subjected to a short-circuit fault). The idea behind the generic control feature of VRR can be the following (Akhmatov et al, 2003(a)).

- 1) In normal operation, the rotor resistance shall be low for minimising the power losses.
- 2) When the grid fault is registered, the rotor resistance is increasing. By this way, the critical speed of the wind turbine, ω_{CR} , is expanded. Transient voltage stability is also improved.
- 3) During the faulted operation in the grid, some higher, but still fair power losses in the rotor circuit can be accepted. Otherwise, it can be a risk of thermal damages of the rotor converter.
- 4) When the voltage in the power grid is re-established, the rotor resistance is again reduced to its regular, low value.

The total value of the dynamic rotor resistance, $R_R(t)$, will be, then, the sum of the stationary value of the rotor winding resistance, R_{R0} , and the additional dynamic value, R_{EXT} , generated by the control system. If the stationary value of the rotor resistance is R_{R0} and it is continuously increased to $2R_{R0}$ during the grid fault, this corresponds to the induction generator operating somewhere between the curves T_{E1} and T_{E2} shown in **Fig. 6.9**. The stable operation range with respect to the speed is from ω_1 to ω_{CR2} . This leads to significant expansion of the speed operation range compared to cases of fixed rotor-resistance values. This explains why the VRR feature can be of interest as a possible wind turbine control feature contributing to maintain transient voltage stability (Akhmatov et al, 2003(a)).

The wind farm model with eighty 2 MW wind turbines is applied. The wind distribution pattern is analogous to as described in **Section 6.7**. The wind farm is, however, with pitch-controlled wind turbines equipped with no-load compensated doubly-outage induction generators with VRR. This representation is chosen to cover the issues:

- 1) Maintaining of transient voltage stability of large wind farms.

- 2) A possible risk of mutual interaction between the wind turbines. Such an interaction could occur between the converters of the individual wind turbines in the large wind farm.

For demonstration of the controllability of the VRR feature with respect to maintain transient voltage stability, the pitch control is disabled in the following simulations. This is because the pitch control, acting at the grid disturbances, would improve transient voltage stability (Akhmatov, 2001). It is necessary to distinguish between the controllability of the pitch and of the VRR feature. Otherwise, it would be difficult to make conclusions about influence of the VRR feature on transient voltage stability.

7.1. Generic control scheme

As explained in **Section 6**, the electrical and mechanical parameters of fixed-speed wind turbines equipped with induction generators show fluctuating behaviours at the grid faults. This is seen in the simulated behaviours in **Fig. 7.1**, illustrating voltage instability process. These fluctuations are with the natural frequency corresponding to the shaft torsional mode. The fluctuations are caused by the internal torsional oscillations in the shaft system (Akhmatov et al, 2000(b)). Such fluctuations can be excited by and also used to indicate abnormal operation of the power grid.

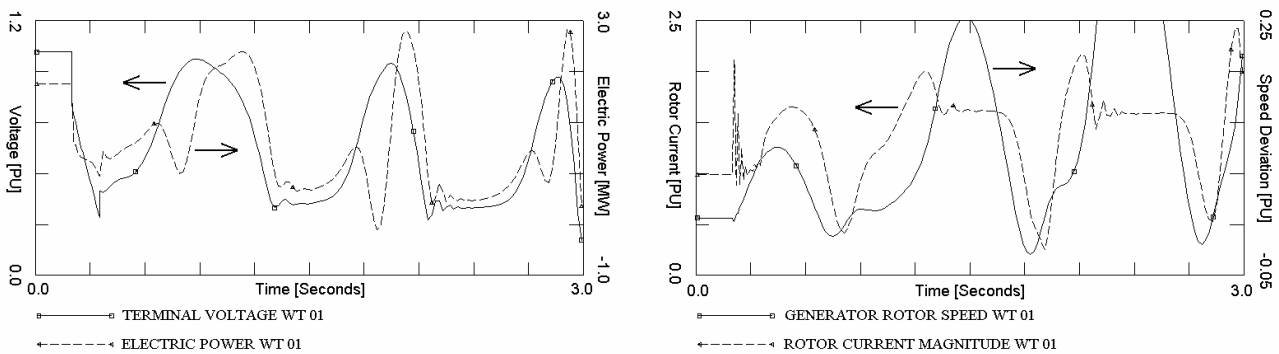


Fig. 7.1. Fluctuating behaviour of the voltage, the electric power, the generator rotor speed and the rotor current magnitude of the wind turbine WT 01 equipped with an induction generator in case of developing of voltage instability at the grid fault. Reported in (Akhmatov et al, 2003(a)).

With respect to generation of the external resistance value, R_{EXT} , it is necessary to choose an input signal to the control system of the rotor converter. The input signal of the generic control system can be chosen by the following requirements (Akhmatov et al, 2003(a)).

- 1) The measuring time delay of the signal, which indicates the grid fault, shall be sufficiently short.
- 2) The monitored parameter shall show the fluctuating behaviour for indication of the grid fault.
- 3) It is an advantage that the parameter shall be compliant with the parameter used for flicker reduction in normal operation. Hence, the same input signal to the control system can be applied in normal as well as in faulted operation of the power grid.

With relation to the requirements above, the rotor current magnitude, I_R , is applied as the input signal to the control system. The generator rotor speed, ω_G , and the rotor current magnitude, I_R , are fluctuating “in-phase”, as shown in **Fig. 7.1**. The measuring time delay of the rotor current magnitude can be very short.

The generator rotor speed fluctuations follow the rotor current magnitude fluctuations with a little delay. It seems to be possible to organise the VRR control by the rotor current magnitude, $R_{EXT}(I_R)$, in means of dynamic expansion of the critical speed, ω_{CR} , in situations where the generator rotor speed, ω_G , is increasing. Visually, it can be understood when considering that the generator rotor speed, ω_G , increases, but the critical speed, ω_{CR} , is moving a little forward the generator rotor speed. Hence, the generator rotor speed is kept in the stable operation range. When the generator rotor speed, ω_G , reduces, the critical speed, ω_{CR} , will also be reduced. Here, the critical speed is moving a little behind the generator rotor speed. Again, the generator rotor speed is kept in the stable operation range.

The generic control scheme of VRR is shown in **Fig. 7.2**. The generic control system consists of the band-pass-filter around the shaft torsional frequency, f_T , and the PI-controller with the gain G_I and the integration time T_I . The generic control system generates the dynamic signal $K_R(t)$ that is limited. The lower limit is $K_{RMIN} = 0$, which implies that the rotor converter absorbs, but does not generates the electric power. The upper limit is K_{RMAX} . In this work, the upper limit $K_{RMAX} = 1$ is applied. This corresponds to that the rotor resistance variations are in the range from R_{R0} to $2R_{R0}$. The dynamic rotor resistance is added to the rotor winding resistance according to:

$$\begin{aligned} R_R(t) &= R_{R0} + R_{EXT}(t) = R_{R0}(1 + K_R(t)) , \\ R_{EXT}(t) &= R_{R0} K_R(t) . \end{aligned} \quad (7.1)$$

The value of the torsional oscillation frequency, f_T , can be computed when knowing the shaft system data using **Eq. (2.17)**. This value can also be received from the wind turbine manufacturer.

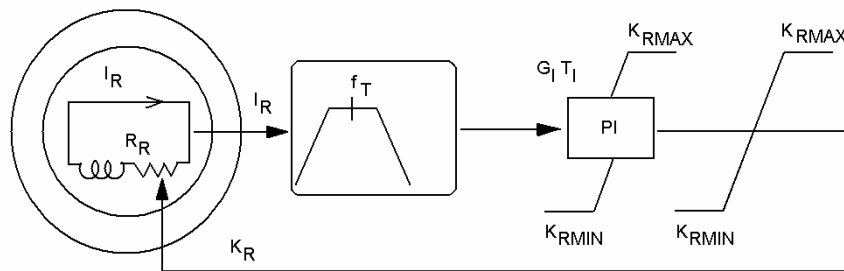


Fig. 7.2. Generic control system of doubly fed induction generator with variable rotor resistance. Reported in (Akhmatov et al, 2003(a)).

In this work, the VRR model deals rather with the VRR functionality than with the detailed representation of the rotor converter and its power electronics. Therefore, the above-described generic model of VRR is applied in investigations of transient voltage stability instead of detailed description of processes in the rotor converter and its switches.

7.2. Influence of control system parameters on voltage stability

Influence of the control system parameters, G_I and T_I , on transient voltage stability at grid faults is illustrated in **Fig. 7.3**. As can be seen, the optimised parameters G_I and T_I shall be in the range around 5 PU and 0.3 s, respectively. These optimised parameters are found for the given data of the wind turbine and its induction generator. When the optimised parameters of the control system are applied, the voltage is re-established without use of dynamic reactive compensation.

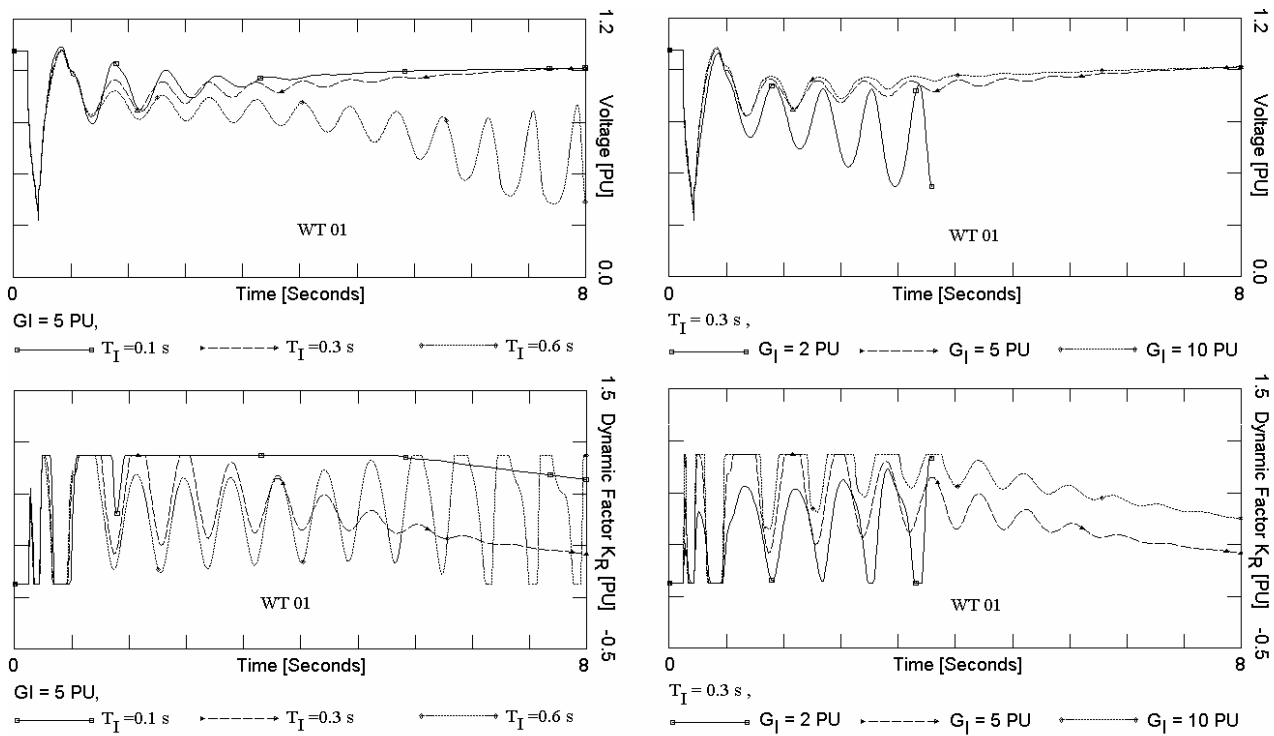


Fig. 7.3. Parameter study with respect to the gain G_I and the integration time T_I . Terminal voltage, V_s , and dynamic factor, K_R , of the wind turbine WT 01. No dynamic reactive compensation is used. Reported in (Akhmatov et al, 2003(a)).

When the short-circuit fault has been cleared and so long as the voltage is recovering, then the fluctuations of the electric and mechanical parameters of the wind turbines will be present. This is illustrated in **Fig. 7.4**. The fluctuations are coherent, e.g. oscillating “in-phase”, and with the frequency of the shaft torsional mode. The fluctuations seen in case of this wind turbine concept are of a longer duration than in case of the wind turbines equipped with induction generators with short-circuited rotor circuits and where the 100 MVar SVC unit is applied (dynamic reactive compensation).

Fluctuations of the generator rotor speed may indicate oscillating loads applied onto the shaft systems and their gearboxes.

When the voltage is re-established, such fluctuations do not appear any longer. So long as the parameters of the fast-acting control system of the variable rotor resistance feature are sufficiently tuned, there is no risk of mutual interaction between the wind turbines in the large wind farm caused by the applied control system.

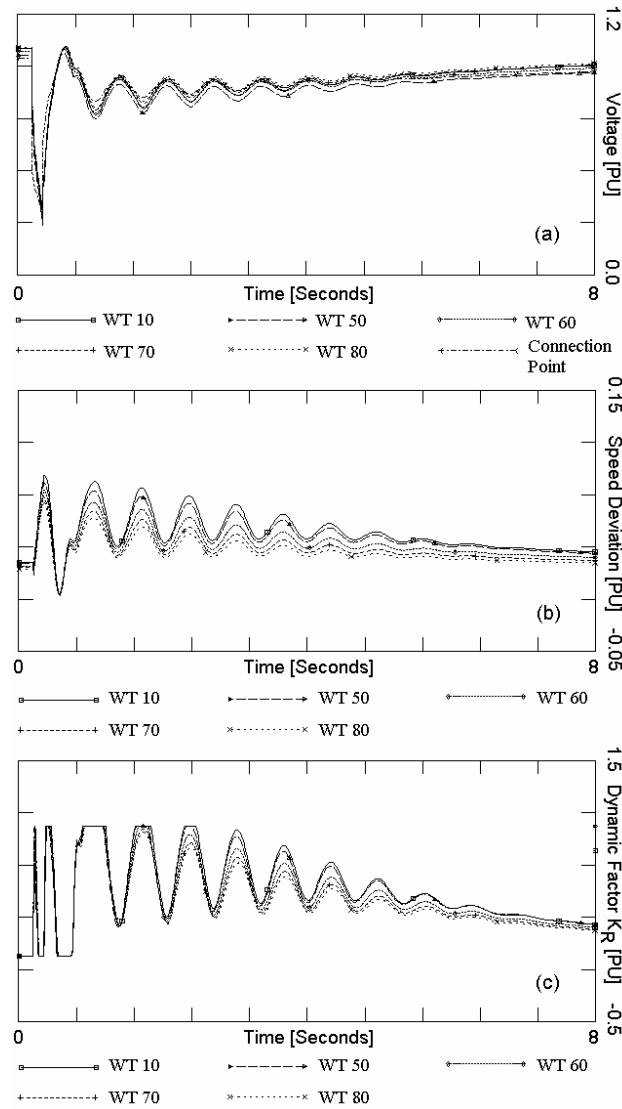


Fig. 7.4. Wind farm operation during voltage re-establishing after the grid fault – coherent fluctuating behaviours of: (a) – terminal voltage of selected wind turbines, (b) – generator rotor speed and (c) – dynamic factor K_R . No dynamic reactive compensation is used. Reported in (Akhmatov et al, 2003(a)).

7.3. Mixed wind farm

A number of simulations have been carried out for investigation whether it is possible risk of mutual interaction between the wind turbines with the VRR control in the large wind farm. Here the wind turbines are with different mechanical parameters. In the simulations, the wind farm consists of the two groups of the wind turbines with different shaft stiffness. The wind turbines in the farm sections 1, 3, 5 and 7 are with the shaft stiffness $K_S = 0.15$ PU/el.rad. and in the farm sections 2, 4, 6 and 8 are with the shaft stiffness $K_S = 0.30$ PU/el.rad. The simulating results are shown in **Fig. 7.5**.

The grid voltage recovers without use of dynamic reactive compensation. First, it is noticed that use of the wind turbines with different mechanical parameters does not necessary lead to more demands of dynamic reactive compensation.

Second, efficient damping of the fluctuations of the voltage at the wind turbine terminals and in the connection point is seen when applying the wind turbines with different shaft stiffness. This conclusion is similar to previously discussed cases of fixed-speed wind turbines equipped with induction generators with shorted rotor-circuits and different shaft stiffness, see **Section 6.13**. The explanation of no mutual oscillations between the wind turbines VRR is similar to case of the wind turbines equipped with induction generators with shorted rotor circuits. It is because of absent synchronising torque in case of (doubly-outage) induction generators. Use of the rotor converter control, operating as adjusting of the rotor-circuit resistance, does not change the picture. The conclusion is made from investigations with the chosen VRR control system and its parameters.

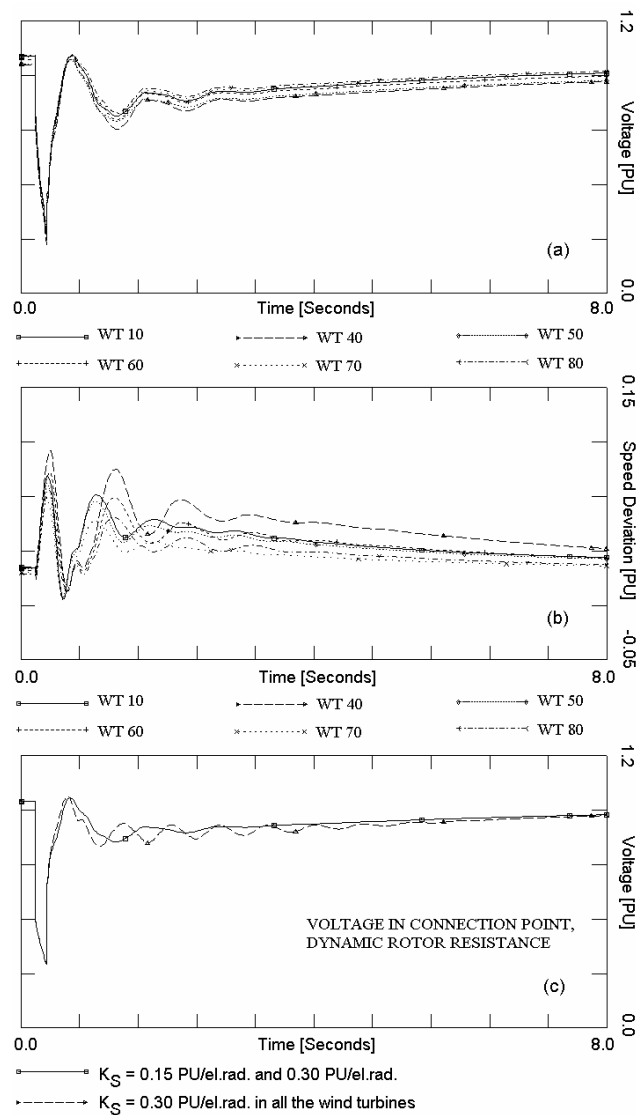


Fig. 7.5. Mixed wind farm with wind turbines of the variable rotor resistance concept, behaviours of: (a) – terminal voltage of selected wind turbines, (b) – generator rotor speed and (c) – voltage in connection point compared to the case of the wind farm equipped with identical wind turbines. Use of wind turbines with different shaft stiffness within the same large wind farm contributes to damping of voltage fluctuations at the grid faults.

7.4. Considerations on protective relay system

In all the simulations given above, it is assumed that the wind turbines equipped with doubly-outage induction generators with VRR maintain grid-connection at the grid fault. This implies that the relay settings are tuned properly, which avoids unnecessary disconnection of the wind turbines. In this concept, the protective system of the generator and the rotor converter shall be represented in power stability investigations.

The protective relay system of the generator itself monitors (i) the voltage, (ii) the machine current, (iii) the grid frequency, (iv) the speed etc. This protective system shall be modelled analogously to case of the fixed-speed wind turbines equipped with induction generators with shorted rotor circuits. The wind turbines can be tripped by (i) over- and under-voltage, (ii) over-current, (iii) frequency deviations, (iv) over-speed etc. This representation is met and discussed in **Section 6.15**.

Notice, furthermore, that the generators of this wind turbine concept are converter-controlled. This implies that the protective system of the converter and its power electronics shall also be taken into account. First, the power electronics of the rotor converter shall be effectively protected against thermal overloads. The thermal overloads can be evaluated from the power losses in the rotor circuit. In the given case, the power losses in the rotor circuit, $P_R = R_R(t)I_R^2$, are found to be within an acceptable range. As illustrated in **Fig. 7.6**, the power losses in case of the VRR feature are between the power losses found in case of fixed rotor resistance (the induction generators with shorted rotor circuits) of R_{R0} and $2R_{R0}$, respectively.

It is kept in mind that thermal overloads can lead to damages of the power electronics of the rotor converter. When thermal overloads are registered, the converter stops switching and blocks. Further operation of the wind turbine depends on the control strategy applied by the manufacturer. The converter blocking is usually followed by tripping of the generator and stopping of the wind turbine. It is thinkable that the converter blocking can be followed by re-start of the converter after awhile. Then the wind turbine continues uninterrupted operation. This operation with the converter re-start will be preferred when the wind turbines shall comply with the Danish specifications (Eltra, 2000).

Second, the converter protective system will monitor the current flowing through the GTO-switches of the converter; it is the rotor current. When the rotor current exceeds its respective relay setting, the converter blocks. This is analogous to case of thermal overloads.

The relay settings for the rotor current are manufacturer-dependent and, unfortunately, not available for this project. Instead, it is chosen here to show the simulated curves of the rotor current magnitudes of selected wind turbines in the large wind farm. Those are shown in **Fig. 7.7**. As can be seen, the rotor current magnitude exceeds slightly the ratio 2 of its rated value during a short while and decays to its regular value. The rotor current magnitude is about 1.5 of its rated value during few seconds. This implies that the converter shall be designed to withstand this current to achieve uninterrupted converter operation at the grid faults. This rotor current behaviour is for the given case, e.g. (i) the given wind turbine data, (ii) the given power grid and (iii) the disturbance. In other situations, the rotor current response may show another behaviour – this will relate to the converter behaviour during a transient event in the power grid.

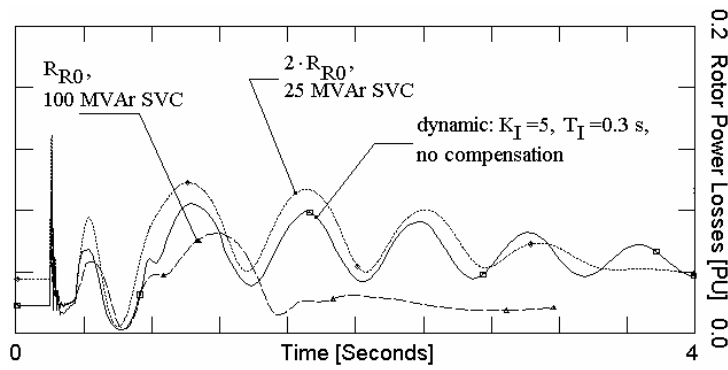


Fig. 7.6. Evaluation of rotor power losses, P_R , with variable and fixed rotor resistance. Reported in (Akhmatov et al, 2003(a)).

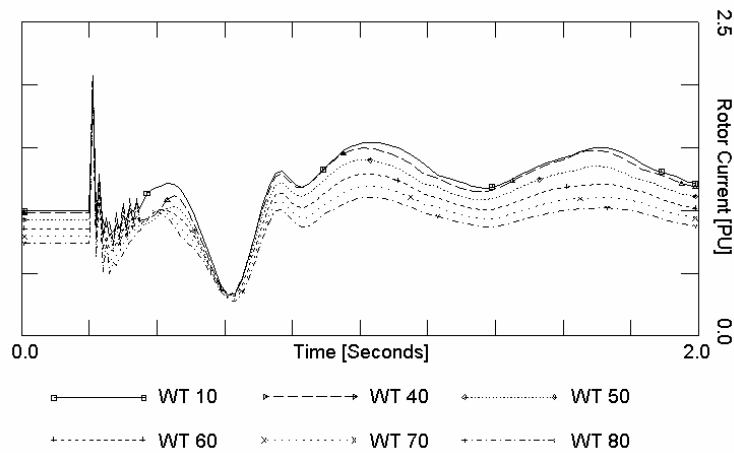


Fig. 7.7. Rotor current magnitude of selected wind turbines in the farm at variable rotor resistance feature.

Representation of the converter protective system is important in power stability investigations. It is because of possible risk of disconnection of a number of wind turbines caused by the converter protection even in situations with no indication of voltage instability.

7.5. Resume

In case of wind turbines with VRR, there are two basic considerations that must be taken into account in power stability investigations. First, the generator is still an induction generator excited from the power grid. The reactive power and the voltage behaviour depend on the speed, which is why concerns about preventing against fatal over-speeding at grid faults will relate to this wind turbine concept. This is similarly to case of wind turbines of the Danish concept.

Second, the generator is controlled by the rotor converter. In power stability investigations, protection of the power electronics of the rotor converter shall be taken into account. It is because the converter may block which may lead to trip of the wind turbines. Tripping of many wind turbines will require establishing of immediate power reserves.

Use of pitch-control, combined with the VRR feature, will be an useful tool preventing fatal over-speeding of the wind turbines.

8. Variable-speed wind turbines – Operation and modelling considerations

As explained in **Section 4**, the wind turbines of the Danish concept are equipped with asynchronous generators with short-circuited rotors. This means that the rotational speed of the wind turbines of the Danish concept is within a narrow range given by the slip of the asynchronous generator. Its value is of 1 to 2 % at rated operation. Therefore these wind turbines are called fixed-speed wind turbines.

The power coefficient, C_P , of the fixed-speed wind turbines is optimised with respect to the most probable wind speed in the installation area. This optimisation requires that the power coefficient, C_P , reaches its optimum at the wind speed above the most probable wind speed because the power is a cubic function of wind. For the given wind turbine on-land in Denmark, this optimisation is made for wind speed around 8 m/s. This means that the power versus rotational speed curve reaches a local maximum at the wind of 8 m/s, as shown in **Fig. 8.1**. In case of the 2 MW fixed-speed wind turbine, which computed curves are shown in **Fig. 8.1**, the optimised rotational speed is 21.5 RPM. At other wind speeds, the power curves of the fixed-speed wind turbine are not related to optimised operation. Further optimisation of the power output, P_M , is only possible with use the blade angle control. However, this further optimisation gives only a slight increase of the power output.

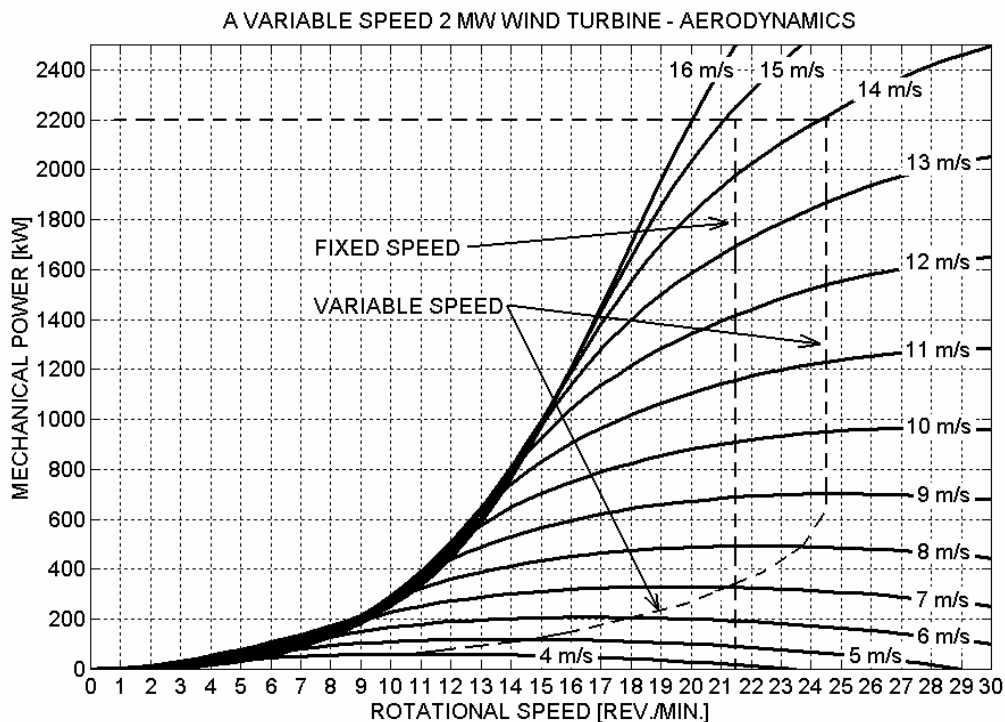


Fig. 8.1. Mechanical power versus rotational speed curves of the 2 MW wind turbine plotted at different incoming wind speeds. The rotor diameter is 61 m. The curves are computed using the BEM-method. Reported in (Akhmatov, 2002(a)).

In case of variable-speed wind turbine, it is possible to produce more mechanical power, P_M , using the wind turbine of the same geometrical configuration, than in case of fixed-speed

operational mode (Zinger and Muljadi, 1997). This is reached by adjusting the rotational speed of the turbine, ω_M , in accordance to the incoming wind, V . The gain is significant in case of wind speeds below the most probable wind where the wind turbine is at sub-synchronous operation (Akhmatov, 2002(a)). The term sub-synchronous operation implies that the rotational speed is below the synchronous speed that is 21.5 RPM for the given wind turbine. This is illustrated in **Fig. 8.1** including comparison between the fixed- and the variable-speed operational modes.

At sub-synchronous operation, the wind turbine is controlled so that the local maximums of the power coefficient curves, C_P , are reached at any wind speed. The other advantage of sub-synchronous operation is that the pressure force – the thrust, T , applied onto the wind turbine and representing mechanical loads is reduced at this operational mode. This is illustrated by the simulated curves in **Fig. 8.2** and **Fig. 8.3**, respectively.

When the rotational speed is reduced, when in sub-synchronous operation, the tip-speed-ratio is also reduced. This implies that the aerodynamic noise impact on the surroundings is reduced in this mode.

The curves in **Fig. 8.1** to **8.3** are computed at the fixed blade-angle, e.g. pitching at higher wind speed than the rated is not taken into account.

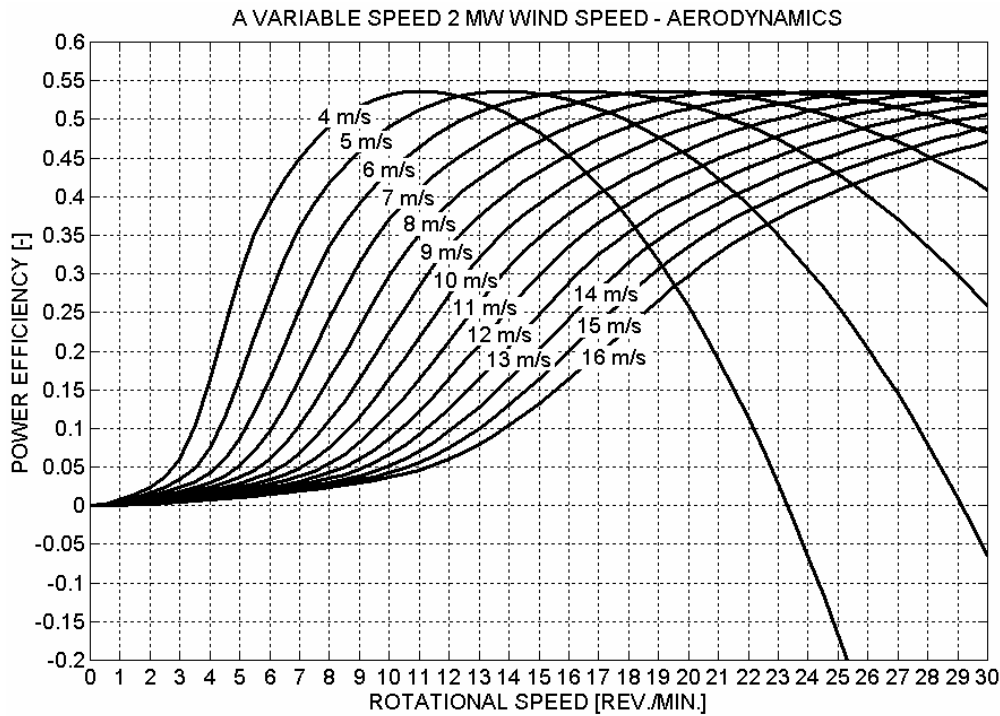


Fig. 8.2. Power coefficient, C_P , versus rotational speed curves of the 2 MW wind turbine plotted at different incoming wind speeds³³. The rotor diameter is 61 m. The curves are computed using the BEM-method. Reported in (Akhmatov, 2002(a)).

³³ Notify that the power coefficient, C_P , is a dimensionless parameter that is usually plotted against the other dimensionless parameter – the tip-speed ratio, λ . In this case, the power coefficient is plotted against the speed to illustrate (for electric engineers) how the optimal power coefficient behaves at different values of incoming wind.

The gain of mechanical power, P_M , at the wind speeds above the most probable wind speed can be higher at variable-speed operation as well, when compared to fixed-speed mode. This is because the optimisation by the power coefficient curves, C_P , is still possible by running the wind turbine in super-synchronous mode. In this operational mode, the rotational speed is above the synchronous speed, e.g. above 21.5 RPM for the given wind turbine. This is again illustrated in **Fig. 8.1** and **Fig. 8.2**. On the other hand, the thrust, T , applied onto the wind turbine construction and the tip-speed will increase at increasing wind, V , and rotational speed, ω_M . For the thrust, it is shown in **Fig. 8.3**. At increasing rotational speed, the centrifugal forces on the generator windings and other rotating parts of the construction are also increasing. The fact that the wind turbine is a *self-bearing construction*, concerns about *safely operation* and prevention of damages of the wind turbine construction shall be taken into account. In other words, the rotational speed and so the mechanical power will be restricted at the wind higher than the rated wind, which is for preventing against possible risk of damages (Hansen, 2000; Akhmatov, 2002(a)).

The other factor, which is taken into account, is the noise impact. The aerodynamic noise increases at increasing tip-speed-ratio (increasing rotational speed). Normally, the tip-speed-ratio may not exceed the value around 7 to get an acceptably low noise.

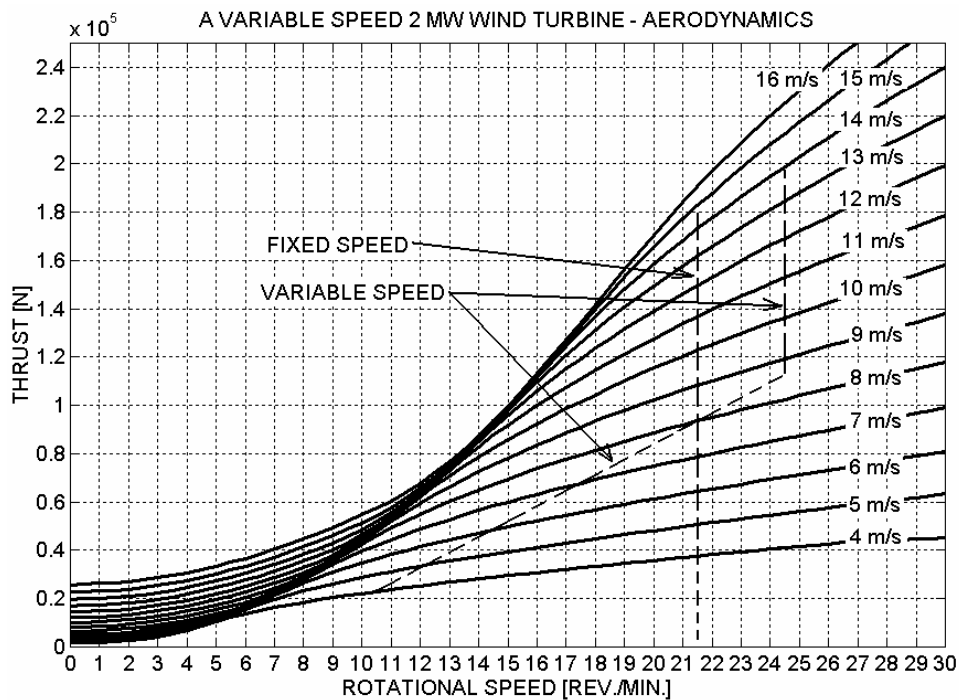


Fig. 8.3. Thrust versus rotational speed curves of the 2 MW wind turbine plotted at different incoming wind speeds. The rotor diameter is 61 m. The curves are computed using the BEM-method. Reported in (Akhmatov, 2002(a)).

The variable-speed wind turbines are, normally, equipped with pitch control. This blade angle control feature is, in the first place, used for further optimisation of the power output, P_M , at the given wind and the rotational speed. At strong wind, the pitch control is applied for restriction of the power output, P_M , and also for reducing mechanical loading on the wind turbine construction. From this viewpoint, it is similar to operation of the blade-angle control of fixed-speed wind turbines.

The variable-speed wind turbines are a promising concept for large (offshore) applications because these wind turbines will produce more energy than the fixed-speed wind turbines of the same construction (Grud, 2000). The variable-speed operation makes it possible to increase the annual energy production by approximately 5 % (Vestas, 2001).

8.1. Range of rotational speed

Consequently, the range of the rotational speed is defined by the following considerations.

- 1) Optimisation of the mechanical power in the sub-synchronous operation at light wind and, partly, in the super-synchronous operation at strong wind.
- 2) Restriction of the power output and of the rotational speed at strong wind for reduction of the mechanical loading on the wind turbine construction and the aerodynamic noise impact.

Optimised values of the rotational speed, ω_M , according to the incoming wind, V , can be produced with use of the BEM-method, **Section 2.1**. The mechanical power of the wind turbine is given by **Eq. (2.6)** which is re-written below.

$$P_M = \frac{1}{2} \rho_{AIR} C_P A_R V^3 ,$$

where A_R denotes the swept area of the wind turbine rotor $A_R = \pi R^2$. Applying the known relation for the tip-speed-ratio

$$\lambda = \frac{\omega_M R}{V} , \quad (8.1)$$

the mechanical power can be re-written according to (Neris et al, 1999; Song et al, 2000).

$$P_M = \frac{1}{2} \rho_{AIR} \pi R^5 \frac{C_P}{\lambda^3} \omega_M^3 . \quad (8.2)$$

In the following, an optimisation algorithm is applied by which the optimal power efficiency, C_P^{OPT} , is reached at the given wind speed, V , by adjusting the rotational speed to its optimised value, ω_M^{OPT} . When the wind turbine operates at the optimised tip-speed-ratio, then:

$$\lambda_{OPT} = \frac{\omega_M^{OPT} R}{V} . \quad (8.3)$$

This leads to the following relation.

$$P_M^{OPT} = \frac{1}{2} \rho_{AIR} \pi R^5 \frac{C_P^{OPT}}{\lambda_{OPT}^3} \omega_M^3 = K_W \omega_M^3 , \quad (8.4)$$

where K_W is the construction-dependent coefficient. **Eq. (8.4)** illustrates the optimisation algorithm for the variable-speed wind turbine. This algorithm computes the optimised value of the rotational speed in accordance to the incoming wind. The result of this optimisation is to reach the optimal

power coefficient, C_P , at any incoming wind, V , and produce more mechanical power, P_M . This is illustrated in **Fig. 8.2**.

As can be seen, the rotational speed shall be proportional to the wind speed when operating within the optimised range. For the given wind turbine, the optimised rotational speed is found 10.5 RPM at the incoming wind 4 m/s. Below this wind speed, the rotational speed is kept on the same level. At the rated operation, where the wind speed is approximately 14 m/s, and at the wind speed above the rated wind, the optimised rotational speed is 24.5 RPM.

In the range from 4 m/s to the 14 m/s, the rotational speed is the linear function of the wind as $\omega_M = A_V V + B_V$, with suitably chosen coefficients A_V and B_V (Papathanassiou and Papadopoulos, 1999; Krüger and Andresen, 2001). The rotational speed versus incoming wind curve is shown in **Fig. 8.4**. The (static) range of rotational speed, ω_M , within the optimised range corresponds to operation between -50% and $+10\%$ with respect to the synchronous speed. This is why this operational mode is called the fully variable-speed operation.

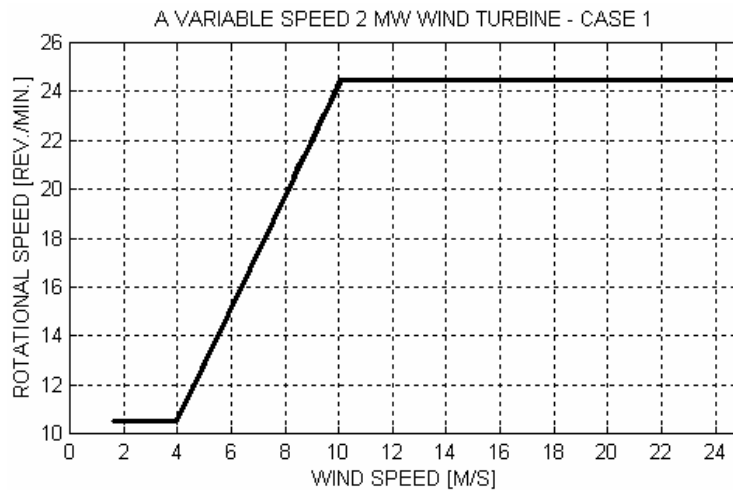


Fig. 8.4. Rotational speed versus incoming wind for the given variable-speed wind turbine. Reported in (Akhmatov, 2002(a)).

The most significant optimisation of the power production, P_M , of the variable-speed wind turbine is achieved by adjusting the rotational speed, ω_M , to its optimised value at the given wind, V .

8.2. Generic versus optimised pitch

Further optimisation of the wind turbine power output, P_M , can be achieved by tracking the global pitch angle, β , to its optimised position at the given wind, V , and the optimised rotational speed, ω_M . The result of this optimisation, with computations of the BEM-method, is illustrated by the curves of the power coefficient, C_P , and the thrust, T , plotted in **Fig. 8.5** and **Fig. 8.6**, respectively. As seen, the variable-speed wind turbine can be optimised by the pitch control in means of a slightly increase of the gain of the mechanical power produced by the wind turbine. This optimisation thinking has only sense when the incoming wind is in the range below the rated wind speed.

Optimisation by the pitch influences slightly on the thrust, T , as well. Its value increases a little as the result of the power optimisation. On this stage, the following considerations are useful (Akhmatov et al, 2002(a)).

- 1) Optimisation by pitch leads only to a slightly increase of the gain in the mechanical power output when the optimisation by the rotational speed is already completed. Here, it is the last couple percent to optimise.
- 2) The optimised pitch values are all found to be close to 0° and, for the given wind turbine, they are slightly negative values.
- 3) Optimisation of the wind turbine is, no-doubt, an important task. The more power is produced, the larger profit will be reached from the same incoming wind. In this investigation, the wind turbine model shall be applied in investigations of transient voltage stability, but not for completion of optimisation of the wind turbine. Thus, refining of the power output is not necessary to include.
- 4) Although detailed optimisation, it is plausible to consider that the wind turbine deviates a little – within a couple percent – from its optimised operational point. It may occur because of dynamic variations in wind etc. Then a little deviation in pitch from the exact optimised value is still a legal consideration for definition of an operational point of the variable-speed wind turbine.

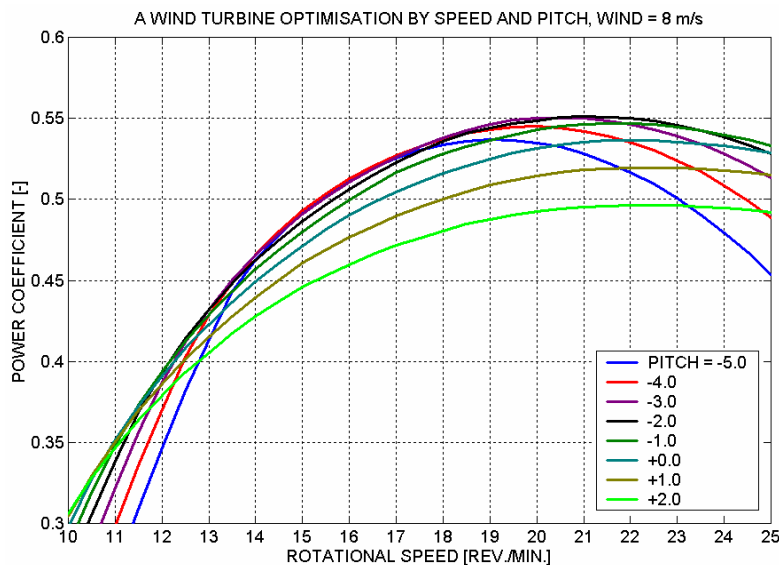


Fig. 8.5. Power coefficient, C_p , at the wind 8 m/s as a function of the rotational speed, ω_M , at the global pitch, β , varying in the range -5° to $+2^\circ$, purposing optimisation of the wind turbine by pitch³⁴. In the given example, the optimised pitch is around -2° , so that slightly below 0° . The gain in the power coefficient is around 0.01 (or 1%). Reported in (Akhmatov, 2002(b))

³⁴ Discussion: notify that the power coefficient, C_p , that is the dimensionless parameter is commonly plotted against the other dimensionless parameter – the tip-speed-ratio. In this case, the power coefficient is plotted against the rotational speed to comply with curves shown in **Fig. 8.2** and **Fig. 8.6**.

Resuming these considerations, the optimisation by pitch at light wind can be omitted in models of variable-speed wind turbines applied in investigations of transient voltage stability. The values of the optimised pitch at light wind can be simply replaced by the value $\beta = 0^\circ$ at any wind below the rated wind.

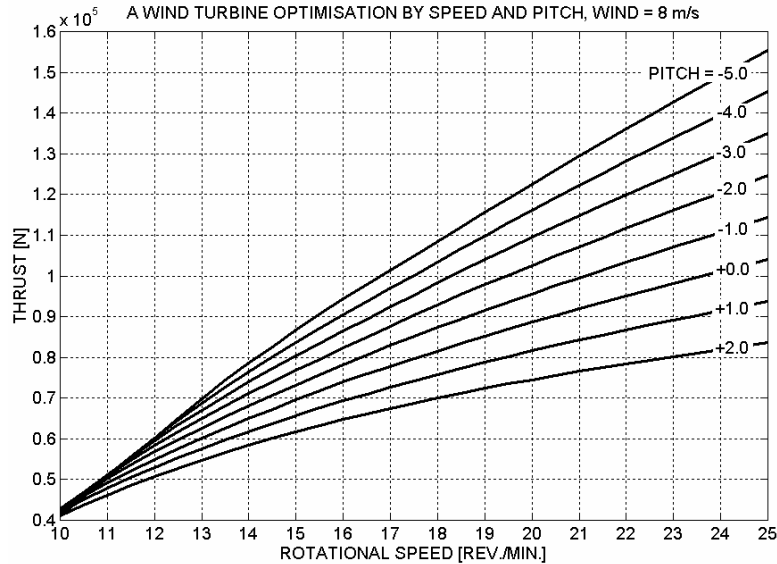


Fig. 8.6. Thrust at incoming wind of 8 m/s as a function of the rotational speed plotted at the global pitch varying in the range from -5° to $+2^\circ$. This curve is given for illustration of the numeric order of values of the mechanical loads applied onto the wind turbine construction. Reported in (Akhmatov et al, 2002(c)).

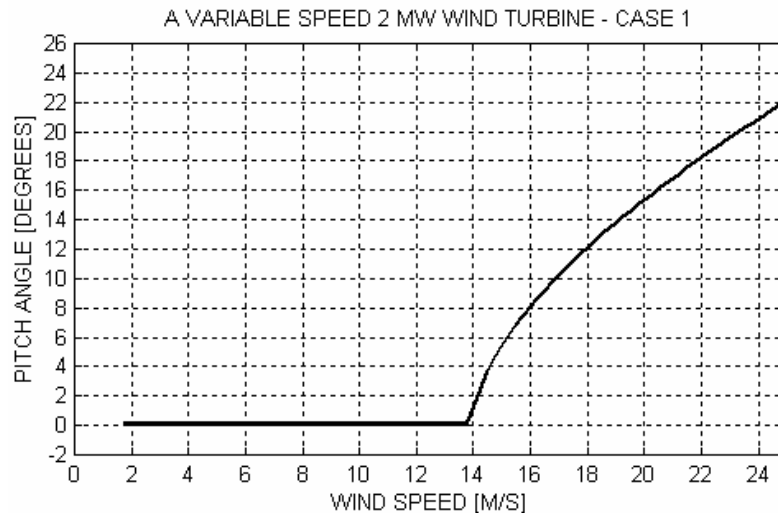


Fig. 8.7. Generic pitch versus wind at optimised rotational speed. Reported in (Akhmatov et al, 2002(a)).

As seen from **Fig. 8.3**, the mechanical loads applied onto the wind turbine construction, which is evaluated by the thrust, T , will increase at increasing wind. The variable-speed wind turbines must be protected against mechanical overloads and possible risk of damages at strong wind. This is achieved by pitching the blades into the position where a part of incoming wind will pass by the wind turbine. The power, P_M , will be kept at its rated value at this operational mode. By pitching, the thrust is reduced. This strategy is similar to case of fixed-speed wind turbines. In this work, the

curve of the global pitch versus incoming wind is computed with use of the BEM-method for the given variable-speed wind turbine. Its curve is shown in **Fig. 8.7**.

By generic way, the pitch angle is set to 0° at incoming wind below the rated wind. At strong wind, e.g. above the rated wind, the global pitch, β , is computed with use of the BEM method purposing to keep the mechanical power at the rated value. This routine relates to initialisation of the generic model of the pitch-control system. The generic pitch control is described in **Section 3**.

8.3. Generator concepts of variable-speed wind turbines

The variable-speed wind turbines are equipped with converter-controlled generators (Slootweg et al, 2003). The two basic concepts are already mentioned in **Section 1**; this work will focus on these two generator concepts.

- 1) Doubly-fed induction generators (DFIG). Here, the rotor circuit of the DFIG is connected to the power network through the partial-load frequency converter.
- 2) Synchronous generators excited with permanent magnets (PMG), which are connected to the ac-grid through the full-load frequency converters.

It seems to be that these two concepts are very similar to each other because the frequency converters are present in the both generator concepts. However, there are several functional differences between these two generator concepts. There are also differences between the control features, which can be applied to the frequency converters to achieve uninterrupted operation of the wind turbines. Therefore it seems to be more reasonable to treat these two generator concepts and their models separately.

The variable-speed wind turbines equipped with PMG and their models are explained in **Section 9** and the variable-speed wind turbines equipped with DFIG in **Section 10**.

9. Variable-speed wind turbines equipped with PMG

Variable-speed wind turbines are a promising concept for large offshore wind farms. One of many possible realisations of this concept is with use of multi-pole, synchronous generators (MPSG) excited by permanent magnets. In this concept, the MPSG are direct-driven and connected to an ac-grid through full-load frequency converters. The main advantages of this concept are that (i) the wind turbines are gearless and (ii) the excitation system is replaced by permanent magnets. The electromagnetic construction of the permanent magnet generators (PMG) is, however, more complex than in case of generators of conventional concepts.

Construction of the MGS is an important issue because it enables the wind turbine to be coupled directly to the generator (Lampola et al., 1995; Grauers, 1996). Several types of constructions of MPSG are proposed for direct-driven wind turbine generators. An overview of these generator types is found in (Grauers, 1996).

Commonly, the permanent magnets are placed in the generator rotor. The stator can either be connected to the ac-grid or to the frequency converter, which is connected to the ac-grid. In case of variable-speed wind turbines, the solution with the full-load frequency converter is common. Use of the frequency converter is essential to link the generator, which operates variable-speed, and the ac-grid, which operates at a fixed electric frequency.

In this investigation, the rotational speed of the rotor, ω_M , varies between 10.5 and 24.5 RPM, depending on incoming wind. This corresponds to the mechanical frequency, f_M , of 0.175 to 0.408 Hz. The electric frequency generated by the synchronous PMG at its terminals, f_E , will be defined by the mechanical frequency, f_M , and the number of pole-pairs, N_{EE} .

$$f_E = f_M N_{EE} . \quad (9.1)$$

In this investigation, the number of pole-pairs $N_{EE} = 32$. For reaching the desired rated power, the PMG may consist of a number of generation units, which are also called sections. These sections are placed on the same rotor shaft (Grauers, 1996).

Furthermore, it is considered that the flux density generated by the permanent magnets, the number of sections and the stator windings are sufficient to generate 2 MW at the rated rotational speed of 24.5 RPM. The rated electric frequency of the PMG will be $f_E^{\text{RAT}} = f_M^{\text{RAT}} N_{EE} = 13$ Hz. Applying **Eq. (9.1)**, the electric frequency at the terminals of PMG varies in the range from 5.6 Hz at light wind to 13 Hz at rated operation in strong wind.

To connect the PMG to the ac-grid, the full-load frequency converter is applied. This frequency converter is controlled by the power electronics with IGBT-switches. The generator-side converter generates the voltage-phasor and the electric frequency at the PMG terminals, which corresponds to the desirable rotational speed of the wind turbine. The generator-side converter operates as a voltage-source converter (VSC) with the voltage, V_G , and the electric frequency, f_E .

In this work, the parameters of the PMG and of the converter are chosen so that the generator is excited by the permanent magnets without use of supplementary arrangements³⁵. In normal operation, there is no exchange of reactive power between the PMG and the generator-side converter. The generator-side converter absorbs only electric power produced by the PMG, P_G . This reduces the generator current in normal operation – the current in the stator windings.

Through the dc-link the electric power generated by the PMG is supplied to the grid-side converter and from this converter to the power grid. The grid-side converter is also a VSC when controlled with IGBT-switches. The grid-side converter can operate reactive-neutral, e.g. no exchange of reactive power between the grid-side converter and the ac-grid. This operation will be suitable in case of a relatively strong power system. Here the terminal voltage of the grid-side converter is around 1.0 PU.

When the power system is relatively weak, the voltage may experience fluctuations even in normal operation. In this case, the grid-side converter can be equipped with reactive-power control, which control reactive power within a pre-dined range.

Let us point-out that the PMG cannot exchange reactive power with the electric power network, because the PMG and the power network are coupled (read also as de-coupled) by the dc-link. Through the dc-link, transfer of the electric power is only possible. Consequently, control of reactive power and voltage in this wind turbine concept is defined by the control system of the grid-side converter.

It would seem to be that, in investigations of transient voltage stability, the variable-speed wind turbines of this concept should be represented with their grid-side converters whereas other parts of the construction are omitted. This simplification would be explained by the fact that reactive power and voltage control would only depend on the control system of the grid-side converter.

However, such a description will be oversimplified in situations with significant voltage fluctuations, which occur at short-circuit faults in the power grid. In such situations, both the restrictions on operation of the frequency converter with a risk of the converter blocking and operation of the generator itself shall be taken into account. This needs a discussion.

Normally, the frequency converter is designed to have the power capacity, which is some above the rated electric power of the generator. Remember that the frequency converter is controlled by the IGBT-switches, which are sensitive to thermal overloads, over-currents and over-voltages (Akhmatov, 2002(a)). To prevent damage of the IGBT-switches, the frequency converter may block. This implies that the IGBT-switches stop switching and disconnect.

The dc-link voltage, the current in the generator- and the grid-side converters and other electrical parameters related to the converter operation are continuously monitored by the converter protective system. When at least one of the monitored parameters exceeds its respective relay settings, the

³⁵ In situations when the generator excitation from the permanent magnets is insufficient, it could be arranged by the permanent magnets in combination with the generator-side converter. In this case, the converter would supply a (less) amount of reactive power to the PMG. Another additional excitation feature could be use of the capacitors either in series with or connected between the three phases of the PMG (Grauers, 1996; Chen et al, 1998). Such details will not influence on the voltage behaviour in the ac-grid, because the generator is not directly connected to the ac-grid and its reactive power demands are not seen from the power system.

converter will block; the blocking time is within few milliseconds. Such short blocking time requires accurate computation both of the converter system and the generator, because the converter may block by an excessive current transient in the generator.

The converter blocking may lead to disconnection of the wind turbine generator. According to the Danish specifications (Eltra, 2000), such disconnection is not acceptable in case of large (offshore) wind farms. The complete model shall be sufficiently accurate to predict the wind turbine operation at transient events in the power network.

The transient behaviour of the generator and the converter will decide operation of the wind turbine during a transient event in the power network. Modelling of variable-speed wind turbines equipped with PMG and frequency converters becomes a multitask project, when the target is investigations of transient voltage stability. The models should be with representations of (i) the generator, (ii) possibly the shaft system and (iii) the rotor aerodynamics, (iv) the frequency converter, (v) its control and (vi) protection.

9.1. Generator model

The generator model consists of (i) an initialisation routine and (ii) a transient model with the state equations. Considered that the electric machine is a symmetrical, three-phased, permanent magnet generator. Furthermore, it is considered that the flux established by the permanent magnets in the stator is sinusoidal (Westlake et al, 1996). The electromotive forces (EMF) are therefore sinusoidal. On these assumptions, the excitation voltage, E_G , is given by the EMF generated by the permanent magnets.

$$E_G = 2\pi f_E \phi , \quad (9.2)$$

where ϕ denotes the magnitude of the flux induced by the permanent magnets of the rotor in the stator phases. The transient model of the PMG is given by the following system of equations (Westlake et al, 1996; Solsona et al, 2000).

$$\begin{cases} \frac{d\psi_D}{dt} = -R_G I_D - \omega_E \psi_Q - V_D , \\ \frac{d\psi_Q}{dt} = -R_G I_Q + \omega_E \psi_D - V_Q , \end{cases} \quad (9.3)$$

$$\psi_D = \phi + L_D I_D , \quad \psi_Q = L_Q I_Q .$$

Here, the electric parameters are given in the D - and Q -axes, the stator flux is $\psi_G = (\psi_D, \psi_Q)$, the terminal voltage of the PMG is $V_G = (V_D, V_Q)$ and the machine current is $I_G = (I_D, I_Q)$. The stator resistance is R_G , the synchronous reactance $X_G = (X_D, X_Q)$ due to saliency and $X_D = \omega_E L_D$ and $X_Q = \omega_E L_Q$, where L_D and L_Q denote the inductance in the D - and Q - axis, respectively. When it is not distinguished between X_D and X_Q , the synchronous reactance is denoted X_G .

The MPSG are characterised by relatively large reactance values, when measured in PU. This statement can be confirmed, when studying the synchronous reactance values of the MPSG of hydro power plants (Chow et al, 1999; Schmidt et al, 2001). The PMG will also be characterised by large synchronous reactances.

As evaluated, the synchronous reactance of the PMG with rated power of 2 MW is in the range of 1.0 PU (Grauers, 1996). In this work, the values of the synchronous reactance X_D and X_Q , the winding resistance R_G and other parameters of the PMG are collected in **Table 9.1**.

Initialisation of the PMG model is with use of the technique known from steady-state computations of synchronous generators with salient rotors. This routine is illustrated in **Fig. 9.1**. When the PMG supplies the electric power P_G and is reactive neutral $Q_G = 0$ (when it is excited by the permanent magnets), the terminal voltage, V_G , and the current, I_G , of the PMG are in-phase. The purpose of initialisation is to find the current components (I_D, I_Q) and the voltage components (V_D, V_Q).

Electric parameter	Value	Electric parameter	Value
Rated generator power, P_G^{RAT}	1.01 MW \times 2	Rated converter power, P_S^{RAT}	2 MW
No-load voltage, V_G	1.40 PU = 966 V	Rated grid frequency	50 Hz
Rotational speed, ω_G	10.5 –24.5 RPM	Rated grid voltage	690 V
Number of pole-pairs N_{EM}	32	Rated DC-link voltage, U_{DC}	1.16 PU =800 V
Reactance X_D	1.05 PU	DC-link capacitor X_{DC}	0.10 PU
Reactance X_Q	0.75 PU	Grid-side smoothing inductor X_S	0.175 PU
Resistance R_G	0.042 PU	Grid-side smoothing inductor R_S	0.014 PU

Table 9.1. Electric data of PMG and electrical system of converter. Reported in (Akhmatov et al, 2003(b)).

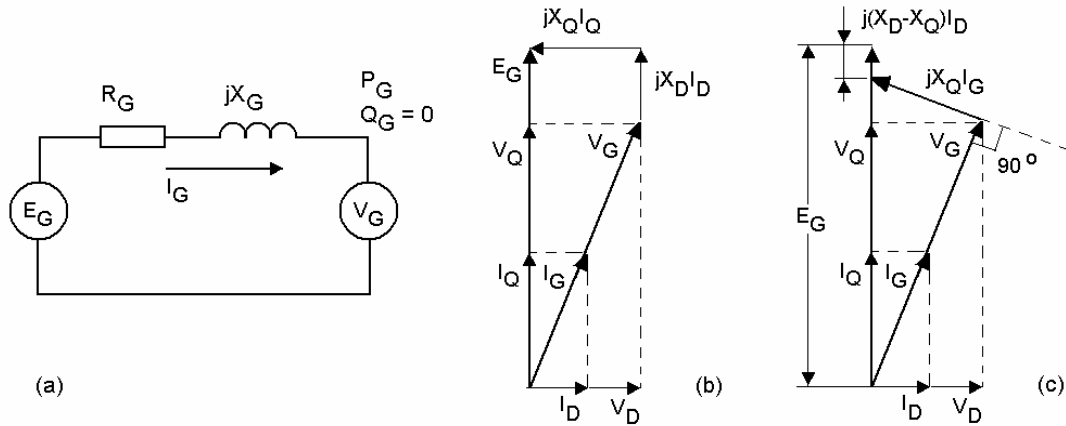


Fig. 9.1. Steady-state representation of PMG: (a) – by a simple network equivalent, (b) – by a vector diagram with neglected R_G , (c) – by a vector diagram with reluctance effects.

The apparent power exchanged between the PMG and the generator-side converter will be:

$$S_G = P_G + jQ_G = V_G \cdot \text{conj}(I_G), \quad (9.4)$$

and $\text{conj}(\cdot)$ denotes complex conjugation. The electric torque, T_E , of the PMG with salient poles is defined from inspection of **Fig. 9.1.c**.

$$T_E = E_G I_Q - (X_D - X_Q) I_D I_Q. \quad (9.5)$$

Notice that the contributions by R_G are neglected in vector diagrams shown in **Fig. 9.1** due to $R_G \ll X_G$.

9.2. Mechanical system representation

Representation of the wind turbine mechanical system covers the shaft system model, the aerodynamic rotor model and the pitch-control model. The aerodynamic model and the generic-level pitch-control model are already discussed in **Sections 2.1**, **Section 3** and **Section 8**.

Representation of the shaft system is not certain in case of direct-driven generators. According to (Kundur, 1994; Akhmatov et al., 2000(a)), the effective shaft stiffness and the inertia constant of the turbine shall be reduced by the product of the gear ratio and the number of pole-pairs squared. The expressions from **Appendix 4.A**, which are re-written below, explain how to compute the effective shaft stiffness in PU/el.rad., K_S , and the inertia constant in seconds, H_M , from their physical values. These must be with respect to the electric system speed, ω_E , to comply with the generator equations written in the PU (Per Unit) system. This gives the transformation between the SI (System Universal) and the PU system.

$$\begin{cases} H_M = \frac{1/2 \cdot J_M \cdot \omega_{E0}^2}{S_B \cdot N_{EM}^2} = \frac{1/2 \cdot J_M \cdot \omega_{M0}^2}{S_B}, \\ K_S = \frac{\kappa}{S_B} \cdot \frac{\omega_{E0}}{N_{EM}^2} = \frac{\kappa}{S_B} \cdot \frac{\omega_{M0}}{N_{EM}}. \end{cases}$$

Here, J_M is the inertia of the turbine in $\text{kg}\cdot\text{m}^2$, κ is the shaft stiffness in $\text{N}\cdot\text{m}/\text{mech.rad.}$, ω_{E0} and ω_{M0} are the rated electrical system speed and the rated mechanical turbine speed in mech.rad./s and el.rad./s , respectively. Further, $\omega_{E0} = \omega_{M0} N_{EM}$ with N_{EM} is the product of the gear ratio and the number of pole-pairs and S_B denotes the rated MVA-base of the generator. In case of the gearless concept, the gear ratio is unity, but the number of pole-pairs can be large. Therefore, $N_{EM} = N_{EE}$. **Table 9.2** illustrates how the parameters of the shaft system will depend on the number of pole-pairs.

Number of pole-pairs	Rated electric frequency, Hz	Inertia constant, s	Shaft stiffness, PU/el.rad.
16	6.53	4.8	3.2
32	13.06	4.8	1.6
64	26.12	4.8	0.8
128	52.24	4.8	0.4

Table 9.2. Dependence of the turbine inertia constant, H_M , and the effective shaft stiffness, K_S , on the number of pole-pairs in a variable-speed wind turbine with a gearless shaft and a MPSG; the turbine inertia $J_M = 2.92 \cdot 10^6 \text{ kg}\cdot\text{m}^2$, the shaft stiffness $\kappa = 4 \cdot 10^7 \text{ N}\cdot\text{m}/\text{rad.}$, the rated mechanical speed $\omega_{M0} = 2.566 \text{ rad./s}$ ($=24.5 \text{ RPM}$) and the MVA-base $S_B = 2 \text{ MVA}$.

Reduction of the effective shaft stiffness, K_S , at increasing number of pole-pairs, N_{EE} , implies that a mechanical shaft twist will result in a larger (dynamic) change of the generator electric angle when the number of pole-pairs is also larger. This conclusion becomes very obvious when recognising that the same electrical angle corresponds to a smaller mechanical angle with increasing

number of pole-pairs. Consequently, the shaft torsional twist will affect operation of the PMG in a more significant way when the number of pole-pairs is larger.

In the case with a PMG with 32 pole-pairs, the shaft system is relatively stiff. In voltage stability investigations, the wind turbine mechanical system could be represented by the lumped-mass model (Akhmatov et al, 2000(c)).

$$2H_M \frac{d\omega_E}{dt} = T_M - T_E . \quad (9.6)$$

The inertia constant of the lumped rotating system of the turbine rotor, H_M , and the generator rotor, H_G , is $(H_M + H_G) \approx H_M = 4.8$ s, when considering that $H_G < H_M$. The parameter ω_E implies the electric speed $2\pi f_E$. Notify a relatively large value of the inertia constant, H_M . This indicates that the rotational speed of the wind turbine and the generator rotor will not change significantly when short-term transient events are seen at the PMG terminals. At a suitable control of the frequency converter, the transients in the ac-grid will not necessarily be seen at the PMG terminals. However, this may depend on the converter action and sequences at faults in the ac-grid.

To complete this discussion, notify that the shaft torsional oscillations are reported in (Westlake et al, 1996) in case of an experimental wind turbine equipped with a PMG with 83 pole-pairs. When the number of pole-pairs is sufficiently large, the shaft system becomes “soft” as it is known for conventional fixed-speed wind turbines (Akhmatov et al, 2000(a)). Here a more detailed model of the shaft system – the two-mass model, should be applied to represent the shaft torsion.

9.3. Frequency converter system and its control

The generic system of a frequency converter in application with a PMG is shown in **Fig. 9.2**. The frequency converter system consists of the generator-side converter with its smoothing inductor, the grid-side converter, and the dc-link connecting these two converters. The converter system is controlled by the IGBT-switches.

The generator-side converter injects the current $J_1 = \frac{P_G}{U_{DC}}$ into the dc-link with the voltage U_{DC} .

The current on the other side of the dc-link is $J_2 = \frac{P_{GC}}{U_{DC}}$ where $P_{GC} = P_S + P_L$ and P_S is the electric

power supplied to the power system and P_L is the power losses in the grid-side converter mains. In steady-state operation and on assumption of no power losses in the dc-link, $P_G = P_{GC}$. At steady-state conditions, the voltage across the dc-link, U_{DC} , is constant, which gives the initialising condition of the dc-link, $U_{DC}(0)$.

When a disturbance occurs, the stationary power equality between the generator power, P_G , and the power received by the grid-side converter, $P_{GC} = P_S + P_L$, is broken. This starts the current flowing through the dc-link capacitor, $I_C = J_1 - J_2$, and leads to fluctuations of the dc-link voltage U_{DC} . Its value, at any time, t , can be computed by the following relation (Akhmatov et al, 2003(b)).

$$U_{DC}(t) = \sqrt{U_{DC}^2(0) + \frac{2}{C} \int_0^t (P_G(\tau) - P_{GC}(\tau)) \cdot d\tau}, \quad (9.7)$$

where C is the value of the dc-link capacitor.

This mechanism corresponds to completion of the power balance on disturbed operation conditions.

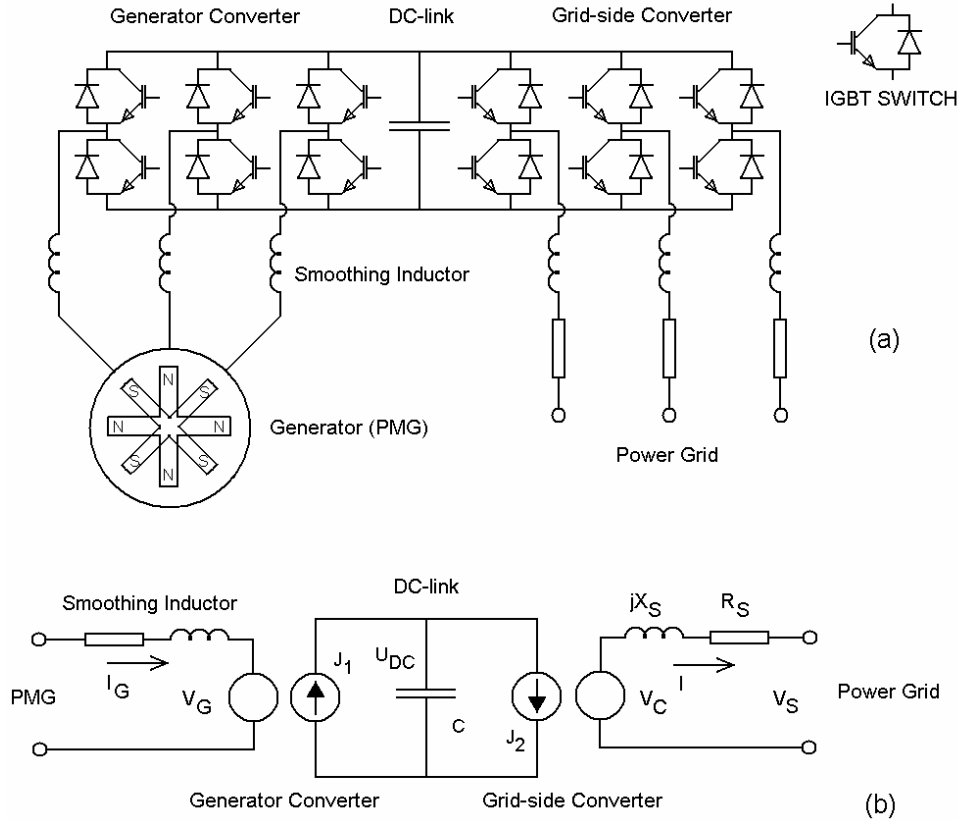


Fig. 9.2. The back-to-back frequency converter for grid-connection of a PMG: (a) – functional scheme, (b) – simplified representation. Reported in (Akhmatov et al, 2003(b)).

The current, I , going through the mains of the grid-side converter with the impedance $R_S + jX_S$ can be computed with use of the well-known relations (Svensson, 1995).

$$\begin{cases} \frac{d\psi_{DS}}{dt} = -R_S I_{DS} - \omega \cdot \psi_{QS} - (V_{DC} - V_{DS}), \\ \frac{d\psi_{QS}}{dt} = -R_S I_{QS} + \omega \cdot \psi_{DS} - (V_{QC} - V_{QS}), \\ \psi_{DS} = X_S I_{DS}, \quad \psi_{QS} = X_S I_{QS}, \end{cases} \quad (9.8)$$

where the differential equations are in the (D, Q) -axis and $\psi_S = (\psi_{DS}, \psi_{QS})$ denotes the flux, $I = (I_{DS}, I_{QS})$ is the current, $V_S = (V_{DS}, V_{QS})$ is the grid voltage and $V_C = (V_{DC}, V_{QC})$ is the voltage generated by the grid-side VSC. The converter mains are also its smoothing inductors in the three

phases. Analogously, the voltage at the PMG terminals $V_G = (V_D, V_Q)$ is controlled by the generator-side VSC, which is taken into account in dynamic simulations.

The complex power exchanged between the grid-side converter and the power system will be:

$$S = P_s + jQ_s = V_s \cdot \text{conj}(I), \quad (9.9)$$

and the power losses in the grid-converter mains are:

$$P_L = R_s I^2 \quad (9.10)$$

Notice that the model of the variable-speed wind turbine with PMG is interfaced to the simulation tool through the mains of the grid-side VSC. The results produced by this part of the model shall be interfaced to the simulation tool PSS/E by an appropriate way.

9.3.1. Control system of generator-side converter

The control system of the frequency converter of the PMG can be organised with use of different schemes (Pöller and Achilles, 2003). In this work, the generic control scheme shown in **Fig. 9.3** is applied. The generic control system is with independent control of the electric power, P_G , and the reactive power, Q_G , of the PMG and given in **Fig. 9.3.a**. Here the electric power of the generator, P_G , is controlled as the power at the receiving end of the transmission line with the reactance X_G . The power is transferred from the sending voltage-source, E_G , to the receiving voltage-source, V_G , (Kundur, 1994; Taylor, 1994).

$$P_G = \frac{E_G V_G}{X_G} \sin \alpha_G \approx \frac{E_G V_G}{X_G} \alpha_G, \quad (9.11)$$

where E_G and V_G denote magnitudes of the voltage-sources and α_G is the angle difference between these two voltage-sources, respectively. Using the same consideration about the transmission line between the two voltage sources (Kundur, 1994; Taylor, 1994), the reactive power, Q_G , is given by:

$$Q_G = \frac{V_G(E_G - V_G)}{X_G} \cos \alpha_G \approx \frac{V_G(E_G - V_G)}{X_G}, \quad (9.12)$$

on assumption of small values of the angle difference α_G . In these terms, the electric power of the PMG is controlled by the voltage angle at the fixed angle of the excitation voltage, E_G .

The magnitude of the excitation voltage, E_G , is proportional to the rotational speed, **Eq. (9.2)**. Since the inertia, H_M , is relatively large, the rotational speed will not change significantly during transient events of a short duration. Consequently, the magnitude of E_G will not change significantly. Therefore, the generator reactive power, Q_G , can be controlled by the magnitude of V_G . The generator is excited by the permanent magnets and magnetisation of the PMG does not influence on the voltage profile in the power system. Therefore, the function of the control system is to keep Q_G at zero at varying electric power, P_G .

The time delays for measuring of the electric and the reactive power are included in the converter model, but the IGBT-switching dynamics in the converter is neglected on assumption that the generator-side VSC is able to follow the reference values of α_G and V_G at any time.

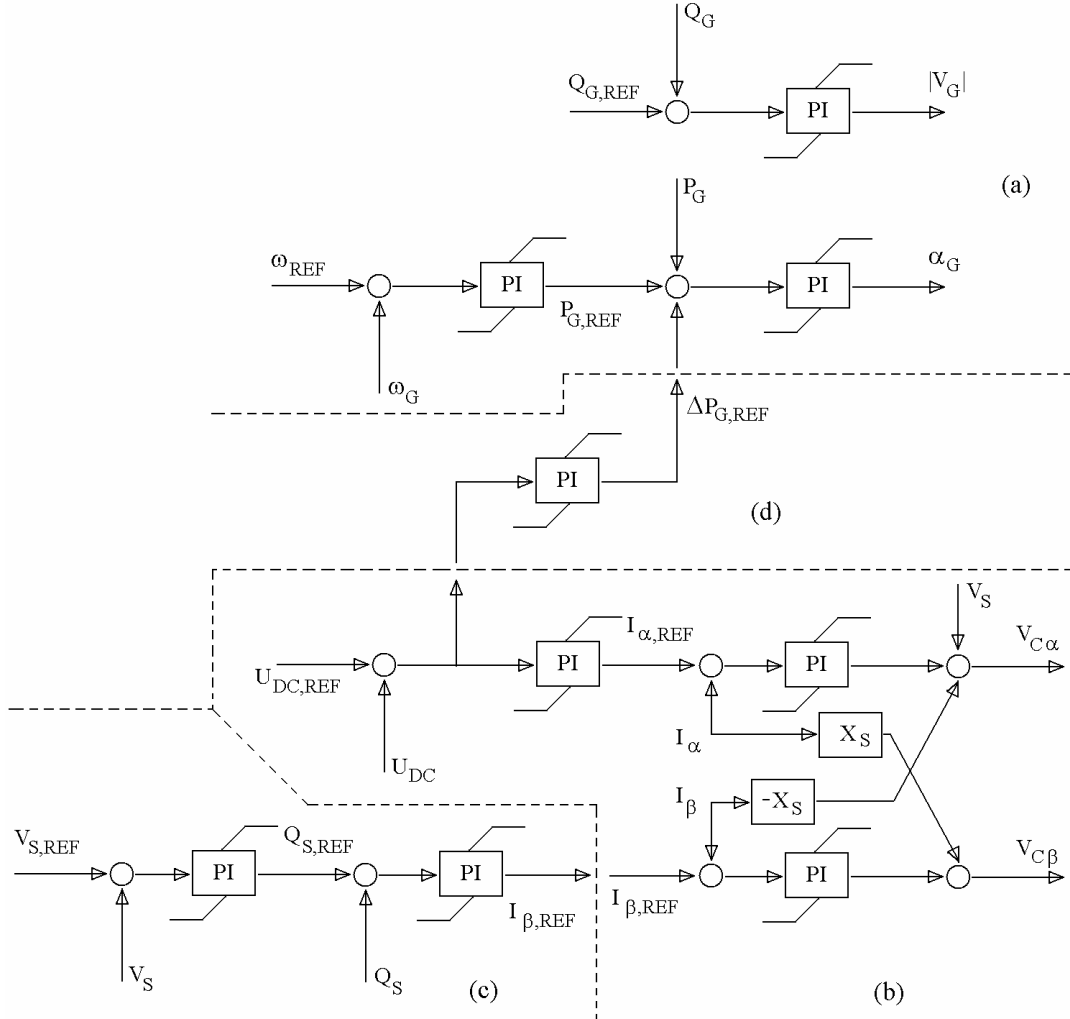


Fig. 9.3. Generic control system of the full-load back-to-back converter: **(a)** – independent control of electric and reactive power of PMG, **(b)** – independent control of dc-link voltage and reactive power of grid-side converter, **(c)** – additional control loops for voltage control by grid-side converter, **(d)** – additional feedback loop for generator control at registering of abnormal grid operation. Figure is, in part, borrowed from (Akhmatov et al, 2003(b)).

9.3.2. Control system of grid-side converter

The control system of the grid-side VSC can be organised in several ways. In this work, this control is arranged with use of the generic control scheme known from control of Statcoms (Schauder and Mehta, 1993; Akhmatov et al, 2003(b)). This generic control is with independent control of dc-link voltage, U_{DC} , and reactive power, Q_S . The generic control system is given in **Fig. 9.3.b**. The grid-side VSC is controlled in a synchronously rotating (α, β) -reference frame. The α -axis is oriented along the terminal voltage vector, V_S , and so $V_S = V_\alpha + jV_\beta = V_\alpha$ and $V_\beta = 0$. The active current component becomes I_α and the reactive current component is I_β , because:

$$S = P_s + jQ_s = V_\alpha (I_\alpha - jI_\beta) = V_\alpha I_\alpha - jV_\alpha I_\beta. \quad (9.13)$$

The control of the dc-link voltage, U_{DC} , is organised with use of two proportional-integral (PI) controllers in series and the reactive current, I_β , is controlled by one PI-controller. The dc-link voltage and the active power, P_s , are regulated by the active current reference in response to an error signal of the dc-link voltage. The reactive power, Q_s , is simply regulated with respect to the setting of the reactive current reference. It is zero when reactive-neutral operation is desired.

The voltage-compensation is given by the cross-coupling in terms of $(V_s - X_s I_\beta)$ and $X_s I_\alpha$, respectively (Schauder and Mehta, 1993). The grid-side converter mains are with resistive losses. This is taken into account in the converter control model, but omitted in **Fig. 9.3.b** for simplification of the drawing.

The switching dynamics of the grid-side VSC is neglected on assumption that the VSC is able to follow the reference values of the voltage-source $V_{C\alpha}$ and $V_{C\beta}$ at any time.

9.3.3. Additional reactive power control

When required, two PI-controllers in series producing the reference signal of the reactive current, $I_{\beta,REF}$, from the voltage error signal can be added to the control system of the grid-side VSC (Akhmatov et al, 2003(b)). It is shown in **Fig. 9.3.c** and can be applied to control reactive power and voltage by the grid-side VSC. This additional control system is chosen because it can be desirable that the grid-side VSC contributes to voltage control at transient events in the power grid.

However, it is kept in mind that this controllability is restricted (Akhmatov et al, 2003(b)). It is because such frequency converters are primarily designed for transferring of the electric power from the generator to the ac-grid with a fixed electric frequency. Therefore the ac-current of the converter, I_s , is dominated by the active component, I_α . For keeping the ac-current of the grid-side converter within the legal range, the reactive current, I_β , and so the reactive power, Q_s , exchanged between the grid-side VSC and the grid will be restricted. Presumably, the reactive power, Q_s , can be in the range of $\pm 10 \%$ of the rated power capacity of the grid-side converter. In case of a 2 MW wind turbine, it gives the reactive power range of ± 200 kVAr, at rated operation of the wind turbine.

9.3.4. Coupling between the two VSC

In the generic control system shown in **Fig. 9.4**, the generator and the grid-side VSC are controlled independently from each other. Normally, a coupling between these two VSC will be introduced. This coupling can be arranged as an additional control loop between the generator power control and the dc-link voltage control, for example. This will make it possible to adjust the power generation when the dc-link voltage deviates from its reference. The negative coupling will contribute to stabilising of the converter system operation.

In this work, the control loop performing the coupling is organised with use of a PI-controller. Other control schemes can be suggested as well (Pöller and Achilles, 2003).

9.3.5. Tuning of frequency converter control

When tuning the converter system control, the proportional gains and the integration times of the controllers are determined. These parameters are set for the given configuration of the control system. The PMG data, the data of the dc-link and the grid-side converter mains must be taken into account. By tuning the following targets shall be reached.

- 1) The controlled parameters shall reach their respective references.
- 2) The response of the converter to a change in a reference signal shall be as fast as possible, but without large overshoots and excitation of transients in the generator- and the grid-side VSC.
- 3) The converter must perform damping of the fundamental-frequency transients in the electric parameters of the PMG and the grid-side converter.
- 4) When the shaft system is taken into account, the converter must contribute to damp the shaft torsional oscillations. This part is omitted in this work.

The generic control of the back-to-back converter is examined by stepping the references of the following parameters.

- 1) The generator power reference, $P_{G,REF}$, at disabled control loop by the speed.
- 2) The reactive power reference, $Q_{S,REF}$, at disabled control loop by the terminal voltage.
- 3) The dc-link voltage reference, $U_{DC,REF}$.

PI-controllers of generator-side converter:			
Gain P_G	Integration time P_G	Gain Q_G	Integration time Q_G
0.07 PU	25 ms	0.07 PU	25 ms
PI-controllers of grid-side converter:			
Gain U_{DC}	Integration time U_{DC}	Gain Q_S	Integration time Q_S
1.50 PU	0.5 s	1.00 PU	0.25 s
2.80 PU	50 ms	2.80 PU	50 ms

Table 9.3. Main parameters of the frequency converter system applied with PMG. Reported in (Akhmatov et al, 2003(b)).

The main parameters of the generic control system of the frequency converter system are collected in **Table 9.3**. The dynamic responses of the converter system are shown in **Fig. 9.4**. All the dynamic responses examined are sufficiently fast. No fundamental-frequency transients in the generator electrical parameters are excited when the converter control system is well-tuned. A delay in the response of the electric power of the PMG to a step in its reference is notified. This delay is caused by the large value of the synchronous reactance of the PMG. A slight fundamental-frequency component is also seen in the response of the electric power of the PMG. It is, however,

not critical for operation of the wind turbine generator because such fundamental-frequency components are damped by the well-tuned converter.

Notice that when other data of the generator, the dc-link capacitor or the grid-side converter are applied or when the control system topology is changed, the converter control shall be tuned again.

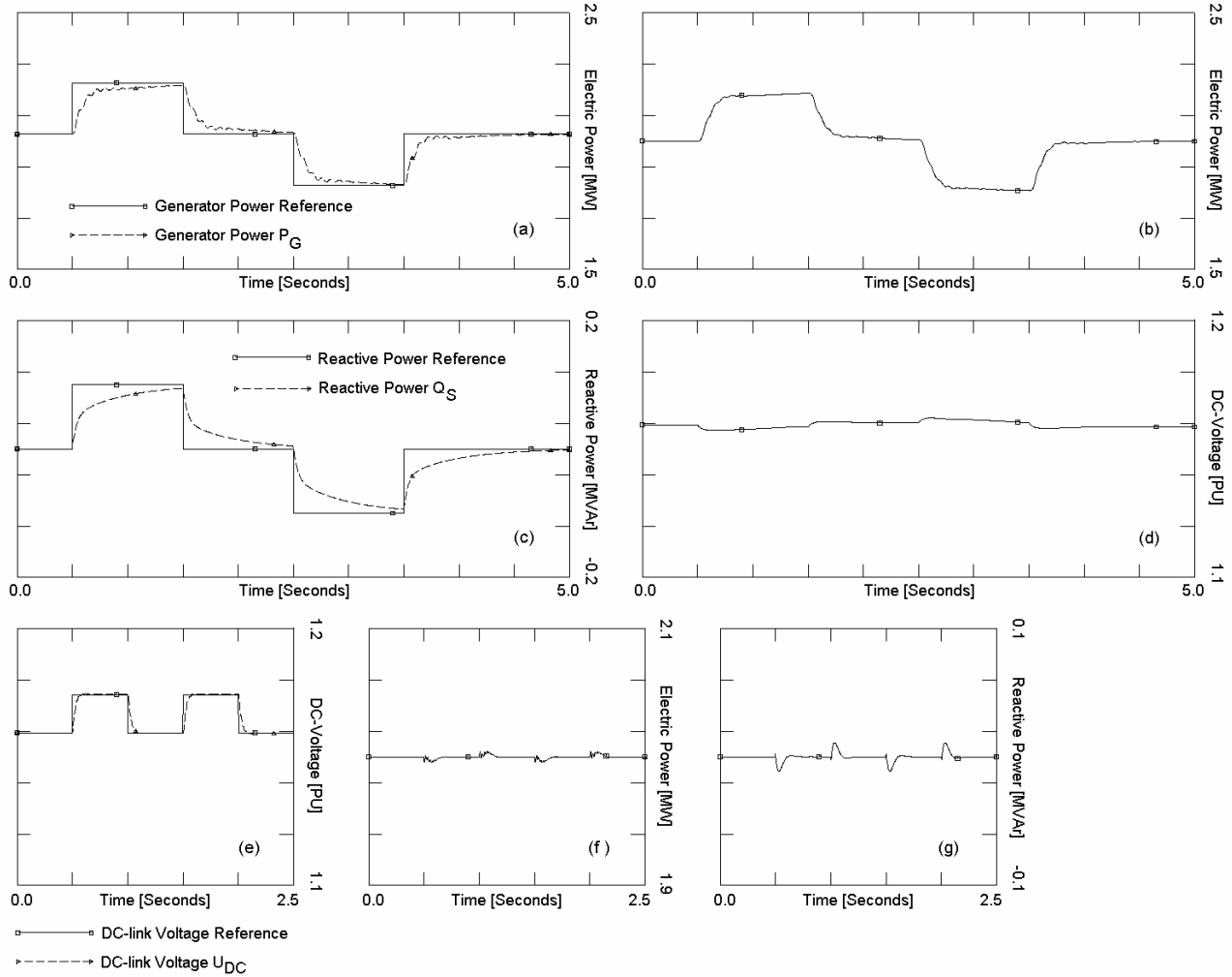


Fig. 9.4. Converter tuning and responses to steps in reference signals: (a) – electric power of PMG, P_G , and (b) – electric power supplied to power system, P_S , as response to step in generator power reference, $P_{G,REF}$, (c) – reactive power exchanged with power system, Q_S , and (d) – dc-link voltage, U_{DC} , as response to step in reactive power reference, $Q_{S,REF}$, (e) – dc-link voltage, U_{DC} , (f) – electric power, P_S , and (g) – reactive power, Q_S , as response to step in dc-link voltage reference, $U_{DC,REF}$. Reported in (Akhmatov et al, 2003(b)).

9.4. Protective system of converter and generator

In investigations of transient voltage stability, the protective systems of the frequency converters must be taken into account. This is necessary because the converter actions will decide the wind turbine operation during the transient events in the power grid. The converter protective system monitors the dc-link voltage, the current of the grid-side converter, the generator current and other electrical parameters and compares the monitored parameters to their respective relay settings. When at least one of the respective relay settings is exceeded, the protective system orders the

converter to block. At blocking, the converter stops switching and trips. This action may lead to disconnection of the wind turbine, which will be in contrast with the TSO's specifications requiring uninterrupted operation of the wind turbine at grid faults.

9.4.1. Evaluation of converter blocking in simulations

Normally, the protective relay settings of the frequency converter can be received from the wind turbine manufacturer (Akhmatov, 2002(a)). When this is not possible, such relay settings can be evaluated. The evaluation must be based on reasonable assumptions and require, at least, basic knowledge about operation of such frequency converters. In this investigation, risk of the converter blocking is primarily evaluated from the behaviour of the dc-link voltage.

The converter tripping limit will not be much above the rated dc-link voltage, which value is set to 800 V in this case. In this investigation, the over-voltage relay setting for the dc-link voltage is therefore set to 1 kV. This implies that the frequency converter will block when the dc-link voltage exceeds 1 kV. The rated voltage is 690 V, see **Table 9.1**. Hence, 1 kV corresponds to 1.45 PU in the chosen PU-system. If the converter tripping limit was significantly above the rated dc-link voltage, this would require over-dimensioning of the frequency converter and increase the price of the wind turbine.

Secondly, the current of the grid-side converter must be paid attention to. It is because the grid-side converter is controlled by the IGBT-switches. The IGBT-switches must not be subject to over-current and thermal over-loads to avoid damages of these power electronics' components. When the current of the grid-side converter exceeds its respective relay setting, the converter will also be ordered to block. Surely, the converter will be ordered to block when the current transients exceed the value of $2I_{\text{RATED}}$ or so. This converter action must also be reflected in investigations of transient voltage stability (Akhmatov, 2002(b)).

The blocking time of the frequency converter controlled by the IGBT-switches can be in the range of a few ms (Akhmatov, 2002(b)).

Keep in mind that the procedure applied in this investigation on evaluation of the converter blocking does not necessarily cover every possible situation. The rated voltage of the PMG applied in the LW72³⁶ wind turbine is 4 kV, which may indicate that the frequency converter may operate at higher dc-voltages than suggested in this work. In practical stability investigations, information about the converter blocking must always be requested from the wind turbine manufacturer.

9.4.2. Generator protection at faults

In many investigations, the generator protection is mentioned as an important issue (Hsu, 2001; Muljadi et al, 1998). Basically, it focuses on the following issues.

- 1) Protection against over-current in the PMG stator-windings. A high value of the generator current, I_G , would cause a serious damage of the machine itself in form of demagnetising the magnets (Muljadi et al, 1998).

³⁶ Mentioned in **Section 1.2**.

- 2) Thermal over-loads of the generator causing the magnets to reach the Curie temperature would also lead to demagnetisation of the magnets (Hsu, 2001).

However, the PMG is separated from the transient fault in the grid by the frequency converter with the dc-link. As found in this investigation, the grid fault affects mostly the grid-side converter and the dc-link, whereas the PMG is not much affected in a case of a grid fault. The converter control must be designed to reduce the stress from the power grid on the PMG. In these terms, grid faults will not necessarily cause damage of the PMG with demagnetising the magnets.

9.5. Uninterrupted operation at transient events

The response of the wind turbines equipped with PMG and frequency converters to a grid fault is examined. The main target of this investigation has been to clarify if there are problems with (i) maintaining of short-term voltage stability and (ii) at the same time uninterrupted operation of such wind turbines. Secondly, the common question about a possible risk of mutual interaction between many grid-connected converters must be answered.

The investigation is made with use of the model of the wind farm consisting of eighty 2 MW wind turbines set-up in **Section 5.1**, but no-load capacitors are not applied in case of the converter-controlled wind turbines. The power generation pattern in the wind farm is similar to **Section 6.7**. The grid disturbance is a three-phased, short-circuit fault of 150 ms duration. The fault is cleared by tripping the faulted line. The fault occurs in the transmission power system, at 132 kV voltage level. Consequences of the grid fault to the power system operation are already discussed in **Section 6.7**.

9.5.1. Uninterrupted operation of converter

The first issue to be explained is how to maintain uninterrupted operation of the frequency converters when a short-circuit fault occurs in the transmission power network. This implies how to achieve the converter operation without protective tripping at the grid fault. In the simulations illustrating this feature, the converter protective systems are disabled for simplification of the computations.

The simulated curves for the wind turbine WT 01 with disabled converter protection are shown in **Fig. 9.5**. The respective curves are plotted for four cases, which can be distinguished by the converter control and the data. In all the four cases, the voltage in the power network is re-established very fast after the fault is cleared. This result indicates that maintaining of short-term voltage stability is not any problem related to this variable-speed wind turbine concept.

When the converter blocks by excessive over-voltage in the dc-link, **Eq. (9.7)** must be taken into account to explain the mechanism behind this voltage increase.

- 1) First, the derivative of the dc-link voltage, dU_{DC}/dt , is proportional to $1/C$. Application of a larger capacitor in the dc-link would reduce the dc-link voltage fluctuations.
- 2) Second, the electric power supplied to the grid drops when the grid voltage drops. Drop of the electric power leads to charging of the dc-link capacitor. Reduction of such voltage drop

would also reduce the dc-link voltage fluctuations. This could be achieved with use of dynamic reactive compensation, for example, an SC acting during the voltage drop.

- 3) Third, using a similar argumentation as in item 2, the power generation from the PMG must be reduced to reduce the dc-capacitor charging. This relates to implementation of a coupling (a feed-back) between the control loops of the generator- and the grid-side converters.
- 4) Fourth, operation of the dc-link at a higher dc-voltage. This option is kept in mind, but will not be present in this work.

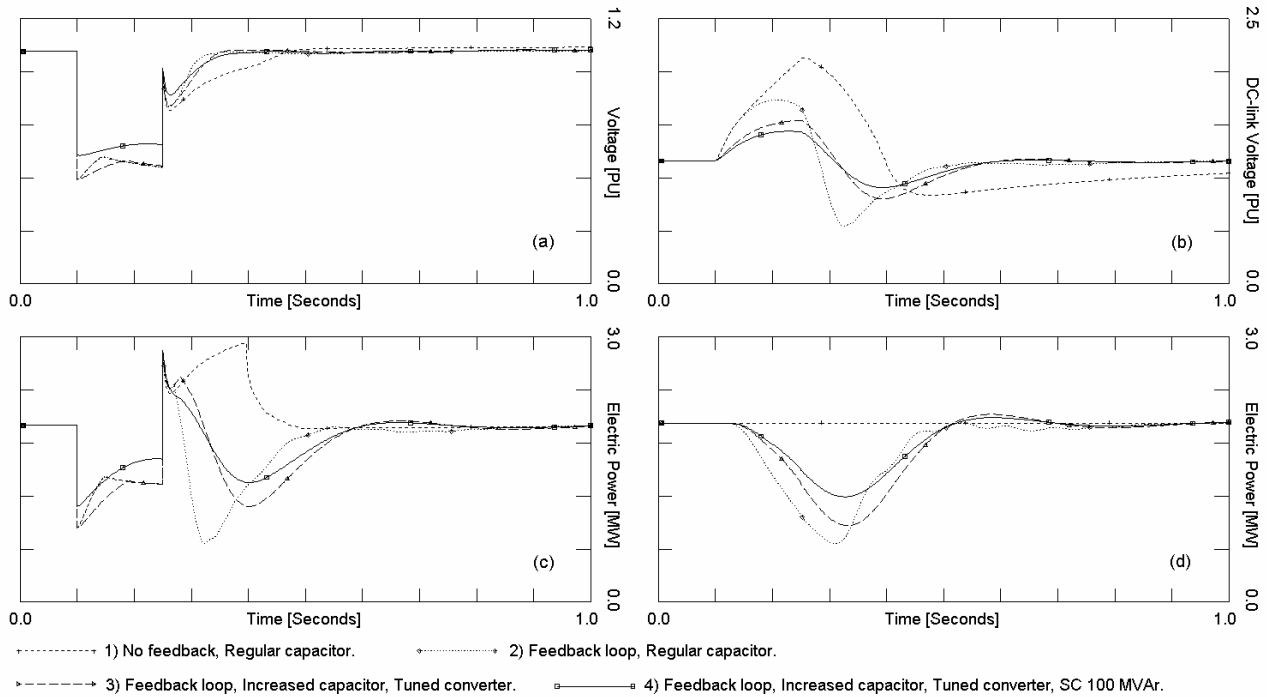


Fig. 9.5. Voltage stability and uninterrupted converter operation of variable-speed wind turbines illustrated by the four simulated cases of converter control feature. Simulated values for wind turbine WT 01: (a) – terminal voltage, V_s , (b) – dc-link voltage, U_{DC} , (c) – electric power supplied to grid, P_s , (d) – electric power generated by PMG, P_g .

Advantages from application of a larger dc-capacitor, implementation of the feed-back in the converter control and use of dynamic reactive compensation to expand the converter tripping limit are explained below. This corresponds also to the marks in **Fig. 9.5**.

- 1) When no one of the suggested arrangements is applied, the dc-link voltage may reach and exceed the converter tripping limit. This will result in the converter blocking, indeed.
- 2) The feed-back between the error signal of U_{DC} and the generator power reference, $P_{G,REF}$, is implemented in the converter control system, **Fig. 9.3.d**. The fluctuation of the dc-link voltage is applied as an indication of abnormal operation of the power grid. The idea behind this feature is to reduce the generator power, P_g , and also the charging dc-current, J_1 , when the discharging dc-current, J_2 , is reduced at drop of P_s at the grid fault. The goal is to minimise a possible risk of over-voltage in the dc-link. When this feed-back is implemented, the fluctuation of U_{DC} is also reduced. Our investigation shows that this feature applied alone performs benefits only at relatively small voltage drop. At a larger voltage drop, this feature

alone is insufficient to reach unblocked converter operation because there are delays in the converter response.

- 3) The feature described in item 2 is combined with the dc-link capacitor increased by the ratio 2.5 of its default value (**Table 9.1**). The converter control system is re-tuned after the dc-link capacitor has been changed. At the grid fault, the dc-link voltage shows a less fluctuating behaviour when compared to the results reached with the feature of item 2. However, the converter will presumably block because the dc-link voltage approaches the converter tripping limit. This is caused by a relatively large voltage drop at the wind turbine terminals. As can be seen, there are two competitive processes starting fluctuation of the dc-link voltage: (i) reduction of the discharging dc-link current, J_2 , due to the terminal voltage drop and (ii) action of the control system reducing the generator power, P_G , and so reducing the charging dc-link current, J_1 . In the given wind turbine, the first process seems to be more rapid than the second one, which causes unacceptably large fluctuation of the dc-link voltage.
- 4) Uninterrupted operation of the frequency converter cannot always be reached by advancing the converter control loops and changing the converter electrical data. Actions of the converter control loops can be delayed due to presence of specific physical parameters of the PMG. This may introduce restrictions on the given generator concept and its control. The main problem seems to be a significant voltage drop in the power grid, which the converter control cannot handle without protective tripping. Therefore, it focuses on reduction of the voltage drop at the wind turbine terminals at the short-circuit fault. This is achieved by incorporation of an SC in the wind farm connection point. In this investigation, the rated power capacity of the SC is 100 MVA.

Notice that the final solution can be a combined feature because the control systems of the frequency converter (with an increased dc-link capacitor and re-tuned control loops) and the controllability of the SC contribute both to uninterrupted operation of the frequency converter at the grid faults. Application of this combined feature results in that the dc-link voltage does not exceed its relay setting and the converter does not block. Notice that the SC is applied to prevent the converter blocking at the grid fault, but not for reasons related to maintaining of short-term voltage stability.

For getting a complete picture, other parameters been important for the converter actions at grid disturbances must be computed and monitored in investigations of short-term voltage stability. Among such parameters there is the current of the grid-side converter, I , because this current is going through the IGBT-switches of the grid-side converter. This current is plotted in **Fig. 9.7** for the four cases (features) described above. As can be seen, the combined control feature reduces also this current. Consequently, a possible risk of the converter blocking is reduced.

Application of the SC increases the total cost of the project. Use of the SC of 100 MVA rated power capacity seems to be an expensive feature when taking into account that the rated power of the wind farm is 150 MW. Notice that uninterrupted operation of the frequency converters requires also increase of the dc-link capacitors. This may also influence the cost of the wind turbines themselves.

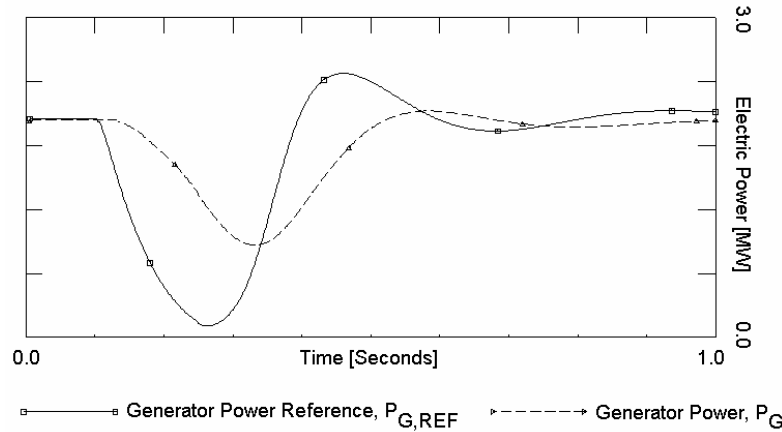


Fig. 9.6. Converter control feature according to item 3. The delay between the generator reference power, $P_{G,REF}$, and the electric power, P_G . The delay is, presumably, due to a large reactance of PMG.

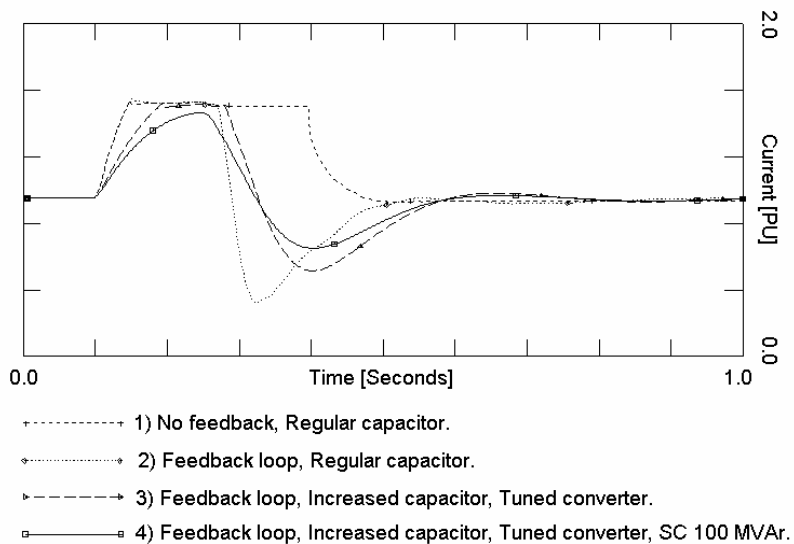


Fig. 9.7. Voltage stability and maintaining uninterrupted feature of variable-speed wind turbines illustrated by the four simulated cases on converter control feature. Simulated current in grid-side converter mains of wind turbine WT 01.

Notice that this presentation does not exclude that better control features of the frequency converters can be suggested to achieve uninterrupted operation of the converters at grid disturbances.

9.5.2. Feature with blocking and re-start of converter

When a risk of the converter blocking at a grid fault is indicated, a feature with blocking and re-start of the frequency converters must be suggested to achieve uninterrupted operation of the wind turbines. Here, the frequency converters are blocked during the grid fault. This means that the wind turbine generators cannot supply the electric power to the grid. The grid-side converters are set to operate as Statcoms, e.g. the wind turbines contribute to control of reactive power and voltage.

After the grid fault has been cleared, the frequency converters re-start and the wind turbine generators continue to supply electric power to the power grid. In the following, this uninterrupted operation feature is explained.

9.5.2.1. Blocking of generator-side converter

When the dc-link voltage approaches or exceeds its tripping limit, the generator-side converter stops switching. The IGBT-switches of the generator-side converter open and the PMG looks into the dc-link capacitor throughout the diode-bridge. This situation is illustrated in **Fig. 9.8.a**. The grid-side converter continues its operation.

The dynamic behaviour of the generator-converter system is characterised by the two competitive processes.

- 1) Charging of the dc-link capacitor throughout the diode-bridge from the PMG.
- 2) Discharging of the dc-link capacitor by the grid-side converter.

Obviously, the dc-link voltage cannot exceed the phase-phase voltage magnitude of the PMG at no-load operation. This value is 1.40 PU and corresponds to the excitation voltage, E_G , induced by permanent magnets, see **Table 9.1**. In other words, blocking of the generator-side converter by opening of its IGBT-switches may prevent fatal over-voltage in the dc-link.

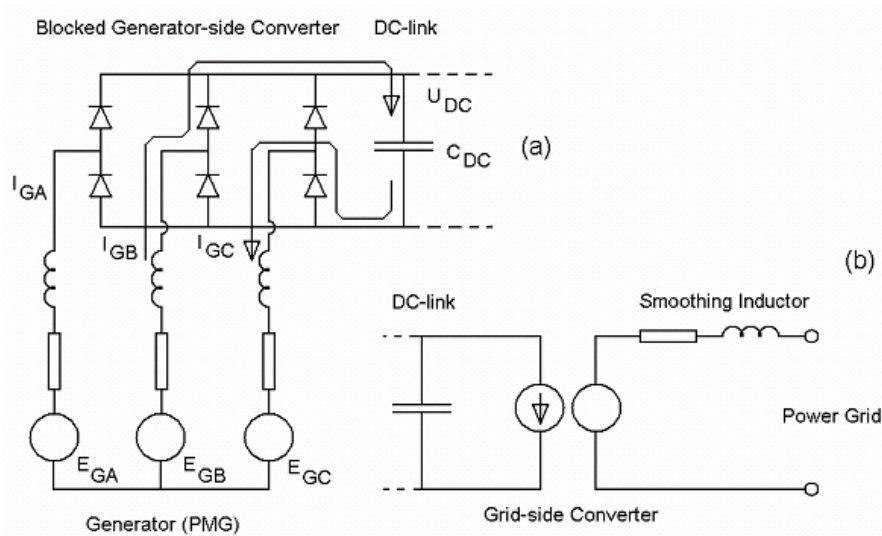


Fig. 9.8. Operation with blocked generator-side converter: (a) – charging of the dc-link capacitor from the PMG, (b) – operation of grid-side converter as a Statcom. It is considered that the converter blocking has occurred at the moment when the phase-current I_{GA} is passing through zero.

On the other hand, discharging of the dc-link capacitor by the grid-side converter can be excessively intense. In this case, the dc-link voltage starts to decay, which will initiate a reactive current in the PMG stator-windings. As found in this investigation, the magnitude of this reactive current may easily reach 2 PU. This is not acceptable because of a risk of demagnetising the

magnets. This implies that co-ordination of the converter control is needed, when executing the blocking sequence.

9.5.2.2. Control co-ordination

The dc-link capacitor discharges because the grid-side converter still supplies an amount of the electric power to the power grid. This can be eliminated when setting the active current reference of the grid-side converter to zero. This is the control co-ordination.

In this situation, the dc-link capacitor will rapidly charge and the dc-link voltage reaches the value being equal to the excitation voltage of the PMG, E_G . When the dc-link capacitor is charging, the current in the PMG stator-windings decays rapidly to zero. This process corresponds to that the magnetising energy accumulated in the current going through the PMG stator-windings is transformed to the electric energy accumulated in the dc-link capacitor (Akhmatov, 2002(b)). This process takes a few ms.

When the dc-link capacitor has charged, the grid-side converter is set to operate as a Statcom, e.g. it contributes to control of reactive power and voltage during and after the grid fault. Its electric scheme is given in **Fig. 9.8.b**. However, this controllability of the grid-side converter is restricted. Here it must be taken into account that the current of the grid-side converter may not exceed its relay settings because of concerns about protection of the IGBT-switches of the grid-side converter against over-currents and thermal over-loads.

9.5.2.3. Re-start of converter

When the grid fault has been cleared and the voltage has re-established, the frequency converter will re-start. The IGBTs of the generator-side converter start switching. The electric power reference of the PMG and the active current reference of the grid-side converter are increased to their original values. This increase is, possibly, by a ramp.

Operation of the wind turbine will re-establish when the electric power reaches its original level (presumably as before the fault). The wind turbine supplies the electric power to the grid, whereas the reactive power exchanged between the grid-side converter and the power system is minimised.

9.5.2.4. Simulation example

The simulation case to illustrate the blocking and re-start converter sequences is carried out with use of the wind farm model with eighty wind turbines; the results for the wind turbine WT 01 operating at rated power are presented. The simulated behaviours of the terminal voltage, V_S , the dc-link voltage, U_{DC} , the generator power and its reference, P_G and $P_{G,REF}$, respectively, and the electric power, P_S , are shown in **Fig. 9.9**.

The events of the simulation case are the following. Initially, the wind turbine and the power system are at normal operation. The frequency converter is controlled by its regular control scheme given in **Fig. 9.3**. At the time $t = 0.5$ s, a short circuit fault occurs in the transmission power network.

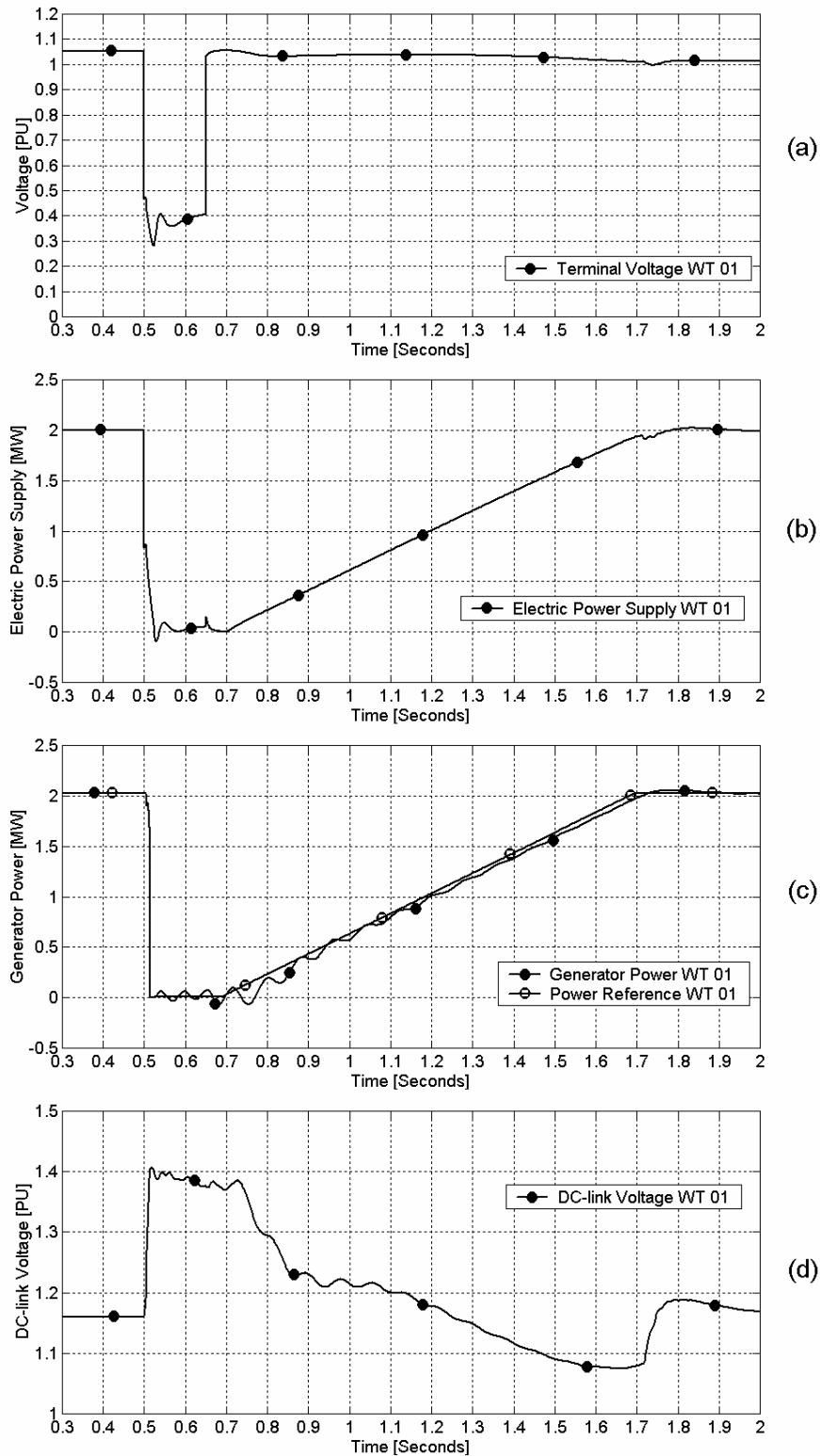


Fig. 9.9. Transient behaviour of a selected wind turbine with converter blocking and re-starting: (a) – terminal voltage, (b) – electric power supplied to grid, (c) – generator power and its reference, (d) – dc-link voltage.

At the short circuit fault, the terminal voltage drops and the dc-link voltage starts approaching to its critical value. The converter protective system registers abnormal operation and orders to block the generator-side converter. The blocking time is very short, been in the range of a few ms.

Shortly after the converter has blocked, the dc-link capacitor is fully charged. The dc-link voltage has reached the value of 1.40 PU corresponding to the excitation voltage magnitude, E_G , and the generator current is zero.

The grid-side converter continues its operation. However, the active current reference is set to zero to minimise discharging of the dc-link capacitor. The grid-side converter operates as a Statcom and contributes to control of reactive power and terminal voltage, V_S . This controllability is restricted. In this investigation, the reactive power limits of the grid-side converter are set to $\pm 20\%$ of the rated power of the grid-side converter (increased ranges in this example when compared to the ranges given in **Section 9.3.3**). This corresponds to ± 400 kVAr for each wind turbine converter.

From simulations it is seen that there will be a little lack of energy accumulated in the dc-link capacitor. This lack occurs due to the cross-coupling in the grid-side converter control. This causes a slight reduction of the dc-link voltage. Reduction of the dc-link voltage starts a reactive current in the PMG stator-windings. However, this current magnitude is so small as insignificant. During blocked operation, the generator-side converter is on stand-by and waits for order to re-start.

At the time $t = 0.65$ s, the grid fault has been cleared. The grid-side converter contributes to re-establishment of the voltage. Shortly after the fault has been cleared, the generator-side converter re-starts. In this simulation example, the converter re-starts approximately 50 ms after the time of the fault clearance.

The generator operation will not be re-established momentarily, but by ramping of the generator power reference, $P_{G,REF}$. This process is illustrated in the curves shown in **Fig. 9.9** and during the time interval from 0.7 s to 1.7 s. In this simulation case, the generator operation and its electric power, P_G , are re-established during 1 s. Notify that other rates of power ramp could be applied.

The power supply to the grid from the grid-side converter is re-established in a similar way. At the time $t = 1.7$ s, the wind turbine operation is completely re-established. The converter control is again organised by its regular control system shown in **Fig. 9.3**.

As can be seen, voltage is re-established with use of dynamic reactive compensation performed by the wind turbine itself, applying the frequency converter. The generator and the converter parameters are default as in **Table 9.1**. Advanced application of the blocking and re-start converter sequences may reduce the total cost of the wind farm.

On the other hand, the frequency converter blocks during the faulting time, which causes that the wind turbines do not supply electric power to the grid during this faulting time. This faulting time is so short that the power loss is negligible.

9.6. On mutual interaction between wind turbines

The common concern with relation to grid-incorporation of large wind farms with a large number of wind turbines controlled by frequency converters is a possible risk of mutual interaction between the converters and their control systems. Such mutual interaction would possibly lead to destabilisation of the wind farm operation and cause tripping of several wind turbines. It could be thought that such mutual interaction would be started by a grid disturbance, for example, by a short-circuit fault in the transmission power network.

With relation to this work, there are two possible issues, which can be investigated. Firstly, if there is a possible risk of interaction between the converters and the control system of the dynamic reactive compensation units – the SC. Secondly, if there is a possible risk of mutual interaction between the control systems of the frequency converters executing blocking and re-start sequences.

As indicated in previous sections, the simulations are made with use of the model of the large wind farm consisting of eighty wind turbines, e.g. with representation of eighty frequency converters.

First, the feature with uninterrupted converter operation combined with application of the SC is examined. **Fig. 9.10** gives the simulated curves for selected wind turbines in the large wind farm, operating at different operational points. As can be seen, the wind turbines show the coherent response at the grid fault. There is no mutual interaction between the wind turbines controlled by the frequency converters (with uninterrupted converter operation). Furthermore, there is no interaction between the frequency converters of the wind turbines and the dynamic reactive compensation unit.

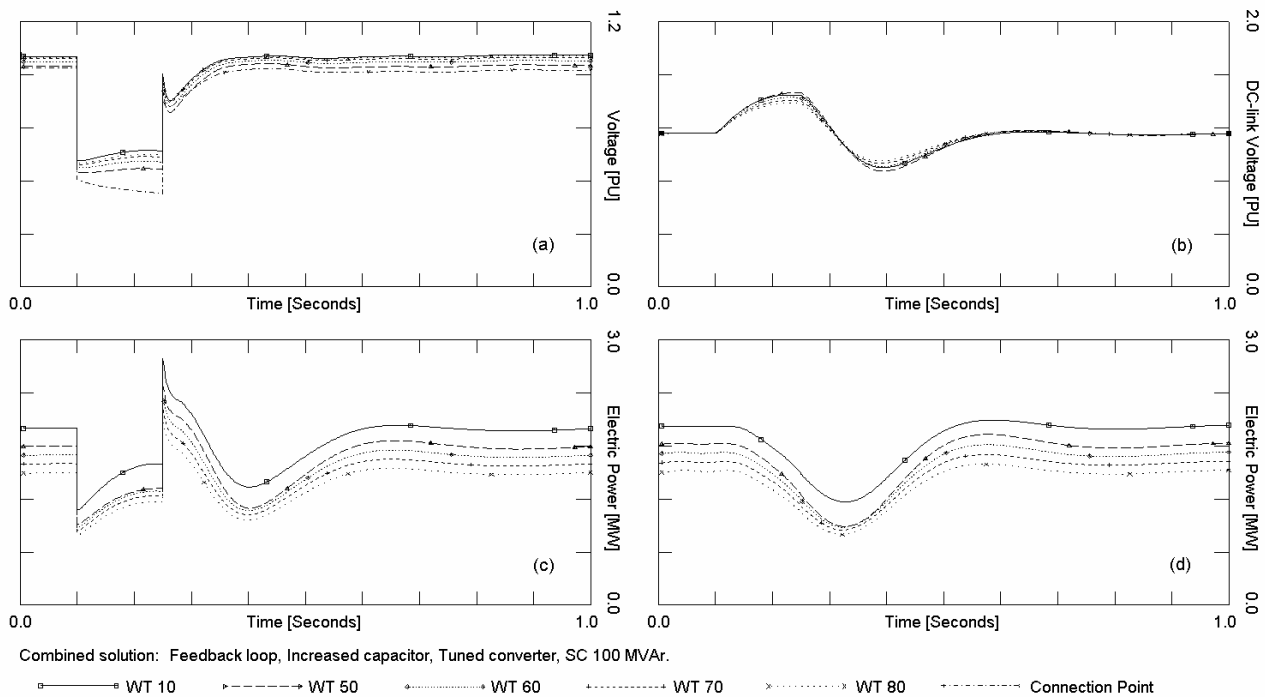


Fig. 9.10. Voltage stability and absence of mutual interaction between wind turbines with PMG and full-load converters. Case with tuned converters and use of SC of 100 MVA rated capacity. Simulated curves for selected wind turbines: (a) – terminal voltage, V_s , (b) – dc-link voltage, U_{DC} , (c) – electric power supplied to grid, P_s , (d) – electric power generated by PMG, P_G .

Second, the feature with the converter blocking and re-start is examined in case of eighty 2 MW wind turbines. The simulation results for selected wind turbines are shown in **Fig. 9.11**. Again, the wind turbines show a coherent response at the grid fault. After the grid fault has been cleared, operation of the wind turbines is re-established without indication of any mutual interaction between the frequency converters.

Generally, it may be expected that in case of well-tuned converters, there is no mutual interaction between the converter-controlled wind turbines.

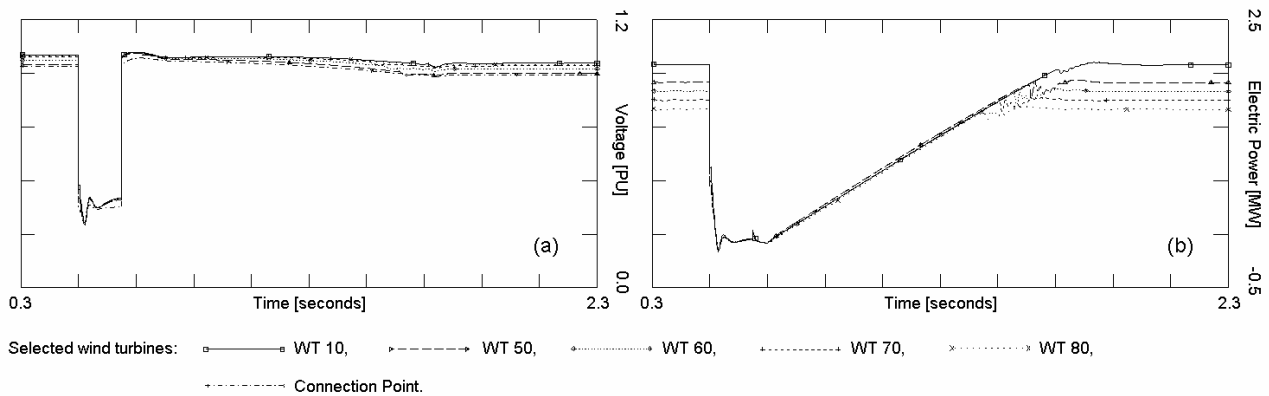


Fig. 9.11. Coherent response of large wind farm with PMG and full-load converters to a short-circuit fault: (a) – terminal voltage of grid-side converters and (b) – electric power supplied by grid-side converters of selected wind turbines. Voltage is re-established without use of dynamic reactive compensation.

9.7. Resume

The variable-speed wind turbines with direct-driven synchronous generators are a promising wind turbine concept for large-scale applications. These wind turbines are connected to the ac-grid through the frequency converters. In the generator concept presented in this work, excitation of the synchronous generators is made with use of permanent magnets instead of electrical excitation. This concept is evaluated with respect to maintaining short-term voltage stability at short-circuit faults.

The PMG does not exchange reactive power with the power grid. Only electric power is transferred through the dc-link of the frequency converters from the generators to the power grid. From this viewpoint,

- 1) The generator excitation mechanism is not entirely important in voltage stability investigations.
- 2) This concept is not critical with respect to voltage instability caused by over-speeding of the wind turbines at the grid faults.
- 3) This concept is not critical with respect to reactive power demands of the generator during the transient event.

Reactive power is exchanged between the grid-side converters and the power system. Normally, the grid-side converters operate reactive-neutral, but can be set to control reactive power and voltage within a restricted range. Operation and controllability of the grid-side converters seem to be sufficient to contribute to voltage re-establishing after the grid fault has been cleared. Incorporation of dynamic reactive compensation is not necessary for voltage re-establishment.

On the other hand, the power electronics of the grid-side converters, which are controlled by the IGBT-switches, and also the dc-links are affected by the transient events in the power systems.

This affection is caused by the voltage drop at the short-circuit faults. At such grid faults, there can be a risk of that the converter blocks. This may even lead to that the wind turbine disconnects. Large wind farms must comply with the Specifications of the transmission system operators, where subsequent disconnection is not allowed (Eltra, 2000).

The main challenge of this wind turbine concept is seen to be maintaining of uninterrupted operation of the wind turbines rather than maintaining of short-term voltage stability. Uninterrupted operation of the wind turbines can be achieved with the following features.

- 1) Application of blocking and re-start sequences of the frequency converters at the grid fault.
- 2) Combination of reinforced converter design (with increased dc-link capacitors, for instance) and application of dynamic reactive compensation. The dynamic reactive compensation is applied to reduce the voltage drop at the grid fault. In this way, the frequency converters are less affected and will probably not block.

Consequently, the converter actions are essential for this wind turbine concept to maintain short-term voltage stability and reach compliance with the Specifications of the transmission system operators (Eltra, 2000). An accurate and sufficiently detailed representation of the converter, its control and protective sequences will be absolutely recommended for investigations of transient voltage stability. The converter actions will, indeed, decide the wind turbine operation during and after the transient event in the power system.

10. Variable-speed wind turbines equipped with DFIG

In this concept, the variable-speed operation is achieved with use of the converter-controlled, doubly-fed induction generators (DFIG). As explained in **Section 8**, the range of the rotational speed, ω_M , in the optimised operational range corresponds to operation at -50% to $+10\%$ (static limit) with respect to the synchronous speed. Dynamically, the speed range can be up to $+30\%$ (Vestas, 2001). According to description of (Vestas, 2001), the variable-speed operation makes it possible to increase the annual power production by approximately 5% .

The DFIG consists of a wound rotor induction generator with a partial-load frequency converter on the slip rings of the rotor. The frequency converter is controlled by the power electronics with the IGBT-switches (Heier, 1996; Müller et al, 2000). Operation of the rotor converter corresponds to adding an external voltage-phasor to the rotor circuit. The voltage-phasor is controlled so that the electric frequency of the rotor circuit corresponds to the desired rotational speed of the rotor. The functional scheme of the DFIG and the frequency converter system is shown in **Fig. 10.1**. The stator of the DFIG is directly connected to the power network and the rotor is grid-connected through the partial-load frequency converter. The DFIG supplies the electric power to the grid from the stator and exchanges the electric power with the grid from the rotor.

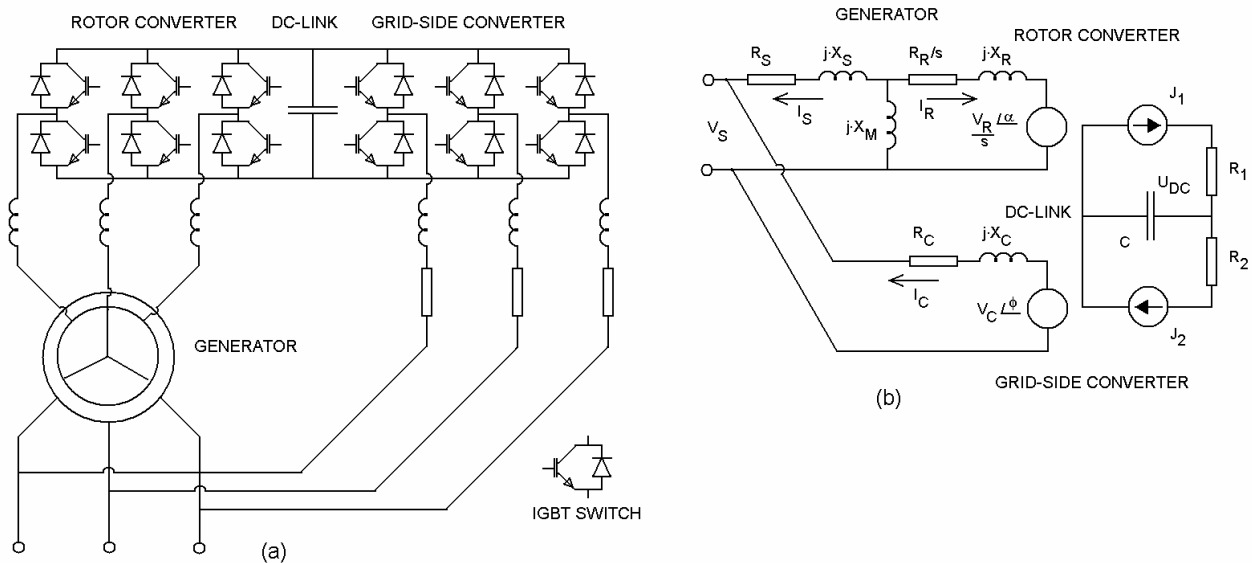


Fig. 10.1. DFIG with the frequency converter system with the dc-link: (a) – a functional scheme, (b) – a simplified representation in steady-state computations. Reported in (Akhmatov, 2003(a)).

Compared to conventional asynchronous generators, the DFIG may have several advantages depending on the realisation of the converter control. Such advantages can be:

- 1) Ability to control reactive power and voltage (Akhmatov, 2002(a)).
- 2) De-coupling of the electric and the reactive power control with independent control of torque and rotor excitation current (Heier, 1996; Zhang et al, 1997).

According to item 2, the DFIG can be excited from the rotor circuit by the rotor converter, but not necessarily from the power grid. Here, we distinguish between two principal situations (Akhmatov, 2002(a)).

- 1) When connected to a strong power system where the voltage is 1.0 PU or around, the DFIG will be excited from the rotor circuit by the rotor converter. The DFIG does not exchange reactive power with the power system. In other words, the DFIG will produce electric power and be reactive-neutral with the power network.
- 2) When connected to a weak power system, characterised by fluctuating voltages, the DFIG can be ordered to produce or absorb an amount of reactive power to control voltage. The DFIG will produce electric power and exchange some reactive power with the grid to reach a desired voltage in vicinity of the connection point.

The converter of the DFIG needs to be rated handling the rotor power only and the excitation of the generator (Heier, 1996; Zhang et al., 1997; Cadirci and Ermis, 1992). The rotor power can be around 25 % of the total generator power. This means that the converter rating should be around 500 kW in case of a 2 MW wind turbine. Reduction of the converter rating is similar to reduction of its size and cost. Use of the converters of smaller ratings is one of the main advantages of this variable-speed concept, compared to the variable-speed wind turbines with the full-load converters.

On the other hand, the converter and its power electronics (controlled by the IGBT-switches) are the most sensitive part of the wind turbine when subjected to transient disturbances in the power network. As the consequence of such disturbances in the power grid, the converter can block (it stops switching and trips) and the wind turbine can disconnect (Akhmatov, 2002(a)). The converter blocks when an order is given by its protective system. The protective system monitors several electrical parameters. Such monitored parameters can be (i) the machine current, (ii) the converter currents, (iii) the dc-link voltage, (iv) the terminal voltage, (v) the electric frequency etc. (Akhmatov, 2002(b)). When at least one of the monitored parameters exceeds its respective relay settings, the converter will block. This implies that the DFIG model shall be sufficiently detailed to perform an accurate representation of the converter blocking sequences in investigations of short-term voltage stability.

The converter action will probably decide operation of the wind turbine and its generator during the transient event that occurs in the power system (Akhmatov, 2002(b)). Accurate and sufficiently detailed modelling of the generator and the converter become an extremely important issue in investigations of short-term voltage stability.

The modelling work presented is made in co-operation with the Danish wind turbine manufacturer Vestas Wind Systems producing the OptiSpeed® variable-speed wind turbines with DFIG. The first Danish large offshore wind farm commissioned at Horns Rev in the year 2002 and connected to the Danish transmission power network contains eighty 2 MW OptiSpeed® wind turbines (Grud, 2000; Jensen 2002). As described by Jensen (2002), the Horns Rev wind farm disconnects at the grid faults, but the wind turbines re-connects again only few seconds after the fault has been cleared. In the wind turbine model it must be possible to compute such or similar tripping and re-connection sequences.

10.1. DFIG modelling in steady-state

Finding of an operational point of the DFIG in steady-state operation corresponds to initialisation (Slootweg et al., 2001). Initialisation of the DFIG model and the power network model is necessary before starting of dynamic simulations.

At initialisation, the following considerations are taken into account. The DFIG consists of a wound rotor induction generator with a converter feeding into the rotor circuit. The generator is with a symmetrical three-phased winding distributed around the uniform air-gap. The generator is doubly-fed which means the following.

- 1) The voltage in the stator, V_S , is applied from the grid.
- 2) The voltage in the rotor, V_R , is induced by the converter. The converter has such a frequency, when superimposed on the rotor speed, this results in a synchronously rotating field in the air-gap.

Only fundamental-frequency components are assumed. Higher harmonics, losses in core and windings, and losses in the converter are all neglected for simplification³⁷. The electric scheme of a DFIG is given in **Fig.10.1.b**. This generator representation corresponds to a modified version of the conventional equivalent circuit given in (Heier, 1996; Müller et al., 2000; Cadirci and Ermis, 1992; Jones and Brown, 1984). On the scheme, V_S is the voltage at the generator terminals, V_R is the magnitude of the rotor voltage-source, and α is the phase difference between the voltages in stator and rotor (Diez et al., 1989). The impedance of the stator, $R_S + jX_S$, the magnetising reactance, jX_M , and the impedance of the rotor, $R_R/s + jX_R$, and the currents in stator, I_S , and in rotor, I_R , are all in stator values.

At initialisation, the electric power operational point is defined by the incoming wind (so that by the power produced by the wind turbine minus losses). The reactive power initialised is in accordance to the control strategy chosen. The electric power and the reactive power are initialised independently from each other, which is similar to synchronous generators. The following is assumed at initialisation.

- 1) The electric power set-point, P_E , is given by the user. This value is the sum of the electric power supplied from the stator to the grid, P_S , and the electric power exchanged with the converter at the rotor slip-rings, P_R . The losses in the converter are neglected, then $P_E = P_S + P_R$.
- 2) The speed slip of the DFIG, s , (also the wind speed and the pitch angle, when necessary) are found from the power set-point using the initialisation algorithm of the wind turbine. This algorithm can be with use of the BEM-method as discussed in **Section 2.1** and **Section 7**.

³⁷ As explained in (Akhmatov, 2003(a)) power losses in the converters of the wind turbines with DFIG do not influence on the voltage profile when executing investigations of short-term voltage stability. Read also our note to Section 4 about assumptions on the asynchronous generator modelling in the dynamic simulation tools. .

- 3) The reactive power exchanged between the DFIG and the power grid is equal to the reactive power in stator, $Q_E = Q_S$. It is because the grid-side converter is considered to be reactive-neutral at normal operation. This consideration is reasonable because the frequency converter rating is maximal 25 % of the generator rating and the converter system is primarily used to supply the electric power from the rotor to the power grid.
- 4) The reactive power from the stator will be zero in case of a strong power system. It will be also set to zero when there is no requirement to control reactive power and voltage by the DFIG. In this case, the DFIG supplies only electric power and excited through the rotor circuit. The power factor of the DFIG is close to unity.
- 5) When required to control voltage at normal operation, the reactive power set-point of the DFIG can be defined as well. Such requirements can be found in the Specifications formulated for the large-scale applications (Eltra, 2000).

As can be seen, (i) the electric and the reactive power, P_E and $Q_E = Q_S$, (ii) the terminal voltage, V_S , and (iii) the speed slip, s , of the DFIG are given at the start of the initialisation. Then, the initialisation of the DFIG model itself must be to find (i) the power distribution between the stator and the rotor, P_S and P_R , (ii) the currents in stator and rotor, I_S and I_R , and (iii) the rotor voltage-source, V_R , induced by the rotor converter. Further, the frequency converter will be initialised, knowing the rotor power, P_R , and neglecting losses.

10.1.1. Initialisation of generator model

In this **Section**, the description of (Akhmatov, 2002(b)) is followed. The initialisation problem of the generator has been solved applying the super-imposing of the currents in stator $I_S = I_{S1} + I_{S2}$ and in rotor $I_R = I_{R1} + I_{R2}$ induced by the voltage-sources $V_1 = V_S$ and $V_2 = V_R/s$. Furthermore, the relations $P_S + jQ_S = V_S \cdot \text{conj}(I_S)$, $P_R + jQ_R = V_R \cdot \text{conj}(I_R)$, and $P_E = P_S + P_R$ have been applied. The super-imposing is illustrated in **Fig. 10.2**.

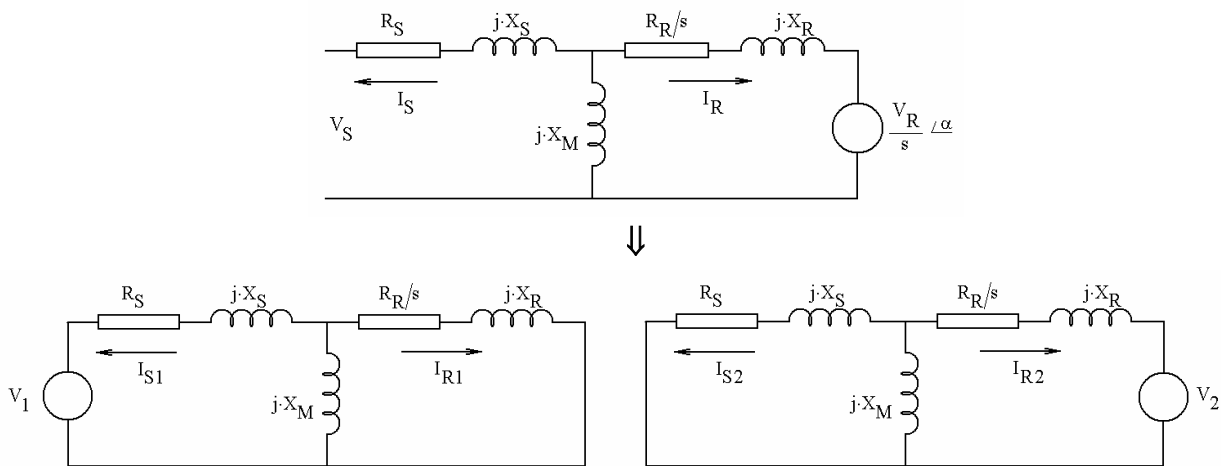


Fig. 10.2. Super-imposing of generator model. Figures are borrowed from (Akhmatov, 2002(b)).

An unambiguous solution of the initialisation problem cannot be found using only the super-imposing, because the number of unknown is larger than the number of equations. The finale solution may be found with use of a selection algorithm applied together with the solutions from the previous super-imposing. The procedure is illustrated by the example below.

Consider that a DFIG (2 MW rating) is at rated operation, $P_E = 1.0$ PU, and the corresponding speed slip is $s = -0.10$. The stator voltage is 1.0 PU and there is no requirement for reactive power control, $Q_S = 0$. The generator parameters are $R_S = 0.00779$ PU, $X_S = 0.07937$ PU, $X_M = 4.1039$ PU, $R_R = 0.0082$ PU and $X_R = 0.40$ PU and found in (Ledesma et al, 1999). The solutions for the electric power and the reactive power are plotted in **Fig. 10.3** as functions of the phase difference, α , with the voltage source magnitude, V_R , as the parameter. In general, the solutions for the electric power must be in the range from 0.0 to 1.0 PU (the generator cannot supply more power than the mechanical power produced by the turbine rotor). The solutions for the reactive power must be in the range from -1.0 PU and 1.0 PU, which is restricted by the generator power capacity.

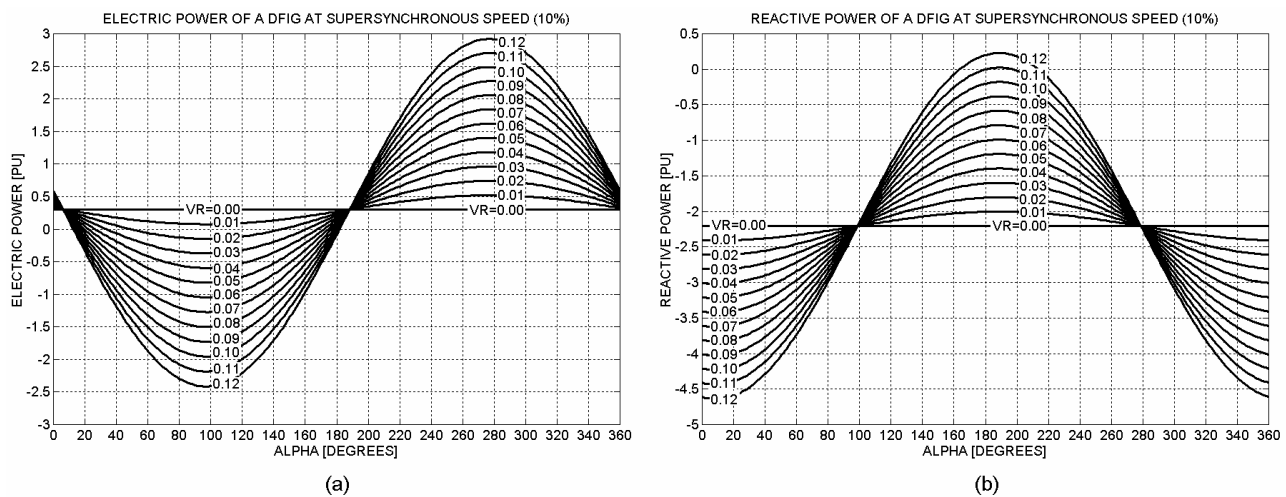


Fig. 10.3. The electric power, P_E , – (a) and the reactive power, Q_S , – (b) of a DFIG at given terminal voltage and slip as functions of the phase difference, α , and the rotor voltage source magnitude, V_R . Reported in (Akhmatov, 2002(b)).

In this case, the solutions related to $P_E = 1.0$ PU and $Q_S = 0.0$ PU are of interest. These solutions are within the ranges 200° to 210° for α and between 0.11 PU and 0.12 PU for V_R , respectively. Then, the solution for the initialisation of the DFIG can be found within the given (reduced) ranges. Applying iteration, the solution is found at $\alpha = 206^\circ$ and $V_R = 0.115$. Plots of the electric power, the reactive power and the currents in stator and rotor are given in **Fig. 10.4**.

As found in this example, $P_R \approx \pm P_E$ and $V_R \approx \pm V_S$. These relations are said to be general for a DFIG in a case when $Q_S = 0$ (Cadirci and Ermis, 1992; Pena et al, 1996). In rated operation and $Q_S = 0$, the currents are close to 1.0 PU.

Another well-known (Heier, 1996; Zhang et al, 1997; Cadirci and Ermis, 1992) general statement for the DFIG power distribution is the following. The electric power is always supplied from the stator to the power grid, independently from the speed slip. The electric power is supplied from the rotor circuit to the power grid at super-synchronous operation and absorbed by the rotor

circuit at sub-synchronous operation (whereas the electric power supply from the stator mains to the grid is increased by the same value).

In case of synchronous operation, the electric power is absorbed by the rotor in means of covering the power losses on the rotor resistance, $P_R = V_R^2/R_R$. The general statements can be used for a simple verification of whether the operational point of the DFIG, found at the initialisation, is in agreement with the expectations on the power distribution between the stator and the rotor circuit.

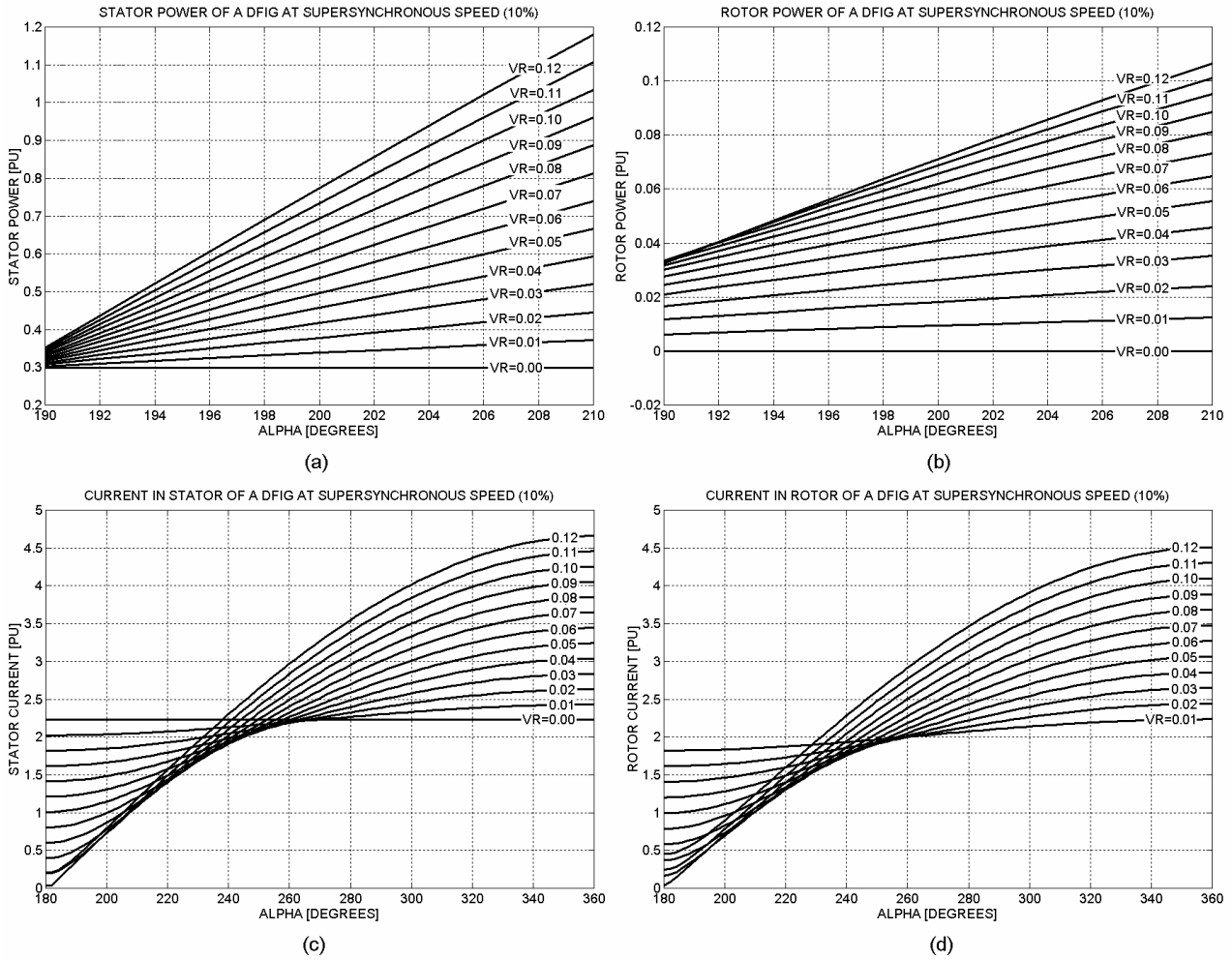


Fig. 10.4. Electric power supplied from stator – (a) and rotor – (b), and currents in stator – (c) and in rotor – (d) within the reduced ranges for the phase difference, α , and the rotor voltage, V_R . Reported in (Akhmatov, 2002(b)).

10.1.2. Initialisation of converter model

Knowing the rotor power, P_R , found from the initialisation routine of the DFIG, the charging current of the dc-link can be initialised as $J_1 = P_R/U_{DC}$ and the discharging current of the dc-link will be $J_2 = J_1$ and $J_2 = P_{GC}/U_{DC}$. The electric power P_{GC} is the power transferred through the dc-link to the grid-side converter, with neglected losses, $P_{GC} = P_R$. All these expressions are by inspection of the electric circuit of the converter in **Fig. 10.1.b**.

The relations for the converter model initialisation with power losses in the dc-link are given in (Akhmatov, 2003(a)).

The interface of the grid-side converter is initialised knowing the total power supplied by the wind turbine to the grid, P_E , and the power supplied from the generator stator mains, P_S , from the initialisation routine of the DFIG. Applying the relation $P_C = P_E - P_S$, the electric power, P_C , exchanged between the grid-side converter mains to the power grid is found. With neglected power losses in the converter mains, $P_C = P_R$. The reactive power set-point is given by Q_C and assumed to be zero (the grid-side converter is reactive neutral at normal operation). Hence, the initialisation is given by the following relation.

$$P_C + j \cdot Q_C = V_s \cdot \text{conj}(I_C), \quad I_C = \frac{V_C - V_s}{R_C + j \cdot X_C}. \quad (10.1)$$

The target is to find the magnitude and the phase angle of the grid-side converter voltage source, V_C . With neglected power losses in the converter mains, it is very easy.

The resistance of the smoothing inductor, R_C , cannot always be neglected. It is because its value is important for damping of the current transients of the grid-side converter at grid disturbances (Svensson, 1998). Presence of the resistive component R_C in the model leads to some power losses in the smoothing inductors of the grid-side converter, so P_R is not equal to P_C . In this case, the initialisation routine of the model can be organised as a number of iterative loops with the power balance $P_E = P_S + P_C$ as the checking condition (Akhmatov, 2003(a)).

10.1.3. Verification of DFIG model initialisation

A precise verification of initialisation routine of a DFIG model should be based on measurements or on comparison to computation results of a reliable simulation program. For instance, the simulation program, which is applied by the wind turbine manufacturer. It is because such programs are always verified by the manufacturer.

In this work, verification of the steady-state operation is made using corresponding simulation results offered by the manufacturer Vestas Wind Systems for their 1.75 MW OptiSpeed® wind turbine generator. In the verification of the initialisation routine of the DFIG model, the specific generator parameters given by the manufacturer Vestas are applied. When verifying the initialisation routine, it is assumed $V_S = 1.0$ PU (690 Volts) always. In the model, the power losses in the converter and the slip-rings are neglected, but these are included in the computations by Vestas. Presumably, this will lead to some discrepancies when compared to Vestas' results.

For each case to be verified, the manufacturer Vestas has given the total electric power, the power distribution in stator and rotor and the currents in stator and rotor. The slip and the reactive power $Q_S = 0$ are given by Vestas for each case as well.

Using the total electric power, P_E , the reactive power, Q_S , the slip, s , and the voltage in stator, V_S , the initialisation routine defines the power distribution in stator, P_S , and rotor, P_R , and the currents in stator, I_S , and rotor, I_R . These parameters found for each case are compared to the parameters kindly offered by the manufacturer Vestas. In **Table 10.1** some of verification results are shown as deviations between the results given by the manufacturer Vestas and the results found by the initialisation routine:

$$\Delta X = 2 \cdot \left| \frac{X_1 - X_2}{X_1 + X_2} \right| \cdot 100 \% , \quad (10.2)$$

where ΔX is the deviations given in **Table 10.1**, X_1 and X_2 denote the values given by Vestas and the values found by the initialisation routine, respectively. As can be seen, there is a good agreement between computations offered by Vestas and the values reached by the initialisation routine. For the values of the currents in stator and rotor, small discrepancies are seen which need more explanation.

Total power, PU	Slip, -	Stator power, %	Rotor power, %	Stator current, %	Rotor current, %
0.290	-0.0133	0.29 %	25.8 %	0.23 %	1.68 %
0.570	-0.1200	0.25 %	2.22 %	0.26 %	3.18 %
0.850	-0.1200	0.29 %	2.62 %	0.17 %	3.74 %
1.000	-0.1200	0.35 %	3.13 %	0.29 %	2.70 %

Table 10.1. Verification of initialisation of the DFIG model against computations given by the manufacturer Vestas. Reported in (Akhmatov, 2002(a)).

In calculations – the initialisation routine of the DFIG model, the value of the terminal voltage is consequently kept at the rated value of $V_s = 690$ Volts. In the computations by Vestas, the terminal voltage has been around its rated value, but not exactly. In the initialisation routine of the DFIG model, the power losses in the converter are neglected, but the converter losses are included in the computations by the manufacturer Vestas, as it is in a real DFIG. This explains the possible discrepancies at the verification.

When the DFIG is close to the synchronous speed, the power exchanged between the rotor circuit and the grid through the converter is small, which is why even small discrepancies may lead to a large relative discrepancy in percent. This explains the 25.8 % discrepancy in the rotor power in the first row of **Table 10.1**.

The results presented in **Table 10.1** are for the super-synchronous operation only. The model of the DFIG must also predict accurate results at synchronous operation, e.g. where the slip is zero. It is because of possible risk of divergence at the slip $s = 0$. Therefore, the manufacturer Vestas requested more validation and kindly offered their results obtained at synchronous operation. The results of this validation are collected in **Table 10.2**, again with use of the relative deviations by **Eq. (10.2)**.

Total power, PU	Slip, -	Stator power, %	Rotor power, %	Stator current, %	Rotor current, %
0.290	0.0	0.02 %	6.45 %	0.72 %	1.29 %
0.570	0.0	0.08 %	10.25 %	1.32 %	1.67 %
0.850	0.0	0.06 %	7.90 %	2.84 %	2.23 %
1.000	0.0	0.10 %	6.83 %	3.19 %	1.90 %

Table 10.2. Verification of initialisation of the DFIG model against computations given by the manufacturer Vestas at synchronous operation.

The discrepancies between the results of the initialisation routine of the DFIG and the results kindly given by the manufacturer Vestas are also small in case of the synchronous operation of the DFIG. There is no risk of divergence in the model at the slip $s=0$. The discrepancies are explained by the same argumentation as in previous cases with relation to **Table 10.1**.

The manufacturer Vestas has agreed that, when the same data set is applied, the initialisation routine of the DFIG model can be used to represent steady-state operation the DFIG used in the 1.75 MW OptiSpeed® wind turbine from the manufacturer Vestas.

A correct definition of the steady-state operation point is important for computation of the currents in the DFIG (Akhmatov, 2002(b)) and, as will be shown in this work, for conclusions with respect to the converter protection/action at a short-circuit fault in the power networks.

10.2. Transient DFIG model

Modelling of the DFIG in investigations of transient voltage stability contains the following representations (Akhmatov, 2002(a)).

- 1) Modelling of the DFIG with use of the state equations.
- 2) Representation of the converter control system with independent control of the electric power and the reactive power.
- 3) Representation of the protective system (the relay models) of the generator and the converter.

Furthermore, the variable-speed wind turbine is treated as a complex electromechanical system (Akhmatov et al, 2000(b); Akhmatov, 2002(c)) where the shaft system, the aerodynamic rotor and the pitch control are included. As explained in **Section 8** and **Section 10.1**, operation of the DFIG and its parameters must be fitted to the wind turbine aerodynamic characteristics for optimisation of the power output.

Although the formal separation, all these representations shall be treated as *the whole* when working on investigations of short-term voltage stability with variable-speed wind turbines equipped with DFIG.

10.2.1. State equations of DFIG

The state equations of the DFIG can be achieved from the state equations of the induction generator. The difference is the presence of a finite induced voltage-source, $V_R = (V_{DR}, V_{QR})$ in the rotor circuit. The state equations of induction generators with shorted rotor-circuit are given by **Eqs. (4.1)**. Those are re-written below for contingency of this presentation.

$$\begin{cases} V_{DS} = R_S I_{DS} - \omega_S \psi_{QS} + \frac{d\psi_{DS}}{dt}, & V_{QS} = R_S I_{QS} + \omega_S \psi_{DS} + \frac{d\psi_{QS}}{dt}, \\ V_{DR} = R_R I_{DR} - s\omega_S \psi_{QR} + \frac{d\psi_{DR}}{dt}, & V_{QR} = R_R I_{QR} + s\omega_S \psi_{DR} + \frac{d\psi_{QR}}{dt}, \\ T_E = \psi_{DS} I_{QS} - \psi_{QS} I_{DS}. \end{cases} \quad (10.3)$$

Commonly, **Eqs. (10.3)** are adapted for investigations of dynamic small-signal stability by neglecting the stator flux transients $\frac{d\psi_{DS}}{dt} = 0$ and $\frac{d\psi_{QS}}{dt} = 0$ (Kundur, 1994; Feijóo et al, 2000). This simplified representation is also often applied in investigations of transient voltage stability (Gjengedal et al, 1999; Ledesma et al, 1999) with large fluctuations of the voltage at transient grid disturbances. The validity of this simplification is often explained by independent control of the electric power and the reactive power of these generation units. With such independent control, the behaviour of the rotational speed, ω_G , and the terminal voltage, V_S , are de-coupled. Therefore, the voltage profile after the fault clearance will presumably not be affected by the generator rotor speed history at the faulting moment (which is seen in case of conventional induction generators, **Section 4**).

In other words, neglecting of the stator flux transients in the generator state equations may only lead to neglecting of the fundamental-frequency transients in the machine current (Akhmatov, 2002(a)). This simplification will not influence the results of investigations of short-term voltage stability so long as the converter maintains uninterrupted operation and the wind turbine does not disconnect.

The fundamental-frequency transients in the machine current can be of a significant character when the power grid is subjected to a short-circuit fault with a more or less significant voltage drop (Akhmatov, 2002(a)). In case of the DFIG with their specific converter control, the transients in the machine current are also influenced by the specific control system of the converter (Akhmatov, 2002(a)), which complicates further the situation.

It is kept in mind that the converter is controlled by the IGBT-switches, **Fig. 10.1.a**. The IGBT-switches must be protected against over-current through the IGBT, over-voltage across the IGBT and thermal over-loads. It is obvious that the rotor current, I_R , is the current going through the IGBT of the rotor converter. The current in the mains of the grid-side converter, I_C , is the current going through the IGBT of the grid-side converter. The dc-link voltage, U_{DC} , is the voltage applied across the IGBT (Akhmatov, 2003(a)).

The frequency converters of the DFIG are commonly designed to handle the rotor power (and the magnetisation of the generator from the rotor circuit) only. This restriction is because application of partial-load frequency converters having a relatively low power capacity is the basic advantage of this variable-speed concept (Akhmatov, 2002(a)). On the other hand, this restriction makes the frequency converter to be the most sensitive part of the electric generator in the wind turbine. The current going through the rotor converter and the current of the grid-side converter must be restricted by the protective reasons (Akhmatov, 2002(a)). A number of electric parameters, which are the currents in stator, rotor and grid-converter mains, the dc-link voltage, the terminal

voltage, the electric frequency and other parameters are monitored. When at least one of the monitored parameters exceeds its respective ranges, the converter will block due to *the converter protection against overloads* at disturbances in the power network.

Again, the converter design is optimised to reduce its power capacity and cost. Therefore the setting of the converter protection against over-current is not much above the rated current (Akhmatov, 2002(c)). This explains why accurate prediction of the current at the grid faults becomes extremely important for reaching accurate results of investigations of short-term voltage stability (Akhmatov, 2002(c)).

The same argumentation can be derived for necessity of accurate prediction of the dc-link voltage and the current in the grid-side converter (Akhmatov, 2003(b)).

When the converter has blocked, its controllability is also lost (Akhmatov, 2002(c)). In such operation situations, argumentation (for use of simplified generator models) about independent control of electric and reactive power of the DFIG becomes meaningless. Furthermore, when the converter blocks, this may lead to disconnection of the wind turbine itself if any converter re-start routine is not applied. In this case, the outcome of investigations of short-term voltage stability will be power loss and the requirement to be suggested must be incorporation of power reserves or arranging of the converter re-start routine.

As demonstrated in (Akhmatov, 2002(a)) with use of the detailed DFIG model, the rotor converter may already block when the voltage drops from 1.0 PU to 0.8 PU at the DFIG terminals. This illustrates sensitivity of the converter protection at transient events in the power network. It is also demonstrated that it can be the model-dependent outcome of investigations of transient voltage stability (Akhmatov, 2002(c)).

When the simplified model has been applied, the DFIG and the converter maintained uninterrupted operation at the same voltage drop. In this case, the reduced representation with neither indication of needs of power reserves nor needs of the converter re-start. This inconvenience is simply unacceptable in practical stability investigations.

We are talking about the model-dependent outcome, which may have serious consequences for the power system stability. This model-dependent outcome is expressed by the following:

- 1) Voltage recovery and uninterrupted converter operation predicted with use of the reduced generator model (the common third-order model).
- 2) Converter blocking by over-current (transients in rotor current) with use of the fifth-order generator model.

This discrepancy is model-dependent and has a significant character, which is why the contact was taken to the Danish manufacturer Vestas producing the OptiSpeed® wind turbines. The manufacturer Vestas agreed that it is necessary to apply at least the fifth-order generator model in investigations of transient voltage stability (Akhmatov, 2002(a)). This is necessary to reach accuracy of the predicted current behaviour and accurate prediction of the converter action (Akhmatov, 2002(a)). The common third-order model of the DFIG, where the fundamental-frequency transients in the machine current are disregarded, will be over-simplified. This simplification of the generator model may lead to misleading results with respect to the converter

action (protection with blocking versus uninterrupted operation) and therefore with respect to the outcome of investigations of short-term voltage stability.

10.2.2. Shaft system model

When the control of electric power and reactive power is de-coupled in the DFIG, the shaft torsional oscillations will be seen in the speed fluctuations, but do not affect the voltage behaviour. From this viewpoint, the shaft system could be represented by the lumped-mass model in investigations of short-term voltage stability, although the shaft system is relatively soft in such drivers.

On the other hand, the converter will probably block during and after the grid fault. Then the electric power and the reactive power are not necessarily de-coupled at the grid fault. Secondly, the machine current will follow fluctuations of the generator rotor speed (Akhmatov, 2003(b)). This current behaviour is important for the converter operation because the converter protective system monitors the machine current and the converter can block by over-current, as discussed in **Section 10.2.1**.

Furthermore, there is a risk of excitation of the shaft system of the DFIG at grid disturbances. As explained in (Akhmatov, 2002(a)), this shaft excitation may have fatal consequences for the wind turbine operation. When the damping of the shaft system oscillations is poor, the shaft torsional oscillations can be with an increasing magnitude (Akhmatov, 2002(a)). This behaviour introduces specific demands and restrictions on the converter control, which must be present in the wind turbine model. Insufficient damping of the shaft torsional oscillations may result in disconnection of the wind turbines equipped with the DFIG. This will probably lead to power loss and demands on incorporation of immediate power reserves.

Taking these considerations into account, the shaft system of the wind turbines equipped with DFIG must be represented with use of the two-mass model with **Eqs. (2.9)**. Remember also our discussion in **Section 2.2**.

10.2.3. Converter system model

The model of the frequency converter system is with representation of the rotor converter, the grid-side converter, the dc-link and the converter control (Akhmatov, 2003(a)). This representation is chosen for reaching accuracy of the simulation results. This complexity is required to reach accuracy of predicted action of the converter at the grid faults (Akhmatov, 2003(a)).

10.2.3.1. Rotor converter model

The rotor converter control is arranged in a synchronously rotating (α, β) -reference frame. The α -axis is oriented along the terminal voltage vector, V_s . In this way, the electric power and the reactive power are controlled independently from each other. The control scheme of the rotor converter is organised in a generic way with two series of two PI-controllers (Heier, 1996; Zhang et al, 1997; Pena et al, 2000; El-Hwang Kim et al, 2000). The control system is illustrated in **Fig.**

10.5.a. The switching dynamics of the IGBT-switches of the rotor converter is neglected, when assuming that the rotor converter is able to follow the reference values $V_{R\alpha}$ and $V_{R\beta}$ at any time.

Furthermore, the PI-controller is added to produce the reference signal of the electric power from the speed error signal (Akhmatov, 2002(c)). This additional control loop is illustrated in **Fig. 10.5.b**. As found in (Akhmatov, 2002(c)), this functionality contributes to damping of the torsional oscillations in the shaft system of the wind turbine. This prevents mechanical excitation of the shaft system of the DFIG and also a risk of unnecessary disconnection and stop of the wind turbine caused by mechanical excitation.

Notice that the active current reference, $I_{R\alpha,REF}$, can be controlled directly by the speed, ω_G . Such control schemes have been reported in (Heier, 1996; Røstøen et al., 2002). Røstøen et al (2002) have reported that such control schemes can be applied to damp the shaft torsional oscillations in the DFIG as well.

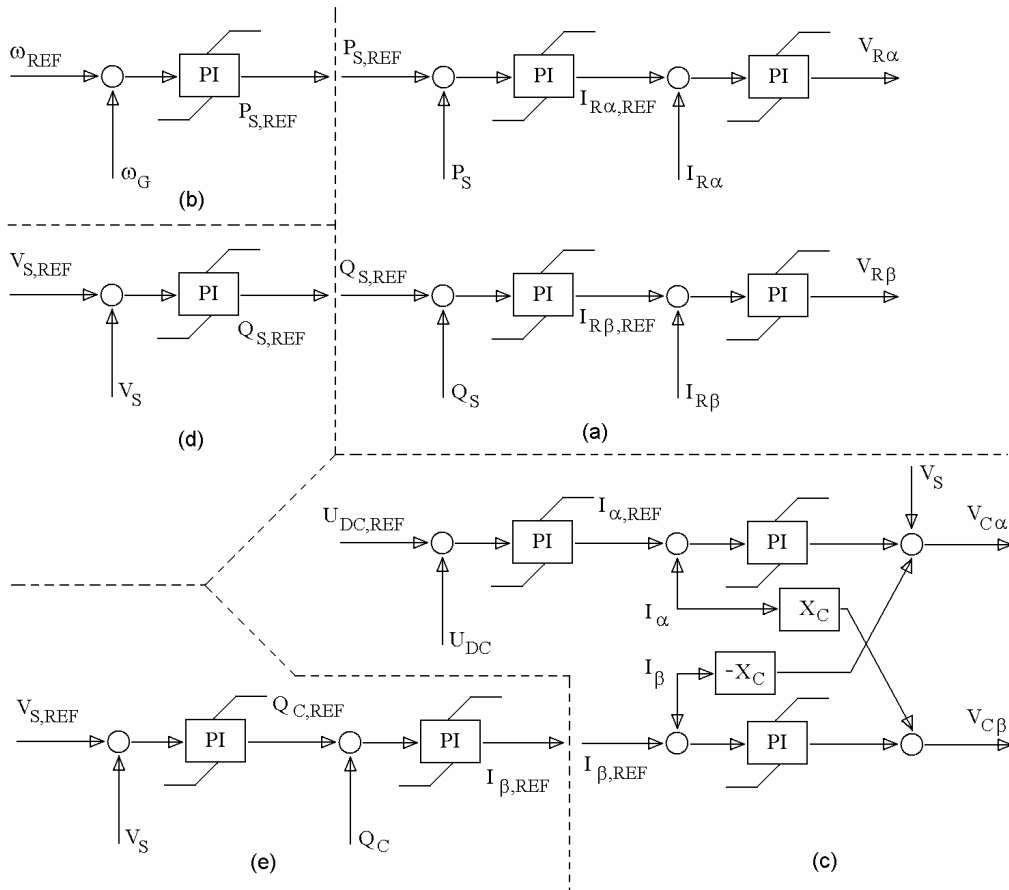


Fig. 10.5. Generic control scheme of DFIG: (a) – generic control scheme of the rotor converter, (b) – additional PI-controller to damp torsional shaft oscillations, (c) – generic control scheme of the grid-side converter organised as a Statcom, (d) and (e) – additional control loops for voltage and reactive power control by the rotor converter, respectively, the grid-side converter. Reported in (Akhmatov, 2003(a)).

10.2.3.2. Modelling of DC-link and grid-side converter

The current going through the capacitor of the dc-link is $I_C = J_1 - J_2$. In (Akhmatov, 2003(a)), it is found that the dc-voltage across the capacitor, U_{DC} , at any time, t , can be expressed by:

$$U_{DC}(t) = \sqrt{U_{DC}^2(0) + \frac{2}{C} \int_0^t (P_R(\tau) - P_{GC}(\tau)) \cdot d\tau}, \quad (10.4)$$

where $U_{DC}(0)$ is the initial dc-voltage, C is the capacitance and τ is an independent variable. This equation is with neglected power losses in the dc-link. The relation for the dc-link with power losses is suggested in (Akhmatov, 2003(a)).

The grid-side converter control is similar to control of a Statcom (Næss et al., 2002). Therefore, its generic model can be set up in a similar way (Pena et al., 1996; Schauder and Mehta, 1993). **Fig. 10.5.c** gives the generic scheme of the grid-side converter control. The converter is controlled in the same (α, β) -reference frame as the rotor converter – this *assumption* is made in this work for simplification. The control of the dc-link voltage is organised by two PI-controllers in series and the control of the reactive current by one PI-controller (Schauder and Mehta, 1993). The electric power is regulated by varying the active-current reference signal in response to error of the dc-link voltage. The reactive power is regulated with respect to setting of the reactive-current reference. Also in this case, the switching dynamics of the converter is neglected because of the assumption that the grid-side converter is able to follow the reference values $V_{C\alpha}$ and $V_{C\beta}$ at any time.

The voltage-compensation is shown by the cross-coupling in terms of $(V_S - X_C I_\beta)$ and $(X_C I_\alpha)$, respectively. Since the grid-side converter lines are with resistive losses, this must be taken into account in the converter control model (Akhmatov, 2003(a)). This is made in this model, but not shown in **Fig. 10.5.c** for simplification.

The Danish manufacturer Vestas Wind Systems has kindly helped with tuning of the parameters of the generic control system of the both converters for getting realistic simulation results.

10.2.3.3. Optional control of reactive power and voltage

A PI-controller producing the reference signal of the reactive power from the voltage error signal can be added to the rotor converter control scheme (Akhmatov, 2002(c)). This is made in this investigation and shown in **Fig. 10.5.d**. Notice that this control loop is optional and introduce dynamic exchange of reactive power between the DFIG and the power grid and dynamic voltage control.

Two PI-controllers in series producing the reference signal of the reactive current from the voltage error signal can be added to the control system of the grid-side converter. This is also done in this investigation and the additional control loop is given in **Fig. 10.5.e**. This loop is arranged for dynamic reactive power and voltage control by the grid-side converter. Notice that other realisations of this grid-side converter control can be suggested.

This control feature will however need control co-ordination between the rotor and the grid-side converters when the reactive power control by the voltage error has already been arranged in the rotor converter (Akhmatov, 2003(a)). This controllability of the converter system can be useful during the process of voltage re-establishing, after the grid fault has been cleared (Akhmatov, 2002(c)). This control can also be applied to keep the voltage within the desired range, when the DFIG feeds into a weak power system (Akhmatov, 2002(d); GE Wind Energy, 2002; Tapia et al.,

2001). Notice that the control of reactive power and voltage with use of the frequency converter system is not necessarily present in every wind turbine equipped with a DFIG and a frequency converter. Presence of this control is manufacturer- and specification- dependent³⁸. This reactive power control can possibly be added to the basic converter control when this is requested by the customer (GE Wind Energy, 2002).

The subject about controllability of the back-to-back converter system with respect to the reactive power and the control coordination has been discussed in (Akhmatov, 2003(b)).

10.2.3.4. Why do not neglect grid-side converter

In investigations of transient voltage stability, the converter system of the DFIG is commonly represented with only the rotor converter. The grid-side converter is considered very fast and often is disregarded (Akhmatov, 2002(c); Pena et al, 1996; Gjengedal et al, 1999; Pena et al, 2000; Røstøen et al, 2002). In this work, the converter system of the DFIG is modelled with the rotor and the grid-side converters and the dc-link in between. Why is it not any good idea to neglect the grid-side converter?

Consider a simple network shown in **Fig. 10.6.a**. Here, the DFIG is connected to the grid with the short circuit ratio (SCR) of 20 with respect to the generator rated power capacity. The power grid is subjected to a balanced fault resulting in a voltage drop to 0.85 PU at the DFIG terminals. The two following cases are compared.

- 1) The control scheme of the DFIG is only given by the rotor converter model, **Fig. 10.5.a**. This is on the common assumptions when the grid-side converter is neglected (Akhmatov, 2002(a); Pena et al, 1996; Gjengedal et al, 1999; Pena et al, 2000; Røstøen et al, 2002).
- 2) The converter system is with the rotor and the grid-side converter with the dc-link in between, which is controlled by the control schemes given in **Fig. 10.5.a** and **Fig 10.5.c**.
- 3) In the both cases, the shaft system is lumped.

The protective system model, see **Section 10.2.1** and **Section 10.2.4**, is disabled in these simulations. The behaviour of the terminal voltage, the rotor current and the dc-link voltage are computed with these two converter representations and shown in **Fig. 10.6**. As can be seen, the model with representation of only the rotor converter predicts a higher value of the transients in the rotor current than it is found with the model containing the grid-side converter and the dc-link. A possible explanation on the discrepancy can be that the dc-link capacitor, working as the energy storage, interacts with the rotor converter. The dc-link capacitor exchanges the electric energy with the rotor circuit during the transient events. This energy exchange is seen as fluctuations of the dc-

³⁸ The wind turbines can be equipped with extra control loops to control reactive power and voltage when this is requested by the transmission system operator or the customer. Notify that the DFIG- wind turbines in the large wind farm at Horns Rev, western Denmark, are with the quasi-dynamic control of reactive power (Sørensen and Hilden, 2003), whereas the wind turbines of the same concept and from the same manufacturer, but incorporated in local sites in Denmark, do not contain this control.

link voltage, U_{DC} . This mechanism introduces delays between the rotor and the grid-side converters and results in smoothing of the profiles of the electric and the reactive power of the DFIG. When the feedback via the converter control loops is introduced, this results in smoothing of the machine current transients at the grid fault.

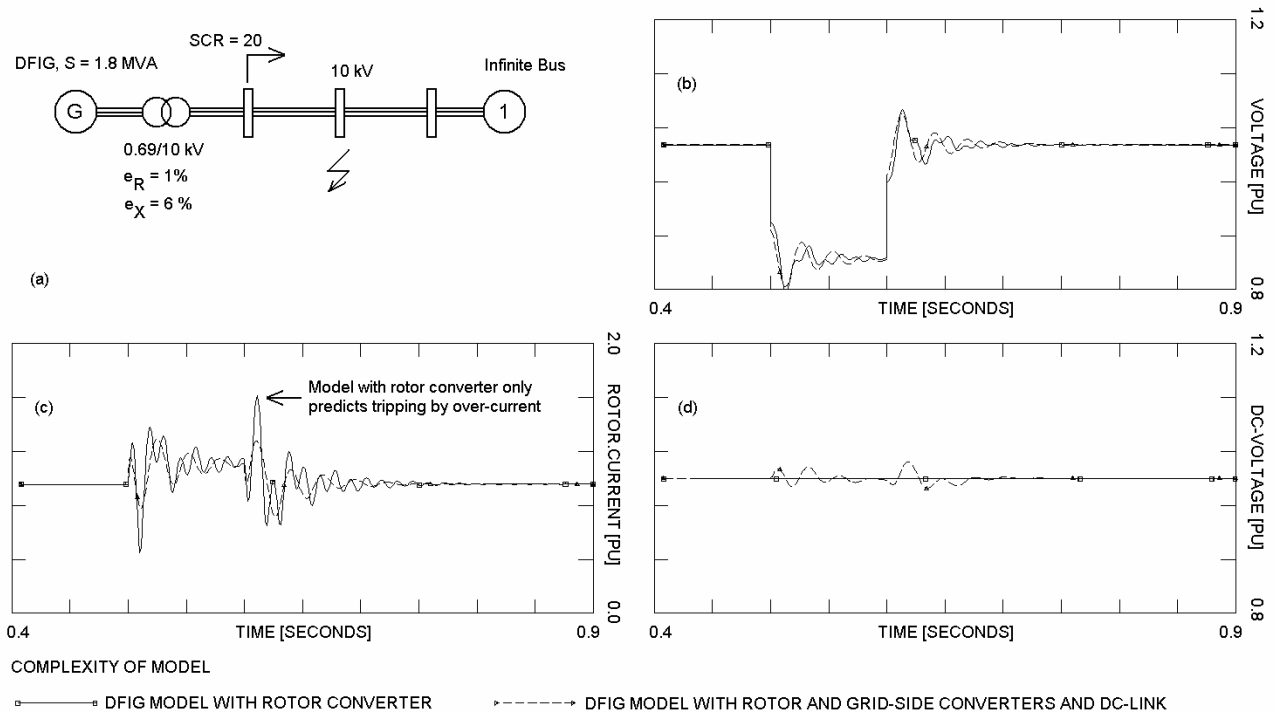


Fig. 10.6. Test of DFIG model with only the rotor converter model versus with the model with the converter system and the dc-link in between: (a) – the test network, (b) – terminal voltage, (c) – rotor current magnitude, (d) – dc-link voltage. Reported in (Akhmatov, 2003(a)).

This mechanism is not represented in the model with only the rotor converter due to *the assumption* of keeping a constant value of U_{DC} at any time (Pena et al, 1996; Gjengedal et al, 1999). Therefore, it is expected that the model with only the rotor converter may predict excessively intense transients in the rotor current.

In this particular example, the rotor current computed with use of the model with only the rotor converter exceeds the relay settings of the converter protective system. This reduced model will predict that the converter blocks by over-current in the rotor circuit. But this is not the case when the detailed model regarding the grid-side converter and the dc-link is applied. Here, the rotor current keeps within the legal operation range, which is why the detailed model predicts uninterrupted operation of the converter system.

The result is not trivial, but principal, which is why discussions about the model-dependent discrepancies and their reasons were taken up with the Danish manufacturer Vestas Wind Systems. The manufacturer Vestas has a solid practical experience with manufacturing of the variable-speed wind turbines equipped with DFIG and the converter technique. The manufacturer Vestas has agreed that the DFIG model with representation of only the rotor converter may predict excessively intense current transients in the generator and in the converter. Representation of the converter system with the rotor converter, the grid-side converter and the dc-link in between is, therefore,

recommended in investigations of short-term voltage stability. This detailed converter representation has been applied in this project.

At the present moment, it is chosen to publish this result due to its principal character, but it must be said that more investigations about the details of the converter system modelling are necessary. In (Akhmatov, 2003(b)), it is shown that the discrepancy caused by the different complexity details of the converter system models plays a part with relation to the converter blocking and re-starting sequences. The converter model details may also influence prediction of the damping characteristics of the converter control applied to damp torsional oscillations in the shaft system of the DFIG- wind turbines. This subject will be discussed with examples in **Section 11.4.2.3**.

10.2.4. Protective system and converter blocking

As it has been discussed in **Section 10.2.1**, the frequency converter system must be modelled with the protective system, which monitors operation of the converter, the generator and the power network (at the generator terminals) and may order the converter to block when abnormal operation has been registered. The main function of the protective system is protection of the IGBT-switches from electrical and thermal over-loads of any kinds.

The protective system monitors (i) the machine current and (ii) the current in the grid-side converter, (iii) the dc-link voltage, (iv) the terminal voltage, (v) the electric frequency etc. and orders the converter to block when at least one of the monitored parameters exceeds its respective relay limits. Typical characteristic time of the converter blocking can be of a few ms (Akhmatov, 2002(a)).

As found in (Akhmatov, 2002(a); Akhmatov, 2003(b)), the most common reason of the rotor converter blocking is due to protection from over-current in the rotor circuit. This kind of protection is the most frequent because the converter power capacity is restricted and the upper limit of the rotor converter current is not much larger than the rotor current at rated operation.

Generally, blocking of the rotor converter can be organised by the two arrangements:

- 1) The IGBT-switches stop switching and open. The rotor circuit opens and looks into the diode-bridge and the dc-link capacitor³⁹. This procedure is chosen to perform fast demagnetising of the rotor circuit (Akhmatov, 2002(a)). The dc-link capacitor is charged by the rotor current going through the diodes and the rotor current stops shortly after the converter has blocked. When the rotor current has decayed to zero, the rotor circuit is demagnetised. In this process, the magnetic energy of the current, which was going through the rotor circuit inductance, is transformed to the electric energy of the dc-link capacitor, which is charged-up. As found in (Akhmatov, 2002(a)), the whole process can take a couple ms. In investigations of short-term voltage stability, this transient behaviour is of less importance. Therefore the rotor current can simply be set to zero when simulating the converter blocking (Akhmatov, 2002(a)). When the rotor circuit has been demagnetised, the generator is seen from the power system as an inductor with the (stator-circuit) impedance $Z_S = R_S + jX_S$. In other words, it starts to absorb

³⁹ The same blocking routine has been discussed for the concept with the frequency converter of the PMG where the generator-converter blocks with opening of the IGBT-switches, see **Section 9.4.1** and **Section 9.5.2**.

a less amount of reactive power (Akhmatov, 2002(a)). In case of many machines operating in this way, this may affect voltage stability of the power system because of quantity of the “reactors” absorbing reactive power. Typically, the wind turbines will disconnect very shortly after the converters have blocked. Therefore such reactive power absorption may have a temporary character and the wind turbine disconnection may have a positive impact on the power grid.

- 2) The IGBT-switches stop switching, the rotor circuit has short-circuited and the rotor converter has tripped. Here, the rotor current may increase significantly at the moment of short-circuiting of the rotor circuit, which is why short-circuiting through a finite external resistance must be applied (Akhmatov, 2002(a)). When the rotor circuit is short-circuited, the generator becomes a conventional induction generator that is significantly over-speeded. Remember that the DFIG has been at super-synchronous operation before the converter has blocked. When the rotor circuit has short-circuited /closed through the external resistor, the generator starts to absorb an amount of reactive power (Akhmatov, 2002(a)). In case of many machines operating with such a blocking sequence, the amount of absorbed reactive power can also be significant. This may affect voltage stability of the power system. Typically, the wind turbines trip shortly after the converters have blocked. Fast disconnection of such generators may have a positive impact on the voltage profile in the power grid.

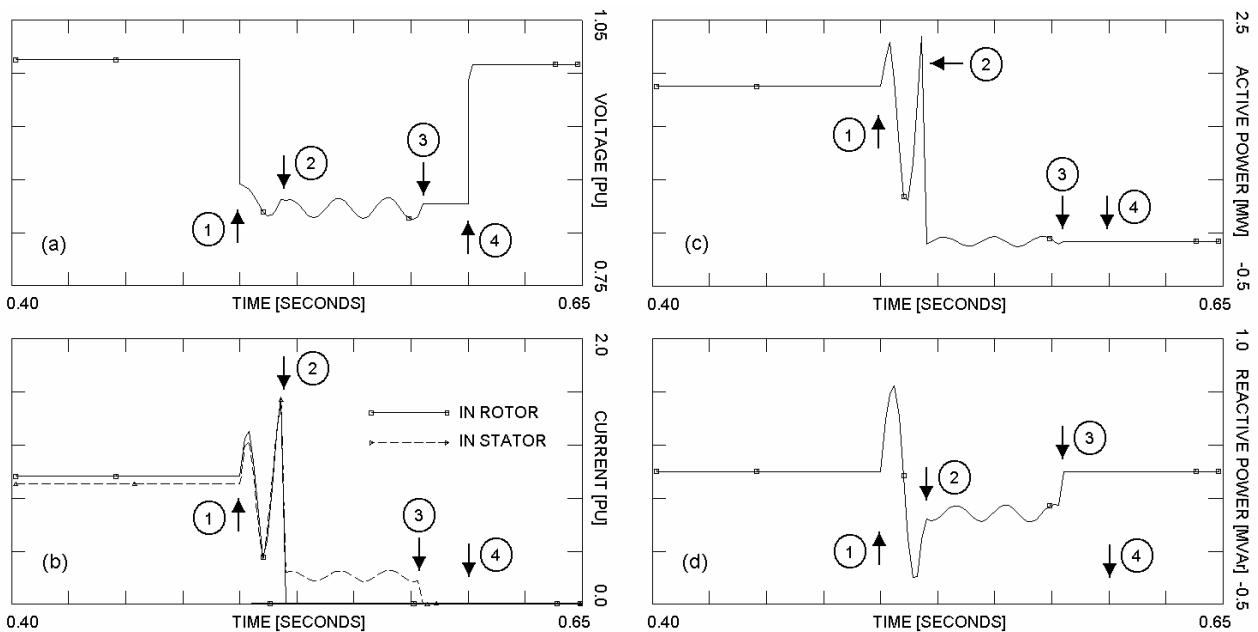


Fig. 10.7. Simulated electric values of the DFIG at a short circuit fault where the converter blocking is followed by opening of the rotor circuit: (a) – terminal voltage at grid-side, (b) – currents in rotor and stator, (c) – electric and (d) – reactive power. Reported in (Akhmatov, 2002(b)).

The simulated behaviour of the DFIG at the converter blocking is shown in **Fig. 10.7**, **Fig. 10.8** and **Fig. 10.9**. The plotted curves are, in this case, reached with use of only the rotor converter representation, e.g. with neglected representation of the grid-side converter, (Akhmatov, 2002(a)).

This model reduction is made for simplification, but this is sufficiently illustrative for this investigation. In the simulated behaviour, the following events are marked.

- 1) The moment when the short circuit fault has occurred in the power network.
- 2) The moment when the rotor converter has blocked and the rotor circuit has subsequently acted (either opened or closed).
- 3) The moment when the generator has tripped.
- 4) The moment when the fault has cleared.

As can be seen, the generator trips very shortly after the converter has blocked. This eliminates absorption of reactive power by the generator and its negative impact on the power system. Therefore the tripping time must be short.

This wind turbine tripping at the grid disturbances will be common for this wind turbine concept. In other words, this action is independent from the manufacturer. This action will be present in local wind turbine sites in Denmark because the wind turbines incorporated in the local sites are not assigned to any specifications of the transmission system operator (Eltra, 2000).

When incorporated in the large wind farms and feeding directly into the transmission power systems, the wind turbines must comply with the Specifications of the TSO. Subsequent tripping of the wind turbines in the large wind farms at the grid faults will not be accepted⁴⁰.

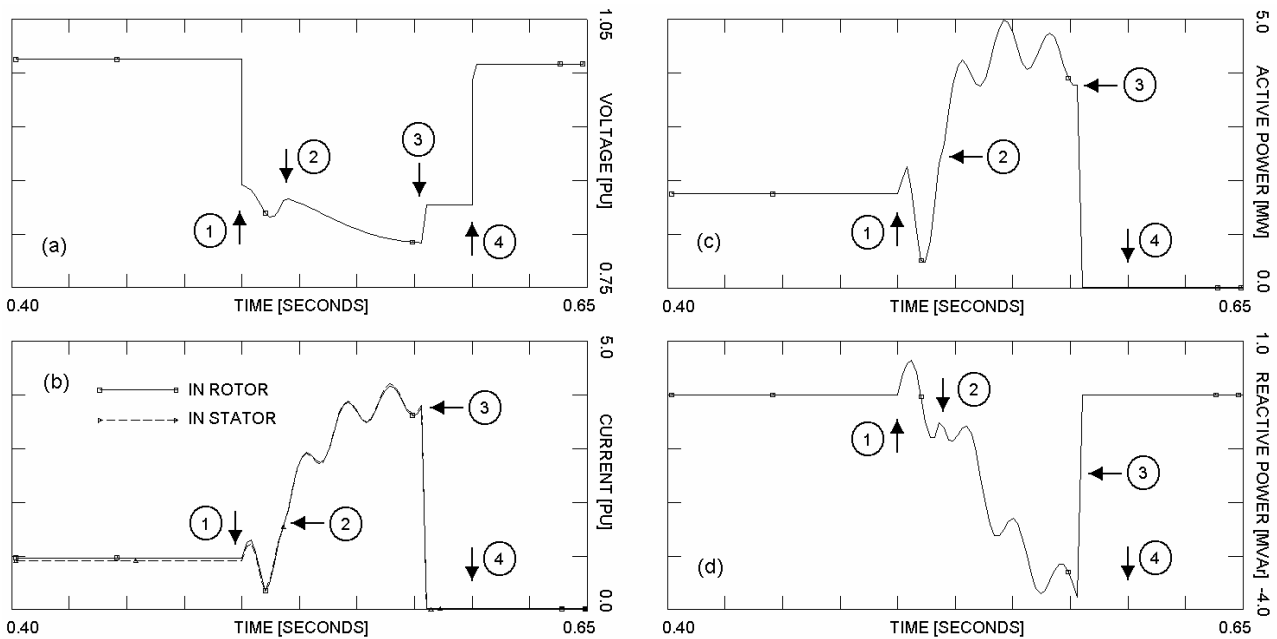


Fig. 10.8. Simulated electric parameters of the DFIG at a short circuit fault where the converter blocking is followed by closing of the rotor circuit: (a) – terminal voltage at grid-side, (b) – currents in rotor and stator, (c) – electric and (d) – reactive power. Reported in (Akhmatov, 2002(b)).

⁴⁰ Interpretation: the wind turbines are equipped with the protective relays and therefore can trip. This tripping is possible, but not acceptable. Either subsequent tripping reached in simulations or uncontrollable voltage decay leading to tripping may indicate that the solution does not comply with the Specifications formulated by the TSO (Eltra, 2000).

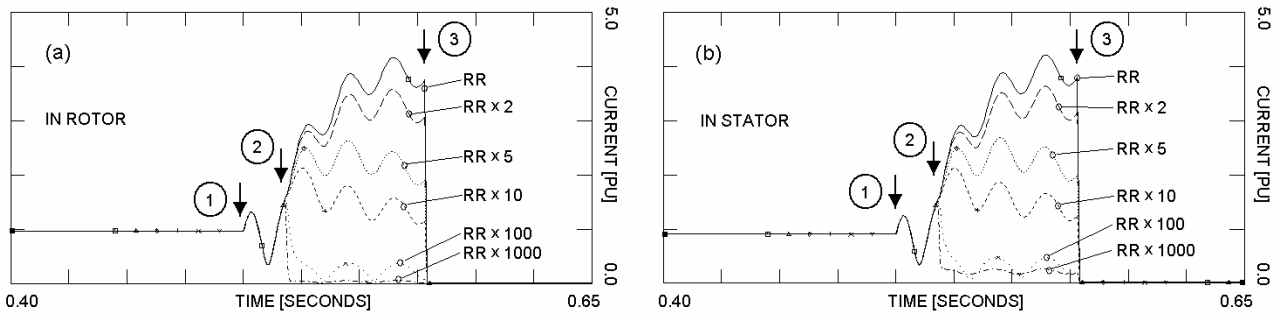


Fig. 10.9. Simulated currents in rotor and stator of the DFIG at a short circuit fault where the converter blocking is followed by closing of the rotor circuit through an external resistance. Reported in (Akhmatov, 2002(b)).

10.2.5. Interface to simulation tool and network model

Interface of the DFIG model must be arranged to exchange the simulation results of the user-written DFIG model and the network solution performed by the simulation tool PSS/E. When viewed from the power system, the DFIG is given by two Norton-equivalents (Akhmatov, 2002(a)). This corresponds to the equivalent of the generator with the synchronous impedance $Z' = R_S + jX'$ and the current source, J_G , as described in (Kundur, 1994; Feijóo et al, 2000), and the equivalent of the grid-side converter with the impedance of the converter-to-grid lines, $Z_C = R_C + jX_C$, and the current source, J_C , as suggested in (Akhmatov, 2002(a)). This interface representation is shown in **Fig. 10.10.a**. The superimposing of the impedances and the current sources is given in **Fig. 10.10.b**.

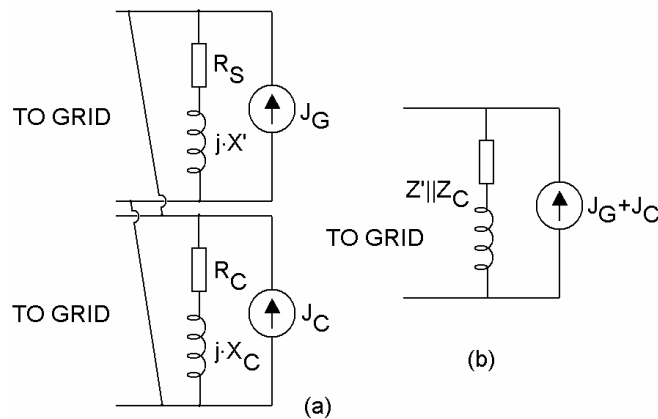


Fig. 10.10. Norton-equivalent of the DFIG and the grid-side converter. Reported in (Akhmatov, 2002(a)).

When interfacing the transient model of the DFIG to the dynamic simulation tool, it is need to acknowledge the constraint of the dynamic simulation tool where the stator flux transients are ignored. The stator flux transients are represented internally in the DFIG model, which is sufficiently for representing the fundamental-frequency transients in the currents and the interfacing to the dynamic tool are taken into account. The reasons for and the ways of doing this are described in (Knudsen and Akhmatov, 1999) in case of conventional asynchronous generators.

10.2.6. Numeric stability of model

The characteristic time constants of the model parts and of the processes in the wind turbine are sketched in **Fig. 10.11**.

The characteristic time intervals of the different parts and processes are in the range of 10^{-4} s to 10 s (Akhmatov, 2003(a)). This may introduce numeric stability problems within the model and also at interaction between the model and the dynamic interface of the simulation tool PSS/E. The tool PSS/E is a fixed integration step tool. Although such inconvenience, the user-written model must be numerically stable, which means performing the same results within an interval of the fixed integration steps. Furthermore, the user-written model must neither conflict with other (standardised) models of the simulation tool nor with the tool interface. For achieving this goal, so-called stiff integration routines can be applied (Ibrahim, 1997)⁴¹. This must be combined with accurate implementation of the model into the simulation tool, respecting its interface.

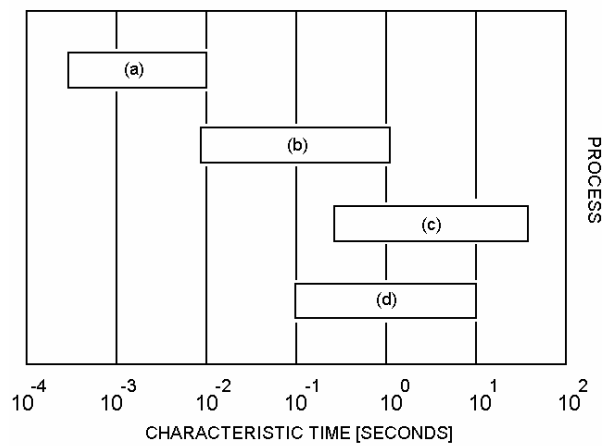


Fig. 10.11. Processes plotted versus their respective characteristic time constants: (a) – interaction between the converters and the generator, (b) – fundamental-frequency model of the generator, (c) – pitch control, wind turbine mechanics, (d) – interaction between grid and wind turbine generator at balanced faults. Reported in (Akhmatov, 2003(a)).

For validation of the numeric stability of the model, the protective relays have been disabled in the model since *the numeric response* of the model to a large disturbance has been investigated. The simulations have been executed in case of a balanced short-circuit fault (in vicinity of the generator terminals). Here, the terminal voltage of the wind turbine with the DFIG is reduced to 0.15 PU during the faulting time, see **Fig. 10.6.a**. The converter control is given by all the schemes shown in **Fig. 10.5**. The simulations have been carried out with different fixed integration steps from 0.1 ms to 10 ms and the results are plotted in **Fig. 10.12** for the steps up to 4 ms.

The simulation results are identical in the range of the fixed integration steps from 0.1 ms to 2 ms, and only at 4 ms a very slight deviation is seen. When using larger integration steps, the

⁴¹ In this work, the author has applied an integration routine which is more complex than suggested in (Ibrahim, 1997). The borders between the different processes within the wind turbine model must be well-defined to reach a successful numeric integration.

deviation increases. Use of smaller time steps is not reasonable because of a risk that the slow processes in the present model and also in the standardised models of the tool PSS/E may accumulate computational errors. Such standardised PSS/E models are typically executed at the default step of 10 ms. Use of smaller steps increases also the total computation time.

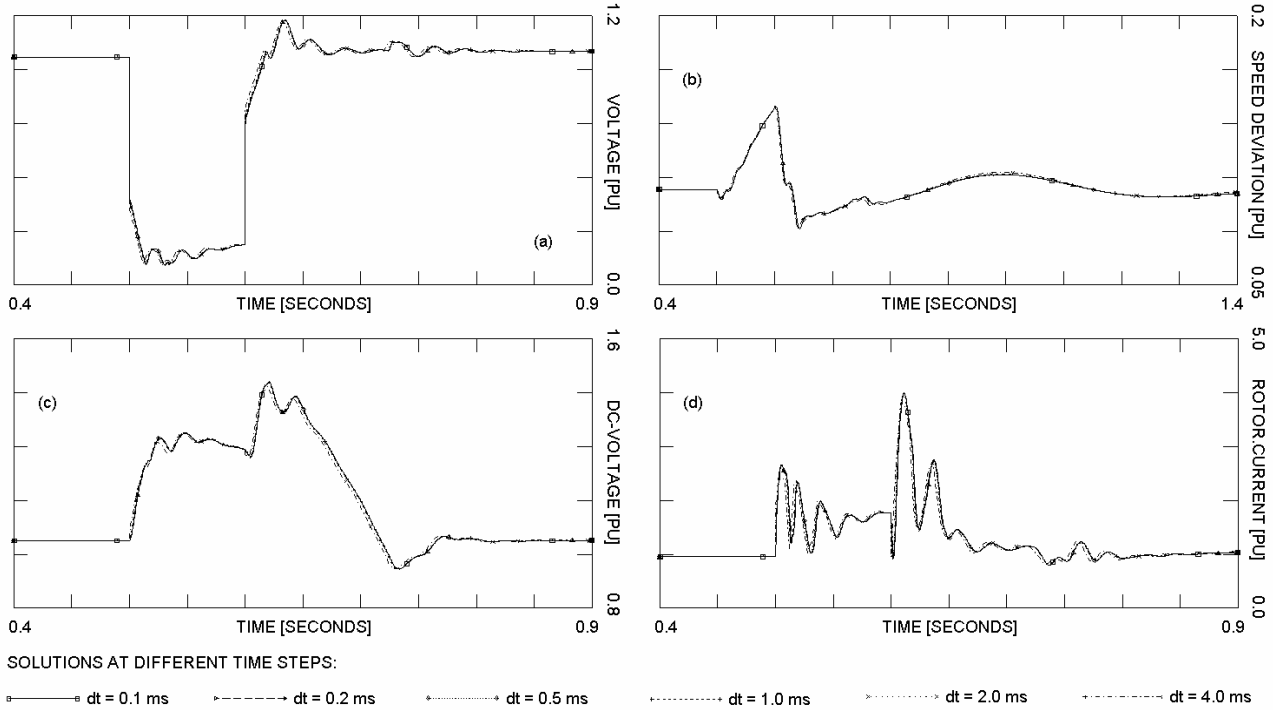


Fig. 10.12. Numeric stability of model of variable-speed wind turbine equipped with DFIG and its converter controls: (a) – terminal voltage, (b) – generator rotor speed, (c) – dc-link voltage, (d) – rotor current. Protective relays are disabled in simulations. Reported in (Akhmatov, 2003(a)).

Even when executing the presented model at “unfair” conditions, the model maintains numeric stability. In the following computations have commonly be made with the integration time step of 1 ms.

10.3. Notification of problems

At the grid fault, operation of the variable-speed wind turbine equipped with the converter-controlled DFIG depends mostly on the converter action and its protective system (Akhmatov, 2003(b)). The grid fault can lead to the converter blocking and ordering of the wind turbine generator to trip. In this case, the wind turbines will disconnect and stop. As already explained, this operation relates to the wind turbines erected in many local wind turbine sites in Denmark. In such local sites, the wind turbines are not assigned to the Specifications of the transmission system operator (Eltra, 2000). Subsequent tripping of many wind turbines will lead to significant power loss. Therefore incorporation of immediate power reserves can be requested (Radtke, 2002).

So long as there are no specifications formulated for the local wind turbine sites with respect to maintaining of uninterrupted operation, this tripping action is fully legal.

When a risk of subsequent tripping is indicated in case of a large wind farm assigned to the Specifications of the TSO, this implies that the solution chosen does not comply with the Specifications of the TSO (Eltra, 2000; Radtke, 2002).

As can be seen from the results shown in **Fig. 10.12**, there can be a risk of the converter blocking due to the following reasons.

- 1) The converter blocks due to over-voltage in the dc-link, see **Fig. 10.12.c**.
- 2) Over-current in the rotor circuit, **Fig. 10.12.d**.
- 3) Over-current in the grid-side converter (not shown in **Fig. 10.12**, but notified in this study case).

As found in (Akhmatov, 2002(a)), the most common reason of the rotor converter blocking is protection from over-current transients in the rotor circuit. Such over-current transients may occur at the following events (Akhmatov, 2002(b)).

- 1) When a short-circuit fault occurs in the power grid.
- 2) When the fault has cleared.
- 3) When the generator has re-connected to the grid or when the converter has re-started (Akhmatov, 2003(b)). This behaviour is not present in **Fig. 9.12**, but experienced from investigations carried out during this project.

Notice that the results shown in **Fig. 10.12** are simulated on the assumption of the co-incident conditions, when (i) the wind turbine is at rated operation (strong wind) and (ii) the fault results in a large voltage drop. At the rated operation, the current in the generator and in the frequency converter is closer to the respective relay settings than when the factual operation point is below the rated operation point.

Normally, the wind turbine production pattern is according to the probability distribution function of wind in the given area. It follows the Weibull distribution (Zinger and Muljadi, 1997; Lange et al, 2001). When assuming that the most probable wind speed in a selected Danish offshore site can be around 8 to 10 m/s (Lange et al, 2001), at such conditions the variable speed wind turbine of 1.8 MW power capacity will produce about 1.0 MW electric power. This will correspond to the most probable operation point of the wind turbine in the selected site, whereas the rated operation will be less often (Akhmatov, 2003(a)).

The large voltage drop may imply that the fault is in the vicinity of the wind turbine, electrically seen. If the fault occurs far, electrically seen, from the generator terminal, the voltage drop will also be small.

Anyway, this investigation has shown that even when the factual operation point is below the rated operation point, there can be a risk of exceeding of the relay settings by over-current in the rotor circuit and by over-voltage in the dc-link when the voltage drops down to 0.5 PU or below (Akhmatov, 2003(a)).

Concerns about protection of the rotor converter, the grid-side converter and the dc-link from risks of over-current in the rotor converter (and also in the grid-side converter) and over-voltage in

the dc-link might be of a general character for this wind turbine concept. This observation is extremely important for understanding the roles of interaction between the DFIG- wind turbines and the electric power grids.

This is also important for reaching accurate and realistic simulation results and for investigations of short-term voltage stability with incorporation of many variable-speed wind turbines with DFIG into power systems.

10.4. Uninterrupted operation feature of wind turbines

The previous discussion has focused on blocking of the frequency converters when the transmission power network is subjected to a short-circuit fault and the voltage drops. Possibly, the wind turbine trips shortly after the converter has blocked. This action has been the level of technology in figures of the year 2001. According to the description of Jensen (2002), the variable-speed wind turbines with DFIG in the Horns Rev offshore wind farm (western Denmark) will disconnect from the grid at faulting situations in the transmission power network. The wind turbines will automatically re-connect few seconds after the fault has cleared.

First, the description by Jensen (2002) indicates that the converter protection and its blocking are important issues, when investigating short-term voltage stability and grid-incorporation of large wind farms with variable-speed wind turbines equipped with DFIG. Second, this description indicates that the frequency converters of DFIG can re-start few seconds after the grid fault has cleared.

In this work, the uninterrupted operation feature, first suggested in (Akhmatov, 2002(a)), will be described and discussed. This feature consists of the following.

The idea behind this feature is that the wind turbines do not trip when the converters have blocked due to the grid fault. The wind turbines continue their operation with the generators with short-circuited rotor circuits. This idea is presented in our work (Akhmatov, 2002(c)). When the rotor converter has blocked, the controllability of the rotor converter is naturally lost. The generators become conventional induction generators. In such operation situations, there is no independent control of electric and reactive power in these units. Over-speeding of the wind turbines is prevented with use of the pitch control, as demonstrated in **Section 6.12**. Here the speed is kept around the pre-defined value with use of the pitch control (Akhmatov, 2002(c)).

When the fault has cleared and when the voltage and the frequency in the power network have been re-established (by operation of conventional power plants and dynamic reactive compensation), the rotor converter will synchronise and re-start. When the rotor converter has re-started, the units are again with independent control of electric and reactive power, which corresponds to normal operation of the wind turbines (before the grid fault occurrence). Advantages of this uninterrupted operation feature are obvious.

- 1) It can be realised with use of frequency converters of relatively small power capacities. Here use of small and cheap converters relates to one of the main advantages of the DFIG concept.
- 2) The wind turbines supply the electric power to the power grid at the transient event. Incorporation of immediate power reserves is not needed.

- 3) By the above-mentioned, the wind turbines will contribute (passively by being in operation and supplying electric power to the power grid) to re-establishing of the electric frequency in the power network at the transient event.
- 4) The feature complies with the Specifications of the TSO and therefore have perspectives for large-scale wind farms.

On the other hand, the controllability of the rotor converter and the DFIG is only possible to use after the rotor converter has re-started, but not during the transient event when the rotor converter blocks. In other words, this feature requires successful re-start of the rotor converter. When the rotor converter has blocked, the grid-side converter can be set to control reactive power and voltage in vicinity of the generator. The controllability of the grid-side converter can, however, be restricted because of a limited power capacity of this converter.

10.4.1. Case of strong power networks

In the case of a strong power grid, it is *expected* that the voltage and the electric frequency will re-established with use of the control of the power grid itself, which is defined by the controllability of large power plants. The requirement of uninterrupted operation of the large wind farms can simply be achieved by the procedure suggested above.

Here the controllability of the grid-side converter is not needed to contribute to reactive power and voltage control in the vicinity of the wind farm connection point, but still useful. This control can also be useful to perform a successful re-start of the rotor converter in the first try (Akhmatov, 2003(b)). Read more about a successful re-start of the rotor converter in the first try in **Section 11.4.2**.

10.4.2. Case of weak power networks

In the case of a weak power network, it is probably not convenient to wait for voltage re-establishment after the grid fault has cleared. It is because there can be a risk of voltage instability initiated by the grid fault. In such a situation, the converter will not re-start and the wind turbines disconnect when uncontrollable voltage decay is developing.

When the wind turbines have been erected in a weak power network, the grid-side converter should be set to control reactive power and voltage at the faulting events. The rotor converter must re-start relatively fast, perhaps before the voltage has completely re-established, and contribute to reactive power control to maintain transient voltage stability. It can also be necessary to combine the control arranged with use of the frequency converters of the wind turbines with other equipment performing dynamic control of reactive power and voltage. This can be SVC, Statcom, SC and discrete components (capacitor banks).

Notify that fast re-start of the converters operating in weak power networks is not always possible. Some results about this topic are described in **Section 11.4.2.2**.

10.4.3. Blocking and re-start sequences of rotor converter

The electric scheme of blocking of the rotor converter is shown in **Fig. 10.13**. The protective relays of the DFIG and the frequency converter are enabled in the simulations. The protective system monitors the voltage, the current, the electric frequency, the dc-link voltage etc. When at least one of the monitored parameters exceeds its respective relay settings, then the rotor converter blocks. When blocked, the converter stops switching and trips (Akhmatov, 2002(b)). When the rotor converter has blocked, the rotor circuit is closed through an external resistor, R_{EXT} (Akhmatov, 2003(b)). The relaying and blocking time is a few ms (Akhmatov, 2002(a)). The external rotor resistor, R_{EXT} , has a current-limiting function, as demonstrated in (Akhmatov, 2002(a)).

This procedure gives the *blocking sequence* of the rotor converter. When the rotor converter has blocked, operation of the generator corresponds to operation of an induction generator with a short-circuited rotor circuit and an increased rotor resistance.

In several descriptions, this feature with closing the rotor circuit through an external resistor is denoted the crow-bar protection. Such descriptions stop often at this stage without introduction of the converter re-start routine. We mean that the converter re-start is essential to demonstrate the ability of uninterrupted operation of the present wind turbine concept. Therefore, this presentation continues with introduction of the converter re-start and suggestions on its practical realisation.

During operation when the rotor converter has blocked, the rotor converter control system continues monitoring the rotor current, the terminal voltage, the active and the reactive powers and the generator rotor speed. The rotor converter is waiting for the order to re-start. The rotor converter *de-blocking sequences* are the following.

- 1) Synchronisation.
- 2) Re-start of the rotor converter.

When the current and the terminal voltage are within their respective pre-defined ranges during a given time period, the rotor converter starts *synchronisation*. At synchronisation, the rotor converter starts switching and the external resistance, R_{EXT} , has switched off. **Fig. 10.14** gives the rotor converter control schemes at synchronisation. The control system resets the PI-controllers by the measured values of the generator rotor speed, the active and the reactive powers, the (α, β) -components of the rotor current etc. The (α, β) -components of the rotor voltage source are set to $V_{R\alpha} = R_{EXT} \cdot I_{R\alpha}$ and $V_{R\beta} = R_{EXT} \cdot I_{R\beta}$. This routine corresponds to that the rotor voltage source, V_R , is controlled by the proportional controllers with the gains R_{EXT} by the (measured) rotor current, I_R . The entire control scheme monitors and resets the PI-controllers at any time-sample. The rotor converter is waiting for the order to re-start.

When the synchronisation seems to be complete, the control system of the rotor converter control shifts to the regular control system given in **Fig. 10.5.a-b**. This is the rotor converter *re-start*.

At this stage, there can be a risk of that the rotor converter can again block. This blocking risk can be due to a risk of excessive transients in the rotor current. Such excessive current transients may occur at the shifting of the control system from the control given in **Fig. 10.14** to the regular

control given in **Fig. 10.5.a-b**. Incomplete synchronisation of the rotor converter can be among the blocking reasons.

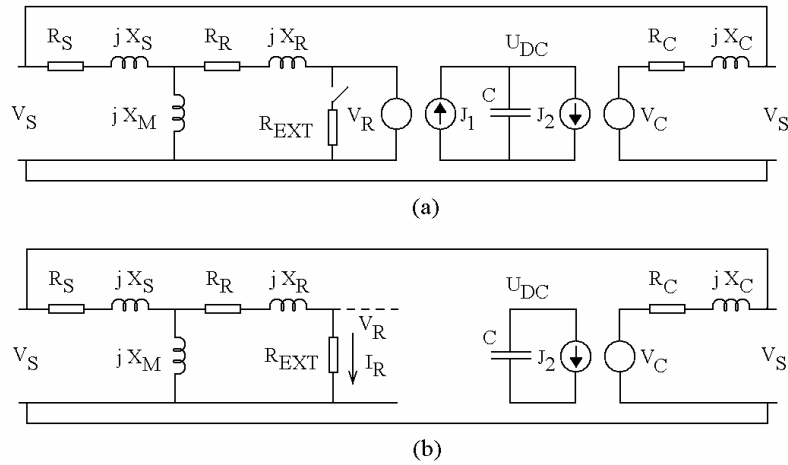


Fig. 10.13. Schematic representation of DFIG and converters: **(a)** – cases of normal, uninterrupted operation of the frequency converters, synchronisation of rotor converter by $V_R = R_{EXT} I_R$, or re-start of rotor converter, and **(b)** – case of blocked rotor converter and grid-side converter operating as a Statcom. Reported in (Akhmatov, 2003(b)).

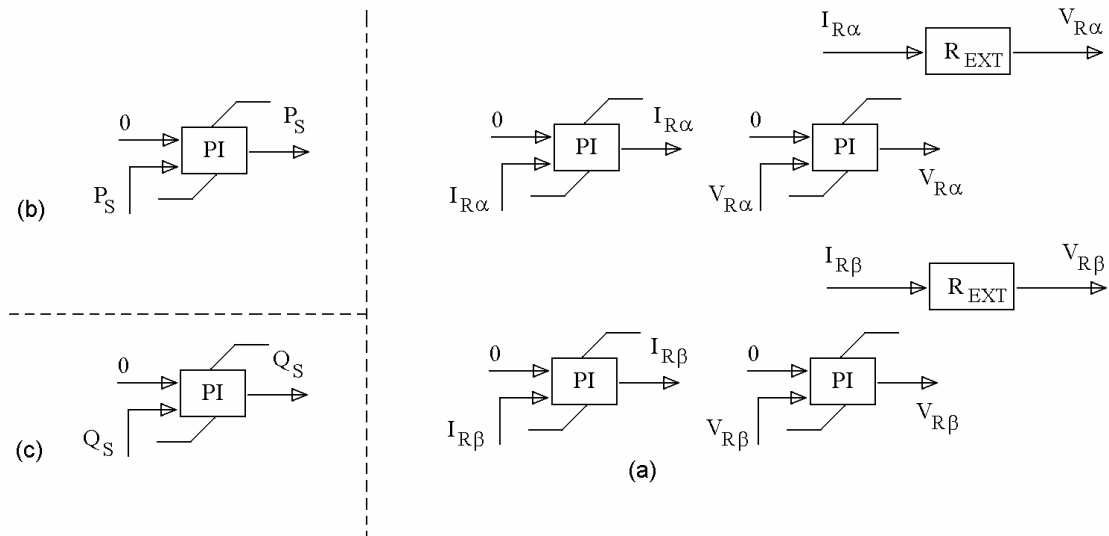


Fig. 10.14. Generic control scheme of rotor converter at synchronisation: **(a)** – generic control scheme of the rotor converter resetting the PI-controllers, **(b)** – resetting of additional PI-controller producing electric power reference by speed, **(c)** – resetting of additional PI-controller producing reactive power reference by voltage. Reported in (Akhmatov, 2003(b)).

Practically said, the synchronisation of the rotor converter is never complete. This synchronisation incompleteness may be caused by presence of the measuring delays of the monitored parameters, which are applied to reset the PI-controllers. This may introduce error signals at the moment of re-start. These error signals are the differences between the reference signals and the factually measured parameters. Such error signals can quickly distribute throughout the proportional gains of the PI-controllers and affect operation of the rotor converter.

A risk of excessive transients in the rotor current when the rotor converter re-starts can also be reduced by independent re-start of the control loops of the rotor converter control for the active power control loop, producing the reference $V_{R\alpha}$, and the reactive power control loop, producing the reference $V_{R\beta}$, respectively. In this way, the rotor current transients at the moment of the rotor converter re-start may be replaced in time. Consequently, the total contribution to the rotor current transients at the moment of the rotor converter re-start will be reduced.

When the rotor circuit is short-circuited /closed through the external resistance, there is no electric power transfer between the rotor circuit and the power network via the frequency converter. From the moment of synchronisation, the electric power $P_R = V_R \cdot \text{conj}(I_R)$ is exchanged between the rotor circuit and the grid-side converter through the dc-link. Therefore, the electric power will be supplied to or absorbed from the power grid at the grid-side converter terminals from the moment of synchronisation.

Notice that this converter action feature has been suggested in this work by inspection of the simulated curves shown in **Fig 10.12**, when the protective system model has been disabled. Other actions of the frequency converter for reaching uninterrupted operation of the wind turbine may also be suggested and implemented into the converter control. *Remember that the action of the frequency converter will decide operation of the DFIG and the wind turbine at transient events in the power network*⁴². In the years to come, we will see more to advanced converter control where the target is to comply with the specifications of the transmission system operators and the customers of the large wind farms. Voltage re-establishment without subsequent disconnection of the large wind farms at transient events in the power networks is the key term in such technical specifications.

10.4.4. Value of external rotor resistance

If the rotor circuit is simply closed through a low-resistance contact, the generator will operate as a strongly over-speeded asynchronous generator with a risk of an excessive reactive current (Akhmatov, 2002(c)). The external resistance, R_{EXT} , is applied to reduce the rotor current magnitude when the rotor converter has blocked. When choosing the value of R_{EXT} , a number of considerations must be taken into account.

- 1) The current transients in rotor circuit must be damped efficiently before the converter synchronisation and the converter re-start will take place.
- 2) The value of the external resistance should not be much large to minimise of a risk of excessive rotor current transients when the resistance will trip to re-start the rotor converter.
- 3) In this work, it is also found that the value of R_{EXT} influences the reactive power demands of the generator. This must be taken into account to minimise such reactive power demands.
- 4) In general, the value of R_{EXT} to be chosen fits to the generator electrical data. When the generator is replaced by another generator with another dataset, a new value of the external rotor resistance should be applied.

⁴² This statement is so important to understand and keep in mind that we have repeated this from a previous section.

In the following simulations, the value $R_{EXT} = 20 R_R$ have been applied (Akhmatov, 2003(b)).

10.4.5. Reactive power control co-ordination

At operation with the short-circuited rotor circuit and at the synchronisation, the rotor converter control is inactive. The DFIG absorbs an amount of reactive power from the power network, which is necessary for the generator excitation. This behaviour is known from operation of conventional induction generators. Since the control of the rotor converter is inactive, the reactive power demands must be covered with use of dynamic reactive compensation incorporated into the power network in vicinity of the wind farm connection point.

This dynamic reactive power compensation can be arranged with use of (i) discrete components, (ii) continuous control components and (iii) combination of discrete components and the continuous control components. The superior control system of the large wind farm can also have access to the control loops of the dynamic reactive power control and order this to act (i) to reduce the voltage drop at the grid faults and (ii) to perform dynamic reactive power control when the frequency converters of the wind turbines have blocked.

To reduce the voltage drop at the grid fault, the Synchronous Condensers and/or Statcoms must be applied because these units are able to generate their terminal voltage. To take over the reactive power control when the frequency converters have blocked, the SVC in combination with a capacitor-bank can be applied. This choice depends on the factual operational situation in the power network and the power network itself, but there are no general roles.

On the other hand, the frequency converters can be applied to control reactive power and voltage, which may reduce demands of dynamic reactive compensation from other equipment in the power grid (Akhmatov, 2002(c)). This application will require (i) fast re-start of the rotor converter and (ii) use of the grid-side converter to control reactive power when the rotor converter has blocked (Akhmatov, 2003(b)).

Notice that the power capacity of the grid-side converter is smaller than the power capacity of the generator, which is why the reactive power controllability of the grid-side converter is smaller as well. This means that the reactive power control must mainly be performed with use of the rotor converter whereas the grid-side converter operates as a supplementary control unit when the rotor converter control is inactive or insufficient to generate a required amount of reactive power.

At the grid fault, the grid-side converter must not block, but continue its operation and wait for fast re-start of the rotor converter. During this time, the grid-side converter must be set to control (i) the dc-link voltage, U_{DC} , to be within the given range and (ii) the reactive power to contribute to faster voltage re-establishment. When the rotor converter has blocked, operation of the grid-side converter is analogous to a Statcom, which is seen from **Fig. 10.13.b**. Therefore it should be possible to set the grid-side converter to control reactive power within a range with use of the control schemes in **Fig. 10.5.c** and **Fig. 10.5.e**.

When the grid-side converter is set to control reactive power and voltage, this control feature must be implemented with application of the control co-ordination between the rotor converter and the grid-side converter to avoid conflicts (Akhmatov, 2003(b)). In this work, this control co-ordination is organised by the following. The grid-side converter is only set to control reactive

power when the rotor converter has blocked. When the rotor converter operates normally or has re-started, the grid-side converter is again set to be reactive neutral. The main reactive power control is realised with use of the rotor converter with the control schemes in **Fig. 10.5.a** and **Fig. 10.5.d**.

When the rated power capacity of the grid-side converter is around 25 % of the DFIG rated power and the rated power of the wind farm is 150 MW, then dynamic reactive power control organised with use of the grid-side converters may correspond to incorporation of a Statcom with the rated power capacity of 37.5 MVAR. It does not look much, but notify that this "Statcom" feeds into the local power network of the wind farm and therefore can be efficient to improve the voltage profile at the DFIG terminals. This will contribute to fast re-start of the rotor converters.

10.4.6. Example with uninterrupted operation of wind turbines

After the short-circuit fault has cleared, the voltage in the power network must re-establish without subsequent disconnection of the wind turbines in the large wind farms. This is the main requirement of the Specifications formulated by the TSO (Eltra, 2000). The uninterrupted operation feature suggested for the DFIG- wind turbines is illustrated by a simulated behaviour the selected wind turbine, WT 01, in the large wind farm. The large wind farm model consists of eighty 2 MW variable-speed wind turbines equipped with DFIG and partial-load frequency converters⁴³. The model, the electric power supply pattern in the farm and the grid fault are according to the description of **Section 6.7**.

When the grid fault occurs, the voltage drops. This initiates the machine current transients, the transients in the grid-side converter current and the dc-link voltage fluctuations (Akhmatov, 2002(d); Akhmatov, 2003(b)). As already been explained, this behaviour leads to the rotor converter blocking. The feature with fast re-start of the rotor converter is illustrated with simulation results shown in **Fig. 10.15**. From the start of simulation to the time $t = T_1$, the power system is at normal operation. At the time T_1 , the short-circuit fault has occurred in the transmission power network.

At the time $t = T_2$, the rotor converter has blocked by over-current (transients) in the rotor circuit. The rotor circuit has closed through the external resistor, R_{EXT} . When the rotor converter has blocked, the wind turbine operates as a pitch-controlled wind turbine equipped with an induction generator with an increased value of the rotor resistance. Pitch-control prevents the wind turbine from fatal over-speeding. This operation prevents the power system from voltage instability which could be started by the wind farm. The positive impact of the blade-angle control on short-term voltage stability has been explained in **Section 6.12**.

⁴³ In this investigation, we have applied the most advanced model of such variable-speed wind turbines. All the eighty wind turbines have been modelled by their individual models with representation of the transient DFIG model, the frequency converter model with the rotor converter, the grid side converter and the dc-link in between and the protective system. The shaft system is essentially modelled with use of the two-mass model. The rotor is with the aerodynamic model with dynamic inflow phenomena, which is more accurate than use of C_P -representation, and the pitch control. Sufficient numeric optimising of the model code made it possible to complete the investigation in acceptable time.

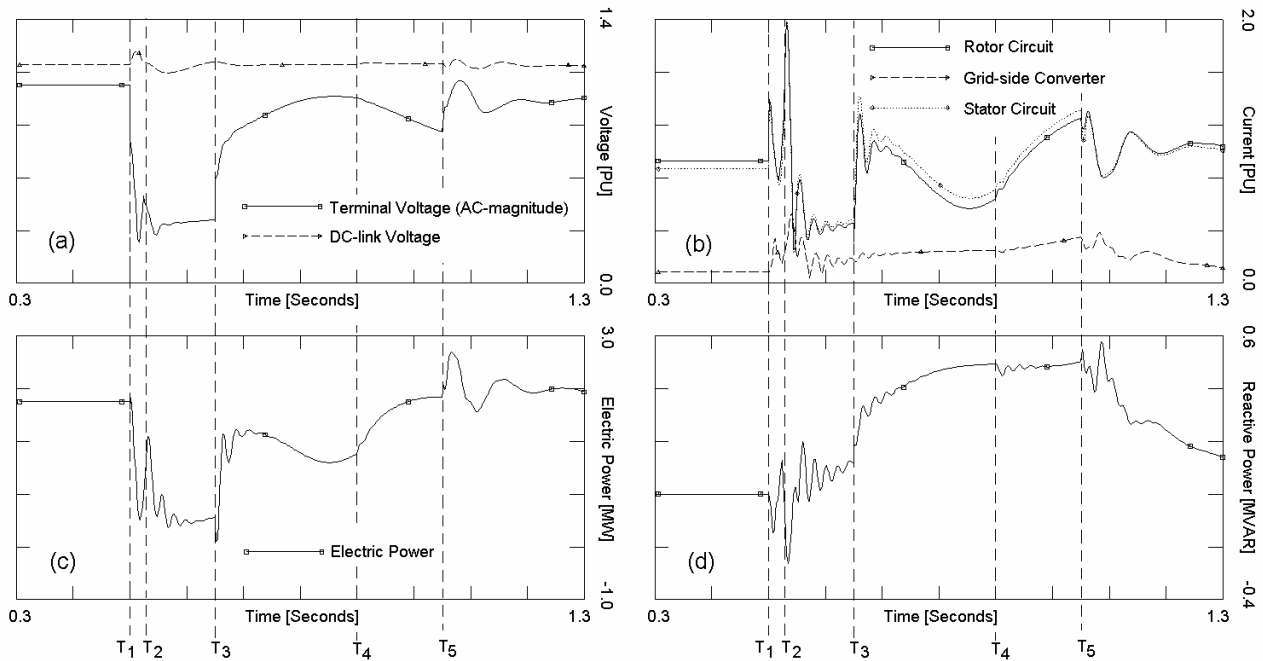


Fig. 10.15. Uninterrupted operation feature of wind turbine WT 01 with fast re-start of the rotor converter: (a) – terminal and dc-link voltages, (b) – current in rotor circuit and grid-side converter mains, (c) – electric power, (d) – reactive power of grid-side converter. Reported in (Akhmatov, 2003(c)).

The grid-side converter operates as a Statcom. It controls the dc-link voltage and contributes to control of the reactive power and the voltage in the vicinity of the wind turbine terminals. This control contributes to fast re-establishing of voltage in the grid and to fast re-start of the rotor converter, but is restricted by the power capacity of the grid-side converter.

The grid fault has cleared at the time $t = T_3$. Shortly after the fault has cleared, the voltage and the grid frequency have been re-established within their respective ranges. At this moment, the rotor converter synchronisation starts. The rotor converter starts switching and the external resistance has disconnected from the rotor circuit. At synchronisation, the rotor converter prepares to re-start. Synchronisation begins at the time $t = T_4$ and prevents the rotor converter from to block at the re-starting sequence, which could be caused by excessive transients in the rotor current or unacceptably large fluctuations of the dc-link voltage.

At the time $t = T_5$, the rotor converter has re-started. After the rotor converter has re-started, normal operation of the wind turbine has re-established. The feature with fast re-start of the rotor converter is applied to achieve uninterrupted operation of the wind turbines in the large wind farm at grid disturbances.

As demonstrated, it is possible to organise uninterrupted operation of variable-speed wind turbines equipped with DFIG and partial-load converters when a short-circuit fault occurs in the transmission power network. At the fault, the rotor converter blocks, indeed. When the rotor converter has blocked, the DFIG operates as a conventional asynchronous generator and supplies electric power to the power grid. The control system of the rotor converter will re-start shortly after the grid fault has cleared. This will re-establish normal operation of the frequency converter and the wind turbine itself. This procedure has been discussed with the Danish manufacturer Vestas Wind Systems, producing the OptiSpeed® wind turbines. The manufacturer Vestas Wind Systems

has agreed that the principle described in this report could be applied to achieve uninterrupted operation of the wind turbines of this variable-speed concept.

10.5. On mutual interaction between wind turbines

Among the concerns of incorporation of large wind farms into the power networks there is a possible risk of mutual interaction between the converter control systems of a large number of the variable-speed wind turbines. Such concerns are enforced in situations with fast-acting frequency converter systems of the DFIG and in situations when the rotor converters execute blocking and re-start sequences in a short time-interval, at the grid fault. These concerns are often expressed by the question whether the wind turbines or the control of their frequency converters start to oscillate against each other. Answering this question should be a part of voltage stability investigations and therefore has been performed in this work.

In this simulation example, maintaining of voltage stability is achieved without use of dynamic reactive compensation. The grid-side converters of the DFIG are set to control reactive power and voltage at the transient event when the rotor converters have blocked (Akhmatov, 2003(b)). The rotor converters have re-started after the grid fault has cleared. The simulated curves for the selected wind turbines operating at different operation points are shown in **Fig. 10.16**. The simulations do not indicate any risk of mutual interaction between the different wind turbines within the large wind farm. The variable-speed wind turbines equipped with DFIG show coherent response at the grid fault.

This positive result is reached for the given control strategy of the variable-speed wind turbines and the given power system. This shows that the control strategy applied in this work is robust to external disturbances affecting the converter control. When another control strategy is applied, similar investigations about a risk of mutual interaction between the control systems of the frequency converters should be made.

However, it is commonly assumed that the well-tuned converters will not interact with each other, independently from the conditions of the power grid (Slootweg, 2003).

10.6. Resume

The variable-speed wind turbines equipped with DFIG and partial-load frequency converters are a promising wind turbine concept for large (offshore) wind farms. In case of DFIG, excitation of the generators can be organised with use of the rotor converter, e.g. from the rotor converter via the rotor circuit, but not from the power grid via the stator mains. Use of partial-load frequency converters is one of the main advantages of this concept because small converters imply small sizes and lower prices of the converters.

In investigations of short-term voltage stability, the DFIG must be modelled with at least the fifth-order model containing representation of the fundamental-frequency transients in the machine current. Such transients are initiated at short-circuit faults in the electric power network and may cause blocking of the rotor converter.

The frequency converter must at least be modelled with representation of the rotor converter and its control and protection. Representation of the grid-side converter and its control and protection is

strongly recommended to reach acceptable accuracy of the predicted rotor current behaviour. The last mentioned conclusion is in contrast to the commonly used assumptions dealing with disregarding of the relatively fast-acting grid-side converter in voltage stability investigations.

In this investigation, it is found that the grid-side converter and the dc-link may contribute to smoothing the machine current transients. An accurate prediction of the machine current transients in the model is essential to reach an accurate prediction of the rotor converter action at the grid disturbances.

Representation of the dc-link in the converter system model makes it possible to monitor the dc-link voltage behaviour in the model and predict the converter blocking caused by excessive fluctuations of the dc-link voltage. Keep in mind that the frequency converter can block by over-voltage in the dc-link. Furthermore, representation of the grid-side converter opens opportunity to investigate the ability of this converter to control reactive power and voltage at the grid faults. Also, this makes it possible to investigate the impact of the grid-side converter and its control on the power network.

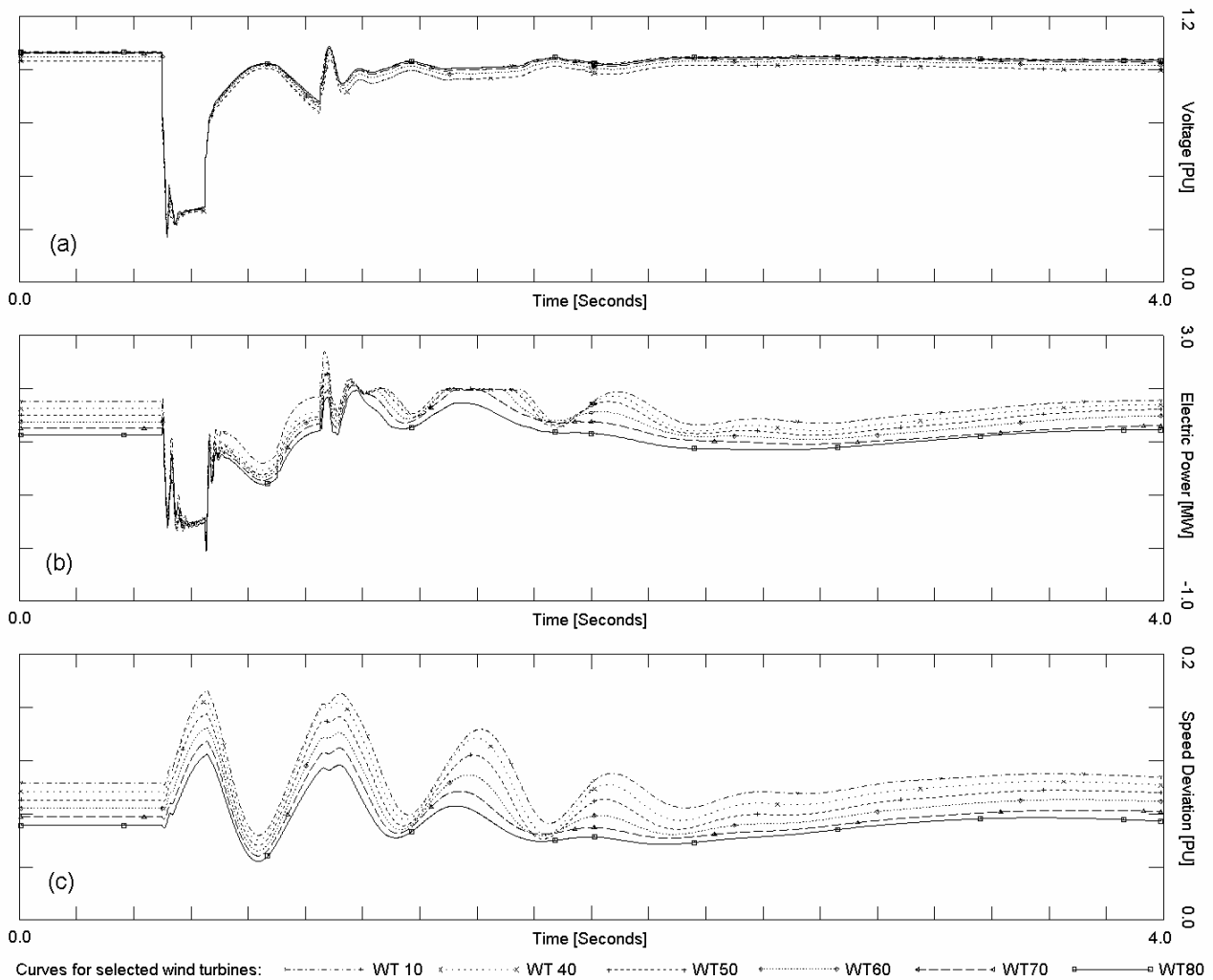


Fig. 10.16. Simulated response of selected wind turbines to a short-circuit fault: (a) – terminal voltage, (b) – electric power, (c) – generator rotor speed deviation (minus slip of DFIG). Reported in (Akhmatov, 2003(c)).

The converter action will decide operation of the wind turbine and its generator at transient events in the power system.

This variable-speed wind turbine concept has been evaluated with respect to maintaining of short-term voltage stability at grid faults. The frequency converters can contribute to control reactive power and voltage in the grid. Mainly, this control is arranged with use of the rotor converters. In situations when the rotor converters have blocked and so their control is inactive, the grid-side converters can be set to control reactive power and voltage. However, the controllability of the grid-side converter is restricted because of their relatively small power capacity. The reactive power control arranged with use of the grid-side converters may improve the voltage profile at the generator terminals and, in this way, contribute to fast re-start of the rotor converter.

The transmission system operator and the customer of the large wind farms have to request this dynamic reactive power control performed by the frequency converters. In the case of such requesting, the wind turbine manufacturers will start to use this dynamic reactive power control feature in their products (GE Wind, 2002). When no dynamic reactive power control has been requested, the converter-controlled DFIG will operate as reactive-neutral components, e.g. these generators are excited by the rotor converters via the rotor circuits and do not exchange reactive power with the power systems.

The frequency converters, their IGBT-switches and the dc-link are affected by the grid faults, when a sudden voltage drop occurs. At the grid faults, there can be a real risk of that the rotor converter blocks by over-current in the rotor circuit or by over-voltage in the dc-link. Such converter blocking is often followed by disconnection of the wind turbines. This protective disconnection is a common behaviour seen in the local wind turbine sites in Denmark, but this is not allowed in the case of large wind farm, which have to comply with the Specifications of the TSO (Eltra, 2000). Sudden (and unexpected) disconnection of many wind turbines will demand immediate power reserves, which may increase the cost of the project and its negative impact on the power system.

The main challenge of this variable-speed concept is rather maintaining of uninterrupted operation of the wind turbines than maintaining of short-term voltage stability. It is found that the voltage will re-establish without use of dynamic reactive compensation. Protective tripping of the large wind farm does not cause voltage instability. The voltage recovers, but protective tripping indicates that the solution does not comply with the Specifications of the TSO (Eltra, 2000). Request of uninterrupted operation of the wind turbines can be met with use of the control feature with fast re-start of the rotor converters, which may block at the grid fault. It is found that the voltage will also re-establish without use of dynamic reactive compensation, when the control feature with use of fast re-start of the rotor converters is applied.

In other words, the frequency converter operation sequences and its control are essential for this wind turbine concept for (i) maintaining of transient voltage stability and (ii) avoiding subsequent trip of the wind turbines at the grid faults.

11. Power system analysis with large amount of wind power

Now experiences with modelling of wind turbines of different concepts and results of investigations of short-term voltage stability are resumed and applied in cases of large power systems. Such large power systems, which are treated in this investigation, contain a large amount of wind power and local combined heat-power (CHP) generation. In such large power systems, there are several factors influencing the outcome of a transient event in the grid.

In the Danish power system, the majority of wind power is dispersed throughout the power grid. The majority of the wind turbines is of the conventional Danish concept, **Section 1** and **Section 4**, e.g. the fixed-speed wind turbines equipped with induction generators. These wind turbines are collected into relatively small local sites. The rated power capacities of such local sites are in the range from few MW up to 40 MW, which is the offshore wind farm at Middelgrund close to the Copenhagen shore and connected to the local cable network of Copenhagen. Such local sites are connected to the local distribution networks. The wind turbines in such local sites are not assigned to any technical specifications from the transmission system operator⁴⁴.

This implies that (i) the wind turbines produce so much electric power as wind blows and (ii) they do not contribute to dynamic reactive power and voltage control. When a short-circuit fault occurs, operation of the wind turbines in local sites may depend on their protective relays.

This statement must be interpreted as that the wind turbines will trip if at least one of the respective relay settings has been exceeded. If the wind turbines continue uninterrupted operation during and after the short-circuit fault, their induction generators will absorb reactive power from the electric power at the voltage re-establishing process. In other words, an uncertainty is introduced about operation of decentralised wind turbine sites at the grid disturbances.

The local CHP units are typically owned by small co-operatives and generate so much power as possible when the electricity tariffs are favourable. These units do not contribute to dynamic reactive power and voltage control either. Again, their operation at the grid disturbances is decided by their protective relays. This will also introduce an uncertainty about operation of local CHP units at the grid faults.

How much does it mean for operation of the large power network? When an amount of local generation is relatively small, it has no significant impact on the grid operation. But the situation can be much different when the part of local generation in the power generation mix is significant.

The conventional power systems in all the developed countries are traditionally built-up about large power plants feeding into the transmission power networks. In eastern Denmark, the transmission power system is at the voltage levels of 132 kV and 400 kV. With rapidly increasing penetration of wind power, the power generation pattern in the Danish power system has changed. From being absolutely dominated by the large power plants, the power generation becomes a mix between the power supply from (i) conventional power plants and large wind farms feeding into the transmission network and (ii) many local wind turbine sites and CHP units feeding into the local

⁴⁴ We repeat our notification given in **Section 1** that the transmission system operator will develop a set of technical specifications for the wind turbines connected to the grids with the voltages below 100 kV. At the moment when this investigation has been carried out, no such specifications have been.

distribution networks at the voltage levels below 100 kV. Notice also that the local generation units feed into the power networks at the low voltage levels, where the consumption has traditionally been located. This situation may relate to a new technical trend which is named active-networking.

Significance of this issue is seen from the counts for eastern Denmark. Here the season-dependent peak power consumption is in the range from 750 MW to 3700 MW (Bruntt et al, 1999). The total power capacity of renewable generation units, including (i) the offshore wind power, (ii) the local wind turbine sites on-land and (iii) the CHP units will be around 1000 MW. The largest concentration of the decentralised wind turbine sites is seen in the region of the island of Lolland (Bruntt et al, 1999). The Rødsand /Nysted offshore wind farm has also been commissioned in the same area that is characterised by excellent wind conditions. The island of Lolland is located south to the main Danish island of Zealand where the main consumption centres are located around Copenhagen, the capital of Denmark, see **Fig. 11.1**.

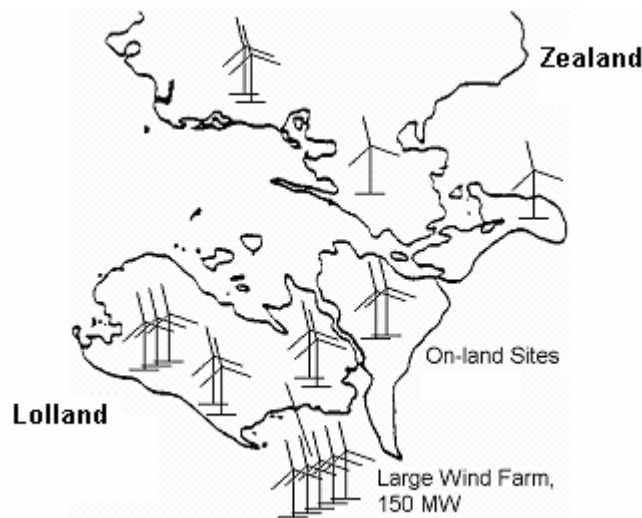


Fig. 11.1. Wind power penetration in the eastern Danish power system.

In case of the eastern Danish power system, the problem with power transport throughout the transmission power system will be introduced. This is specific for this case because the major wind turbine sites are at south and the consumption centres with the developed (strong) power system are located at north of the region. Before the large wind power penetration in the Lolland region came, this region had a relatively low consumption and received electric power from the large power plants at north. The wind power penetration in many local sites has changed the power flow in the (transmission) power network and now the consumption centres at north receive electric power from the local generation sites located at south.

Similar patterns can be found in other power systems. This will perhaps occur in the power grid in the U.K. where large wind power projects have recently been announced (Twidell, 2002). This may be the general problem formulation that relates to several power systems because the large wind power sites are located where the wind conditions are good, but commonly far from the consumption centres and also from the strong power networks. This implies that the wind turbines may be incorporated into relatively weak power networks, at peripheries of the transmission power systems.

The challenge of reliable operation of such power systems becomes an important issue. Among the questions related to maintaining short voltage stability and reliable power supply can be the following.

- 1) Definition of the worst case operation with respect to voltage stability and also with respect to a risk of power loss.
- 2) Questions related to operation of the wind turbines in local sites at the grid faults.
- 3) Question related to operation of the local CHP units at the grid faults.
- 4) Access to strong power networks for grid-connection of the large wind farms and compliance with the Specifications of the TSO (Eltra, 2000).
- 5) Incorporation of dynamic reactive compensation and what kind.
- 6) Demands of immediate power reserves when several local units will disconnect.
- 7) Choosing wind technology to large (offshore) applications because there will be many factors from the power system which may influence operation of the large wind farms.
- 8) Applicability of the results reached in this investigation in other power systems.

The tasks listed above will be explained and illustrated with a number of examples in this presentation.

11.1. Model of large power system

The sketch of the large power system which is used in this investigation is shown in **Fig. 11.2**. The whole power system can be separated into a number of areas characterised by (i) The electricity production and consumption pattern, (ii) the amount of incorporated wind power and local CHP and also (iii) the strength of the power system.

Area 1 is characterised by good wind conditions and consequently by significant penetration of wind power located in many local sites on-land. There are also a few local CHP units. The wind power capacity incorporated in this area is considered about 500 MW. The power system consists of a number of 0.7 –10 –50 kV local distribution networks connected by few 132 kV transmission lines. The power consumption is low and the power system is considered weak. Through the long transmission line, which is marked (1) in **Fig. 11.2**, the area 1 is connected to the entire power system with the consumption centres. In other words, the power is transported from the wind power incorporated in area 1 to the entire power network through this long transmission line.

Area 2 is characterised by relatively poor wind conditions on-land. In this area there is not much grid-incorporated wind power on-land. But many local CHP units of approximately 400 MW total power capacity dominate the electric power generation in this area. There are also a number of relatively large consumption centres and large power plants. The power grid is with a number of 0.7 –10 –50 kV local power distribution networks (with the local CHP generation) connected to the 132 kV meshed transmission power system. The power system in this area is considered relatively strong.

The meshed power system in area 3 is considered strong and contains the main power consumption centres and the main large power plants controlling voltage and frequency in the

transmission power network. Wind conditions are poor. Therefore there are only few wind turbine sites and also few local CHP units.

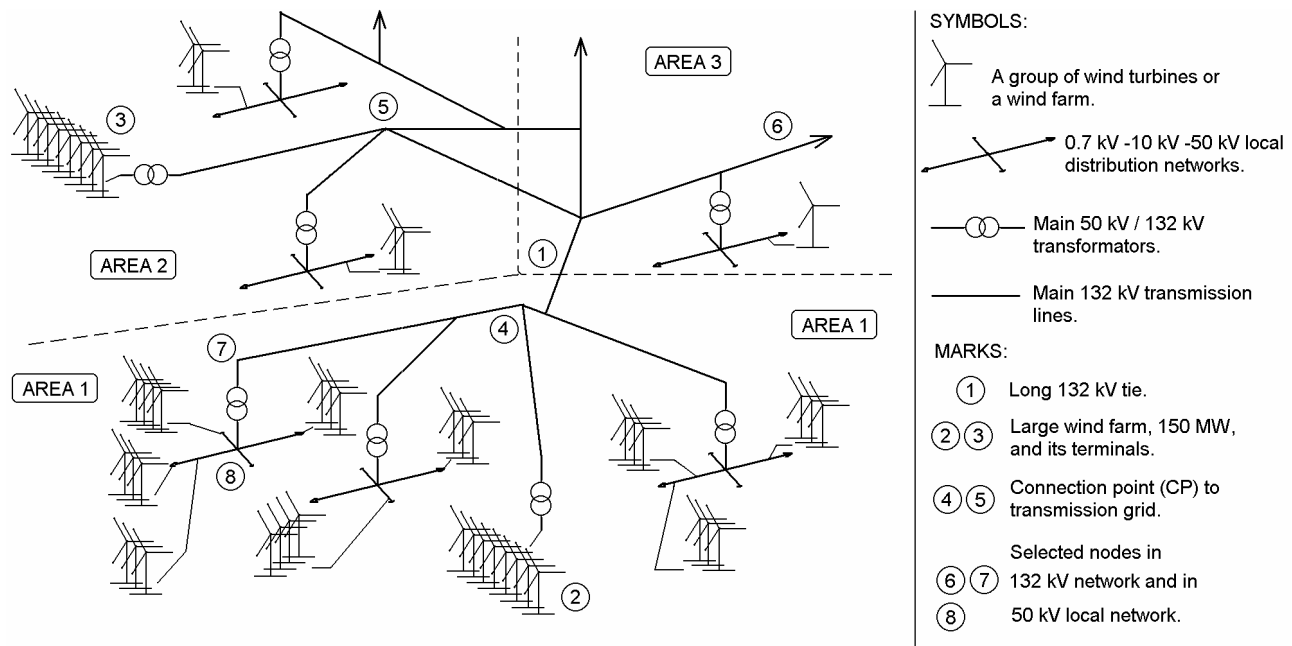


Fig. 11.2. Sketch of large power system model.

Furthermore, a large (offshore) wind farm of 150 MW rated power has been connected to the transmission power network. The large wind farm must comply with the Specifications of the Danish TSO (Eltra, 2000). The large wind farm has been incorporated *either* into the transmission power network of area 1 – marked (2) *or* into the transmission power network of area 2 – marked (3) indicated in **Fig. 11.2**. These two cases are present for evaluation of significance of the access to strong power networks.

The cases to be investigated represent the classical situation similar to a number of power networks used for investigations of short-term voltage stability. This is the bottleneck connecting two areas with consumption and generation, which is in the present case relates to the long weak tie between the power grid of area 1 and the entire power system. Here this classical situation is combined with grid-incorporation of large amount of wind power in area 1.

The model of the large power system is implemented into the simulation tool PSS/E, which is applied at NESA for investigations of power system stability. The company NESA helped kindly with implementation of the power system model.

11.1.1. Modelling of large power plant units

The large power plant units are thermal power units equipped with synchronous generators. The synchronous generators are with excitation control and their turbines are with governing control. Furthermore, a number of the power plant units are equipped with Power System Stabilisers (PSS).

Via the transformers, the large generation units feed directly into the transmission power network. The large power plant units and their equipment control are represented using the standardised models of the simulation tool PSS/E. The data of the generators and their control

systems are applied in accordance with recommendations of the company NESAs. In simulations, accurate implementation and data of the large power plants are necessary to get a sufficiently realistic response of the power plant models to the grid faults.

11.1.2. Modelling of large consumption centres

Dynamic load models, which represent large consumption centres in this investigation, are voltage- and frequency- dependent. This dependency is applied because the dynamic load characteristics influence voltage behaviour at the grid disturbances (Taylor, 1994). Especially, the voltage-dependence of dynamic loads plays a part and needs sufficiently accurate representation in investigations of short-term voltage stability.

In this work, this voltage-dependence is given with use of the PSS/E standardised model CONL, e.g. the load conversion model. Its operation corresponds to the ZIP-model, as the load is composed of constant impedance (Z), constant current (I) and constant power (P) components (Kundur, 1994). The mathematical description of such load conversion is given with use of the polynomial expression.

$$P(V) = P(V_0) \cdot \sum_{l=0}^2 a_l \cdot (V/V_0)^l, \quad Q(V) = Q(V_0) \cdot \sum_{l=0}^2 b_l \cdot (V/V_0)^l. \quad (11.1)$$

Here P and Q are the voltage-dependent electric power and reactive power of the load, respectively. V is the factual voltage and V_0 is the rated voltage where $P(V_0)$ and $Q(V_0)$ are the electric power and the reactive power of the load at rated voltage. The parameters of this model are the coefficients a_0 , a_1 , a_2 and b_0 , b_1 , b_2 , which define the proportion of each component (Kundur, 1994). These coefficients are chosen in accordance to recommendations of the company NESAs.

Notice that such load representations will be sufficiently accurate in the limited range of voltage. According to (Taylor, 1994), **Eqs. (11.1)** will still predict accurate response when the voltage drop is not large. When the voltage drop at the load terminals is sufficiently large, then more accurate load models would be required. For example, more accurate models should be necessary for representation of induction motors at significant voltage fluctuations. Inaccuracy of representation of the dynamic loads will consequently introduce inaccuracy in the simulated results⁴⁵. On the other hand, it is not always possible to find and apply a detailed representation of every each load in the grid in such investigations of short-term voltage stability of large power systems⁴⁶.

The frequency-dependence of the dynamic loads is with use of the standardised PSS/E model LOADFA. Its operation corresponds to introduction of the frequency-dependence of the electric and reactive power

⁴⁵ Notice that sensitivity of the voltage profile to the load model coefficients has been registered in this investigation. Reduced load representation with constant electric power and constant reactive power, which are independent from the dynamic voltage behaviour, should not be applied instead of dynamic load models.

⁴⁶ Request information about average data of the dynamic load models from the local power company or from Nordel when investigating voltage stability in a Scandinavian grid.

$$P(f) = P(f_0) \cdot (f / f_0)^A, \quad Q(f) = Q(f_0) \cdot (f / f_0)^B, \quad (11.2)$$

and also of the active and reactive current components

$$I_D(f) = I_D(f_0) \cdot (f / f_0)^C, \quad I_Q(f) = I_Q(f_0) \cdot (f / f_0)^D. \quad (11.3)$$

Here P , Q , I_D and I_Q are the frequency-dependent electric power, reactive power, active current component and reactive current component of the load, respectively, f is the factual frequency and f_0 is the rated frequency. $P(f_0)$, $Q(f_0)$, $I_D(f_0)$ and $I_Q(f_0)$ are the electric power, the reactive power, the active current component and the reactive current component of the load at rated frequency, respectively. The coefficients A , B , C and D are the parameters of this model and chosen in accordance to recommendations of the company NESAs.

The dynamic load representations with use of **Eqs. (11.1) to (11.3)** are considered suitable for this investigation.

11.1.3. Modelling of local CHP units

Local CHP units do not contain dynamic reactive power and voltage control. The generators feed directly into the local distribution networks and assumed to be at rated operation when they are in operation (consideration of favourable tariffs). Therefore the local CHP units are simply represented by their synchronous generator models with the lumped inertia of the generator rotors and the turbines. The synchronous generators are given with use of the standardised models of the simulation tool PSS/E.

Furthermore, the protective relay models are included into the representation of local CHP units in investigations of short-term voltage stability. The relay models monitor the voltage, the grid frequency, the machine current and the speed of the generation units and order tripping when at least one of the monitored values exceeds its respective relay settings. The relay settings and the characteristic relay times are in accordance with recommendations of the company NESAs.

11.1.4. Representation of local wind turbine sites

When representing the wind turbines in many decentralised sites, it is taken into account that the majority of wind turbines in Denmark are fixed-speed wind turbines equipped with no-load compensated induction generators⁴⁷. Therefore the wind turbines in local sites are represented with use of the dynamic model of stall-controlled wind turbines. In investigations of short-term voltage stability, the wind turbines are treated as complex electromechanical systems (Akhmatov et al, 2000(a)). The model consists of the following parts, **Section 4**.

⁴⁷ Discussion: the older Danish wind turbines are no-load compensated. The wind turbines erected in Denmark after the year 1996 may be assumed as full-load compensated. Notice that the local wind turbines are often owned by groups of farmers and co-operatives which are paid for the electric power supply. There are no requirements on (and therefore no sufficient attention to) maintenance of the capacitor banks applied to arrange the full-load compensation of the local wind turbines. In this investigation, we have assumed that all the local wind turbines are no-load compensated.

- 1) The fifth-order model of induction generators (Knudsen and Akhmatov, 1999).
- 2) The two-mass representation of the shaft system.
- 3) The aerodynamic rotor model in terms of C_p - λ -curves, **Section 2.1**.
- 4) The protective relay model. The relay model monitors (i) the voltage, (ii) the machine current, (iii) the grid frequency and (iv) the speed and trips the wind turbine when at last one of the monitored values exceeds its respective relay settings (Akhmatov, 2002(a)). The relay model disconnects first the no-load capacitors and so the induction generators. This procedure is applied to prevent tripped induction generators from over-excitation and over-voltages.

The wind turbine induction generators are grid-connected on the 0.7 kV level and through their transformers feed into the local distribution networks. The local wind turbine sites are represented in the power system model with use of their single-machine equivalents (Knudsen and Akhmatov, 2001). In other words, the local wind turbine sites are given by their re-scaled wind turbine models. This is valid on the assumption derived in (Akhmatov and Knudsen, 2002). Here all the wind turbines in the given site are with identical data and at similar operation points. The large power system model contains more than sixty local wind turbine sites on-land (Knudsen and Akhmatov, 2001).

11.1.5. Representation of large wind farms

The large wind farms are also represented with use of single-machine equivalents, at similar considerations of (Akhmatov and Knudsen, 2002) as in case of decentralised wind turbine sites. This will also simplify the modelling process and reduce the computation time, when modelling a single wind turbine with a re-scaled (increased) power capacity instead of a large number of wind turbines in the large wind farm⁴⁸.

In this work, the two wind turbine concepts are examined. First, it is considered that the wind farm is with fixed-speed, active-stall wind turbines, **Section 4** and **Section 6**. This may relate to the Rødsand /Nysted offshore wind farm containing seventy-two fixed-speed wind turbines from the Danish manufacturer Bonus Energy.

Second, it is considered that the wind farm is with variable-speed wind turbines equipped with DFIG and partial-load frequency converters, **Section 10**. This case may relate to the Horns Rev offshore wind farm consisting of eighty variable-speed wind turbines from the Danish manufacturer Vestas Wind Systems.

The large wind farms must comply with the Specifications of the Danish TSO (Eltra, 2000). This requires that the voltage must be re-established, after a short-circuit fault of 100 ms duration has cleared, without subsequent disconnection of the large wind farm. Notice that it is not always convenient to omit representation of the protective relay systems of the wind turbines in the large wind farms. In some situations, the requirement of uninterrupted operation of the wind farm must be reflected in representation of the wind farm model. For example, in case of the converter-

⁴⁸ Why is it possible? Pay your attention to the modelling with use of the PU-system.

controlled generators, this requires implementation of the converter re-start feature in the wind turbine model, **Section 10.4**.

All kinds of wind turbines are equipped with their protective relay systems and therefore may trip at the grid faults. This protective disconnection may occur when uncontrollable voltage decays has been registered in the power grid. Subsequent disconnection of the large wind farm will imply that the solution does not comply with the Specifications of the TSO, independent from the voltage behaviour after the wind farm has tripped.

11.2. Assumptions on power system operation

In all the simulated cases, the total power consumption (at normal operation conditions) is set to approximately 2000 MW. The rated power capacity of the local generation units is 900 MW. When the large wind farm of 150 MW has been taken into account, this corresponds to that the wind turbines and the CHP units can cover more than 50 % of the total power consumption in this large power system.

It is considered that the large wind farm is constructed in the area with excellent wind conditions. Presumably, the large wind farm operates always at rated operation point. This will also give the worst case with respect to maintaining of transient voltage stability of the power system when the solutions leading to disconnection of the large wind farm are not valid (Akhmatov et al., 2000(c)).

It is considered that the power tariffs are favourable and the local CHP units generate so much electric power as possible. Therefore these units are assumed to be at rated operation in all the simulating cases. The controllability of the large power system with respect to reactive power and voltage is performed by the large power plants. However, reduction of power supply from and even switching off the large power plants will be necessary to prevent the power system from over-generation. This will naturally reduce the controllability of the power system. The CHP units do not contribute to dynamic reactive power and voltage control. From this argumentation, the worst case will occur when the CHP units are at rated operation and the power supply from the large power plants is reduced – exactly the operational conditions been assumed for the large power system.

Often it is considered that the wind turbines in on-land sites are at rated operation. Such operational conditions correspond to extremely strong wind that must be around 14 m/s or stronger. The most probable wind in Denmark is around 6 to 10 m/s, depending on the location. This corresponds to around 60 to 70 % of the rated power of the modern wind turbines. Situations where the power generation from the on-land wind turbines exceeds these 70 % will be more seldom.

The wind turbines in local sites may be disconnected by their protective relays at grid disturbances. When the wind turbines are closer to the rated operation, then their operation parameters (the machine current and the speed) are also closer to their respective relay settings. It may be expected that the wind turbines at rated operation are tripped faster from the grid than the wind turbines at lower operational points than the rated operation point. When the wind turbines have tripped, this “eliminates” demands of reactive compensation of the over-speeded wind turbines at the voltage re-establishment process. From this viewpoint, the rated operation is not necessarily the worst case with respect to maintaining of short-term voltage stability. Therefore the study cases

with the power generation in the local wind turbine sites in the range from 60 to 90 % of the rated power have been simulated.

When resuming the operational conditions assumed above, the power generation from the wind turbines and the local CHP units will be in the range from 42.5 to 50 % of the actual power consumption in the large power system.

11.3. Operation of local generation units at grid disturbances

The electric power supplied from the local generation units exceeds significantly the power supplied from the large wind farms assigned to the Specifications of the TSO (Eltra, 2000). The rated power capacity of wind power in the local sites corresponds to approximately *three* large wind farms!

At the grid disturbances, operation of the wind turbines in the local sites can be decided by action of their protective systems. Since the rated power capacity of wind power in the local sites is so large, this will affect operation of the power system, indeed. Therefore accurate and reasonable assumptions on representation and action of the local wind turbine sites are important for reaching meaningful results and conclusions.

11.3.1. Consideration of small power loss

First, it is considered that the large wind farm is commissioned at the node (2) in the weak power system of area 1 with the connection point at the transmission power network at the node (4), **Fig. 11.2**. The large wind farm is with fixed-speed, active-stall wind turbines. The large wind farm is at rated operation and the local wind turbine sites are at 60, 70, 80 or 90 % level, respectively, from case to case.

In simulations, the consideration of small power loss is met by disabling the protective relay models when representing the local wind turbine sites and the CHP units. Such an assumption is commonly applied in investigations of short-term voltage stability for simplification (Bruntt et al, 1999; Akhmatov et al, 2000(b)).

The induction generator data are given in **Appendix 4.A** and the mechanical system data are collected in **Table 11.1**. The mechanical system data that are applied for representation of the local wind turbine sites correspond to the typical data of a Danish medium-sized wind turbine (Akhmatov et al, 2000(a)). Notice that the construction of the wind turbines in the large wind farm is enforced. It is because those are active-stall wind turbines to be operated at sea, e.g. they shall withstand larger mechanical loads. Enforcing the mechanical construction of fixed-speed wind turbines will also contribute to improve short-term voltage stability (Akhmatov et al, 2003(a)).

Decentralised wind turbine sites			Large wind farm		
H_G	H_M	K_S	H_G	H_M	K_S
0.5 s	2.5 s	0.3 PU/el.rad.	0.5 s	4.5 s	0.6 PU/el.rad.

Table 11.1. Data of mechanical construction of wind turbines.

Regarding to the wind turbines in the large wind farm, the active-stall control is (typically) organised with the reference signal $X_{\text{REF}} = P_{\text{REF}}$ and the controlling signal $X = P_E$. According to the argumentation of (Akhmatov, 2001), this will correspond to fixed-pitch operation at the transient event of a short duration in the power system.

The grid disturbance is the 100 ms, three-phased, short-circuit fault in the transmission power network. The fault is *either* subjected to the node (6), which is far from the area 1, *or* to the node (7), which is in the area 1 with strong concentration of local wind turbine sites. When the fault has cleared, the lines connected to the faulted node have tripped. The simulation results are given in **Fig. 11.3**. The following is resumed.

- 1) The worst case with respect to maintaining short-term voltage stability will be present when the local wind turbine sites are at 90 % level, which is the maximal generation level in this investigation.
- 2) With insufficient amount of dynamic reactive compensation, *voltage collapse* will be predicted from investigations of short-term voltage stability.
- 3) To maintain short-term voltage stability, it will be necessary to incorporate two SVC units. The rated capacity of each SVC unit shall be 200 MVar (capacitive). The SVC units shall be incorporated at the node (4) and also at the node (8) where concentration of grid-connected wind power is largest. The SVC model has been applied in **Section 6** and it is according to the description of (Noroozian et al, 2000).
- 4) Another solution can be to incorporate two SC units with 150 MVA rated power capacity of each unit. Again, the SC units shall be located at the node (4) and at the node (8).
- 5) No immediate power reserves are necessary due to *the assumption* on minimal disconnection of the local generation units.
- 6) The worst case occurs when the short-circuit fault occurs at the node (6), but not at the node (7). Although the node (7) is close to concentration of the local wind turbine sites in the weak power system of area 1. The node (6) is electrically far from the local wind turbine sites and in the strong power grid of area 3.

All the conclusions listed up above seem to be trivial, except of the conclusion of item 6. This needs more explanation. The large power plants located in area 3 control reactive power and voltage in the transmission power network. They control also reactive power and voltage in the transmission power network of area 1. When the short-circuit fault occurs at the node (7), the power plants located in area 3 will still contribute to dynamic control of reactive power and to re-establishment of voltage in the whole power system. In other words, the voltage drop in area 1 has a local character and does not affect operation of the large power plants in area 3.

In contrast, the voltage drop will be present throughout the strong power system of area 3 when the short-circuit fault occurs at the node (6). When the fault has cleared, a number of transmission lines around the faulted node (6) are tripped. This contributes also to weak the power system of area 3. The fault is not of local character any longer, but may affect operation of the whole power system and the large power plants in a significant way. Therefore this fault may have more serious consequences for operation of the power system and for the voltage re-establishment process.

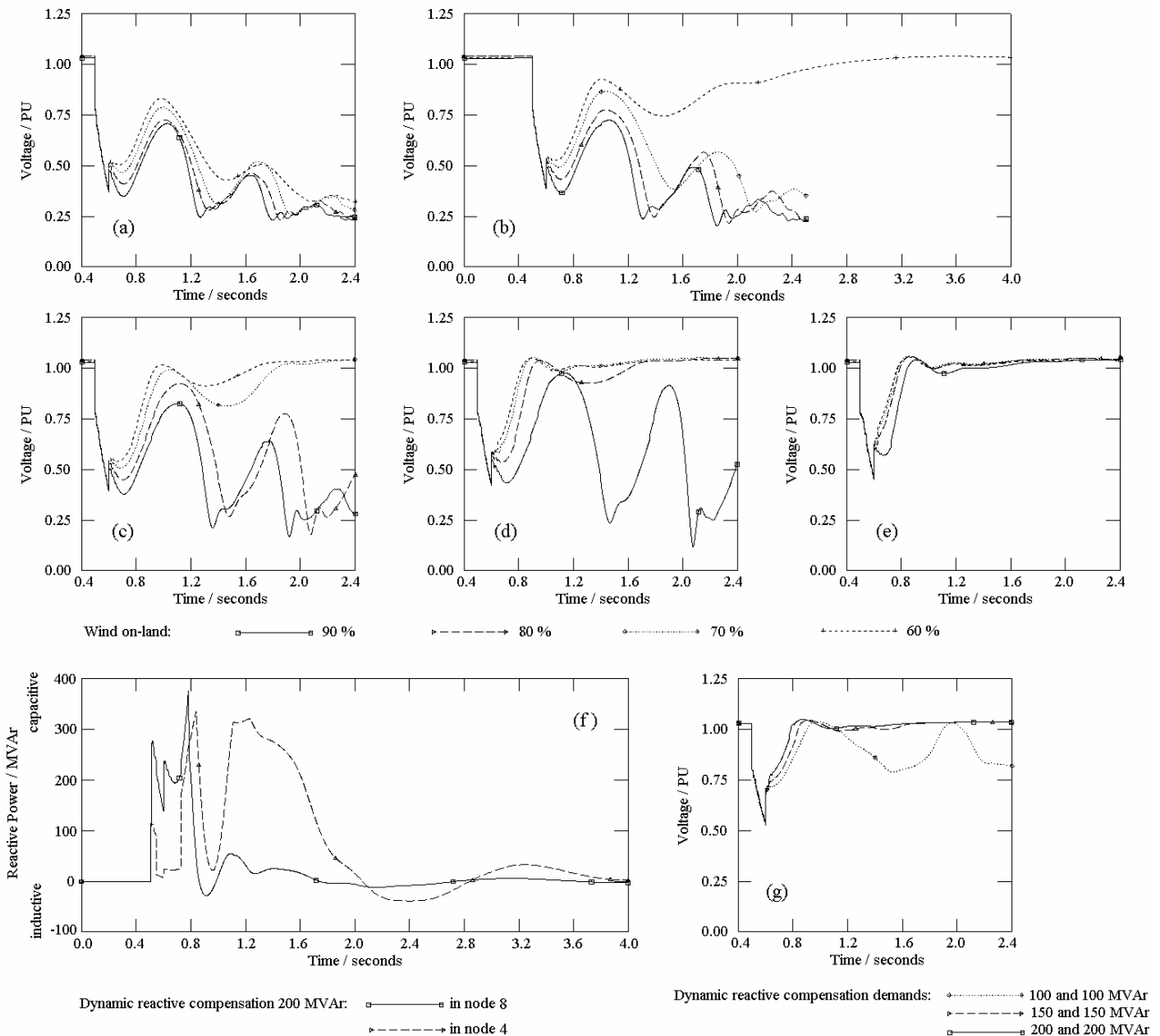


Fig. 11.3. Simulation case when disconnection of local generation units is minimal by disabling the relay models. Simulated curves show voltage at node (2) at different operation conditions in local wind turbine sites. Short-circuit fault occurs at node (6), and capacities of the SVC units are: (a) – none, (b) – 100 MVar in node (4), (c) – 100 MVar both in node (4) and in node (8), (d) – 150 MVar both in node (4) and in node (8), (e) – 200 MVar both in node (4) and in node (8). Operation of SVC units: (f) – with 200 MVar both in node (4) and in node (8), at 90 % wind in and the fault occurs at node (6). Voltage in node (2) at different rated capacities of SVC units both in node (4) and (8): (g) – at 90 % wind and when the fault occurs at node (7).

11.3.2. On risk of mutual oscillations between local wind turbine sites

There is a common concern of a possible risk of mutual oscillations between many local wind turbine sites in the large power system. Such mutual oscillations could be started by a transient event in the power system.

When the wind turbines are with identical parameters of their mechanical constructions, the wind turbines show coherent response to a transient event in the power grid. This implies that the

electrical and the mechanical parameters of different wind turbine sites oscillate together, “in-phase”, but not against each other. A similar conclusion has been reached from simulations made with use of the model of the large wind farm consisting of eighty wind turbines (Akhmatov et al., 2003(a)).

Concerns about a possible risk of mutual oscillations between several wind turbine sites would perhaps relate more to situations where the wind turbines are with different parameters of their mechanical constructions. It is because the natural frequency of such oscillations is the shaft torsional mode (Akhmatov et al., 2000(a)) and the oscillations will be characterised by different natural frequencies at different parameters of the wind turbine constructions.

Therefore a number of simulations are made where the shaft stiffness of the half part of the local wind turbine sites is kept at 0.3 PU/el.rad. In the second half part of the local sites, the shaft stiffness is changed to 0.6 PU/el.rad. The simulation results show that the wind turbines in different local sites show more or less coherent response, e.g. those are oscillating “together” and “in-phase”, see **Fig. 11.4**. No mutual oscillations between the local wind turbine sites with different shaft stiffness are seen. This conclusion is similar to the conclusion reached in (Akhmatov et al., 2003(a)) where the same problem has been investigated in a case of the large offshore wind farm consisting of eighty wind turbines.

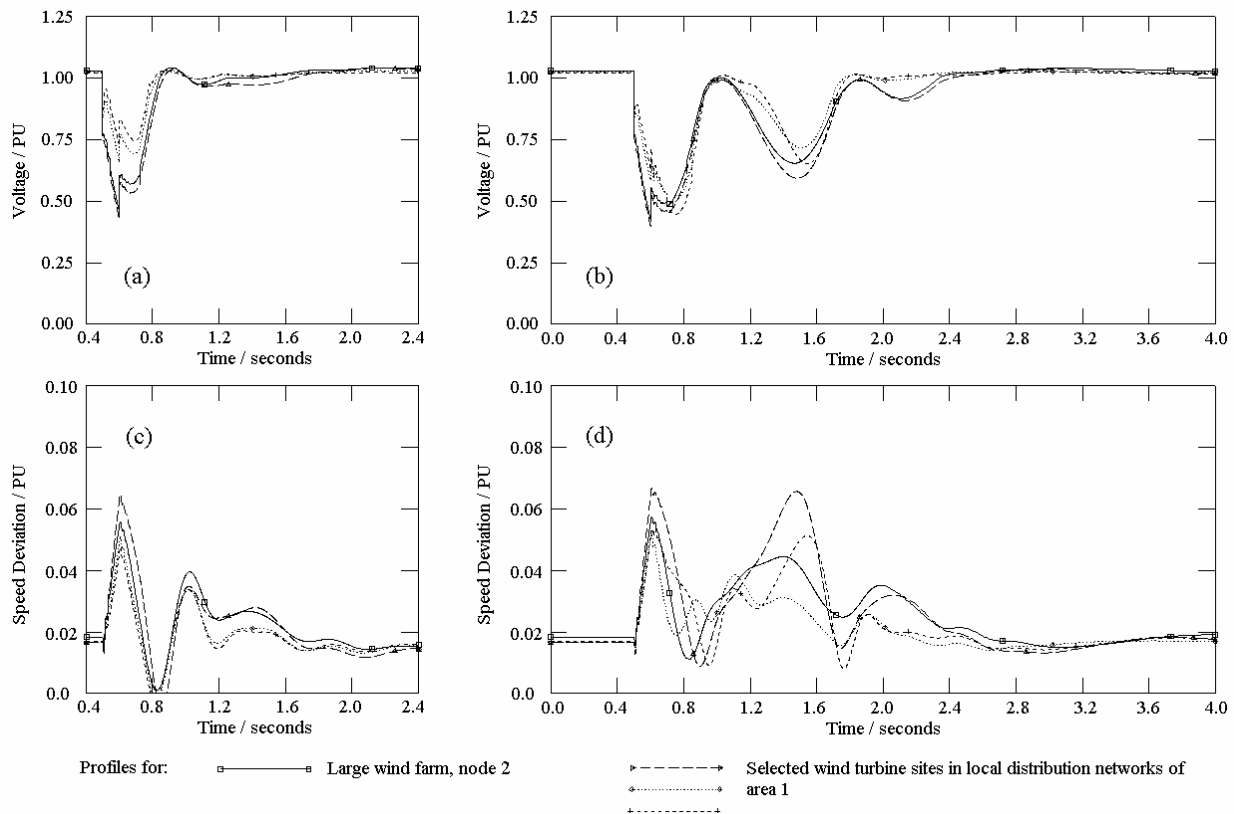


Fig. 11.4. No risk of mutual oscillations between decentralised wind turbine sites (90 % wind) at short-circuit fault at node (6). Voltage in selected wind turbine sites: **(a)** – with identical shaft stiffness $K_S = 0.3$ PU/el.rad. and 200 MVar SVC units in node (4) and in node (8), **(b)** – with different shaft stiffness $K_S = 0.3$ and 0.6 PU/el.rad. and 150 MVar SVC units in node (4) and in node (8). Speed in selected wind turbine sites: **(c)** – with identical shaft stiffness $K_S = 0.3$ PU/el.rad., **(d)** – with different shaft stiffness $K_S = 0.3$ and 0.6 PU/el.rad.

Furthermore, enforcing of the mechanical construction, even in the half part of the local wind turbine sites, has reduced demands of dynamic reactive compensation. In this case, the total reduction of dynamic reactive compensation is 100 MVar. When the shaft stiffness is set to 0.6 PU/el.rad. in all the sites, this leads to improvement of voltage profile at the voltage re-establishing, see **Fig. 11.5**. But it does not lead to further reduction of demands of dynamic reactive compensation, in this particular case.

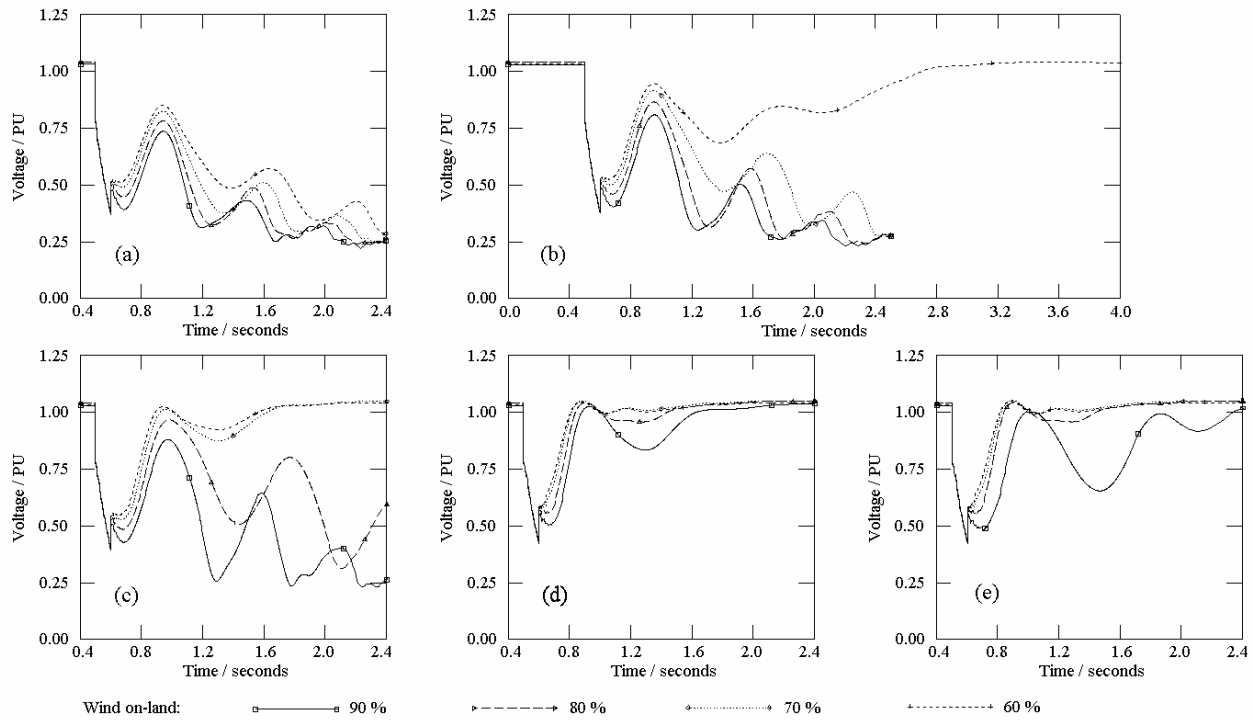


Fig. 11.5. Consideration of minimal trip of decentralised generation sites. Voltage in node (2) at different wind conditions at decentralised wind turbine sites and when the shaft stiffness $K_S = 0.6$ PU/el.rad. The fault occurs at node (6). Capacities of SVC units: (a) – none, (b) – 100 MVar in node (4), (c) – 100 MVar both in node (4) and (8), (d) – 150 MVar both in node (4) and (8), (e) – 150 MVar both in node (4) and (8), but when the shaft stiffness $K_S = 0.3$ and $K_S = 0.6$ PU/el.rad. in the decentralised wind turbine sites.

As can be seen, accuracy of data of the wind turbines is an important issue in investigations of short-term voltage stability. Receiving accurate data of the local wind turbine sites must be taken seriously. But it is not always possible to receive the data for all the local sites. In this case, it can be considered that investigations are carried out with use of estimated, typical data of the local wind turbines. For example, this can be with use of the same data set for all the local wind turbine sites. This is acceptable because no mutual oscillations between the wind turbine sites, independently from their mechanical system data, will be present.

In power system analysis, conservative estimations are often applied to provide a stability margin. When making a conservative estimation, the worst case must be applied in simulations. The worst case will relate to the wind turbine shaft systems having the smallest shaft stiffness'.

11.3.3. Evaluation of disconnection and power loss

Wind turbines (in local sites) and local CHP units are equipped with protective relays. Those protective relays may disconnect the local generation units at abnormal operation of the power system. It will depend on (i) the relay settings and (ii) the operation conditions of the local generation unit and the power grid itself whether this unit disconnects or maintains uninterrupted operation.

In the following simulations, the relay models of all the local generation units are enabled. The relay settings of wind turbines are in accordance with data of the wind turbine manufacturers and recommendations of the company NESAs (Akhmatov et al, 2001). The relay settings of CHP units are according to the Danish recommendations (KR-88). The relay models disconnect the respective generation units automatically when the relay settings have been exceeded. At the start of dynamic simulations, it is rather not to say how many units will disconnect.

The mechanical data of the wind turbines are as in **Table 11.1**. The power loss caused by protective disconnection of the local generation units is collected in **Table 11.2**. The simulated curves achieved with enabled relay models of the local generation units are shown in **Fig. 11.6**. When analysing the results of this investigation, the following conclusions have been made.

- 1) It can be problematical to define the worst case with respect to maintaining of short-term voltage stability. In all the simulation cases with different power generation levels in the local wind turbine sites, the voltage recovery rates seem to be similar. But in the cases with strong wind in the local wind turbine sites, a stronger tendency to voltage oscillations and instability there is seen than in the cases with 60 % wind.
- 2) Risk of voltage collapse is minimal, but there can be a risk of *over-voltage* due to sudden disconnection of many wind turbines in the local sites in the periphery of the transmission power network.
- 3) Function of dynamic reactive compensation has changed its character. It must be capacitive during re-establishment of voltage just after the fault has cleared⁴⁹. But it must be inductive

⁴⁹ The target is to get voltage recovery without any subsequent tripping of the large wind farm. Notify that there are two conditions in this formulation made by the Danish TSO (Eltra, 2000). Incorporation of dynamic reactive compensation of +100 MVar might look to be in contrast with the conclusion about a minimal risk of voltage collapse because this dynamic capacitive compensation is exactly applied to get voltage to recover after the grid fault has cleared. When no dynamic capacitive compensation is applied, the simulations predict voltage instability characterised by rapid voltage decay. In this situation, the large wind farm will disconnect and the voltage recovers. We do not get voltage collapse in this power system, but the solution does not comply with the Specifications of the Danish TSO because the large wind farm trips (Eltra, 2000). Notify that uncontrollable voltage decay in such simulated situations does not necessarily imply that the outcome of the grid fault will be voltage collapse. Such voltage decays will most probable lead to trip of the large wind farm. What happens with the voltage after the large wind farm has tripped depends on the factual operation situation and the power grid itself; in the case of the present power system, voltage recovers when the wind farm trips.

later to absorb an immediate surplus of reactive power coming from tripped wind turbines. This is necessary to prevent possible risk of over-voltage.

- 4) For getting voltage re-establishment within the pre-defined voltage band, is necessary to incorporate at least one SVC unit of ± 100 MVar either in node (4) or in node (8). The same goal can be achieved with use of an SC of the same rated power capacity located in the same nodes.
- 5) *Power loss* caused by tripping of the local generation units may be significant. In this particular case, immediate power reserves in the range from 83 up to 719 MW can be demanded, depending on the pre-fault operation situation. This amount of immediate power reserves corresponds to approximately one-third of the total power consumption in the large power system. The worst case with respect to power loss occurs at *co-incidence* of strong wind and a short-circuit fault occurring at the node (6). At moderate wind, the power loss is much less and mainly caused by protective disconnection of many local CHP units.
 - a. Notify that such co-incident events are very seldom in the Danish power system. In the most time, the operation conditions of the local wind turbine sites are characterised by moderate wind. This implies that even in the case of a serious transient disturbance in the transmission power network, the power loss can be relatively small.
 - b. Notice that three-phased short-circuit faults in the transmission power network are very seldom events. Mostly, we have single-phased or two-phased short-circuits in the transmission lines (touching of two phases in wind, accidents with birds etc.). Such events do not cause a significant voltage drop in the faulted node as this would occur at the three-phased fault.
 - c. Typically, local disconnection of a less number of local wind turbines can be registered at single- or two-phased faults in the grid. The co-incidence of the strong wind and serious, three-phased short-circuit faults is very seldom and represents the absolute worst case scenario with respect to transient voltage stability and power loss.
- 6) The worst case, which is characterised by amount of tripped power, is again reached when the fault occurs in the node (6), e.g. in the strong power system of area 1, but not when the fault occurs in the node (7), e.g. the weak power system of area 3 with the main concentration of wind power.
- 7) Enforcing the mechanical construction of wind turbines in some of or in all the local wind turbine sites, in this case this implies increasing the shaft stiffness $K_S = 0.6$ PU/el.rad., results in improving the voltage profile at recovering process. But it does neither reduce demands of dynamic reactive compensation nor power loss in this particular case. (Not shown in plots).

In **Section 11.3.1** it is found that it should be incorporated two 200 MVar SVC units on the assumption of minimal tripping of the local generation units and minimal power loss. In the following, the consequence of incorporation of such two SVC units has been evaluated, but with enabled relay models of the local generation units. As can be seen from the simulated curves in **Fig. 11.6**, the voltage profiles have improved when more dynamic capacitive reactive compensation has been applied.

Power loss will still be present, but of a less amount. Namely, it will be up to 556 MW, which corresponds to 27 % of the total power consumption in the large power system. This power loss is again for the worst case present at co-incidence of strong wind and a serious grid disturbance.

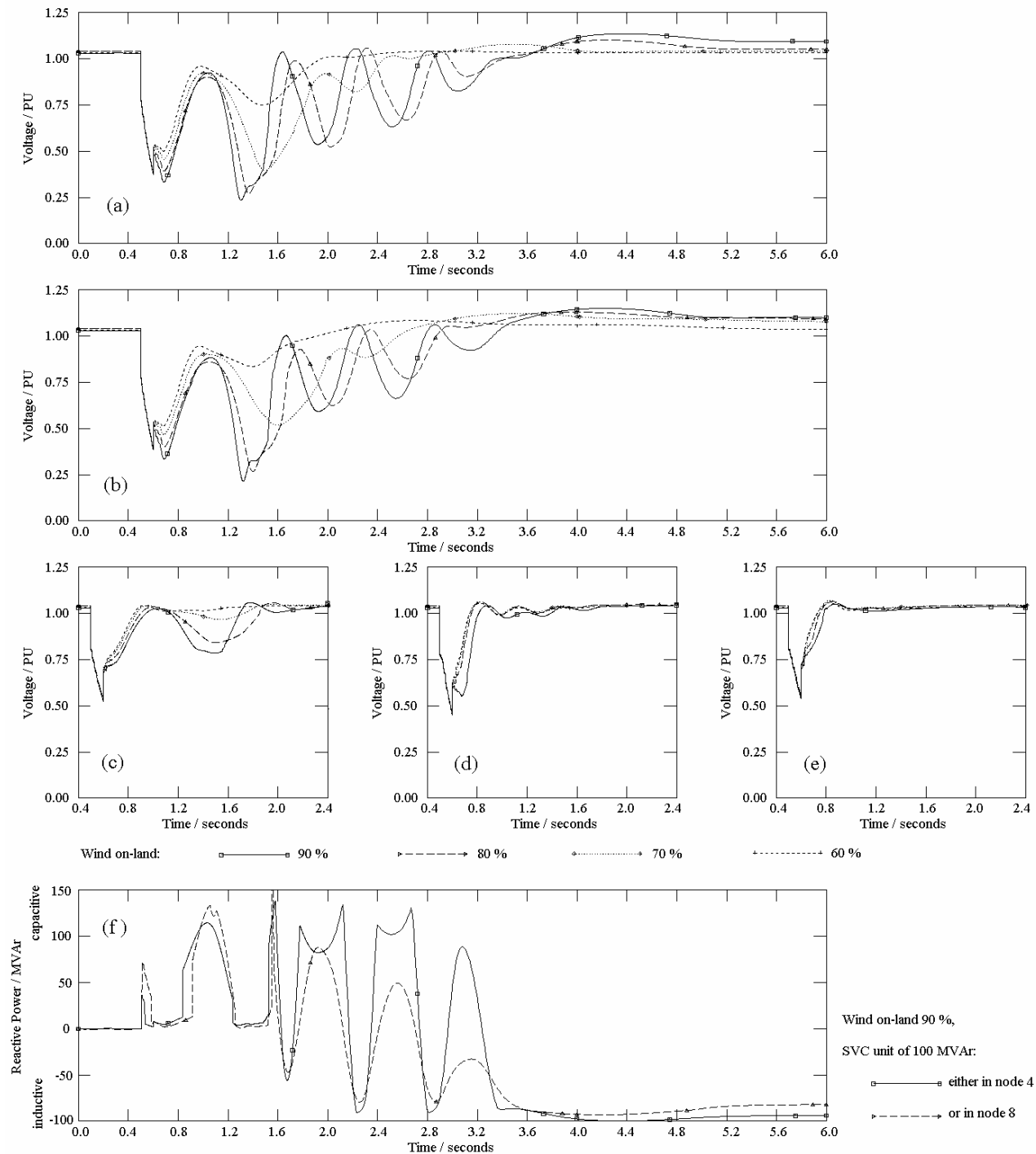


Fig. 11.6. Simulation results with protective tripping of local generation units by their relays at different generation levels of local wind turbine sites. Voltage in node (2): (a) – when 100 MVar SVC unit is established in node (4) and the fault in node (6), (b) – with 100 MVar SVC unit established in node (8) and the fault in node (6), (c) – with 100 MVar SVC unit in node (4) and the fault in node (7), (d) – with 200 MVar SVC units both in node (4) and in node (8) and the fault in node (6) and (e) – the same but the fault is in node (7). Function of SVC unit of ± 100 MVar established either in node (4) or in node (8): (f) – response to the fault in node (6).

The counts for power loss are summarised in **Table 11.3**. Incorporation of immediate power reserves may still be necessary to cover the worst case situations, though large SVC units (capacitive) are applied. This outcome would be overseen when possible protective tripping of the local generation units is disregarded.

Faulted node	Wind in decentralised sites, %	Trip of CHP, MW	Trip of wind turbine sites, MW
6	60	326	0
	70	326	238
	80	326	375
	90	326	393
7	60	83	0
	70	83	0
	80	83	143
	90	83	240

Table 11.2. Power loss due to trip of local generation units, dynamic reactive compensation is an ± 100 MVar SVC unit in node (4).

Faulted node	Wind in decentralised sites, %	Trip of CHP, MW	Trip of wind turbine sites, MW
6	60	326	0
	70	326	5
	80	326	11
	90	326	230
7	60	81	56
	70	81	121
	80	83	138
	90	83	156

Table 11.3. Power loss due to trip of local generation units, dynamic reactive compensation is 200 MVar SVC units both in node (4) and in node (8).

Incorporation of large dynamic reactive compensation units does not necessarily prevent tripping of many local generation units and significant power loss in the worst case situations. For minimisation of such power loss with incorporation of a significant amount of dynamic reactive compensation, the relay settings of the local generation units must also be adjusted (Akhmatov et al, 2001).

11.3.4. Preventing grid from possible risk of over-voltage

There can be a possible risk of over-voltage due to such sudden tripping of many wind turbines in the local sites in the periphery of the transmission power network. Such sudden tripping may produce immediate and significant surplus of reactive power in the large power system. In this

particular case, this problem is observed and solved with use of a combined SVC unit, which contains capacitive and inductive sub-units.

Dynamic reactive power control of large power plants can be very useful to prevent the power grid from over-voltage. This control of the large power plants was not sufficient in this particular case, which is why the inductive SVC sub-unit of –100 MVar is applied. Keep in mind that the reactive power is produced and absorbed locally. It is not desirable to transmit reactive power throughout the power system (this may demand large voltage gradients throughout the transmission power network). The large power plants control reactive power and voltage in areas 2 and 3. But this control does not seem to be sufficient at the periphery of the transmission power network in area 1. This fact may explain why incorporation of the inductive SVC sub-unit in area 1 has been needed.

Automatic tripping of the shunt capacitors and switching-on of the shunt reactors in the power network of area 1 when registering over-voltage in the (local distribution) networks will also contribute to minimise a possible risk of over-voltage in area 1. This solution should be combined with use of continuous control performed by the SVC. In (Taylor, 1994) it is mentioned that the SVC control system can order the shunt capacitors and reactors located in the vicinity of the SVC.

If over-voltage has occurred and distributed throughout the power network of area 1, power loss would be larger because of a risk that more local generation units would trip, but this time the tripping would be by over-voltage⁵⁰.

11.3.5. Resume

It becomes clear that impact from local generation units at the grid faults to the power system operation may be decided by action of their protective systems. Accurate modelling of the local generation units and of their relay models is important in investigations of short-term voltage stability of power systems with a large amount of local power generation.

Normally, the main concern of investigations of short-term voltage stability has been a risk of voltage collapse (Bruntt et al, 1999). The risk of voltage collapse is commonly connected with increased demands of dynamic reactive power (capacitive) of the induction generators after the fault has cleared, when such dynamic reactive control cannot be met by the power system or the large power plants (Bruntt et al, 1999). Such common conclusions of a possible risk of voltage collapse have been reached on the assumption that the local wind turbines do not trip at uncontrollable voltage decay in the power grid. In such investigations, the wind turbine relay models were always disregarded due to the assumption of minimal power loss. This common assumption has however been in contrast to the other assumption of such investigations: the power loss due to the wind turbine tripping is minimal when the operation point is around 60 % of their rated operation, whereas the investigations have always been carried out at the rated operation of the wind turbines.

⁵⁰ In simulations, such developed over-voltage could start an avalanche-like process where more disconnection of the local wind turbines and increasing over-voltage were following each other (but only till an upper limit of the voltage which could be reached in this power network). But we do not believe that we would observe such an operation situation in a realistic power network because other protective equipment (for example, reactors) would interfere and minimise such a risk of over-voltage.

When the protective relay models are regarded, other results can be reached. A possible risk of voltage collapse caused by a lack of dynamic control of reactive power and voltage is not the major concern. This is because the local wind turbine sites trip when abnormal operation has been registered. Uncontrollable voltage decay can be among triggering mechanisms which get the local wind turbines to trip. This tripping “eliminates” problems dealing with a lack of dynamic reactive power compensation in the power system. Therefore there will not be any risk that uncontrollable voltage decays reaches to develop to voltage collapse. When a sufficient number of wind turbines have disconnected, the voltage will presumably re-establish.

On the other hand, the major concern of the power system stability can be power loss due to protective disconnection of local wind turbine sites and local CHP units. When this disconnection has a significant character, this will lead to demands of immediate power reserves. In the most operation situations, the power loss will be of a minor character, whereas the power loss may be of a significant character when the wind turbines operate close to their rated operation points. Incorporation of dynamic reactive compensation such as SVC, Statcom and SC will, indeed, improve the voltage profile when the voltage is re-establishing after the grid fault has cleared. But such (expensive) arrangements in the grid do not necessarily reduce power loss in a significant way.

Second, among the concerns on the power system stability there is a possible risk of over-voltage in the periphery of the transmission system networks. This result is firstly presented in this report. This over-voltage risk is present because disconnection of many wind turbines equipped with induction generators may lead to immediate and significant surplus of reactive power. When such reactive power surplus is present in the periphery of the transmission power network, dynamic control of reactive power performed by the large power plants is not always sufficient to absorb this reactive power surplus. This situation can be when the large power plants are electrically far from the periphery of the transmission power network, which is the source of the problem. In such situations, incorporation of dynamic reactive compensation (inductive) can be required in the periphery of the transmission power networks or in the distribution networks⁵¹.

11.4. Access to strong power grid

As explained above, incorporation of large (offshore) wind farms into the power networks is often present at the periphery of the transmission power networks. Therefore investigations of short-term voltage stability correspond to an almost classical problem formulation when the large wind farm is

⁵¹ Discussion: Let us estimate the requirements on inductive reactive compensation caused by a significant trip of the local wind turbines. There are 500 MW rated power in the wind turbine sites and these wind turbines are no-load compensated. As a rule of a thumb, we may say that the induction generators absorb 250 MVAR (a half of the rated power capacity installed) where the no-load capacitors supply 125 MVAR (one-fourth of the rated power capacity) and the other 125 MVAR are absorbed from the entire network. The induction generators trip with their no-load capacitors. If all the wind turbines have been at rated operation and all the wind turbines have tripped at the grid fault, there will be a reactive power surplus of 125 MVAR. This should be the maximal rated power capacity of inductive compensation to prevent a risk of over-voltage in the power network. Notice that in simulations, we should apply the compensation unit with -100 MVAR to prevent the grid from over-voltage, which is close to this roughly estimated value. Notice also that the short-circuit capacity of the network should be taken into account to evaluate this value and this impact on the power system.

incorporated into a weak power grid. In some situations, it can be possible to access relatively strong power networks to connect the large wind farm. In case of the electric power network shown in **Fig. 11.2**, there are chosen two possible connection points whereat the large wind farm can be connected to the transmission power network.

- 1) The first possible connection point is at the node (4) in the weak power system of area 1. This possible connection point is at the periphery of the transmission power network and separated from the strong power grid by the long tie (1) – the bottleneck.
- 2) The second possible connection point is at the node (5) in the relatively strong power system of area 2. The power network of area 2 is a meshed, transmission power system accessing the large power plants of area 3.

A connection point with an access to strong power networks can be difficult to find because the large wind farms are often constructed in rural areas. Usually, the power networks are not much developed in such rural areas. Therefore the majority of situations with grid-incorporation of the large (offshore) wind farms will be similar to the case of item 1 – grid-connection to a weak power network.

In a minor number of cases, it will be possible to access the relatively strong power grid, which corresponds to item 2. For example, a connection point in a strong power network can be accessed in situations where the large wind farm is commissioned offshore not far from the urban areas and so the developed transmission power networks on-land. In such situations, the large offshore wind farm is connected at the node in the strong power system on-land via the sea /underground cable.

The following presentation will demonstrate importance of accessing a connection point in the strong power grid. The presentation is given for the two wind turbine concepts, which are the most common in Denmark.

- 1) Fixed-speed, active-stall wind turbines equipped with induction generators.
- 2) Variable-speed, pitch-controlled wind turbines equipped with DFIG and partial-load frequency converters.

The large wind farms must comply with the Specifications of the Danish TSO (Eltra, 2000). This compliance with the Specifications has been reflected in the modelling work relating to the large wind farms – complexity of the wind turbine models and the control feature representations. The presentation will also show how operation of a large amount of local wind power may affect operation of the large wind farm and its control.

11.4.1. Large wind farm with fixed-speed wind turbines

First, it is considered that the large wind farm is located at the node (2) and connected at the node (4) in the weak power system of area 1, **Fig. 11.2**. This location and the connection point have been proposed due to excellent wind conditions of area 1, respectively, because this connection point is the closest node of the transmission power network of area 1 to the wind farm terminals.

Investigations of short-term voltage stability have made when the short-circuit fault occurs at the node (6) in the strong power system – the worst transient event. As it has been explained in **Section 11.3.3**, incorporation of at least ± 100 MVar dynamic reactive compensation (the SVC unit) will be necessary to comply with the Specifications (voltage recovery without subsequent trip of the large wind farm) and to prevent the power grid from over-voltage in the post-fault operation. Such demands of dynamic reactive compensation are found necessary when the fixed-speed wind turbines operate fixed-pitched at the grid fault. The voltage re-establishment must be reached by the efforts of the power system.

Notice also that the voltage profiles are slightly improved when the SVC unit is incorporated at the node (8), instead at the node (4). In other words, incorporation of dynamic reactive compensation is preferred in the area with the major concentration of the local wind turbine sites rather than at the connection point of the large wind farm. This indicates that the main problem with maintaining of short-term voltage stability should rather be connected with these local sites than with the large wind farm. This conclusion is not unexpected.

- 1) The total rated power of the wind turbines in the local sites corresponds to approximately three large wind farms.
- 2) The local wind turbine sites do not trip immediately at the moment when the fault has occurred. The majority of the wind turbines are still in operation in one second or so after the fault has cleared. During this operation, their induction generators absorb a large amount of reactive power and slower voltage recovery. They start first to disconnect when the voltage has exceeded the under-voltage relay settings.
- 3) The local wind turbine sites are modelled with lighter turbines and softer shaft systems than those in the large wind farm, **Table 11.1**. Therefore they over-speed more and faster than those in the large wind farm, whereas excessive over-speeding may cause voltage instability and initiate uncontrollable voltage decay in the grid (Akhmatov et al, 2003(a)).

11.4.1.1. Use of power ramp

Investigations of (Akhmatov, 2001; Akhmatov et al, 2003(a)) have shown that operation of the large wind farms can be stabilised with use of power ramp at transient events in the power system. Power ramp is achieved with application of the active-stall control for temporarily reduction of the mechanical power of the wind turbines. This control must act at the transient events in the power system. The target of application of the power ramp is to prevent fatal over-speeding of fixed-speed wind turbines. Ability of the power ramp to stabilise the large wind farm is demonstrated in **Section 6.12**, where the post-fault operation of a large wind farm with eighty fixed-speed wind turbines has been examined.

In this investigation, the power ramp has been applied to stabilise the large wind farm commissioned at the node (2) of the power network. This case differs from that described in **Section 6.12** due to presence of impact from the large power system. This impact is characterised by presence of several factors which can influence operation of the large wind farm and its control.

Consider that the signal to activate that power ramp is given 200 ms after the grid fault has occurred at the node (6). The regular control system of active-stall is disabled. The reference angle of active-stall, β_{REF} , is set to the value β_{ORDR} , **Section 3**. This corresponds to the blade-angle position where the operation point of the large wind farm is 20 % of the rated power at the given wind. Notice that the faulting time is 100 ms. This implies that the activation of the power ramp occurs shortly after the fault has cleared. The pitch rate, $d\beta/dt$ is in the range of ± 5 °/s corresponding to the pitch rates at normal operation of the wind farm.

When the voltage has re-established, the power ramp mode is cancelled. The regular control system of active-stall has again re-started. This occurs 3 sec. after the power ramp has been activated. **Fig. 11.7** shows the simulated curves with use of the power ramp. As can be seen, the voltage has recovered with use of power ramp and dynamic reactive compensation (capacitive) will not be necessary in this case.

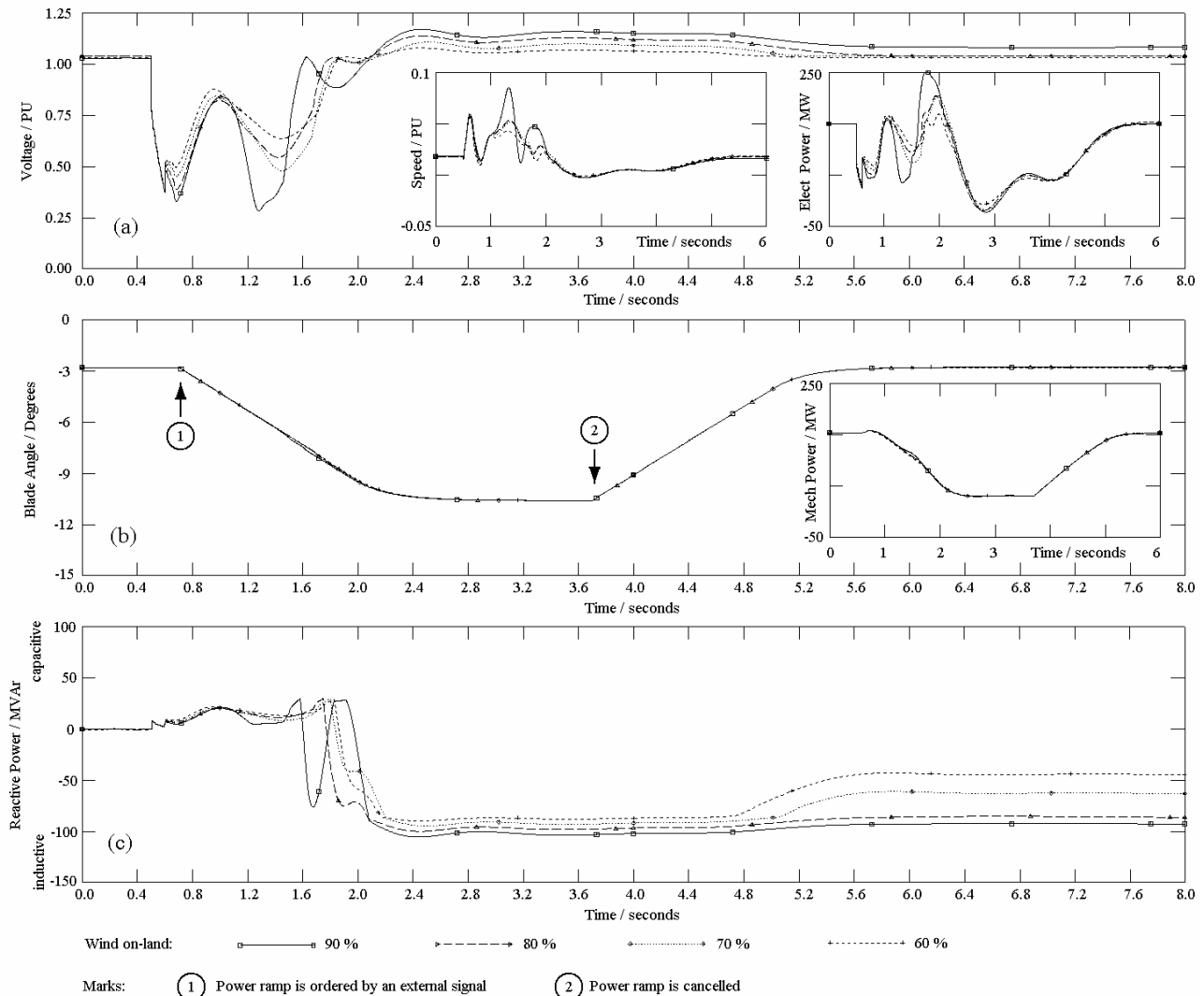


Fig. 11.7. Use of power ramp when the grid fault occurs at node (6): (a) – voltage in node (2), generator rotor speed of the large wind farm (insertion) and electric power of the farm (insertion), (b) – blade angle at power ramp and mechanical power of the large wind farm (insertion), (c) – reactive power of SVC unit in the node (4).

Again, a significant amount of local generation units will be disconnected when the local wind turbines are close to their rated operation. Power loss due to tripping of local wind turbine sites and local CHP units is of a similar value as in the previous case. First, this indicates necessity of immediate power reserves when the wind in on-land sites is strong. Second, significant surplus of reactive power may occur, which produce over-voltage in the periphery of the transmission power network. To prevent the power grid from a possible risk of over-voltage, incorporation of reactive compensation (inductive) will be required. This can be achieved with establishment of the -100 MVar either in the node (4) or in the node (8) of the weak power system of area 1.

Notice that voltage recovers slower in the case with 70 % wind in the local sites than in the case with 80 %. This is because the wind turbines, when operating at 80 % of their rated operational points, disconnect faster than those operating at 70 %. Slower disconnection leads to larger absorption of reactive power during the post-fault operation. This relation is mentioned to illustrate importance of accurate considerations about the operation points and the protective relays of many local wind turbine sites.

11.4.1.2. Case of strong power system

Now it is considered that the large (offshore) wind farm is connected at the node (5) in the relatively strong power system of area 2. The wind farm is at rated operation (150 MW) and reactive-neutral with the transmission power network at the connection point.

The short-circuit fault has applied to the node (6) in the strong power network of area 3. The wind turbines operate fixed-pitched at the grid fault. **Fig. 11.8** shows the simulated curves from this simulation case. As can be seen, voltage has re-established without use of dynamic reactive compensation (capacitive). It is because the power grid is sufficiently strong. Use of power ramp is not necessary for voltage recovery at the grid faults, either.

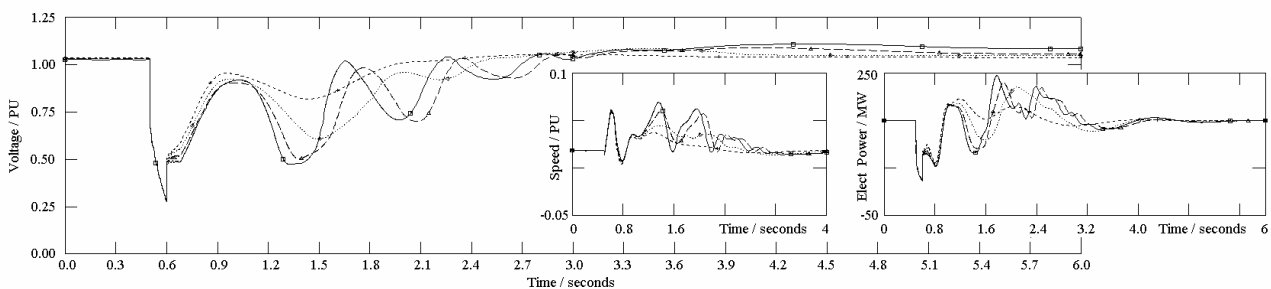


Fig. 11.8. Simulation case with large wind farm connected at node (3) in strong power network of area 2 and wind from 60 % to 90 % in local sites. Voltage profile when the fault occurs at node (6). Insertions: generator rotor speed and electric power of the large wind farm. Voltage re-establishes without use of dynamic reactive compensation (capacitive) or other control features.

Again, protective disconnection of many local generation units may occur as the result of the grid disturbance. Establishing of (i) immediate power reserves to cover power loss and (ii) reactive compensation (inductive) in the weak power network of area 1 to prevent this network from a risk of over-voltage will be necessary. These requirements are needed at strong wind in on-land sites.

11.4.2. Large wind farm with variable-speed wind turbines

Consider that the large wind farm is grid-connected at node (5) of the relatively strong power network of area 2. The large wind farm is with variable-speed, pitch-controlled wind turbines equipped with DFIG and partial-load frequency converters. The dynamic model of such wind turbines is described in **Section 10**.

The converter system model includes representations of the rotor converter and the grid-side converter with the dc-link in between. This converter system representation is necessary according to explanations of **Section 10** and (Akhmatov, 2003(a)). The blocking and re-start sequences of the partial-load converter are according to **Section 10.4** and (Akhmatov, 2003(b)).

The fixed-speed wind turbines in the decentralised sites are at 90 % of rated operation. The short-circuit fault occurs at the node (6) in the strong power system of area 3, which gives the worst fault event. **Fig. 11.9** shows the simulated curves with relation to the large wind farm operation. Keep in mind that operation of the variable-speed wind turbines at transient events is decided by their converter action.

The fault has occurred at the time $t = T_1$ and resulted in a large voltage drop at the wind farm terminals. At the time $t = T_2$, the rotor current transients have exceeded the relay settings by over-current, which is why the rotor converter has blocked. The IGBT of the rotor converter stop switching and the rotor circuit is closed through an external resistor (Akhmatov, 2003(b)). The short-circuit fault has cleared at time $t = T_3$. At the time $t = T_4$ the rotor current transients are sufficiently dissipated in the external resistor. Here the rotor converter synchronisation starts (Akhmatov, 2003(b)). Synchronisation has completed at the time $t = T_5$.

During operation with the rotor converter blocked and also at synchronisation, the grid-side converter contributes to dynamic reactive power control. As can be seen, this dynamic reactive control with use of the grid-side converter contributes to (i) faster voltage re-establishment and (ii) more successful re-start of the rotor converter (reducing the current transients at re-start).

First, the rotor converter control loop of the reactive power has re-started. At this moment, the dynamic control of reactive power and voltage with use of the grid-side converter is disabled. The DFIG is more efficient to control reactive power and voltage than the grid-side converter because its power capacity is larger than that of the grid-side converter.

At the time $t = T_6$, the rotor converter control loop of the electric power has re-started. The control loops re-start is replaced in time to reduce risk of excessive current transients (Akhmatov, 2003(b)). Such excessive transients could occur in the rotor circuit and cause that the rotor converter would again block at the moment of re-start⁵².

When the large wind farm is with variable-speed wind turbines and incorporated into the strong power system of area 2, the following is concluded.

⁵² Discussion: at the public presentation, a soft converter restart has been discussed. In terms of the soft restart discussed, the electric power could be ramped up by the converter control. Probably, such soft restart would minimise the current (transients) at the converter restart. This feature is not described in this thesis. In this work, the electric power is increased through a simple Laplace filter at the converter restart, which is more or less similar to the soft restart with power ramp. Exact converter design is not a part of this project.

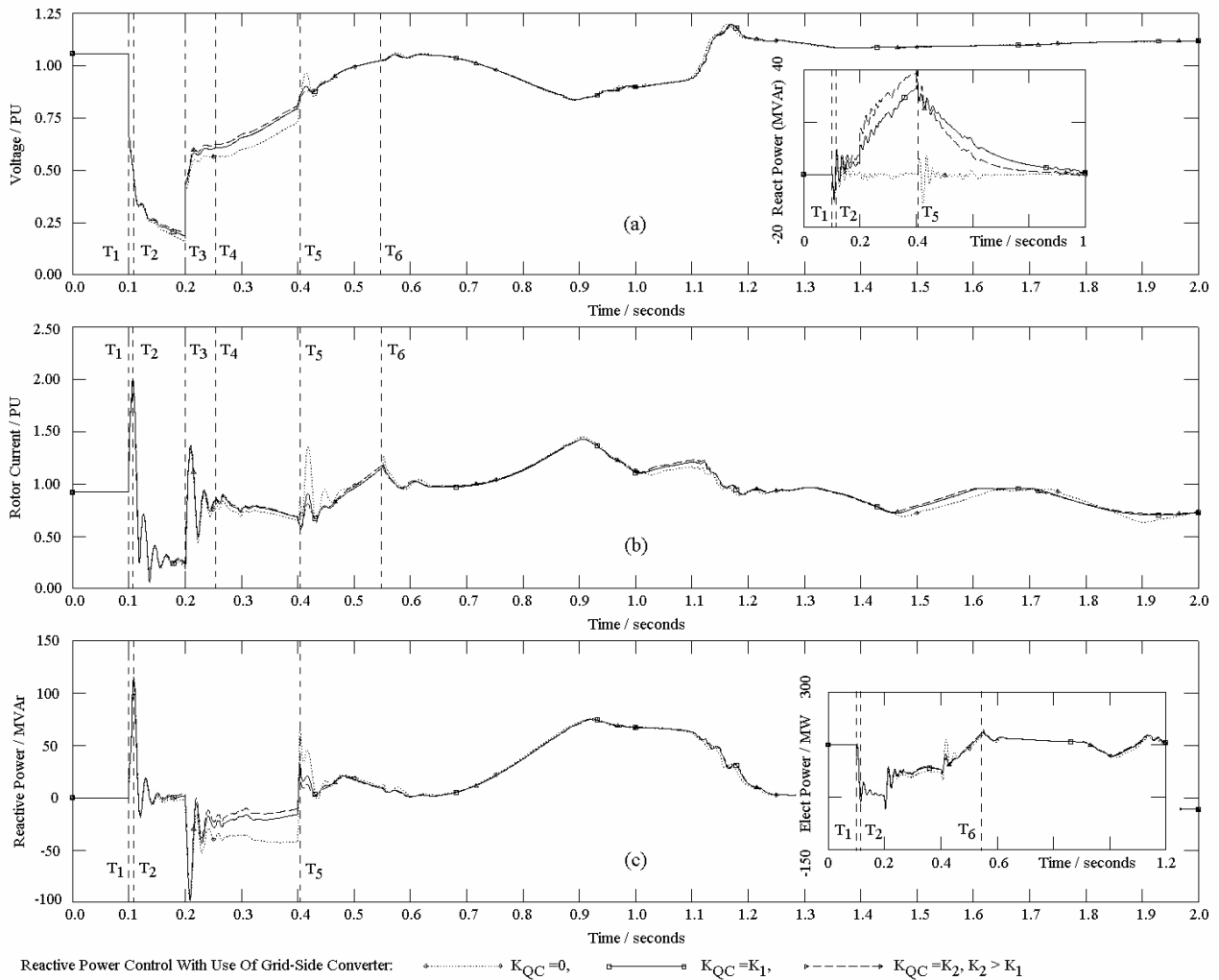


Fig. 11.9 Simulation results for the large wind farm with a connection point at the node (5) in the strong power network of area 2: **(a)** – terminal voltage at node (3) at different controllability of grid-side converter, reactive power of grid-side converter (insertion), **(b)** – rotor current with marked converter sequences, **(c)** – reactive power of DFIG and its electric power (insertion).

- 1) The rotor converter will block at the grid fault and fast re-start after the fault has cleared. Primarily, the rotor converter blocks because a significant voltage drop occurs at the short-circuit fault in the grid and initiates excessive current transients in the DFIG.
- 2) The grid-side converter is applied to dynamic control of reactive power and voltage in the vicinity of the wind turbine terminals, when the rotor converter has blocked or at synchronisation.
- 3) Investigations have also been made when the fixed-speed wind turbines in the local sites are at 60 % to 80 % of the rated operation. In all the investigated cases, fast re-start of the rotor converter has been successful. In other words, operation conditions of the local wind turbine sites do not affect the converter actions of the variable-speed wind turbines in the large wind farm.
- 4) Again, significant power loss may occur as the result of disconnection of the local generation units at the grid fault. This occurs at strong wind in on-land sites. Incorporation of reactive

compensation (inductive) into the weak power network of area 1 can be necessary to prevent this power network from a possible risk of over-voltage.

- 5) Incorporation of this inductive compensation in the power network of area 1 is necessary because the dynamic control of reactive power performed by the large wind farm (with use of the frequency converters) will perhaps not be efficient. This is because the large wind farm feeds into the strong power network of area 2, whereas the problems with over-voltage are seen in area 1. The control and the problem to be fixed are displaced through a distance. Keep in mind that reactive power must be generated and absorbed locally. Transport of reactive power over long distances is not convenient because this would require large voltage gradients in the transmission power network.

11.4.2.1. Incorporation into weak power systems

The large wind farm with variable-speed wind turbines equipped with DFIG and partial-load frequency converters is commissioned at the node (2) of the weak power network of area 1. Its connection point at the node (4) is surrounded with many local sites with fixed-speed wind turbines.

First, consider that the fixed-speed wind turbines in the local sites are at 90 % of rated operation. The short-circuit fault occurs at the node (6) of the strong power network of area 3, at the time $t = T_1$. This is the worst transient event in the power grid. **Fig. 11.10** shows the simulated curves with relation to the large wind farm operation.

The rotor converter blocks at the time $t = T_2$ due to excessive current transients in the rotor circuit. Also in this case, the rotor converter blocks with closing of the rotor circuit through an external resistor. Shortly after the external resistor has been taken in operation, the rotor current transients are efficiently damped on this external resistor. But the rotor converter synchronisation and re-starting wait for complete re-establishment of voltage and frequency in the transmission power network. This waiting time is of a few sec. and introduced in this case to perform successful re-start of the converter *at the first try*.

During operation with the rotor converter blocked:

- 1) The grid-side converter is set to contribute to dynamic reactive power and voltage control.
- 2) When the rotor circuit has closed, the generator operates as an over-speeded asynchronous generator. The generator absorbs a large amount of reactive power and, in this way, contributes to prevent the grid from a possible risk of over-voltage. Notice that this operation is not the most efficient way to prevent such over-voltage.
- 3) The pitch control prevents excessive over-speeding of the large wind farm and, in this way, contributes to stabilisation of the wind farm operation at the post-fault operation (Akhmatov, 2001).

At the time $t = T_3$, the rotor converter has synchronised and, at the time $t = T_4$, the rotor converter has re-started. After the rotor converter has re-started, it contributes to dynamic control of reactive power and voltage in the weak power network of area 1. The DFIG absorbs an amount of reactive

power and contributes to preventing of over-voltage. Further incorporation of dynamic reactive compensation (inductive) does not seem to be necessary.

Again, significant power loss may occur due to protective disconnection of many local generation units since the wind is strong in on-land sites (90 % operation). Therefore establishing of immediate power reserves may be requested in such operation situations.

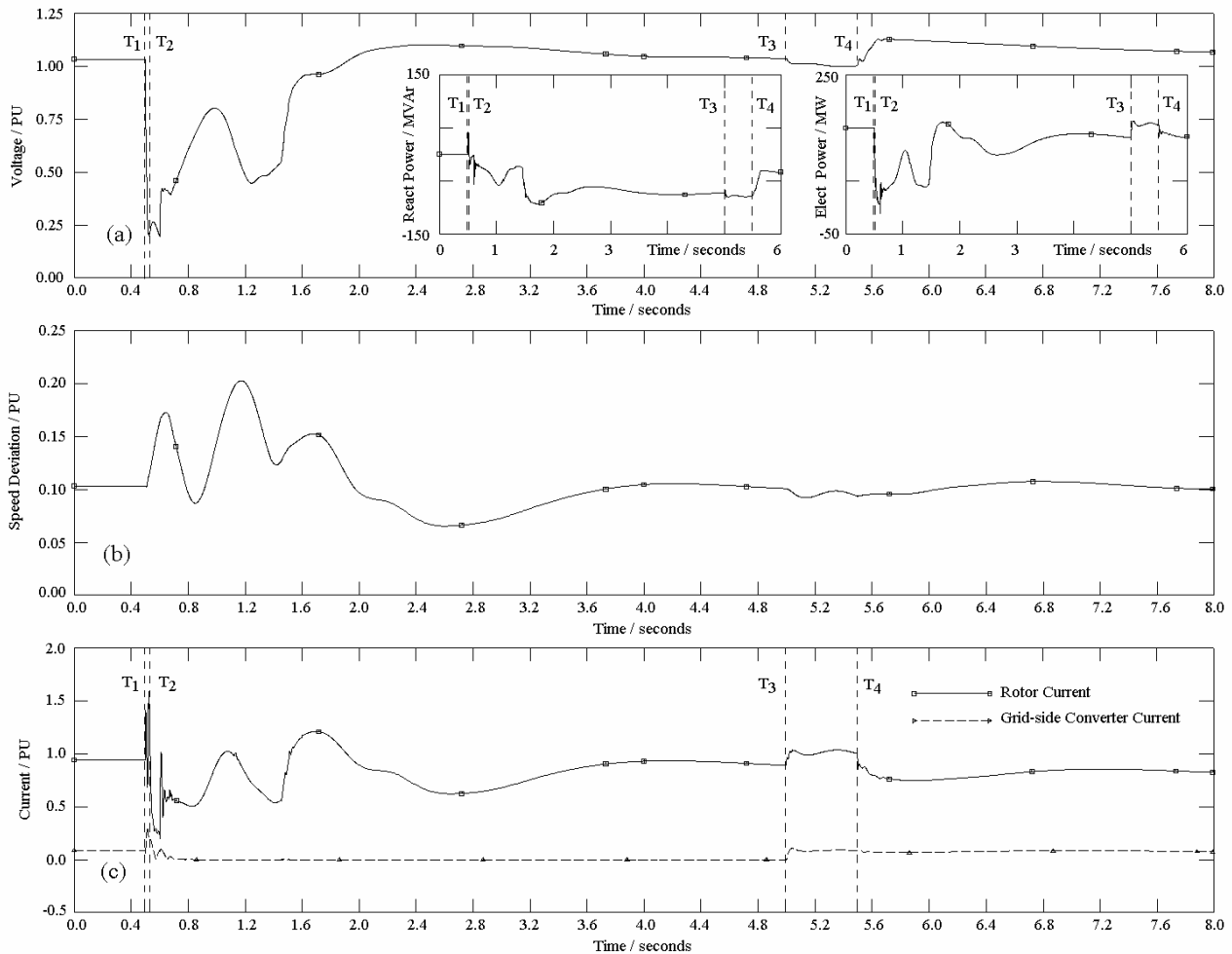


Fig. 11.10. Simulation results for the large wind farm with connection point at the node (4) in the weak power network of area 1. Converter re-starts few sec. after voltage has re-established: (a) – terminal voltage at node (4), reactive power and electric power of DFIG (insertions), (b) – generator rotor speed, (c) – current in the rotor, respectively, in the grid-side converter.

11.4.2.2. Fast converter re-start in weak power networks?

When the short-circuit fault occurs in the power network, the voltage drops. The induction generators in the local wind turbine sites supply reactive power to the power network till the moment when the fault has not cleared. After the fault has cleared, the induction generators absorb reactive power, which is necessary to re-establish their normal operation. The amount of reactive power absorbed by the induction generators depends on operation points of the wind turbines. The

reactive power absorption of the induction generators after the fault has cleared (i) slows process of voltage recovery and (ii) may cause large voltage fluctuations.

In the weak power network of area 1, a significant voltage drop and large voltage fluctuations may occur during and after the transient event. The weak power system is characterised by a relatively low value of the short-circuit capacity, S_{SC} . In the given power network, S_{SC} is around 1000 MVA or lower. Here the voltage fluctuations, ΔV , show a stronger dependence on the reactive power absorption of the induction generators, Q , than in the strong power network. This relation is due to a strong sensitivity of voltage to changes of reactive power.

$$\frac{\Delta V}{V} \propto \frac{Q}{S_{SC}}. \quad (11.4)$$

If the rotor converter has fast re-started, e.g. before complete re-establishment of voltage and frequency in the weak power network, then such voltage fluctuations may affect operation of the converter. When the voltage fluctuations are sufficiently large, the rotor converter can again block. In this case, the converter blocks shortly after it has re-started. This may introduce restrictions on how fast the converter would re-start, when operating in a weak power network.

Now consider that the wind turbines in the local sites are at 60 % of rated operation. When the short-circuit fault has cleared, the reactive power absorption of the induction generators is not much large. Therefore voltage fluctuations are relatively small. In this case, only a minor number of the local wind turbine sites disconnect.

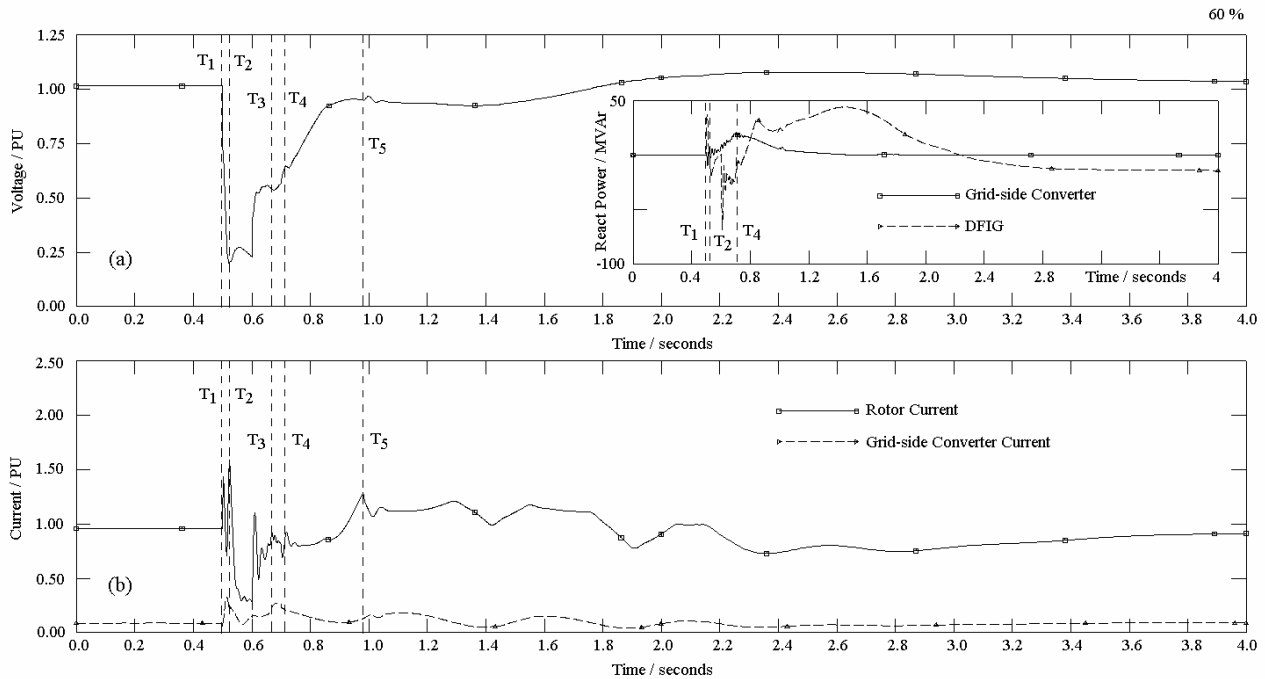


Fig. 11.11. Large wind farm with variable-speed wind turbines when local sites at 60 % wind. Large wind farm is at node (2) of weak power system and fault is at node (6). The curves are: **(a)** – terminal voltage of large wind farm and reactive power of grid-side converter, respectively, of DFIG (insertion), **(b)** – current in rotor circuit and grid-side converter, respectively.

The simulated curves are shown in **Fig. 11.11**. The following events are notified: (i) the short-circuit fault occurs at the node (6) at the time $t = T_1$, (ii) the rotor converter has blocked at the time $t = T_2$, (iii) the converter has synchronised at the time $t = T_3$, shortly after the fault has cleared, (iv) the reactive control loop and the electric power control loop have re-started at the time $t = T_4$ and T_5 , respectively. Notice that the rotor converter re-starts fast when the fault has cleared. When the voltage is re-establishing, the voltage profile does not contain drops or fluctuations, which could again cause the rotor converter blocking. The converter contributes to dynamic control of reactive power and voltage. The converter-controlled DFIG supplies reactive power to re-establish voltage and absorbs reactive power in the post-fault operation to prevent the grid from a possible risk of over-voltage.

At last, consider that the local wind turbine sites are at 90 % of rated operation. The simulated curves for the large wind farm are shown in **Fig. 11.12**.

The short-circuit fault occurs at the node (6) and at the time $t = T_1$. The rotor converter has blocked at the time $t = T_2$. This is caused by excessive current transients in the rotor circuit. The converter has synchronised at the time $t = T_3$, when the fault has cleared and the rotor current transients are suppressed. In this case, it is chosen to make fast converter re-start. At the time $t = T_4$ and T_5 , the reactive power control loop, respectively, the electric power control loop have re-started. Here the converter has re-started before the voltage in the power network has completely re-established and the local wind turbine sites have not tripped yet. The idea with this fast converter re-start should be to contribute to faster voltage re-establishment using the controllability of the frequency converter.

The over-speeded induction generators of the local wind turbine sites absorb a large amount of reactive power before these wind turbines reach to trip. First, the voltage profile is strongly affected by this reactive power absorption. Second, the voltage fluctuations are significant which is caused by the shaft torsional oscillations in the local wind turbines. Combination of these two mechanisms produces a significant voltage drop, which starts around the time $t = T_5$. The dynamic control of reactive power and voltage performed by the frequency converter is applied to reduce this voltage drop and to meet reactive power demands in the local wind turbine sites. But the power capacity of the frequency converter is not sufficiently large to prevent this large voltage drop. The voltage drop continues to develop and the rotor current of the DFIG increases rapidly. Finally, the rotor converter blocks again due to excessive current in the rotor circuit, at the time $t = T_6$ ⁵³.

After this second converter blocking, operation of the large wind farm with DFIG and partial-load frequency converters will be similar to that described in **Section 11.4.2.1**. The converter will probably wait for complete re-establishment of voltage and frequency in the power network of area 1 before the next try to re-start.

⁵³ Discussion: perhaps the converter operation could be improved if the electric power was temporarily reduced in operation of the grid when the voltage and the frequency had not been re-established yet. Notify that the DFIG supplied both electric and reactive power before the converter had blocked due to the voltage drop started at the time $t = T_5$. If the electric power supply was reduced, the converter should only handle/control the reactive power which is why the rotor current was reduced at such critical moment of operation. This discussion was made at the public presentation and it is chosen to bring this in this report.

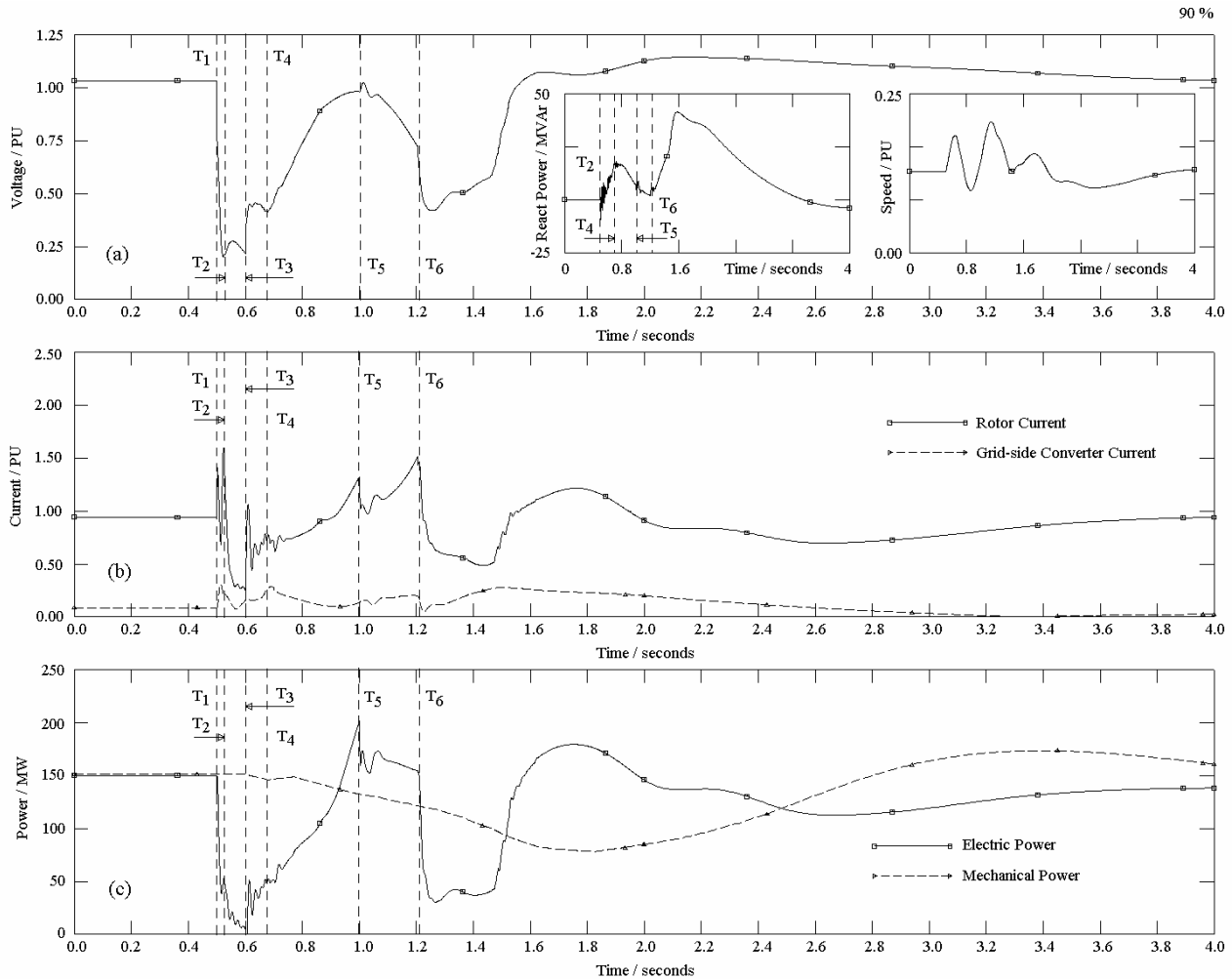


Fig. 11.12. Large wind farm with variable-speed wind turbines when local sites are at 90 % wind. Large wind farm is at node (2) of weak power system and fault is at node (6). The curves are: **(a)** – terminal voltage of large wind farm and reactive power of grid-side converter (insertion) and generator rotor speed (insertion), **(b)** – current in rotor circuit and grid-side converter, respectively, **(c)** – electric and mechanical powers of large wind farm, respectively.

Notice that the converter action has been affected by operation conditions of the weak power network and many local sites with fixed-speed wind turbines.

This discussion should demonstrate that the converter re-start routine can be influenced by the operation conditions of the local wind turbines when the large wind farm feeds into a weak power system. This is different from the results of investigations carried out on the strong power network.

11.4.2.3. Damping of speed fluctuations

The results showing impact of the frequency converter modelling details on the damping of the shaft torsional oscillations are presented. In this investigation, the two converter representations have been compared.

- 1) The reduced converter model where the rotor converter and its control are represented whereas the grid-side converter and its control are disregarded.

- 2) The detailed converter model with representation of the rotor converter, the grid-side converter and the dc-link in between, including the respective control loops.

The frequency converter control is given in **Fig. 10.5** when the detailed converter model is applied. When the reduced converter model is applied, the control loops of the grid-side converter are disregarded and the dc-link voltage assumed constant.

The simulation cases relate to the large wind farm incorporated into the strong power network of area 2, **Section 11.4.2**. First, the results reached with use of the detailed converter model are discussed. The gain of the reactive power control loop of the grid-side converter is kept $K_{QC} = K_1$ whereas the gain K_{PREF} of the PI-controller producing the electric power reference, P_{REF} , from the speed error signal is the parameter of this investigation. **Fig. 11.13** shows the generator rotor speed behaviour reached with use of the detailed converter model at different gains K_{PREF} . Notice the following:

- 1) When the tuning of the control loops of the frequency converter is insufficient, there can be a risk of excitation of the shaft torsional oscillations (Akhmatov, 2002(a); Akhmatov, 2003(b)). This may occur when K_{PREF} is zero or low.
- 2) Moderate values of the gain K_{PREF} must be chosen to reach efficient damping of the shaft torsional oscillations (Akhmatov, 2003(b)).
- 3) The most efficient damping is reached when $K_{PREF} = K_4$.

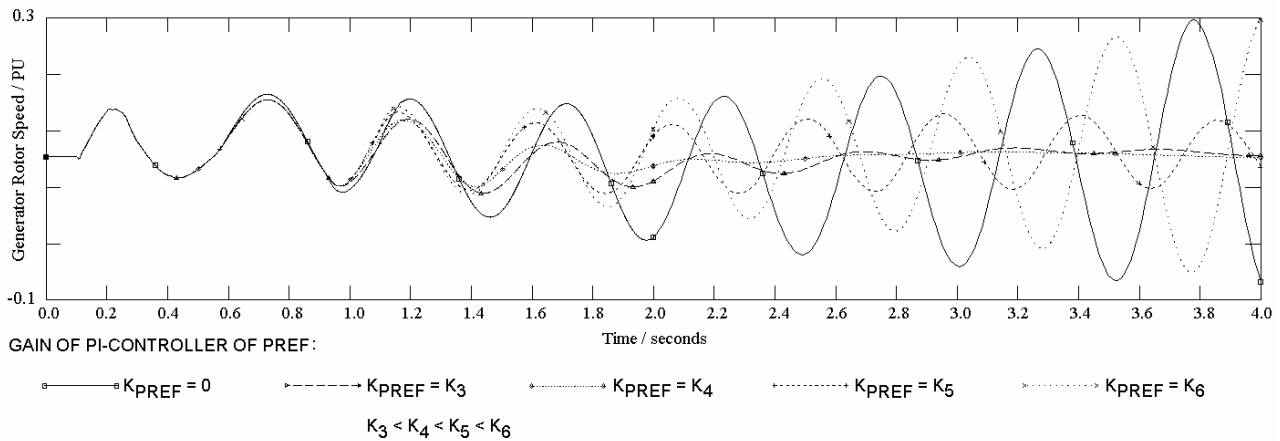


Fig. 11.13. Damping of shaft torsional oscillations using the PI-controller producing P_{REF} . Curves are computed at different gains of this controller. Reported in (Akhmatov, 2003(b)).

When the reduced converter model has been applied, the gain K_{PREF} should be in the range of K_6 to give the best damping of the shaft torsional oscillations. When the reduced converter representation has been applied, the simulations predicted insufficient damping and excitation of the shaft torsional oscillations when the gain $K_{PREF} = K_4$. This result is in contrast to the result predicted with use of the detailed converter model.

Obviously, an accurate representation of the partial-load frequency converter is significant for evaluation of the damping of the shaft torsional oscillations in variable-speed wind turbines

equipped with DFIG. Notice that the physical converter consists of the rotor converter, the grid-side converter and the dc-link in between. Therefore the detailed converter model is closer to the physical converter than the reduced model. When the reduced converter model is applied in investigations with use of the data of the well-tuned physical converter, there can be a risk of inadequate results with respect to the damping of the shaft torsional oscillations in such wind turbines. Use of the reduced converter model should be avoided in investigations dealing with tuning of the converter parameters for damping of such shaft torsional oscillations.

11.4.3. Character of dynamic reactive compensation

Considerations about use of dynamic reactive compensation in the power grids with a large amount of wind power are resumed in the following. This is given in accordance to the considerations and the goal of investigations of short-term voltage stability. **Fig. 11.14** illustrates predicted demands of dynamic reactive compensation (SVC) in the four different cases. Notify that the results relate to cases when the large wind farm is incorporated in the weak power network of area 1.

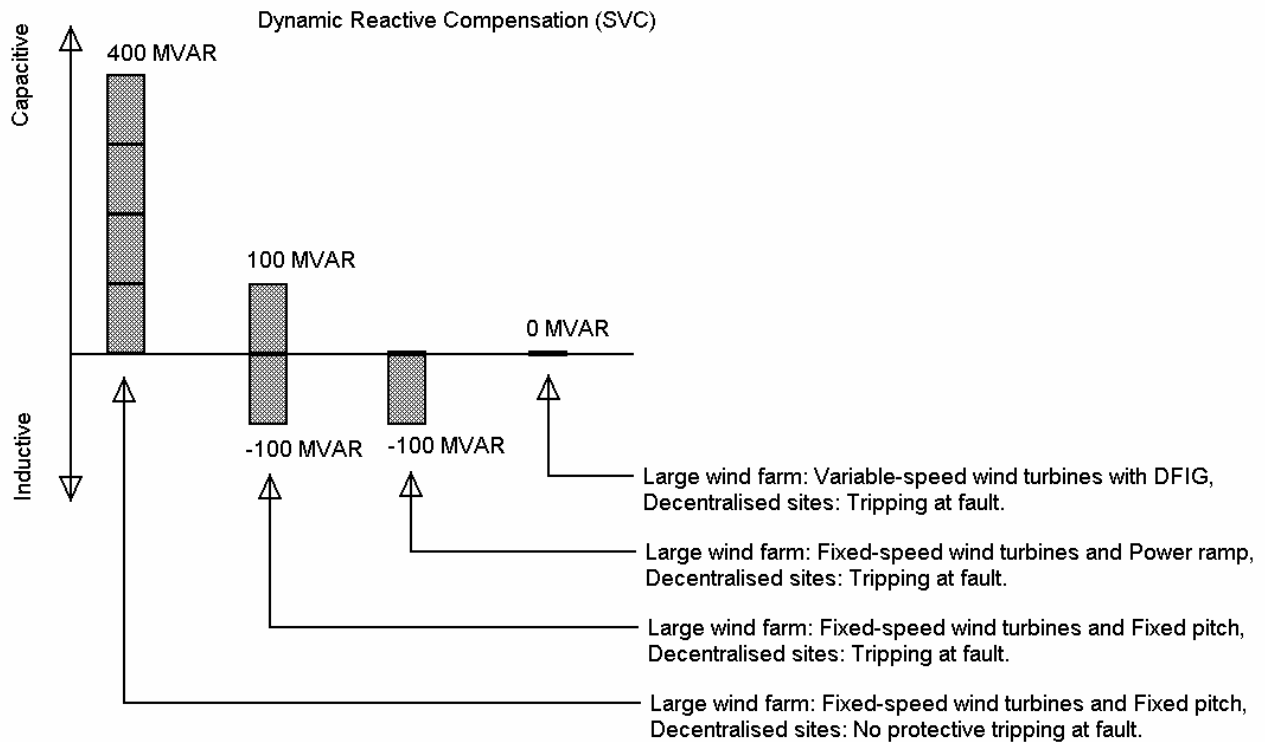


Fig. 11.14. Demands of dynamic reactive compensation versus action of wind turbines in local (decentralised) sites and in large wind farm.

As can be seen, predicted demands of dynamic reactive compensation are strongly dependent on (i) assumptions made for action of the fixed-speed wind turbines in the local sites and (ii) on the wind technology chosen for the large wind farm. This result shows also significance of an accurate and suitable representation of the local generation units and the wind turbines in the large wind farms.

The comparison given in **Fig. 11.14** has not only technical, but also economic interest because there can be a significant difference in the costs of the solutions with incorporation of dynamic reactive compensation.

However the predicted demands of dynamic reactive compensation depend also on the access to the connection point of the large wind farm at the strong power network. When the large wind farm has been incorporated into the strong power system of area 2, no dynamic reactive compensation is needed to voltage re-establishment in the grid. There will be only required -100 MVar of dynamic inductive compensation in the power network of area 1 to avoid a risk of over-voltage in this weak power network. This requirement is specific for the given power system. This result is not dependent from the wind technology chosen for the large wind farm which is why the cheapest solution can be chosen for the large wind farm.

11.4.4. Co-incidents of events – Worst case

The worst case of the outcome of short-term stability investigations can be defined according to:

- 1) Short-term voltage stability which relates to demands of dynamic reactive compensation to avoid uncontrollable voltage decays and fluctuations.
- 2) Power loss which is the result of protective disconnection of the local generation units.
- 3) Location of the faulted node.
- 4) Use of inadequate wind technology for the large wind farms.

The absolutely worst case may appear at co-incidence of such events as:

- 1) Strong wind and large power generation in the local CHP units. In this case, there will be a risk of uncontrollable voltage decay which may result in disconnection of many local generation units and even in outage of the large wind farm.
- 2) When the grid fault occurs in the node (6) of the strong power network of area 3 which affects operation and control of the large power plants.

However such co-incident events are seldom. Keep in mind that the most probable operation situations will be when the wind turbines on-land are at 60 to 70 % of their rated operation. Here the consequences of a short-circuit fault, which occurs in the transmission power networks and may cause a large voltage drop, will not be very drastic with respect to (i) problems with voltage instability, (ii) amount of power loss or (iii) risk of over-voltage in the periphery of the transmission power networks. In other words, operation of the large power network sketched in **Fig. 11.2** is not much affected by serious grid disturbances in the most probable operation situations.

Only in a minor number of operation situations, power generation in the local wind turbine sites approaches 80 to 90 % of rated power. In such situations, the consequences of a three-phased short-circuit fault in the transmission power network can be serious.

Notice that the investigation has been made in cases with a three-phased, short-circuit fault whereas the most probable events are single-phased or two-phased short-circuit faults. At such

events, the voltage drop is smaller than in the case of three-phased faults. In the case of a single-phased short-circuit fault, the positive-sequence voltage at the faulted node drops to around 80 % of its rated value whereas the voltage can drop to zero in a case of the three-phased short-circuit fault. Therefore, the power network operation will be affected in a less significant way in the majority of the fault events.

The faulted node location plays also a part when the impact of the fault events on the power network operation shall be clarified. In this particular case, the worst event occurs when the fault is at the node (6) of the strong power network of area 3. The faults which occur at the periphery of the transmission power network affect operation of the network in a less significant way.

The arrangements with (i) establishment of immediate power reserves and (ii) incorporation of dynamic reactive compensation of both signs will relate to the operation situations with such co-incident events which are seldom. In other words, these arrangements and controls will only be taken in operation in a minor number of situations. In the majority of operation situations, these arrangements and controls will have a less significant effect on operation of the large power network.

Primarily, inadequate operation of the local generation units such as wind turbines and CHP at co-incident events will require establishment of immediate power reserves and dynamic reactive compensation in the grid. Immediate power reserves, when these are arranged with operation of the large power plants at stand-by, will be applied at strong wind (and also at favourable power tariffs). In other situations, such power reserves are probably not necessary.

Once established, dynamic reactive compensation units will be present in the large power network. But their action is mostly acknowledged at strong wind when the problems with uncontrollable voltage decay and fluctuations may be notified at the grid faults. The dynamic reactive compensation units will also act at the grid faults which occurs in the situations at light wind. In situations at light wind, this action can be less important for the power system operation.

Notify that the worst case situation can be made worse when the large wind farm consists of the wind turbines which do not contribute to maintaining short-term voltage stability or even suppress voltage recovery due to absorption of a significant amount of reactive power at the grid faults. Choice of inadequate wind technology to be in the large wind farm should also be placed among such co-incident events. How often this "event" will be present depends on many factors which are not always of a technical character. Notify that the term "wind technology" may include the wind turbines themselves and also the dynamic compensation units delivered by the wind turbine manufacturer as a part of the total solution for the large wind farm.

12. Conclusion

The results of the work presented could be separated into two basic parts.

- 1) Dynamic wind turbine modelling.
- 2) Investigations of power system stability where the dynamic wind turbine models are applied.

It is kept in mind that such a formal separation is not always appropriate to follow because the target of the investigations influences on the model complexity considerations.

12.1. Conclusion to modelling part

Dynamic wind turbine models covering the four basic wind turbine concepts are set up, which are:

- 1) Fixed-speed wind turbines equipped with induction generators. These are (i) fixed-pitch or (ii) with blade-angle control. The generic blade-angle control model can be applied to represent (i) pitch or (ii) active-stall control.
- 2) Pitch-controlled wind turbines equipped with doubly-outage induction generators with variable rotor resistance control.
- 3) Variable-speed, pitch-controlled wind turbines equipped with DFIG and partial-load frequency converters.
- 4) Variable-speed, pitch-controlled wind turbines equipped with direct-driven, multi-pole, synchronous PMG and frequency converters.

The dynamic wind turbine models of the presented complexity should be applied to investigate short-term voltage stability. The target of investigations has influenced the complexity of the models developed.

12.1.1. On generator modelling

The generator models should at least be the fifth-order models with representation of the fundamental-frequency transients. The common third-order generator models are always not sufficiently accurate to be used in investigations of short-term voltage stability.

- 1) In case of induction generators, the common third-order models can predict over-pessimistic behaviour of the generator rotor speed and the voltage at short-circuit faults.
- 2) In case of all the generator concepts, the common third-order models do not acknowledge the fundamental-frequency transients in the machine current. Such current transients are extremely important to predict the protective relay system action.
- 3) Especially in the case of DFIG with partial-load frequency converters, the rotor current transients can be the common reason of the rotor converter blocking.
- 4) In case of direct-driven PMG, there can be a risk of demagnetising the permanent magnets caused by excessive over-current. Also in this generator concept, accuracy of the predicted

current behaviour seems to be important. The control applied to ride-through featuring may not excite excessive current transients in the PMG.

The protective relay system is a part of the generator representation when investigating short-term voltage stability.

12.1.2. On shaft system modelling

The shaft system provides a coupling between the turbine rotor and the generator rotor. In the most cases, the shaft systems contain a gearbox and are characterised by a relatively soft coupling. This soft coupling is expressed by relatively low values of the shaft stiffness. Therefore the shaft systems of fixed-speed wind turbines should rather be represented with the two-mass models than with the lumped-mass models.

- 1) The two-mass model predicts fluctuations of the electrical and the mechanical parameters of the wind turbine and its generator at transient events in electric power networks. The natural frequency of such fluctuations is the shaft torsional mode. Such fluctuations are absent when applying the lumped-mass model.
- 2) The two-mass model predicts also a larger over-speeding of fixed-speed wind turbines than with use of the lumped-mass model. This is important in voltage stability investigations because excessive over-speeding leads to voltage instability.

In case of variable-speed wind turbines equipped with DFIG, such torsional oscillations will lead to the generator speed and electric power fluctuations. When the rotor converter is in operation, the speed fluctuations will not influence the voltage behaviour. It is because the speed and the voltage are controlled independently from each other in such systems.

- 1) However the generator rotor speed fluctuations may become excessive and cause the wind turbine disconnection. This behaviour can be common for this wind turbine concept (Akhmatov, 2002(a)). Also, a control system damping such speed fluctuations should be a part of the dynamic wind turbine model.
- 2) The natural frequency of the shaft torsional mode is in the range of few Hz, which is close to the natural frequency of the electric power grid. This may introduce a risk of oscillations between the wind turbines and the electric power grid (synchronous generators of the conventional power plants).
- 3) When the rotor current behaviour follows the generator speed fluctuations, there can be a risk of that the rotor current will easier approach its relay setting than in case of stiff shaft systems. This behaviour may cause the rotor converter blocking.

The direct-driven wind turbines can also be characterised by a soft coupling between the turbine rotor and the electromagnetic field in the generator when the number of pole-pairs is sufficiently large.

The two-mass model requires more data and is more complex than the lumped-mass model. It is necessary to apply the two-mass model in investigations of short-term voltage stability, but not always.

- 1) When the shaft stiffness is sufficiently low, the two-mass model should be applied in investigations of short-term voltage stability.
- 2) When the shaft system is relatively stiff, e.g. it is characterised by the shaft stiffness around 3.0 PU/el.rad. or larger, the lumped-mass model can be applied without loss of accuracy.

12.1.3. On aerodynamic rotor and blade-angle control modelling

The aerodynamic rotor model gives the coupling between the wind turbine mechanical power and the rotational speed. Often it is modelled with use of the (pre-calculated) C_P - λ - β - curves. Although this representation corresponds to the turbine rotor being in equilibrium (the static representation), this can be applied to represent the dynamic wind turbine response in investigations of short-term voltage stability.

- 1) This static representation can be applied in cases of (i) fixed-pitch and (ii) active-stall controlled wind turbines without loss of accuracy.
- 2) In cases of pitch-controlled wind turbines, the mechanical power will be characterised by over-shoots at relatively fast pitching. Such over-shoots can be computed with use of the Øye model where unsteady inflow phenomena are taken into account (Øye, 1986).
- 3) When the static representation with use of C_P - λ - β - curves is applied to represent pitch-controlled wind turbines, this can result in loss of accuracy. Especially when fast pitching is present. This fact must be kept in mind when representing pitch-controlled wind turbines with their C_P - λ - β - curves and interpreting /analysing the investigation results.

The blade-angle control is represented with use of a generic control system and a servo. There are restrictions on the pitch rate.

- 1) In case of pitch-controlled wind turbines, such restrictions are due to prevention the wind turbine from excessive over-shoots in the mechanical torque.
- 2) In case of active-stall wind turbines, the restrictions are due to a stronger sensitivity of the power output to the blade-angle position than in the case of pitch-controlled wind turbines.

12.1.4. On converter modelling

The frequency converters perform independent control of the electric and the reactive power of the wind turbine generators. Hence, the generator rotor speed and the voltage at the generator terminals are de-coupled. The converter system model must contain (i) a representation of the electric parts of the converter, (ii) the converter control system (modelled in a generic way), (iii) the converter

protective system containing the converter blocking and also (iv) the converter re-start sequences when it is required.

Commonly, the partial-load frequency converters of DFIG are only represented with the rotor converter whereas the grid-side converter and the dc-link models are disregarded. This reduction of the converter system model is agreed due to the common assumption on that the grid-side converter is sufficiently fast and can always follow its references (the dc-link voltage and the reactive current). However, this assumption is only valid so long as the grid voltage is within a pre-defined range around the rated grid voltage. Disregarding the grid-side converter becomes invalid when the grid voltage drops at the grid fault. In this work, necessity of detailed modelling of the partial-load frequency converters of DFIG has been demonstrated.

- 1) When the terminal voltage drops, the electric power supplied from the grid-side converter drops also. At such operation conditions, the dc-link voltage starts increasing and does not necessarily follow its reference. The dc-link voltage is one of the parameters monitored by the protective system. When the dc-link voltage exceeds its relay setting, the converter blocks.
- 2) The converter protective system monitors also the rotor current of DFIG. This current must be computed with sufficient accuracy because excessive over-current in the rotor circuit is among the most common reasons of the rotor converter blocking. When the converter system is only represented with the rotor converter, excessively high values of the rotor current transients can be predicted. Therefore the reduced converter model where the grid-side converter and the dc-link are neglected can predict more frequent converter blocking than will occur.
- 3) The grid-side converter can be set to dynamic control of reactive power and voltage in the vicinity of the wind turbine terminals. This supplementary control is useful when operating with the rotor converter blocked. This supplementary control is however restricted because the power capacity of partial-load converters is limited.
- 4) Accurate representation of the converter system is also required to predict accurate damping of the shaft torsional oscillations.

In cases of wind turbines connected to the ac-grid via the frequency converters, accuracy of the converter representation is important as well. It focuses again on accurate predictions of the converter sequences and the converter actions at transient events in the power networks. The converter may block at (i) over-voltage in the dc-link, (ii) excessive current transients, (iii) frequency deviations in the grid and (iv) under- and over-voltage at the terminals. The grid-side converter can be ordered to dynamic control of reactive power and voltage within a restricted range.

For the both variable-speed concepts, the converter actions will decide the wind turbine operation at the grid faults. Therefore accurate representations of the converter, its protection and the blocking and re-start sequences are absolutely necessary in investigations of short-term voltage stability.

12.1.5. On model validation

Parts of the dynamic wind turbine models are validated against (i) measurements and (ii) results of other simulation tools containing validated models. The results of validation are very positive.

12.2. Conclusion to part with power system studies

The dynamic wind turbine models have been applied to investigate short-term voltage stability.

- 1) In a case of a large (offshore) wind farm consisting of eighty wind turbines.
- 2) With use of a detailed model of a large power system with eighty decentralised wind turbine sites and a large wind farm.

The rated power of the large wind farm is 150 MW. In simulations with use of the large power system, the wind turbines and the CHP units cover around 50 % of power consumption. Here, the total power capacity of the wind turbines in the local (decentralised) sites is around 500 MW, which approximately corresponds to three large wind farms.

In all the investigations, it is distinguished between local wind turbine sites and large (offshore) wind farms. The local wind turbine sites feed into the local distribution networks. The wind turbines in such local sites are not obliged to maintain grid-connection at grid faults and so they may disconnect at abnormal operation of the power network.

The large wind farms are connected to the transmission power networks and must comply with the Specifications of the Danish TSO (Eltra, 2000). The wind turbines in the large wind farms are also with protective relays and may therefore trip. However the Specifications of the Danish TSO require that the voltage shall re-establish without subsequent tripping of the large wind farms.

12.2.1. Reduced wind farm equivalents

It is possible to represent a large wind farm by a reduced equivalent. Such an equivalent may consist of a single wind turbine model with a re-scaled power capacity, which is why this is termed a single-machine equivalent. Reduction to the single-machine equivalent is possible when the wind turbines are (i) with similar data and (ii) operate at similar operation points. The equivalent predicts collective response of the large wind farm at short-circuit faults in the electric power networks.

When the wind turbine data or their operational points are much different, such reduced equivalents may predict inaccurate results.

Typically, investigations of short-term voltage stability are executed on the assumption that the large wind farm is at rated operation. In this case, the single-machine equivalent is applicable and may also reduce computational time.

12.2.2. Voltage stability considerations – Fixed-speed wind turbines in large wind farms.

In the case of fixed-speed wind turbines equipped with induction generators, fatal over-speeding is the main reason of transient voltage instability. Improving of transient voltage stability is similar to

prevent the fixed-speed wind turbines from excessive over-speeding. Such excessive over-speeding is initiated by a lack of the electric torque of induction generators. The electric torque is proportional to the terminal voltage squared. Therefore excessive over-speeding may occur when the power grid is with a deficit of reactive power and voltage control.

A possible way to improve short-term voltage stability is to incorporate dynamic reactive compensation and reinforce the power network. Such reactive compensation can be (i) with continuous control, e.g. SVC, Statcom and SC, (ii) with discrete elements, for example thyristor-switched capacitors and inductors, or (iii) with combination of continuous-controlled and discrete components. The SVC and the Statcom can be set to order the discrete components in the vicinity of their connection points to switch and contribute to reactive power and voltage control in the grid.

The generator parameters influence also short-term voltage stability. For example, the dynamic reactive compensation demands can be reduced when applying induction generators with (i) an increased or (ii) a dynamic-varying rotor resistance. The last mentioned might correspond to the variable-rotor resistance feature described in this work.

Demands of the dynamic reactive compensation can also be reduced when enforcing the wind turbine mechanical construction. This reduction is achieved with increase of (i) the turbine inertia and (ii) the shaft stiffness.

Short-term voltage stability can significantly be improved when the blade-angle control is set to act at transient events in the electric power networks. Here, the wind turbine power is reduced with action of the blade-angle control. This decelerates the wind turbines, prevents excessive over-speeding and stabilises the wind farm operation at the grid faults. In many situations, the dynamic reactive compensation demands can be reduced or even avoided when the blade-angle control is applied to stabilise the wind farm operation at the grid faults.

Since the large (offshore) wind farms are connected to the transmission power network through a long cable, the machine current transients do not seem to be excessive to trip the wind farm when the fault is in the transmission power network. Presumably, a risk of subsequent tripping does not seem to be related to fixed-speed wind turbines erected in the large wind farms.

Accessing strong power networks is an important issue when the large wind farm consists of fixed-speed wind turbines.

- 1) Demands of dynamic reactive compensation (its capacitive part) can be reduced when the large wind farm has accessed a connection point in the strong power network.
- 2) Voltage can re-establish with minimal application of the control present in the wind turbines themselves (fixed-pitch operation instead of active-stall acting at grid faults).

Fixed-speed wind turbines are the concept which is compliant with the Specifications of the TSO (Eltra, 2000).

This conclusion has been reached because voltage in the grid can re-establish without subsequent tripping of the large wind farms equipped with such fixed-speed wind turbines. Incorporation of dynamic reactive compensation units (at the connection point, for example) can be a part of the total solution delivered for the large wind farm.

12.2.3. Voltage stability considerations – Variable-speed wind turbines in large wind farms.

Maintaining of short-term voltage stability does not seem to be a problem related to variable-speed wind turbines of the investigated concepts. Over-speeding does not necessarily lead to voltage instability because the generator speed and the voltage are controlled independently from each other (so long as the frequency converters of the variable-speed wind turbines are in operation).

On the other hand, maintaining of uninterrupted operation at transient events can be the main challenge of such variable-speed wind turbines. It is because the frequency converters of the variable-speed wind turbines are controlled with the IGBT-switches, which are sensitive to electric and thermal over-loads. The IGBT-switches need to be protected against thermal over-loads, over-current (transients) and over-voltage. The converter can block in a few ms at over-current in the generator and the converter, over-voltage in the dc-link and other events, which are interpreted as abnormal operation and may damage the IGBT-switches. The wind turbines may trip when the converters have blocked at such transient events.

The power capacity of the frequency converters is not much larger than the rated power which shall be transmitted through these devices at normal operation. Then, the protective relay settings for the current, for instance, are not much larger than the rated current. Already at the voltage drop of around 0.5 PU, the frequency converters will block. Development of the re-start sequences of such frequency converters is necessary to maintain uninterrupted operation of the variable-speed wind turbines at the grid faults.

In this work, such converter re-start features are suggested for (i) the partial-load frequency converters of DFIG and (ii) the frequency converters of direct-driven, multi-pole PMG. In both cases, it is demonstrated that (i) the converters are able to re-start and (ii) the wind turbine operation has re-established shortly after the grid fault has cleared.

Again, accessing of a connection point in the strong power networks is important.

- 1) This accessing may allow fast re-start of the rotor converters of variable-speed wind turbines with DFIG. The converter can be re-started before the voltage and the frequency have completely re-established.
- 2) When the rotor converter has fast re-started, this converter can order the DFIG to control reactive power and voltage. This may reduce demands of dynamic reactive compensation in the grid.
- 3) When connected to the weak power networks, fast converter re-start is not always possible. Here, the converters will probably wait for the order to re-start till the voltage and the frequency have completely re-established. The other way can be development of better re-start sequences with independent re-start of the control loops for the electric and the reactive power.

Development of such fast re-start sequences of the frequency converters makes these variable-speed concepts to be compliant with the Specifications of the TSO (Eltra, 2000).

In simulations which must demonstrate that the solution with the converter re-start complies with the Specifications of the TSO, accuracy of the converter model is extremely important.

12.2.4. Voltage stability considerations – Local sites

Behaviour of the local generation units at the grid faults is mostly decided by their protective relays. It is rather not to say whether (i) the local wind turbines will disconnect shortly after the grid fault has occurred, (ii) the local wind turbines will not trip, but absorb an amount of reactive power and slow voltage re-establishing or (iii) the local wind turbines will absorb reactive power during a while, contribute to start of uncontrollable voltage decay and then trip.

In this work it is found that the behaviour mentioned in item (iii) can be present when the local wind turbines are many and operate at the operation points being close to the rated operation. The wind turbines in local sites trip around 1 to 2 seconds after the moment of the grid fault has occurred because the voltage starts to decay from this moment. This behaviour may first result in slowing of voltage re-establishment and then in power loss due to protective disconnection of the local wind turbines and the local CHP units. This behaviour is very inappropriate from the viewpoint of the reliable operation of the power system.

This behaviour of the local wind turbine sites may influence the required functionality of the dynamic reactive compensation to be incorporated into the power grid.

- 1) Shortly after the grid fault has cleared, the dynamic reactive compensation unit must supply an amount of reactive power to contribute to voltage re-establishment in the power system. Partly, this must cover reactive power absorption of the local wind turbines.
- 2) In a short while, it can be necessary to set the dynamic reactive compensation unit to absorb reactive power to prevent the power grid from a risk of over-voltage. This requirement is made because tripping of many local wind turbines may produce an immediate surplus of reactive power at the periphery of the power system and increase the voltage above the allowed range.
- 3) Consequently, the dynamic reactive compensation unit must contain both capacitive and inductive components⁵⁴.

In many previous investigations, a risk of voltage collapse has been considered as the main problem of the power systems with a large amount of wind power.

This work is among the first investigations, which concludes that the problem of voltage collapse is not necessarily present in such power networks.

The wind turbines will automatically disconnect when uncontrollable voltage decay has been indicated. When the wind turbines in the local sites have tripped, this has “reduced” demands of dynamic reactive compensation (capacitive) and “eliminated” a risk of voltage collapse in the

⁵⁴ However, the capacitive part of the compensation unit can be excluded.

- (1) When the large wind farm is with fixed-speed, active-stall wind turbines and the blade-angle control is set to act at the grid faults to stabilise the wind farm operation.
- (2) When the large wind farm is with variable-speed wind turbines with DFIG and partial-load frequency converters. The frequency converters are set to control reactive power and voltage, when the converters can fast re-start shortly after the grid fault has cleared.

power system. However, the problem of a risk of voltage collapse is replaced with two other challenges.

- 1) Power loss occurs at disconnection of such local wind turbines. Immediate power reserves should be incorporated to cover such power loss.
- 2) When many wind turbines have tripped, there can be a risk of over-voltages in the periphery of the transmission power network.

Preventing the power network from a risk of over-voltage can be achieved with incorporation of an inductive compensation unit. Such over-voltage may occur in the weak power system, at periphery of the transmission power network. In some situations, the DFIG and their frequency converters of the large wind farm can be applied to contribute to voltage control. But it is kept in mind that converter power capacity is restricted. Besides, fast re-start of the converter is not always possible when the large wind farm, which consists of the DFIG- wind turbines, is connected to a weak power network.

The other important result of this work is that the main problem of the large power system with a large amount of local wind power can be power loss due to tripping of many local generation units. This can be solved with establishing of immediate power reserves.

Notify that such problems dealing with (i) a risk of uncontrollable voltage decays, (ii) a risk of serious power loss due to intense disconnection of the local generation units and (iii) a risk of over-voltage at the periphery of the transmission power network are present at co-incidence of (i) the local wind turbines are close to their rated operation and (ii) serious grid disturbances have occurred. Such problems will be seen very seldom.

In the majority of operation situations, the wind turbines generate around 60 % of the installed power capacity in the local sites. In such operation situations, neither tendency to uncontrollable voltage decay nor significant power loss caused by protective tripping of the local wind turbines have been seen even in cases of serious grid faults. Therefore neither special requirements for dynamic reactive compensation nor immediate power reserves are required in the majority of operation situations in the grid.

Only at strong wind when the local wind turbines are at 80-90 % of the rated power, power loss due to protective tripping can be significant and incorporation of immediate power reserves can be required. Such power reserves could be performed with the large power plants at stand-by. However, it is discussible how convenient this solution would be for an appropriate operation of the power system.

12.2.5. On mutual interaction between wind turbines

A risk of mutual interaction between wind turbines is of common concerns. In this work, it is explained that there is no such a risk in case of fixed-speed wind turbines equipped with induction generators because there is no synchronising torque. This conclusion is confirmed with simulations made on (i) a large wind farm model with representation of eighty wind turbines and (ii) a large

power system with a large number of local wind turbine sites distributed throughout the power system.

Mutual interaction between variable-speed wind turbines (controlled with the frequency converters) is not observed in this work. This result is in agreement with a consideration that there is no such mutual interaction in the case of well-tuned converters. This conclusion is reached from simulations with a large wind farm model with representation of eighty variable-speed wind turbines.

12.3. Practical application of results

The dynamic model of fixed-speed, fixed-pitch wind turbines equipped with induction generators is applied to represent local wind turbine sites in practical investigations of power system stability. The dynamic model of active-stall wind turbines is applied to represent large wind farms in practical investigations of power system stability. These investigations are carried out at the consulting division of the Danish power company NESA for the customers of NESA in Denmark and abroad.

The dynamic model of variable-speed wind turbines equipped with DFIG and partial-load frequency converters has also been applied in practical investigations of power system stability for the customers of NESA world-wide. The main part of this model has been developed in this project.

The feature with use of active-stall control acting at grid faults to stabilise the wind farm operation at the grid faults will be applied at the Danish offshore wind farm at Rødsand /Nysted (150 MW rated power, the year 2003).

This work describes the tools, the controls, the patterns and the ideas about (i) wind turbine modelling of the four main wind turbine concepts and (ii) execution and assumptions of practical investigations of short-term voltage stability. These tools, controls, patterns and ideas would be useful to apply in investigations of short-term voltage stability in YOUR power network. However, there are no general rules or general relations which could automatically be valid for every possible power network /every possible operation situation in the power network. The outcome of investigations of short-term voltage stability carried out on large power networks depend on the power network itself and its control and influenced from several factors. If we change something in this network, then we have changed the considerations of our investigations. Therefore investigations of short-term voltage stability on incorporation of wind power into the power networks will be required in every single case that is also in the case of YOUR power network.

Investigations of short-term voltage stability on incorporation of wind power into the power networks become the power engineers' work.

Literature

- Ackermann, T., Leutz, R., Hobohm, J. (2001(a)). World-wide offshore potential and European projects, *In IEEE Power Engineering Society Summer Meeting*, Vancouver, Canada, vol.1, pp. 4-9.
- Ackermann, T., Andersson, G., Söder, L. (2001(b)). Distributed generation: a definition, *Electric Power Systems Research*, vol. 57, pp. 195-204.
- Akhmatov, V. (1999). *Development of Dynamic Wind Turbine Models in Electric Power Supply*, M.Sc. Thesis, Dept. of Electric Power Engineering, Technical University of Denmark, 108 p., in Danish.
- Akhmatov, V., Knudsen, H. (1999). Modelling of windmill induction generators in dynamic simulation programs, *In International IEEE Power Tech. Conference*, Budapest, Hungary, Paper BPT99-243-12.
- Akhmatov, V., Knudsen, H., Nielsen, A.H. (2000(a)). Advanced simulation of windmills in the electric power supply, *Electrical Power and Energy Systems*, vol. 22, no. 6, pp. 421-434.
- Akhmatov, V., Nielsen, A.H., Knudsen, H. (2000(b)). Electromechanical interaction and stability of power grids with windmills, *In IAESTED International Conference on Power and Energy Systems*, Marbella, Spain, pp. 398-405.
- Akhmatov, V., Knudsen, H., Bruntt, M., Nielsen, A.H., Pedersen, J.K., Poulsen, N.K. (2000(c)). A dynamic stability limit of grid-connected induction generators, *In IAESTED International Conference on Power and Energy Systems*, Marbella, Spain, pp. 235-244.
- Akhmatov, V., Knudsen, H., Nielsen, A.H., Pedersen, J.K., Poulsen, N.K. (2001). Short-term stability of large-scale wind farms, *In European Wind Energy Conference EWEC-2001*, Copenhagen, Denmark, Paper PG 3.56.
- Akhmatov, V., Nielsen, A.H. (2001). Fixed-speed active-stall wind turbines in offshore applications, *In Topical Expert Meeting on Large Scale Integration into The Grid, IEA R&D Wind Annex XI*, Hexham, U. K., 5 p.
- Akhmatov, V. (2001). Note concerning the mutual effects of grid and wind turbine voltage stability control, *Wind Engineering*, vol. 25, no. 6, pp. 367 –371.
- Akhmatov, V., Knudsen, H. (2002). An aggregate model of grid-connected, large-scale, offshore wind farm for power stability investigations – Importance of windmill mechanical system, *Electrical Power and Energy Systems*, vol. 24, no. 9, pp. 709 –717.
- Akhmatov, V. (2002(a)). Modelling of variable-speed wind turbines with doubly-fed induction generators in short-term stability investigations, *In 3rd International Workshop on Transmission Networks for Offshore Wind Farms*, Stockholm, Sweden, p. 23.
- Akhmatov, V. (2002(b)). Variable speed wind turbines with doubly-fed induction generators, Part I: Modelling in dynamic simulation tools, *Wind Engineering*, vol. 26, no. 2, pp. 85-107.
- Akhmatov, V. (2002(c)). Variable speed wind turbines with doubly-fed induction generators, Part II: Power system stability, *Wind Engineering*, vol. 26, no. 3, pp. 171-188.
- Akhmatov, V., Knudsen, H., Nielsen, A.H., Pedersen, J.K., Poulsen, N.K. (2003(a)). Modelling and transient stability of large wind farms, *Electrical Power and Energy Systems*, vol. 25, no. 1, pp. 123-144.

- Akhmatov, V., Nielsen, A.H., Pedersen, J.K., Nymann, O. (2003(b)). Variable-speed wind turbines with multi-pole synchronous permanent magnet generators and full-load converters, Part I: Modelling in dynamic simulation tools, *Wind Engineering – re-submitted after revision*.
- Akhmatov, V. (2003(a)). Variable-speed wind turbines with doubly-fed induction generators. Part III: Model with the back-to-back converters, *Wind Engineering*, vol. 27, no. 2, pp. 79 -91.
- Akhmatov, V. (2003(b)). Variable-speed wind turbines with doubly-fed induction generators. Part IV: Not-interrupted operation features at grid faults with converter control co-ordination, *Wind Engineering- re-submitted after revision*.
- Akhmatov, V. (2003(c)). An aggregate model of a large wind farm with variable-speed wind turbines equipped with doubly-fed induction generators, *Wind Engineering – accepted*.
- Akhmatov, V. (2003(d)). On mechanical excitation of electricity producing wind turbines at grid faults, *Wind Engineering*, vol. 27, no. 4, pp. 257-72.
- Barocio, E., Messina, A.R. (2003). Normal form analysis of stressed power systems: Incorporation of SVC models, *Electrical Power and Energy Systems*, vol. 25, no. 1, pp. 79-90.
- Bruntt, M., Havsager, J., Knudsen, H. (1999). Incorporation of wind power in the East Danish power system, *In International IEEE Power Tech. Conference*, Budapest, Hungary, Paper BPT99-202-50.
- Cadirci, I., Ermis, M. (1992). Double-output induction generator operating at sub-synchronous and super-synchronous speeds: steady-state performance optimisation and wind-energy recovery, *IEE Proceedings-B, Electric Power Applications*, vol. 139, no. 5, pp. 429-442.
- Cathey, J.J., Cavin, R.K., Ayoub, A.K. (1973). Transient load model of induction motor, *In IEEE PES Winter Meeting*, New York, USA, pp. 1399-1406.
- Chaviaropoulos, P.K. (1996). Development of a state-of-the art aeroelastic simulator for horizontal axis wind turbines, Part I: Structural aspects, *Wind Engineering*, vol. 20, no. 6, pp. 405-421.
- Chen, Z., Spooner, E., Norris, W.T., Williamson, A.C. (1998). Capacitor-assisted excitation of permanent-magnet generators, *IEE-Proceedings on Electric Power Applications*, vol. 145, no. 6, pp. 497-508.
- Chow, J.H., Glinkowski, M.T., Murphy, R.J., Caese, T.W., Kosaka, N. (1999). Generator and exciter parameter estimation of Fort Patrick Henry hydro unit 1, *IEEE Transactions on Energy Conversion*, vol. 14, no. 4, pp. 923-929.
- Diez, A., Garcia, D.F., Cancelas, J.A., López, H. (1989). Adaptive control of an asynchronous eolic generator using the field-oriented technique, *In Electrotechnical Conference “Integrating Research, Industry and Education in Energy and Communication Engineering”*, MELECON’89, Mediterranean, pp. 99-103.
- Eel-Hwan Kim, Sung-Bo Oh, Yong-Hyun Kim, Chang-Su Kim (2000). Power control of a doubly fed induction machine without rotational transducers, *In 3rd International Conference on Power Electronics and Motion Control, PIEMC-2000*, vol. 2, pp. 951-955.
- Ekelund, T. (1998). Dynamics and control of structural loads of wind turbines, *In American Control Conference*, Philadelphia, Pennsylvania, pp. 1720-1724.

- Eltra (2000). *Specifications for Connecting Wind Farms to the Transmission Network*, 2nd Ed., ELTRA Transmission System Planning, Denmark: ELT1999-411a.
- Eltra (2003). 2,315 MW wind power in West Denmark, *In Eltra Magasinet*, vol. 6, no. 2, p. 2 (in Danish).
- Enercon (2002). The E-112 prototype is coming, *Wind Blatt*, no. 4, pp. 2-5.
- Feijóo, A., Cidras, J., Carrillo, C. (2000). A third order model for the doubly-fed induction machine, *Electric Power Systems Research*, vol. 56, pp. 121-127.
- Freris, L. (1990). *Wind Energy Conversion Systems*, Prentice Hall, New York, 388 p, in Chapter 4.
- GE Wind Energy. (2002). *Patented VAR Control Technology*, GE Wind Energy, General Electric Company, GEA-13345 (05/02 5M).
- Gere J.M, Timoshenko S.P. (1997). *Mechanics of Materials*, PWS Publishing Company, Boston Mass., 912 p, in Chapter 7.
- Gjengedal, T., Gjerde, J.O., Sporild, R. (1999). Assessing of benefits of adjustable speed hydro machines, *In IEEE International Power Tech 99 Conference*, Budapest, Hungary, Paper BPT99-439-21.
- Grauers, A. (1996). *Design of Direct-driven Permanent Magnet Generators for Wind Turbines*, Chalmers University of Technology, Göteborg, Sweden, Technical Report No. 292, 133 p.
- Grud, P. (2000). State of the art offshore wind technology, *In Workshop Offshore-Windenergienutzung Technik, Naturschutz, Planung*, Deutsches Windenergie-Institut GmbH, Wilhelmshafen, Germany, pp. 26-37.
- Hansen, A., Bindner, H. (1999). *Combined Variable Speed/ Variable Pitch Controlled 3-bladed Wind Turbine: Control Strategies*, Risø National Laboratory, Roskilde, Denmark, 47 p.: Risø-R-1071(DA), in Danish.
- Hansen M.O.L. (2000). *Aerodynamics of Wind Turbines: Rotors, Loads and Structure*, James & James, London, U.K., 144 p.
- Heier, S. (1996). *Windkraftanlagen im Netzbetrieb*, 2.Aufl., Teubner, Stuttgart, Germany, 396 p.
- Hinrichsen, E.N., Nolan, P.J. (1982). Dynamic stability of wind turbine generators, *IEEE Transactions on Power Apparatus Systems*, vol. PAS-101, no. 8, pp. 2640-2648.
- Hinrichsen, E.N. (1984). Controls for variable pitch wind turbine generators, *IEEE Transactions on Power Apparatus and Systems*, vol. PAS-103, no. 4, pp. 886-892.
- Holdsworth, L., Jenkins, N., Strbac, G. (2001). Electrical stability of large, offshore wind farms, *In IEE AC-DC Power Transmission Conference*, Publication No. 485, pp. 156-161.
- Hsu, J.S. (2001). Flux guides for permanent magnet machines, *IEEE Transactions on Energy Conversion*, vol. 16, no. 2, pp. 186-191.
- Ibrahim, E.S. (1997). Digital simulation of electromagnetic transients, *Electric Power Systems Research*, vol. 41, pp. 19-27.

- Incropera, F.P., Dewitt, D.P. (1996). *Introduction to Heat Transfer*, 3rd Edit., New York, Wiley, 801 p.
- Jensen, J.K. (2002). A balancing act: What demands does wind power make on a grid?, *Renewable Energy World*, vol. 5, no. 5, pp. 57-66.
- Jensen, K.H. (2002). *Transient Analysis of Superconducting Cables*, Ph.D. thesis, Dept. of Electric Power Engineering, Technical University of Denmark, Lyngby, Denmark.
- Johansen, J. (1999). *Unsteady Airfoil Flows with Application to Aeroelastic Stability*, Risø National Laboratory, Roskilde, Denmark, 89 p.: Risø-R-1116, in Chapters 8 and 9.
- Jones, B.L., Brown, J.E. (1984). Electrical variable speed drives, *IEE Proceedings-A*, vol. 131, no. 7, pp. 516-558.
- Knudsen, H., Akhmatov, V. (1999). Induction generator models in dynamic simulation tools, *In International Conference on Power System Transients IPST'99*, Budapest, Hungary, pp.253-258.
- KR-88 (1991). *Grid-Connection of Decentralised Generation Units*, DEFU, Copenhagen, Denmark, Committee Report KR-88, 61 p., in Danish.
- Krüger, T., Andresen, B. (2001). Vestas OptiSpeedTM – Advanced control strategy for variable speed wind turbines, *In European Wind Energy Conference EWEC-2001*, Copenhagen, Denmark, pp. 983-986.
- Kundur, P. (1994). *Power System Stability and Control*, EPRI, McGraw-Hill, New York, 1176 p.
- Lange, B., Barthelmie, R., Højstrup, J. (2001). *Description of the Rødsand Field Measurement*, Risø National Laboratory, Roskilde, Denmark, Report Risø-R-1268(EN), 59 p.
- Larsson, A., Thiringer, T. (1995). Measurements on and modelling of capacitor-connecting transients on a low-voltage grid equipped with two wind turbines, *In International Conference on Power System Transients IPST*, Lisbon, Portugal, pp. 184-188.
- Ledesma, P., Usaola, J., Rodriguez, J.L., Burgos, J.C. (1999). Comparison between control systems in a doubly fed induction generator connected to an electric grid, *In European Wind Energy Conference EWEC-1999*, Madrid, Spain, 4 p.
- Leithhead, W.E., de la Salle, S.A., Reardon, D. (1992). Classical control of active pitch regulation of constant speed horizontal axis wind turbine, *International Journal of Control*, vol. 55, no. 4.
- Leith, D.J., Leithhead, W.E. (1997). Implementation of wind turbine controllers, *International Journal of Control*, 1997, vol. 66, no. 3, pp. 349-380.
- Müller, S., Deicke, M., De Doncker, R. W. (2000). Adjustable speed generators for wind turbines based on doubly-fed induction machines and 4-quadrant IGBT converters linked to the rotor, *In IEEE Industry Applications Conference*, Rome, Italy, vol. 4, pp. 2249-2254.
- Muljadi, E., Butterfield, C.P., Wan, Y.H. (1998). Axial flux, modular, permanent-magnet generator with a toroidal winding for wind turbine applications, *In IEEE Industry Applications Conference*, St. Luis, U.S.A., vol. 1, pp. 174-178.

- Neris, A.N., Vovos, N.A., Giannakopoulos, G.B. (1996). Dynamics and control system design of an autonomous wind turbine, *In Third IEEE International Conference on Electronics, Circuits and Systems ICECS'96*, Rhodes, Greece, vol.2, pp. 1017-1020.
- Noroozian, M., Knudsen, H., Bruntt, M. (2000). Improving a wind farm performance by reactive power compensation, *In IAESTED International Conference on Power and Energy Systems*, Marbella, Spain, pp. 437-442.
- Næss, B.I., Undeland, T.M., Gjengedal, T. (2002). Methods for reduction of voltage unbalance in weak grids connected to wind plants, *In IEEE/CIGRE Workshop on Wind Power and the Impacts on Power Systems*, Oslo, Norway, 6 p.
- Ong, C.M. (1998). *Dynamic Simulation of Electric Machinery, Using Matlab/Simulink*, Prentice Hall PTR, Upper Saddle River, New Jersey, USA, 626 p.
- Papathanassiou, S.A., Papadopoulos, M.P. (1999). Dynamic behaviour of variable speed wind turbines under stochastic wind, *IEEE Transactions on Energy Conversion*, vol. 14, no. 4, pp. 1617-1623.
- Pedersen, J.K., Akke, M., Poulsen, N.K., Pedersen, K.O.H. (2000). Analysis of wind farm islanding experiment, *IEEE Transactions on Energy Conversion*, vol. 15, no. 1, pp. 110-115.
- Pedersen, J.K., Pedersen, K.O.H., Poulsen, N.K., Akhmatov, V., Nielsen, A.H. (2003). Contribution to a dynamic wind turbine model validation from a wind farm islanding experiment, *Electric Power Systems Research*, vol. 64, no. 1, pp. 41-51.
- Pena, R., Clare, J.C., Asher, G.M. (1996). Doubly-fed induction generator using back-to-back PWM converters and its application to variable-speed wind-energy generation, *IEE Proceedings-B, Electric Power Applications*, vol. 143, no. 3, pp. 231-241.
- Pena, R.S., Cardenas, R.J., Asher, G.M., Clare, J.C. (2000). Vector controlled induction machines for stand-alone wind energy applications, *In IEEE Industry Applications Conference*, Rome, Italy, vol. 3, pp. 1409-1415.
- Pretlove, A.J., Mayer, R. (1994). Rotor size and mass – The dilemma for designers of wind turbine generating systems, *Wind Engineering*, vol. 18, no. 6, pp. 317-328.
- Pöller, M., Achilles, S. (2003). Direct drive synchronous machine models for stability assessment of wind farms, *In Proc. of Fourth International Workshop on Large-Scale Integration of Wind Power and Transmission Networks for Offshore Wind Farms*, Billund, Denmark.
- Raben, N., Donovan, M.H., Jørgensen, E., Thisted, J., Akhmatov, V. (2003). Grid tripping and re-connection: Full-scale experimental validation of a dynamic wind turbine model, *Wind Engineering*, vol. 27, no. 2, pp. 205-213.
- Radtke, U. (2002). Wind energy is growing faster than the grid, *Wind Blatt*, no. 6, pp. 8-9.
- Røstøen, H.Ø., Undeland, T.M., Gjengedal, T. (2002). Doubly-fed induction generator in a wind turbine, *In IEEE/CIGRE Workshop on Wind Power and the Impacts on Power Systems*, Oslo, Norway, 6 p.
- Salman, S.K., Teo, A.L.J. (2003). Windmill modelling consideration and factors influencing the stability of a grid-connected wind power based embedded generator, *IEEE Trans. on Power Systems*, vol. 18, no. 2, pp. 793-802.
- Schauder, C., Metha, H. (1993). Vector analysis and control of advanced static VAR compensators, *IEE Proceedings-C*, vol. 140, no. 4, pp. 299-306.

- Schmidt, E., Grabner, C., Traxler-Samek, G. (2001). Reactance calculation of a 500 MVA hydro-generator using a finite element analysis with superelements, *In IEEE International Electric Machines and Drives Conference*, Cambridge, U.S.A., pp. 838-844.
- Sheahan, T. P. (1994). *Introduction to High- Temperature Superconductivity*, New York, Plenum, 580 p.
- Slootweg, J.G., Polinder, H., Kling, W.L. (2001). Initialisation of wind turbine models in power dynamics simulations, *In 2001 IEEE Porto Power Tech Conference*, Porto, Portugal, 6 p.
- Slootweg, J.G., de Haan, S.W.H., Polinder, H., Kling, W. (2003). General model for representing variable speed wind turbines in power system dynamics simulations, *IEEE Transactions on Power Systems*, vol. 18, no. 1, pp. 144-151.
- Snel, H., Schepers, J.G. (1992). Engineering models for dynamic inflow phenomena, *Wind Engineering and Industrial Aerodynamics*, vol. 39, pp. 267-281.
- Snel, H., Schepers, J.G., editors (1995). *Joint Investigation of Dynamic Inflow Effects and Implementation of an Engineering Method*, Netherlands Energy Research Foundation ECN, Petten, the Netherlands, 326 p.
- Song, Y.D., Dhinakaran, B., Bao, X.Y. (2000). Variable speed control of wind turbines using non-linear and adaptive algorithms, *Wind Engineering and Industrial Aerodynamics*, vol. 85, pp. 293-308.
- Svensson, J. (1995). Voltage angle control of a voltage source inverter – Application to a grid-connected wind turbine, *In 6th European Conference on Power Electronics and Applications*, Sevilla, Spain, vol. 3, pp. 539-544.
- Svensson, J. (1998). *Grid-connected Voltage Source Converter – Control Principles and Wind Energy Applications*, Chalmers University of Technology, Göteborg, Sweden, Technical Report no. 331, 34 p.
- Søbrink, K.H., Schettler, F., Bergmann, K., Stöber, R., Jenkins, N., Ekanayake, J., Pedersen, J.K., Pedersen, K.O.H. et al (1998). *Power Quality Improvements of Wind Farms*, Fredericia, Denmark, ISBN No.: 87-90707-05-2.
- Sørensen, J.N., Kock, C.W. (1995). A model for unsteady rotor aerodynamics, *Wind Engineering and Industrial Aerodynamics*, vol. 58, pp. 259-275.
- Sørensen, J.N., Hilden, A. (2003). Remote control and supervision for the Horns Rev offshore windfarm by the VestasOnline™ Professional System, *Wind Engineering*, vol. 27, no. 5, pp. 361-70.
- Sørensen, P., Hansen, A.D., Christensen, P., Mieritz, M., Bech, J., Bak-Jensen, B., Nielsen, H. (2003). *Simulation and Verification of Transient Events in Large Wind Power Installations*, Report Risø-R-1331(EN), Risø National Laboratory, Roskilde, Denmark, 80 p.
- Tapia, A., Tapia, G., Ostolaza, J.X., Saenz, J.R., Criado, R., Berasategui, J.L. (2001). Reactive power control of wind farms made up with doubly-fed induction generators, *In IEEE Porto Power Tech Conference*, Porto, Portugal, vol. 4, 6 p.
- Taylor, C.W. (1994). *Power System Voltage Stability*, McGraw-Hill, Inc., New York, 273 p., in Chapter 3.
- Thiringer, T., Dahlberg, J.A. (2001). Periodic pulsations from a three-bladed wind turbine, *IEEE Transactions on Energy Conversion*, vol. 16, no. 2, pp. 128-133.
- Thiringer, T., Luomi, J. (2001). Comparison of reduced-order dynamic models of induction machines, *IEEE Transactions on Power Systems*, vol. 16, no. 1, pp. 119-126.

- Thomsen, K. (2002). *Determination of Damping for Blade and Tower Mode Shapes*, Risø National Laboratory, Roskilde, Denmark, 40 p.: Risø-R-1371(DA), in Danish.
- Twidell, J.W. (2002). Offshore wind energy – the technical challenge; Report of conference S868, Institution of Mechanical Engineers, London, *Wind Engineering*, vol. 26, no. 5, pp. 329-334.
- Vestas (2001), *OptiSpeed™, Vestas Converter System, General Edition*, Item.no. 947543.R0 – Class 1, Ringkøbing, Denmark.
- Walker, J.F., Jenkins, N. (1997). *Wind Energy Technology*, John Wiley & Sons, London, U.K., 161 p.
- Westlake, A.J.G., Bumby, J.R., Spooner, E. (1996). Damping the power-angle oscillations of a permanent-magnet synchronous generator with particular reference to wind turbine applications, *IEEE Proceedings on Electric Power Applications*, vol. 143, no. 3, pp. 269-280.
- Yamamoto, M., Motoyoshi, O. (1991) Active and reactive power control for doubly-fed wound rotor induction generator, *IEEE Transactions on Power Electronics*, vol. 6, no. 4, pp. 624-629.
- Younsi, R., El-Batanony, I., Tritsch, J.B., Naji, H., Landjerit, B. (2001). Dynamic study of a wind turbine blade with horizontal axis, *European Journal of Mechanics A/Solids*, vol. 20, pp. 241-252.
- Zhang, L., Watthanasarn, C., Shepherd, W. (1997). *Application of a matrix converter for the power control of a variable-speed wind-turbine driving a doubly-fed induction generator*, In *IECON Proceedings, Industrial Electronics Conference*, vol. 2, pp. 906-911.
- Zinger, D.S., Muljadi, E. (1997). Annualized wind energy improvement using variable speeds, In *IEEE Annual Meeting: Industrial and Commercial Power Systems Technical Conference*, Conference Records, pp. 80-83.
- Øye, S. (1986). Unsteady wake effects caused by pitch –angle changes, In *IEA R&D WECS Joint Action on Aerodynamics of Wind Turbines, 1st Symposium*, London, U.K., pp.58-79.
- Öhrström, M., Söder, L. (2003). Installation of a fault current limiter as an alternative to upgrade substation equipment, In *Proc. of Fourth International Workshop on Large-Scale Integration of Wind Power and Transmission Networks for Offshore Wind farms*, Billund, Denmark.

Further Readings

To Section 1: Introduction

- Another record year for European wind industry, *Renewable Energy World*, vol. 6, no. 2, available on: <http://www.jxj.com/magasandj/rew/news/>
- Hansen, L.H., Helle, L., Blaabjerg, F., Ritchie, E., Munk-Nielsen, S., Binder, H., Sørensen, P., Bak-Jensen, B. (2001), *Conceptual Survey of Generators and Power Electronics for Wind Turbines*, Risø National Laboratory, Roskilde, Denmark, 105 p.: Risø-R-1205(EN).
- Slootweg, J.G., De Vries, E. (2003). Inside wind turbines: Fixed vs. variable speed, *Renewable Energy World*, vol. 6., no.1, available on: <http://www.jxj.com/magasandj/rew/news/>

To Section 2: Mechanical system of a wind turbine

Ekelund, T. (2000). Yaw control for reduction of structural dynamic loads in wind turbines, *Wind Engineering and Industrial Aerodynamics*, vol. 85, pp. 241-262.

Snel, H., Lindenburg, C. (1990). Aeroelastic rotor system code for horizontal axis wind turbines: Phatas II, *In European Community Wind Energy Conference*, Madrid, Spain, pp. 284-290.

Krasnov, N.F. (1985). *Aerodynamics, I: Fundamentals of Theory, Aerodynamics of an Airfoil and a Wing*, MIR, Moscow, Russia, 510 p.

Aagaard Madsen, H. (1991). *Aerodynamics and Structural Dynamics of a Horizontal Axis Wind Turbine: Raw Data Overview*, Risø National Laboratory, Roskilde, Denmark, Risø-M-2902, 237 p.

To Section 3: Generic blade angle control

Cardenas-Dobson, R., Asher, G.M. (1996). Power limitation in variable speed wind turbines using pitch control and a mechanical torque observer, *Wind Engineering*, vol. 20, no. 6, pp. 363-387.

Diop, A.D., Nichita, C., Belhache, J.J., Dakyo, B., Ceanga, E. (1999). Modelling variable pitch HAWT characteristics for a real time wind turbine simulator, *Wind Engineering*, vol. 23, no. 4, pp. 225-243.

Leithead, W.E., de la Salle, S.A., Reardon, D. (1991). Role and objectives of control for wind turbines, *IEE Proceedings-C Generation, Transmission and Distribution*, vol. 138, no. 2, pp. 135-148.

To Section 4: Induction generators of fixed-speed wind turbines

Kazachkov, Y.A., Feltes, J.W., Zavadil, R. (2003) Modeling wind farms for power system stability studies, *In IEEE Power Engineering Society Meeting*, Toronto, Canada, 8 pp.

Krause, P.C. (1986). *Analysis of Electric Machinery*, McGraw-Hill Book Company, New York, 564 p., in Chapter 4.

Saad-Saoud, Z., Jenkins, N. (1999). Models for predicting flicker induced by large wind turbines, *IEEE Transactions on Energy Conversion*, vol. 14, no. 3, pp. 743-748.

Sørensen, P., Hansen, A., Janosi, L., Bech, J., Bak-Jensen, B. (2001). *Simulation of Interaction between Wind Farm and Power System*, Risø National Laboratory, Roskilde, Denmark, Risø-R-1281(EN), 66 p.

To Section 5: Modelling of large wind farms

Feijóo, A.E., Cidrás, J. (2000). Modelling of wind farms in the load flow analysis, *IEEE Transactions on Power Systems*, vol. 15, no. 1, pp. 110-115.

Jenkins, N. (1993). Engineering wind farms, *Power Engineering Journal*, no. 4 (April), pp. 53-60.

Magnusson, M., Smedman, A.S. (1999). Air flow behind wind turbines, *Wind Engineering and Industrial Aerodynamics*, vol. 80, pp. 169-189.

Slootweg J.G., de Haan, S.W.H., Polinder, H., Kling W. (2002). Aggregated modelling of wind parks with variable speed wind turbines in power system dynamics simulations, *In 14th Power Systems Computation Conference*, Sevilla, Spain, 6 p.

Slootweg, J.G., Kling, W. (2002). Modelling of large wind farms in power system simulations, *In IEEE Power Engineering Society Summer Meeting*, Chicago, U.S.A., vol. 1, p. 503-508.

To Section 6: Voltage stability of large wind farms with fixed-speed wind turbines

Haslam, S.J., Crossley, P.A., Jenkins, N. (1999). Design and evaluation of a wind farm protection relay, *IEE Proceedings-C Generation, Transmission, Distribution*, vol. 146, no. 1, pp. 37-44.

Haslam, S.J., Crossley, P.A., Jenkins, N. (1999). Design and field testing of a source protection relay for wind farms, *IEEE Transactions on Power Delivery*, vol. 14, no. 3, pp. 818-823.

Miller, T.J.E. (1982). *Reactive Power Control in Electric Systems*, John Wiley & Sons, London, U.K., in Chapter 3, 4 and 8.

Saad-Saoud, Z., Jenkins, N. (1995). Simple wind farm dynamic model, *IEE Proceedings-C Generation, Transmission, Distribution*, vol. 142, no. 5, pp. 545-548.

Saad-Saoud, Z., Lisboa, M.L., Ekanayake, J.B., Jenkins, N., Strbac, G. (1998). Application of Statcoms to wind farms, *IEE Proceedings-C Generation, Transmission, Distribution*, vol. 145, no. 5, pp. 511-516.

Wang, Y., Chen, H., Zhou, R. (2000). A nonlinear controller design for SVC to improve power system voltage stability, *Electrical Power and Energy Systems*, vol. 22, no. 7, pp. 463-470.

To Section 8: Variable-speed wind turbines – Operation and modelling considerations

Blaabjerg, F., Pedersen, J.K. (1997). Optimised design of a complete three-phased PWM-VS inverter, *IEEE Transactions on Power Electronics*, vol. 12, no. 3, pp. 567-577.

Christiansen, P., Kristoffersen, J., Holmstrøm, O., Palmelund, H., Abildgaard, H. (2001). New requirements for grid connection of wind farms, *In 2nd International Workshop on Transmission Networks for Offshore Wind Farms*, Stockholm, Sweden.

Freeman, J.B., Balas, M.J. (1998). Direct model-reference adaptive control of variable speed horizontal-axis wind turbines, *Wind Engineering*, vol. 22, no. 5, pp. 209-218.

Nielsen, P., Blaabjerg, F., Pedersen, J.K. (1999). New protection issues of a matrix converter: Design considerations for adjustable-speed drives, *IEEE Transactions on Industry Applications*, vol. 35, no. 5, pp. 1150-1161.

Shieh, J.J. (2001). Modelling and analysis of a single stage step-up/down three-phased AC to DC converter, *Electrical Engineering*, vol. 83, pp. 115-122.

To Section 9: Variable-speed wind turbines equipped with PMG

Cavagnino, A., Lazzari, M., Profumo, F., Tenconi, A. (2000). A comparison between the axial and the radial flux structures for PM synchronous motors, *In IEEE Industry Applications Conference*, Rome, Italy, vol. 3, pp. 1611-1618.

Chalmers, B.J., Wu, W., Spooner, E. (1999). An axial-flux permanent-magnet generator for a gearless wind energy system, *IEEE Transactions on Energy Conversion*, vol. 14, no. 2, pp. 251-257.

- Di Napoli, A., Carrichi, F., Crescimbeni, F., Noia, G. (1991). Design criteria of a low-speed axial-flux PM synchronous machines, *In International Conference on the Evolution and Modern Aspects of Synchronous Machines*, Zurich, Switzerland, part 3, pp. 1119-1123.
- Lampola, P., Perho, J., Saari, J. (1995). Electromagnetic and thermal design of a low-speed permanent magnet wind generator, *In International Symposium on Electric Power Engineering*, Stockholm, Sweden, part Electrical Machines and Drives, pp. 211-216.
- Lampola, P. (2000). Directly-driven, low-speed permanent-magnet generators for wind power applications, *Acta Polytechnica Scandinavica, Electrical Engineering Series*, Finish Academy of Technology, issue EI 101, pp. 2-62.
- Nielsen, A.H. (1980). *Ironless Motors with Permanent Magnets*, Dept. of Electric Power Engineering, Technical University of Denmark, Publication No. 8003, 59 p.
- Schneider, H., Hartkopf, T., Hagenkort, B., Henschel, M., Jöckel, S., Boldlehner, H.G. (2001). Development of an extremely compact 1.5 MW direct drive permanent-magnet generator system using finite elements, *In European Wind Energy Conference EWEC-2001*, Copenhagen, Denmark, Paper PG 3.47.
- Simsir, N.B., Ertan, H.B. (1999). A comparison of torque capabilities of axial flux and radial flux type of brushless DC (BLDC) drives for wind speed range applications, *In IEEE International Conference on Power Electronics and Drive Systems*, Hong Kong, pp. 719-724.
- Slootweg, J.G., Polinder, H., Kling, W.L. (2001). Dynamic modelling of a wind turbine with direct drive synchronous generator and back to back voltage source converter and its control, *In European Wind Energy Conference EWEC-2001*, Copenhagen, Denmark, Paper PG 3.4.
- Slootweg, J.G., de Haan, S.W.H., Polinder, H., Kling, W. (2001). Voltage control methods with grid-connected wind turbines: a tutorial review, *Wind Engineering*, vol. 25, no. 6, pp. 353-366.
- Slootweg, J.G., Kling, W. L. (2002). Modelling and analysis of impacts of wind power on transient stability of power systems, *Wind Engineering*, vol. 26, no. 1, pp. 3-20.
- Solsona, J., Valla, M.I., Muravchik, C. (2000). Nonlinear control of a permanent magnet synchronous motor with disturbance torque estimation, *IEEE Transactions on Energy Conversion*, vol. 15, no. 2, pp. 163-168.
- Spooner, E., Williamson, A.C. (1996). Direct coupled, permanent magnet generators for wind turbine applications, *IEE-Proceedings-C Electric Power Applications*, vol. 143, no. 1, pp. 1-8.
- Spooner, E., Williamson, A.C., Catto, G. (1996). Modular design of permanent-magnet generators for wind turbines, *IEE Proceedings-C Electric Power Applications*, vol. 143, no. 5, pp. 388-395.
- Spooner, E., Williamson, A.C. (1998). Parasitic losses in modular permanent-magnet generators, *IEE-Proceedings-C Electric Power Applications*, vol. 145, no. 6, pp. 485-496.
- Weh, H. (1995). Transverse flux (TF) machines in drive and generator application, *In IEEE Power Tech International Symposium on Electric Power Engineering*, Stockholm, Sweden, vol. 1, pp. 75-80.
- Wu, W., Ramsden, V.S., Crawford, T., Hill, G. (2000). A low-speed, high-torque, direct-driven permanent magnet generator for wind turbines, *In IEEE Industry Applications Conference*, Rome, Italy, vol. 1, pp. 147-154.

To Section 10: Variable-speed wind turbines equipped with DFIG

- Bhowmik, S., Spée, R., Enslin, J.H.R. (1999). Performance optimisation for doubly fed wind power generation systems, *IEEE Transactions on Industry Applications*, vol. 35, no. 4, pp. 949-958.
- De Battista, H., Puleston, P.F., Mantz, R.J., Christiansen, C.F. (2000). Sliding mode control of wind energy systems with DOIG – Power efficiency and torsional dynamics optimisation, *IEEE Transactions on Power Systems*, vol. 15, no. 2, pp. 728-734.
- El-Lithy, F.M. (1999). Matching a wind turbine with double output induction generator, *Journal of Engineering and Applied Science*, vol. 46, no. 2, pp. 321-336.
- Hoffman, W., Okafor, F. (2001). Optimal control of doubly-fed full-controlled induction wind generator with high efficiency, *In 27th Annual Conference of IEEE Industrial Electronics Society*, Denver, U.S.A., vol. 2, pp. 1213-1218.
- Ioannides, M.G. (1991). Doubly fed induction machine state variables model and dynamic response, *IEEE Transactions on Energy Conversion*, vol. 6, no. 1, pp. 55-61.
- Metwally, H.M.B., Abdel-kader, F.E., El-Shewy, H.M., El-kholy, M.M. (2002). Optimum performance characteristics of doubly fed induction motors using field oriented control, *Energy Conversion and Management*, vol. 43, pp. 3-13.
- Novak, P., Jovik, I., Schmidtbauer, B. (1994). Modelling and identification of drive-system dynamics in a variable-speed wind turbine, *In 3rd IEEE Conference on Control Applications*, vol. 1, pp. 233-238.
- Petersson, A. (2003). Analysis, *Modelling and Control of Doubly-fed Induction Generators for Wind Turbines*, Chalmers University of Technology, Göteborg, Sweden, Report No. 464L, 122 p.
- Wang, Q., Chang, L. (2001). PWM control strategies for wind turbine inverters, *Wind Engineering*, vol. 25, no. 1, pp. 33-40.
- Wasynczuk, O., Sudhoff, S.D., Corzine, K.A., Tichenor, J.L., Krause, P.C., Hansen, I.G., Taylor, L.M. (1998). A maximum torque per ampere control strategy for induction motor drives, *IEEE Transactions on Energy Conversion*, vol. 13, no. 2, pp. 163-169.

To Section 11: Power system analysis with large amount of wind power

- Rodriguez, J.M., Fernández, J.L., Beato, D., Iture, R., Usaola, J., Ledesma, P., Wilhelmi, J.R. (2002). Incidence on power system dynamics of high penetration of fixed speed and doubly fed wind energy systems: Study of the Spanish case, *IEEE Transactions on Power Systems*, vol. 17, no. 4, pp. 1089-1095.
- Slootweg, J.G. (2003). Wind Power Modelling and Impact on Power System Dynamics, PhD thesis at Delft University of Technology, Ridderprint Offsetdrukkerij B.V. Ridderkerk, the Netherlands, 219 p.
- Thiringer, T. (2000). Integration of large sea-based wind parks – how much power electronic devices are needed in order to avoid power quality problems on the grid?, *In IEEE Power Engineering Society Summer Meeting*, Seattle, U.S.A., vol. 2, pp. 1277-1279.

224 Vladislav Akhmatov: Analysis of dynamic behaviour of electric power systems with large amount of wind power

---. (2003). *Efficient Development of Offshore Windfarms (ENDOW)*, Final report to the European Commission: Executive Summary (ERK6-1999-00001), Risø National Laboratory, Roskilde, Denmark, 30 p.

Appendix 2.A. Excitation of wind turbine construction at grid disturbances

When this thesis has been in revision, the article covering this issue has been published in *Wind Engineering*:

V. Akhmatov, Mechanical excitation of electricity producing wind turbines at grid faults, *Wind Engineering*, 2003, vol. 27, no. 4, pp. 257 -272.

Therefore this issue has been removed from this thesis. Order you copy at your library or from the publisher Multi-Science Publishing on: www.multi-science.co.uk.

If you choose to read this article, notify that the expression of the mechanical torque, T_M , must be given by **Eq. (2.5)** of this thesis.

Appendix 4.A. Per Unit system of the wind turbine model

All the electrical and the mechanical parameters of the wind turbine model are in the Per Unit (PU) system. The base values are the following.

- 1) The rated electric power of the wind turbine, P_{BASE} , in Watts.
- 2) The rated terminal voltage of the wind turbine, V_{BASE} , in Volts phase-phase RMS.
- 3) The rated electric frequency at the wind turbine terminals, f_{BASE} , in Hz.

All the other base values are defined with use of the base values above.

- 4) The base impedance of the wind turbine generator $Z_{BASE} = \frac{V_{BASE}^2}{P_{BASE}}$, in Ohm.
- 5) The base machine current $I_{BASE} = \frac{P_{BASE}}{V_{BASE}}$, in Amps.
- 6) The base speed, which is also called the electric system speed, $\omega_{BASE} = 2\pi f_{BASE}$, in el.rad./s.
- 7) The base flux $\psi_{BASE} = \frac{Z_{BASE}}{\omega_{BASE}} I_{BASE}$, in V/s.

Expression of the electrical and mechanical parameters in PU is illustrated by the following examples.

- 1) The stator impedance in PU is given by:

$$R_s + jX_s (PU) = \frac{R_s + jX_s (Ohm)}{Z_{BASE}}.$$

- 2) The electric and the reactive power of the wind turbine generator and its terminal voltage in PU will be:

$$P_E (PU) = \frac{P_E (MW)}{P_{BASE}}, \quad Q_E (PU) = \frac{Q_E (MW)}{P_{BASE}}, \quad V_s (PU) = \frac{V_s (V)}{V_{BASE}}.$$

- 3) The inertia constants of the generator rotor and of the turbine rotor and the shaft stiffness are all given with respect to the electric system speed. Therefore, those parameters are:

$$H_G = \frac{\frac{1}{2} J_G \omega_{0G}^2}{P_{BASE}} = \frac{\frac{1}{2} J_G \omega_{BASE}^2}{P_{BASE} N_{EE}^2}, \text{ in s,}$$

$$H_M = \frac{\frac{1}{2} J_M \omega_{0M}^2}{P_{BASE}} = \frac{\frac{1}{2} J_M \omega_{BASE}^2}{P_{BASE} N_{ME}^2 N_{EE}^2}, \text{ in s,}$$

$$K_s = \frac{\kappa}{P_{BASE}} \cdot \frac{\omega_{BASE}}{N_{ME}^2 N_{EE}^2}, \text{ in PU/el.rad.}$$

Here J_G and J_M are inertia of the generator rotor and the turbine rotor, respectively, in kgm^2 , ω_{0G} and ω_{0M} are the mechanical rotational speed of the generator rotor and the turbine rotor, respectively, in mech.rad./s , N_{ME} and N_{EE} are the gearbox ratio and the number of pole-pairs of the generator, respectively, and κ is the shaft torsional stiffness in kgm^2/s^2 .

The typical dataset of a fixed-speed wind turbine is given in **Table 4.A.1**.

Parameter	Value	Parameter	Value
Rated Power	2 MW	Magnetising Reactance	3.80 PU
Rated Voltage	690 V	Rotor Resistance	0.018 PU
Rated Frequency	50 Hz	Rotor Reactance	0.12 PU
Rated Slip	0.02	Generator Rotor Inertia	0.5 s
Stator Resistance	0.048 PU	Turbine Rotor Inertia	2.5 s
Stator Reactance	0.075 PU	Shaft Stiffness	0.3 PU/el.rad.

Table 4.A.1. Typical data for a 2 MW fixed-speed wind turbine equipped with an induction generator.

Appendix 4.B. Validation of wind turbine model from measurements

Validation of the wind turbine model is made with use of the results of:

- 1) An islanding experiment of the Rejsby Hede wind farm (Pedersen et al., 2000) and (Pedersen et al., 2003).
- 2) A tripping – re-connection experiment executed at the Nøjsomheds Odde wind farm (Raben et al., 2003).

In the both cases, the results of the experiments are kindly offered to this Ph.D. project by the Danish power system operator ELTRA and by the Danish power distribution company SEAS. The experiments and the results of the validation work have been published in the articles:

J. K. Pedersen, K.O.H. Pedersen, N.K. Poulsen, V. Akhmatov, A.H. Nielsen, Contribution to a dynamic wind turbine model validation from a wind farm islanding experiment, *Electric Power Systems Research*, 2003, vol. 64, no. 1, pp. 41-51.

N. Raben, M.H. Donovan, E. Jørgensen, J. Thisted, V. Akhmatov, Grid tripping and re-connection: Full-scale experimental validation of a dynamic wind turbine model, *Wind Engineering*, vol. 27, no. 2, pp. 205 -13.

Therefore this issue has been removed from this thesis. Order you copies at your library or from the publishers Elsevier Science, respectively, Multi-Science Publishing. In the validation work, the two-mass model of the wind turbine shafts has been validated, which has been the primary goal of this validation. Secondly, the model of induction generators has been validated and explained from measurements.

The description below presents more (unpublished) validations of the dynamic wind turbine model.

4.B.1. A case of full-scale validation: Tripping – re-connection of a wind turbine

The majority of the wind turbines in the local sites in Denmark are with fixed-speed wind turbines of the so-called Danish concept. This wind turbine concept is characterised by a three-bladed turbine rotor, a shaft system with a gearbox and an induction generator. Furthermore, the wind turbines can be with the blade-angle control, which can be either pitch or active-stall, for power optimisation at the wind below the rated wind speed. At strong wind, the blade angle control is used to maintain the rated operation point of the wind turbine.

The Rødsand /Nysted offshore wind farm has been taken in operation in eastern Denmark in the year 2003. This wind farm consists of seventy-two fixed-speed, active-stall controlled wind turbines of the Danish concept. The wind turbines are from the manufacturer Bonus Energy. The rated power of the Rødsand wind farm is 150 MW. The wind farm is connected to the transmission power network (at 132 kV voltage level) of the Danish island of Lolland. This large wind farm must comply with the Specifications of the Danish TSO (Eltra, 2000). At transient disturbances in the transmission power network, voltage must re-establish without subsequent disconnection of the

large wind farm.

As known from modelling issues (Akhmatov et al., 2000(a)), the wind turbines of this concept are characterised by a relatively soft coupling between the turbine rotor and the induction generator rotor. This soft coupling is present because the turbine rotor and the induction generator rotor are connected through the shaft of a relatively low stiffness. Typical values of the shaft stiffness of the wind turbines of the Danish concept are the ratio 30 to 100 lower than the shaft stiffness of the conventional power plant units, when measured in PU/el.rad. (Hinrichsen and Nolan, 1982). Therefore the shaft systems of the wind turbines must be represented by the so-called two-mass model. These two masses represent the turbine rotor and the generator rotor, respectively.

The dynamic wind turbine model consists of (i) the induction generator model with representation of the dc-offset in the machine current, (ii) the shaft system represented by the two-mass model and (iii) the aerodynamic model of the rotating turbine. This model has been described in **Section 4** of this thesis. The shaft representation given by the two-mass model has been the most affected part of this simulation model, which is used for investigations of short-term voltage stability. Before this model has been published (Knudsen and Akhmatov, 1999), the wind turbine shafts were considered stiff and the turbine inertia and the generator rotor inertia were lumped together. This is the lumped-mass model.

With representation of the shaft system by the two-mass model and with application of relatively low values of the shaft stiffness, the wind turbine model has predicted the following phenomena (Akhmatov et al., 2000(b)).

- 1) Oscillations of the voltage, the machine current, the electric and the reactive power and the speed of the induction generators of fixed-speed wind turbines at a short-circuit fault in the power network. The natural frequency of such oscillations is the shaft torsional mode and in the range from one to few Hz, which depends on the shaft construction and data.
- 2) Slower re-establishment of voltage in the power grid after the grid fault has cleared and larger demands of dynamic reactive compensation than predicted with use of the lumped-mass model.

Prediction of more demands of dynamic reactive compensation to be grid-incorporated for the same amount of grid-connected wind power seems to be more serious than a risk of voltage oscillations after the fault has cleared. This is because such prediction of more demands of dynamic reactive compensation implies more cost of the total solution with grid-incorporation of wind power than predicted with use of the lumped-mass model.

The Danish power distribution company SEAS has planned and executed a number of experiments to clarify the complexity details, which are needed to model the electricity-producing wind turbines of the Danish concept in investigations of short-term voltage stability. A number of these experiments have been executed at the Nøjsomheds Odde wind farm grid-connected in the area of SEAS. This wind farm consists of twenty-four fixed-speed, active-stall controlled wind turbines equipped with induction generators. The results of this experimental work are of practical interest because:

- 1) The wind turbines are of the same concept which is present in the Rødsand /Nysted offshore wind farm. But the wind turbines in the Nøjsomheds Odde wind farm are of 1 MW rated power.
- 2) The wind turbines are from the manufacturer Bonus Energy, which has also supplied the wind turbines to the Rødsand /Nysted offshore wind farm.

This experimental work has been realised in co-operation with (i) the consulting company Hansen & Henneberg (Copenhagen, Denmark) assisted with measurements, (ii) the manufacturer Bonus Energy contributed with their knowledge about wind turbines and exact data and (iii) the power distribution company NESA assisted with experiment planning and simulations.

Here, the experiment with tripping and re-connection of a selected wind turbine is described. *The main target of this experiment has previously been the validation of the shaft system representation with use of the two-mass model. This target has originally been set because the shaft system representation with use of the two-mass model and the results predicted by this model with respect to voltage stability have been of the most concerns. Later, the validation work has been extended and the results of this experiment have also been used to perform the full-scale validation of the wind turbine model.* The measurements were kindly given by the company SEAS to this industrial PhD project.

The induction generator has been modelled with use of the fifth-order model with representation of the stator current transients. This model is of a higher order than commonly applied in voltage stability investigations – the common third-order induction generator model (Kundur, 1994). The results of this experiment have also been applied to validate this fifth-order induction generator model.

The description of the experiment is given in Section **4.B.1.1**. The details about the wind turbine model are shortly given in Section **4.B.1.2**. The validation work is presented in Section **4.B.1.3**.

4.B.1.1. Experiment

The experiment has been carried out on the Nøjsomheds Odde wind farm in the year 2002. The wind farm is placed in the Danish island of Lolland, just south to the main island of Zealand, see the map in **Fig. 11.1**. The wind farm is separated into four sections, which are organised along the 10 kV underground cable sections with six wind turbines in each section. This cable network is the internal network of the wind farm. Through the 0.7 / 10 kV transformers, the wind turbines are connected to the internal network of the wind farm. The wind farm is connected to the local 50 kV distribution power system through the 10 / 50 kV transformer and, then, through the 50 / 132 kV transformer to the transmission network of the island of Lolland. The short circuit capacity at the connection point viewed into the transmission network (132 kV voltage level) is 350 MVA.

A fragment of the wind farm with relation to the experiment is shown in **Fig. 4.B.1**. Before the start of the experiment, the induction generators and the no-load capacitors of the wind turbines WT 02 to WT 06 were tripped and these wind turbines were temporarily stopped. After the experiment, these wind turbines should be re-connected and continue their normal operation. This implies that the induction motors of these wind turbines were still in operation for forced cooling of the

induction generators of the tripped wind turbines and keeping other vital functions on stand-by. Only the wind turbine WT 01 in the wind farm section 1 was in operation during the experiment.

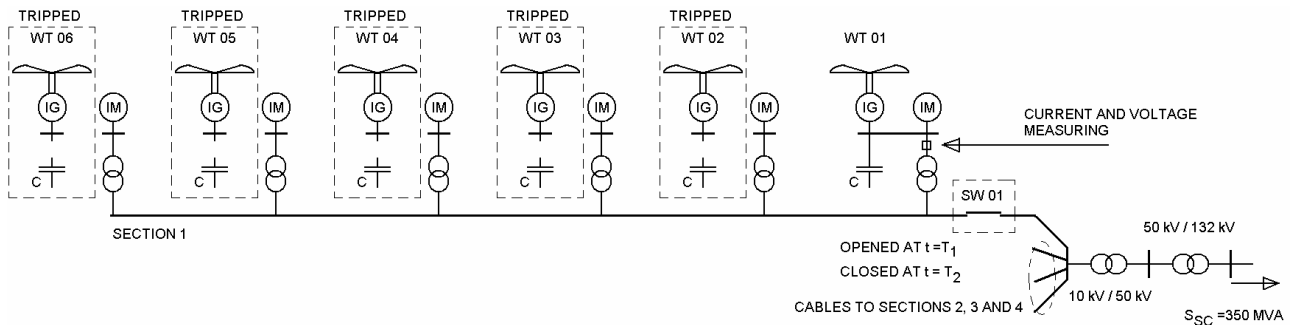


Fig. 4.B.1. A fragment of wind farm with the wind turbine WT 01 from the tripping – re-connecting experiment. Reported in (Raben et al, 2003).

The tripping – re-connection experiment described in this work was carried out at light wind. This condition was needed to reach a successful re-connection of the wind turbine WT 01 to the power system.

At strong wind, excessively large transients in the machine current would occur at re-connection and cause protective disconnection of the wind turbine. This behaviour was seen in a number of experiments factually executed at strong wind (up to 80% of rated power). Second, unacceptably large spikes in the electric torque would occur at re-connection at strong wind and affect the gearbox. As clarified from the simulations at the planning stage, the machine current transients and the torque spikes would presumably reach up to 10 times of the rated machine current, respectively, the rated electric torque at re-connection at rated operation (Raben et al, 2003).

The target has naturally been a non-destructive experiment. Notify that the experiments should be accepted by the power distribution company, the wind farm owners and the wind turbine manufacturers before this could be realised (Raben et al, 2003).

At the time of tripping, T_1 , the switch SW 01 was opened and the section 1 with the wind turbine WT 01 was at islanded operation with the induction motors of the section 1 and its internal network given by the impedance of the cables and the transformers and the cable charging. The duration of islanded operation was about 500 ms in this experiment.

At the time of re-connecting, T_2 , the switch SW 01 was closed and the section 1 with the wind turbine WT 01 was re-connected to the power system. During the experiment, the voltage and the current at the low-voltage side of the 0.7 / 10 kV transformer of the wind turbine WT 01 were measured, as indicated in **Fig. 4.B.1**. The sampling frequency of the measurements was 1 kHz. Therefore delays in the measured signals produced by the equipment can be neglected.

At islanded operation, the no-load capacitor of the wind turbine generator WT 01 was kept connected to the grid. This was for reduction of a possible voltage drop at the terminals of the wind turbine WT 01 at the islanded operation.

The measured behaviour of the phase current, I_L , and the phase-to-phase voltage, V_{LL} , are given in **Fig. 4.B.2**. The current of the no-load compensated induction generator of the wind turbine WT 01 was not zero at islanded operation because the induction motors in the section 1 absorbed an

amount of electric power produced by the wind turbine generator. An amount of reactive power was also exchanged throughout the internal network of the section 1, when taking into account the no-load impedance of the transformers and the cable charging.

At islanded operation and shortly after re-connection, higher harmonics of the fundamental frequency were seen in the measured current. These harmonics were caused by the induction machines, which is reported in previous investigations (Pedersen et al., 2000). The measured voltage had no (significant) drop at islanded operation.

At the time of tripping, $t = T_1$, there was no dc-offset in the measured phase current. However, there was a notable dc-offset in the measured current at the time of re-connection, $t = T_2$. The dc-offset at tripping was absent because opening of the switch SW 01 occurred separately in the three phases, e.g. single phases were disconnected at the phase currents passing through zero in each single phase. This mechanism eliminated the dc-offset in the phase current at tripping.

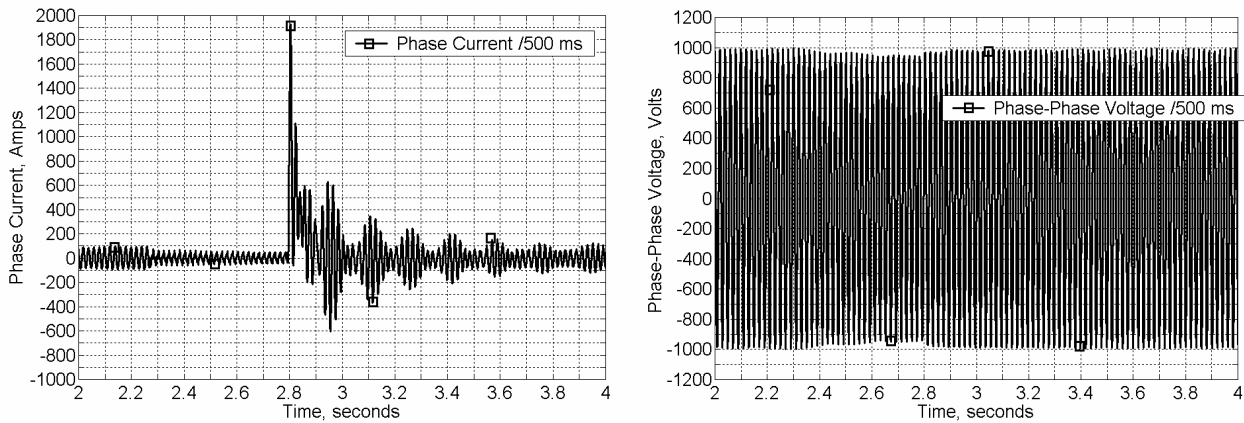


Fig. 4.B.2. Measured phase-current and phase-to-phase voltage. Time of islanded operation is 500 ms.

Closing of the switch SW 01 occurred abruptly at the same time, $t = T_2$, in all the three phases. This abrupt switching-on caused the dc-offset in the phase current at re-connection. This information about switching of the contactors is of a common knowledge. This behaviour is mentioned because this can be important for the generator model assumptions in dynamic simulation tool PSS/E, which has been applied in simulations. This dynamic simulation tool does not contain representation of fundamental-frequency transients in its standardised generator model or in its network solutions.

During and after islanded operation, the voltage magnitude is almost unchanged. The machine current shows a fluctuating behaviour after re-connection has been made. The natural frequency of the current fluctuations is about 7 Hz and cannot only be explained by the dynamic behaviour of the induction generator. The value of the natural frequency indicates that the current fluctuations may relate to the torsional oscillations of the shaft system of the wind turbine WT 01.

4.B.1.2. Computational work

The validation of the dynamic wind turbine model from the tripping – re-connection experiment has been carried out with use of the tool PSS/E. At the moment of these investigations, the simulation

tool PSS/E did not contain any model of electricity-producing wind turbines of sufficient complexity. Therefore, these investigations were carried out with use of the user-written dynamic model of grid-connected wind turbines described in **Section 4**.

The dynamic simulation tool PSS/E is commonly applied in investigations of power system stability of large power systems. The power network models in the simulation tool PSS/E are established by the positive-sequence equivalents, which is a reasonable and acceptable consideration in investigations of power system stability. However, this may introduce a number of restrictions on representation of the transient behaviour in the electric machines and the transient events.

With use the dynamic simulation tool PSS/E, simulation of balanced, three-phased events is possible. The dynamic simulation tool PSS/E is the fundamental-frequency tool, which implies that possible frequency deviations of the simulated events are in the range of 10 % of the nominal electric grid frequency. Higher harmonics of the fundamental frequency are not represented in the simulation tool. Furthermore, all the standardised generator models in the dynamic simulation PSS/E are reduced-order models where the fundamental-frequency transients of the machine currents are disregarded. The last mentioned consideration is in agreement with the interface of the dynamic simulation tool PSS/E and with the common idea of power stability investigations of large power networks. Such assumptions are acceptable in simulations of balanced events in the grid and also in modelling of synchronous generators of large power plants (Kundur, 1994).

From the description above, it becomes clear that the dynamic wind turbine model must have a more advanced model of the induction generator and go beyond the standardised model frames of the dynamic simulation tool PSS/E to perform the validation work with use of the data of the tripping – re-connection experiment.

4.B.1.2.1. Assumptions on dynamic wind turbine model

The dynamic model of fixed-speed, active-stall controlled wind turbines is described in **Section 4**. The control system of active-stall is not present in this validation work. This control system has been by-passed in the simulations of this validation work due to the assumption that this control is relatively slow and does not influence the short-term behaviour of the wind turbine. This means that the blade angle, β , has kept constant in simulations. This simplified representation corresponds to fixed-pitch operation of the wind turbines.

4.B.1.2.2. Induction generator model

The model complexity of induction generators to be applied in investigations of short-term voltage stability has been discussed in **Section 4**. In this presentation, the model complexity is related to the transient events of the experiment.

The balanced three-phased disturbances, which can either be a three-phased short-circuit fault or closing of a three-phased line, may cause the dc-offset in the machine current of the induction generators (Knudsen and Akhmatov, 1999). The dc-offset may be strongly represented in the machine current in the situations when (i) the voltage sudden changes or drops in the vicinity of the

generator terminals and (ii) the generator has been close to its rated operation. This can be present when the voltage drops at the moment of a three-phased short-circuit fault in the power network.

As explained in (Knudsen and Akhmatov, 1999), the dc-offset in the machine current must not be neglected when modelling an induction generator which is subjected to such short-circuit faults. It is because this transient current behaviour influences the braking torque of the induction generator when the fault has occurred. This behaviour of the braking torque influences again the generator rotor speed during the faulting time and, then, the voltage profile after the fault has cleared (Knudsen and Akhmatov, 1999).

In this particular case, the transients in the machine current have occurred at re-closing of the switch SW 01. Presence of the dc-offset in the machine current must be reflected in the model equations of the induction generator.

At unbalanced three-phased disturbances, which can either be tripping of a three-phased line or opening of a switch, the dc-offset in the machine current is eliminated. In the case of the dynamic simulation tool PSS/E, which is built-up about simulation of balanced events in the power grid, this compliance (absent fundamental-frequency transients at three-phased unbalanced events) is achieved with use of the model equations where the fundamental-frequency transients in the stator fluxes have been omitted. In the case of induction generator, this corresponds to use of the common third-order model (Kundur, 1994).

In other words, the induction generator model must predict sufficiently accurate results in the case of balanced as well as unbalanced events in the power grid. This validation work is interesting because the induction generator of the wind turbine WT 01 is subjected to balanced as well as unbalanced three-phased events in the same sample.

In the experiment, the voltage magnitude is, practically said, unchanged at islanded operation. The experiment has been carried out at light wind, which is why the induction generator of the wind turbine WT 01 has been significantly below the rated operation point. Such conditions could be applied to argue for use of the common third-order induction generator model in the validation work. On the other hand, the duration of islanded operation has been large. This has resulted in a notable dc-offset at re-connection. For evaluation of the induction generator model complexity needed in such situations, the simulations have been carried out with two models of the induction generator. The first model contains representation of the dc-offset in the generator equations, which must be active at re-connection, whereas the second model is the common third-order model without such representation of such transient behaviour.

Notice that it is necessary to add the current of the induction generator and the current of the no-load capacitor to perform validation of the phase current in simulations. This notification is in accordance to the measuring scheme of the experiment. The current of the no-load capacitor may contain transients at tripping and re-connection sequences (Larsson and Thiringer, 1995). This behaviour has however been neglected in these simulations according to the interface of the dynamic simulation tool PSS/E.

4.B.1.2.3. Shaft system model

The mechanical system of the wind turbine is represented with use of the two-mass model according to the description given in **Sections 2.2**. A single simulation with use of the lumped-mass model has also been made for comparison with the results predicted with use of the two-mass models.

4.B.1.3. Wind turbine model validation

At the start of the validation work, it is necessary to implement the equivalent of the wind farm internal network with the grid-connected wind turbine and the induction motors in the section 1. The data for the internal network of the wind farm including the cables and the transformers have been received from SEAS and the data of the electricity-producing wind turbines are given by the manufacturer Bonus Energy. Notice that the damping coefficients, D_G and D_M , appearing in **Eqs. (2.9)** have not been received from the wind turbine manufacturer. For simplification, these values are set to zero in the simulations.

The data of the induction motors, which have been received, are only their rated power. Neither electrical parameters nor their operational points have been given. Therefore the electrical parameters of the induction motors have been estimated from so-called typical values (Cathey et al, 1973; Ong, 1998), and their operation points have been initialised as described in the next section. The rated power of the induction motors is small in comparison with the power generated by the wind turbines. Therefore it can be considered that uncertainty of the induction motor data will result in a relatively small uncertainty and so in a small inaccuracy of the simulated results.

4.B.1.3.1. Network model and initialisation

It is essential that the network equivalent is set-up and initialised in an appropriate way. The model of the internal network of the wind farm connected to the local power system (at the 50 kV and the 132 kV voltage levels) has been implemented in the simulation tool PSS/E. This model is similar to the configuration of the wind farm network fragment shown in **Fig. 4.B.1**. In the case of the wind turbines WT 02 to WT 06, which have been disconnected during the whole experiment, their induction motors have only been represented in the wind farm model.

The values of current and voltage of the wind turbine WT 01, which are measured just before the switch SW 01 has opened, are applied to initialise the induction generator of this grid-connected wind turbine in the farm. The induction motors of the disconnected wind turbines in the section 1 are initialised from the current and the voltage measurements during islanded operation. The numeric value of the complex power of the no-load compensated induction generator of the wind turbine WT 01 is computed from:

$$|S| = \sqrt{P_E^2 + Q_T^2} = \sqrt{3} \cdot V_{LL} \cdot I_L,$$

where S is the complex power, P_E is the electric power of the induction generator, Q_T is the reactive power absorbed by the generator minus the reactive power supplied by the no-load capacitor, V_{LL} is the phase-to-phase voltage and I_L is the phase current.

From the measured behaviour which is shown in **Fig. 4.B.2**, the numeric value of the complex power of the no-load compensated induction generator of the wind turbine WT 01 before islanding has been evaluated to 80 kVA. With use of this result and knowing the data of the induction generator and the no-load capacitor, the initial operation point of the induction generator of the wind turbine WT 01 has been found.

At islanded operation, the measured value of the phase current peak has been in the range from 60 to 65 Amps and the voltage magnitude has not changed significantly. This current represents mainly the electric power absorption of the induction motors in the section 1 of the wind farm. With use of the above-described procedure, the operation points of the induction motors have been evaluated. The induction motors absorb approximately 10 kW per a (disconnected) wind turbine. In the post-following dynamic simulations, the induction motors are computed with use of the standardised PSS/E model CIMTR4, which is the common third-order model of induction machines.

In the dynamic simulations, the reactive current of the no-load capacitor is computed in accordance to the PSS/E interface. This implies absence of the fundamental-frequency transient in the capacitor current at opening and at re-closing of the switch SW 01.

4.B.1.3.2. Simulations with two-mass model

The simulated curves of the current and the voltage magnitude of the wind turbine WT 01 are shown in **Fig. 4.B.3**. Additionally, the generator rotor speed is shown in **Fig. 4.B.4**. The simulated curves are in agreement with the measured curves shown in **Fig. 4.B.2**. The dc-offset is seen in the simulated current, analogously to the behaviour of the measured phase current of the wind turbine generator. Presence of the dc-offset results in the current magnitude of ratio 14 at the time of re-connection, when compared to the current magnitude at undisturbed operation. This result is close to the ratio seen in the measured phase-current (approx. 18).

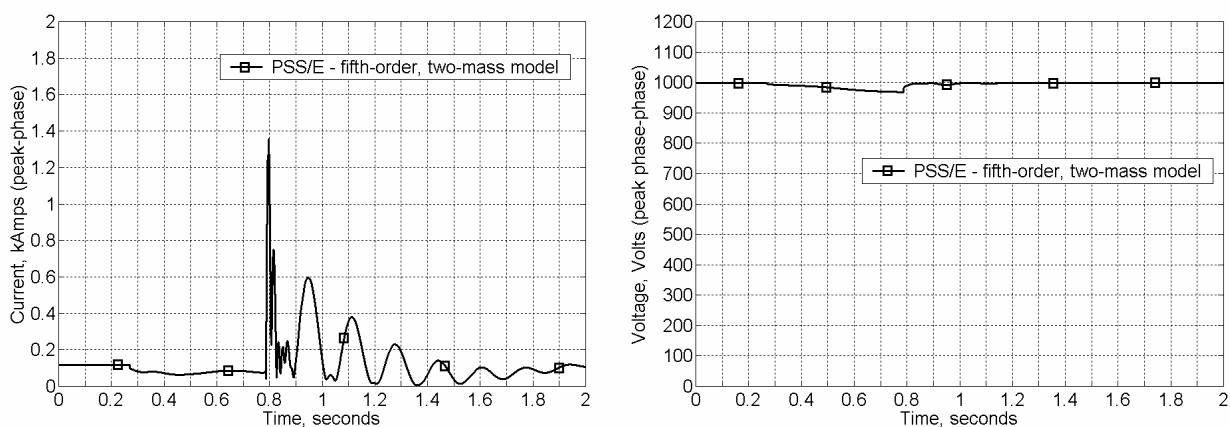


Fig. 4.B.3. Simulated current and voltage magnitude at “the point of measurement”. The two-mass shaft model and the fifth-order induction generator model are applied.

The discrepancy can be due to several reasons. The most plausible are the following.

- 1) The fundamental-frequency current transients in the no-load capacitor are disregarded in the simulations, but these transients are present in the measurements.
- 2) The phase current is measured in a single phase, but the three-phased current-phasor magnitude has been computed. Therefore these values are close to each other, but not necessarily match exactly to each other. Notice that the current-phasor contains the information about the phase-current in all the three phases. The phase currents in the two other phases can have another behaviour which can be characterised by a smaller dc-offset.

The simulated behaviour and the measured behaviour of the current show the same fluctuating behaviour. The natural frequency of these fluctuations in the simulated current is approximately 7 Hz. The fluctuations seen in the current behaviour relate to the shaft torsional oscillations and therefore the same fluctuations are seen in the generator rotor speed. Thus, the fluctuations of the measured phase current, which are seen after re-connection has occurred, can be explained by the shaft torsional oscillations. Notice that the fluctuations of the simulated current of the induction generator follow the oscillations of the generator rotor speed, which confirms the relation between the shaft torsional oscillations and the current fluctuations.

The measured behaviour and the simulated behaviour of the current are characterised with different damping. This difference can be explained by that the damping coefficients, D_M and D_G , are set to zero in simulations, but there is always friction in the rotating parts of the wind turbine construction and, then, damping is not zero in the physical wind turbine.

A very little discrepancy is seen in the natural frequency (7 Hz) of the current fluctuations between the measured and the simulated behaviour. This discrepancy occurs because damping may influence the natural frequency of the shaft torsional oscillations (Akhmatov et al, 2000). On the other hand, this discrepancy is so little that it is assumed negligible. The assumption on the damping coefficients in simulations, $D_G = D_M = 0$, seems to be reasonable in this validation work.

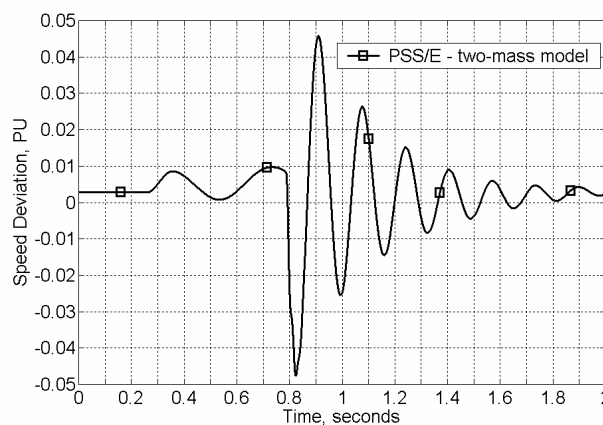


Fig. 4.B.4. Simulated speed deviation (minus slip) of wind turbine generator. The two-mass shaft model and the fifth-order induction generator model are applied.

4.B.1.3.3. Simulations with lumped-mass model

The lumped-mass model corresponds to the assumption that the shaft system of the wind turbine is stiff, $K \rightarrow +\infty$, and the rotating parts of the wind turbine construction are lumped together. According to (Akhmatov et al, 2000(c)), this corresponds to addition $H_G + H_M$. The lumped-mass equations are given by **Eq. (2.6)**. Before the two-mass model has been introduced in (Knudsen and Akhmatov, 1999), the electricity-producing wind turbines were simply computed by the induction generators with large inertia constants in power stability investigations.

The simulated behaviour of the current magnitude and the generator rotor speed is shown in **Fig. 4.B.5**. As can be seen, this simulated behaviour is not in agreement with the measurements because the lumped-mass model of the wind turbine is applied. When the lumped-mass representation is applied, the following discrepancies are seen.

- 1) No fluctuations of the simulated behaviour of the current-phaser magnitude or the generator rotor speed are seen after re-connection has occurred.
- 2) The magnitude of the machine current overshoot at re-connection is much lower than predicted by the two-mass model or seen in the experiment.
- 3) This notification of the current discrepancy at re-connection can be important for relay modelling of the wind turbine generators.

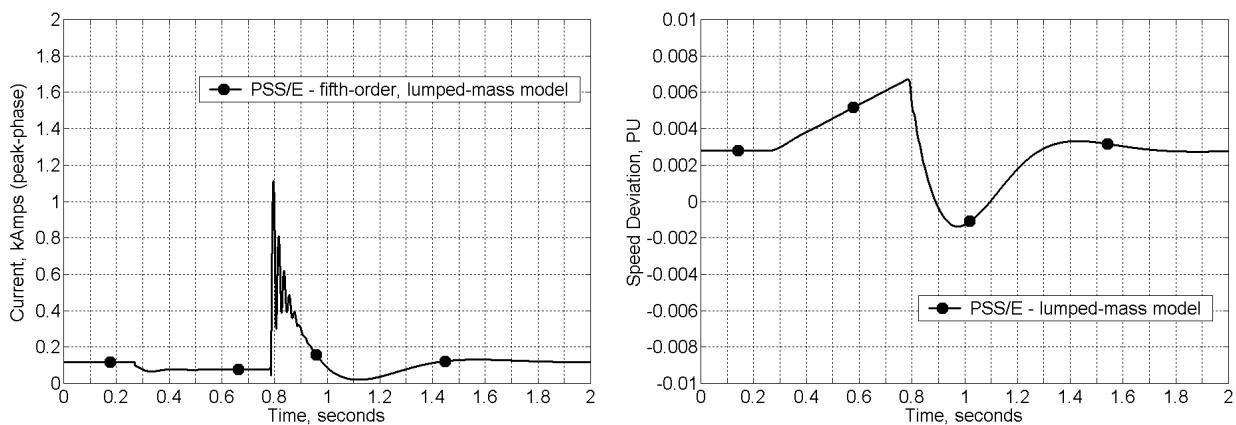


Fig. 4.B.5. Simulated current magnitude and speed deviation (minus slip). The lumped-mass shaft model and the fifth-order induction generator model are applied.

4.B.1.3.4. Simulations with third-order generator model

In this part, the simulation results with use of the common third-order model of induction generators are shown. The shaft system of the wind turbine is given with use of the two-mass model. It is expected that the discrepancy will be seen in the machine current behaviour because the fundamental-frequency transients in the machine current is disregarded at re-connection.

The simulated current-phaser magnitude is shown in **Fig. 4.B.6**. With use of the common third-order model of induction generators, there is no dc-offset in the simulated behaviour of the machine current-phaser. The overshoot of the simulated current-phaser magnitude is of the ratio 8 at the

time of re-connection, when compared to the current magnitude at undisturbed operation. This ratio is much lower than predicted with use of the fifth-order model of induction generators and seen in the experiment. The common third-order model of induction generators predicts this low value of the machine current magnitude at balanced events in the power system because this model does not contain the fundamental-frequency transients in the machine current. In this case such current transients occur at re-connection.

Notice that the fluctuations of the machine current with the natural frequency of approximately 7 Hz are seen in the simulated current behaviour after re-connection has occurred. This behaviour is caused by the shaft torsional oscillations.

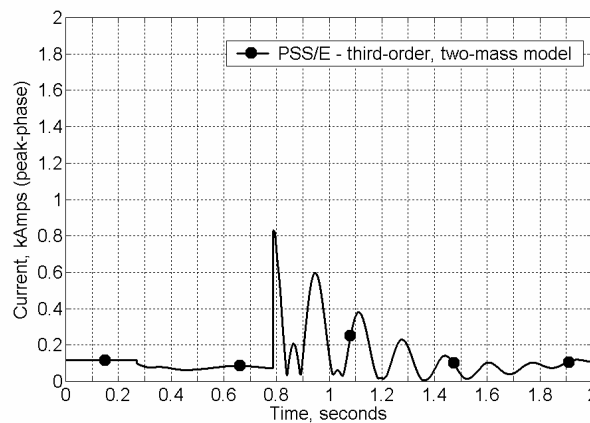


Fig. 4.B.6. Simulated current magnitude. The two-mass shaft model and the third-order induction generator model are applied.

Notice that the experiment applied to the validation work has been carried out at the conditions where it can be difficult to make any definitive conclusions about complexity of the induction generator model, which must be applied in investigations of short-term voltage stability. This is because the representation of the induction generators with use of the higher-order models (with the fundamental-frequency transients in the machine current) is important in the situations when:

- 1) A significant voltage drop occurs in the vicinity of the generator terminals, e.g. at a short-circuit fault in the power grid.
- 2) The induction generators of the wind turbines are at rated operation or so, which is assumed to simulate the worst case.
- 3) At this conditions, the machine current transients will play a part.

In this particular case, the operation point of the induction generator is significantly lower than the rated operation point. Secondly, the terminal voltage magnitude, practically said, does not change during the experiment.

Therefore, the duration of islanded operation has been increased to 500 ms in this experiment to compensate for the conditions when the machine current transients play a part. Notice that the fault duration in the transmission power network can be around 100 ms in the Danish power grid and then this fault will clear with use of the protective relays.

4.B.1.3.5. Discrepancies

Possible discrepancies between the measurements and the simulated results reached with use of the dynamic wind turbine model containing (i) the fifth-order model of induction generators and (ii) the two-mass model of the shaft system need discussion. Although the simulated results reached with use of this dynamic wind turbine model are in good agreement with the measurements, several small discrepancies have been registered. Such discrepancies can be caused by the two basic reasons:

- 1) Restrictions of the simulation tool PSS/E applied in the validation work.
- 2) Uncertainties in the data applied in the validation work.

The restrictions of the simulation tool PSS/E with relation to the validation work have already been mentioned.

- 1) This is the fundamental-frequency tool.
- 2) The simulation tool operates with positive-sequence equivalents of the power systems.
- 3) The fundamental-frequency transients in the machine current are not a part of the simulation tool PSS/E or the standardised generator models found in this tool.

The discrepancies between the measurements and the simulation results, which are caused by the restrictions of the simulation tool, can be the following.

- 1) Presence of higher harmonics in the measurements. Higher harmonics are not in the simulated behaviour of the phase current and the phase-to-phase voltage.
- 2) Presence of unbalanced conditions in the experiment, which is in disagreement with the positive-sequence representations of the network models in the simulation tool.
- 3) Presence of the fundamental-frequency transients in the measured machine current, which is in disagreement with the standardised generator representation in the simulation tool.

The largest discrepancy, which is caused by the restrictions of the simulation tool, between the measurements and the simulation results have presumably been due to absence of higher harmonics in the simulated current-phasor at islanded operation. The other discrepancies in this category are minimised by accurate modelling work.

Uncertainties in the data of the experiment, resulting in the discrepancies, are the following.

- 1) Uncertainties in the data of the wind turbine itself and in the data of the internal network of the wind farm.
- 2) Uncertainty in the initial operation points of the wind turbines and additionally in the operation points of the induction motors.

Among the largest discrepancy between the measurements and the simulation results is due to a lack of the data of the damping coefficients D_G and D_M . This discrepancy is seen when comparing the measured behaviour and the simulated behaviour of the current shown in **Fig. 4.B.2** and **Fig. 4.B.3**, respectively. The other discrepancies with relation to uncertainties in the data have been minimised by careful work with implementation of the wind farm model and accurate initialisation of the model.

Although some discrepancies discussed above have been termed as the largest discrepancies, such discrepancies are very small.

4.B.1.3.6. Results of validation work

The dynamic model of fixed-speed wind turbines equipped with induction generators has been implemented in the dynamic simulation tool PSS/E as a user-written model. This dynamic wind turbine model has applied in practical investigations of short-term voltage stability with incorporation of a large amount of wind power into the eastern Danish power grid. Therefore the validation work has been performed for this model.

In this section, the validation work from measurements of the tripping – re-connection experiment is described. In this experiment, a selected wind turbine in the Nøjsomheds Odde wind farm was at islanded operation with a part of the internal network of the wind farm. Shortly after, the wind farm was again re-connected to the power system. The experiment was carried out on the same type of wind turbines, which have been erected in the Rødsand /Nysted offshore wind farm, but with a lower power capacity than in this offshore wind farm.

The main target of this validation work is the full-scale validation with definition of the complexity details of the dynamic wind turbine model. The wind turbine models of different complexities have been examined and compared to each other and to the measurements. It is found that such models of different complexities can be ranged according to the accuracy of the predicted results. Below, this range of the accuracy of such models is given in the decreasing order when the first model reaches the best accuracy and the last model is characterised by the worst accuracy:

- 1) The dynamic wind turbine model containing the fifth-order model of induction generators and the two-mass model of the shaft system.
- 2) The dynamic wind turbine model containing the common third-order model of induction generators and the two-mass model of the shaft system.
- 3) The dynamic wind turbine model containing the fifth-order model of induction generators and the lumped-mass model of the mechanical rotating system.

This notification is important because it shows that the two-mass model of the shaft system is essential to reach the accurate representation of the fixed-speed wind turbines at the grid faults. This notification shows also the importance of the fifth-order model of induction generators with representation of the fundamental-frequency transients. The dynamic wind turbine model containing the fifth-order model of induction generators and the two-mass model of the shaft system

predicts the best results. The simulated behaviour predicted with use of this model is in a good agreement with the measurements.

Only small discrepancies between the measurements and the simulated results reached with use of this dynamic wind turbine model are present. Such discrepancies have been explained by uncertainties in the wind turbine data (the data for damping are not given) and restrictions of the dynamic simulation tool PSS/E.

The dynamic wind turbine model containing the fifth-order model of induction generators and the two-mass model of the shaft system has been set up in this project and later applied in practical investigations of short-term voltage stability in Denmark and abroad.

4.B.2. Induction generator model validation

The measurements when a wind turbine was subjected to a short-circuit fault with a significant voltage drop are not found in literature. Therefore the response to the short-circuit fault of the user-written model of induction generators in the simulation tool PSS/E has been validated with use of the physical three-phased standardised model of induction generators of the tool Matlab/Simulink. The induction generator model of Matlab/Simulink is a fully-transient model. This validating work is important because investigations of short-term voltage stability cover often situations with balanced three-phased short-circuit faults.

The validation work has made for the common third-order model, respectively, for the fifth-order model of induction generators which are implemented in the dynamic simulation tool PSS/E during this project. This is of importance because the common third-order model is commonly used in investigations of short-term voltage stability and not only with application of the dynamic simulation tool PSS/E.

The fifth-order model of induction generators is with representation of the fundamental-frequency transients in the machine current. This representation is more complex and needs a smaller time step when simulating. This model needs also a more complex implementation in the simulation tool PSS/E because the dynamic interface of this tool corresponds to the common third-order models of such generation units.

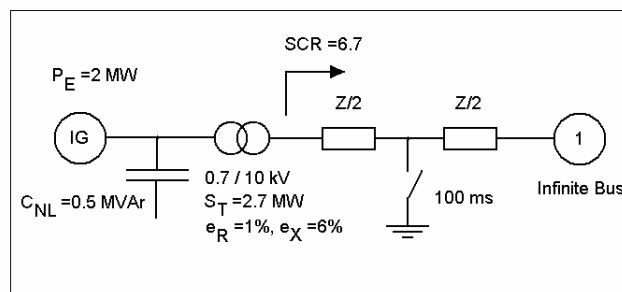


Fig. 4.B.7. Model of the network equivalent with an induction generator.

The validation work has been made with use of a simple network equivalent. It contains the induction generator connected to the infinite bus through a transformer and a line. The induction generator is at rated operation and supplies 2 MW. Its data are given in **Table 4.A.1**. The network

equivalent is shown in **Fig. 4.B.7**. The models of the network equivalents are set up in the simulation tool PSS/E and also in the tool Matlab/Simulink. The models of the network equivalents in these two simulation tools are so close to each other as possible. The transient event is a balanced, three-phased short-circuit fault.

The results of this comparative validation are collected in **Table 4.B.2**. As can be seen, the user-written fifth-order model of induction generators implemented in the tool PSS/E is in agreement with the results predicted by the fully-transient model of Matlab/Simulink. This indicates an accurate implementation of the fifth-order model into the dynamic simulation tool PSS/E.

The results predicted with use of the common third-order model of induction generators seem to show a stronger tendency to over-speeding and to voltage instability of the induction generator. The common third-order model predicts more acceleration of the generator rotor during the transient event than in the case of the transient model of Matlab/Simulink. Generally, this over-acceleration leads to prediction of slower voltage recovery and, in this particular case, to uncontrollable voltage decay after the fault has cleared. Similar conclusions are reached in (Knudsen and Akhmatov, 1999).

The standardised model of induction generators of the simulation tool PSS/E has been the common third-order model CIMTR3, which has been the situation at the start of this project and also when the practical investigations of short-term voltage stability with grid-incorporation of the first large offshore wind farm in Denmark should take place. This explains why implementation of the user-written fifth-order model of induction generators into the dynamic simulation tool PSS/E has been necessary for this project and for the practical stability investigations in Denmark. As the author knows, PTI, which is the supplier of the tool PSS/E, is working on the standardised fifth-order model of induction generators to be offered with the PSS/E package.

Furthermore, the simulated with Matlab/Simulink behaviour of the single-phase machine current, I_L , is compared to the machine current-phasor magnitude, I_S , reached with Matlab/Simulink. As can be seen, the single-phase current magnitude (its peak values) and the three-phased machine current-phasor follow each other. Therefore, the measured single-phase current, I_L , can be applied for model validation when the validation has been made against the simulated behaviour of the machine current-phasor magnitude, I_S . This is only valid on the assumption that the single-phase current, applied for validation, is with a developed dc-offset. This is the case, which has been applied for the validation work described in **Appendix 4.B.1**.

These two behaviours of the currents, I_L and I_S , are close to each other, but does not match exactly. The small discrepancy is present because the single-phase currents in the two other phases are not necessarily with developed dc-offsets.

The validation work and the conclusions reached from this work must be treated very carefully. Notify, for example, that the fifth-order model of induction generators implemented in the dynamic simulation tool PSS/E predicts the fundamental-frequency transients in the machine current when the fault has occurred, but such transients are suppressed when the fault has cleared. This behaviour is also seen in the current-phasor magnitude predicted with use of Matlab/Simulink. This specific behaviour deals with how the fault has occurred and how the fault has cleared.

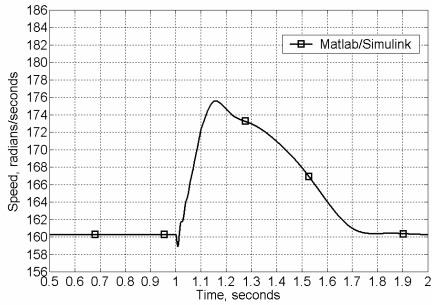
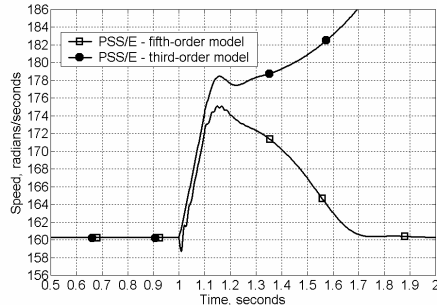
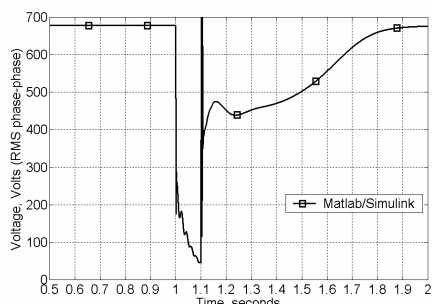
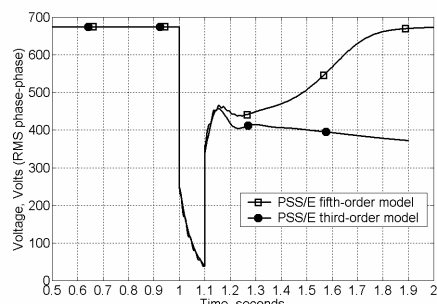
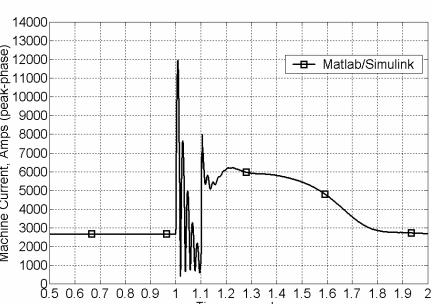
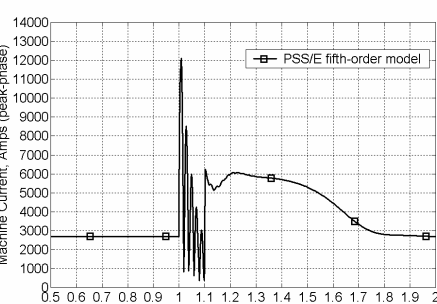
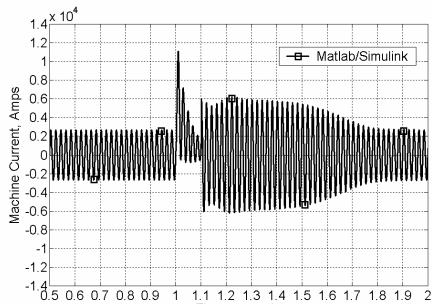
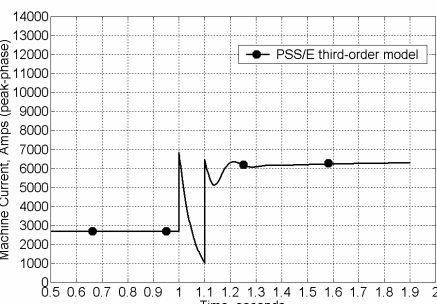
Transient model of Matlab/Simulink	User-written model in PSS/E
 <p>Generator rotor speed – Matlab/Simulink.</p>	 <p>Generator rotor speed – PSS/E.</p>
 <p>Terminal voltage – Matlab/Simulink.</p>	 <p>Terminal voltage – PSS/E.</p>
 <p>Machine current magnitude – Matlab /Simulink.</p>	
 <p>Machine current in one phase – Matlab /Simulink.</p>	 <p>Machine current magnitude – PSS/E.</p>

Table 4.B.2. Comparing between the results of the fully-transient, standardised model of induction generators of Matlab/Simulink and the results of the user-written models of induction generators implemented in the tool PSS/E (the third- and the fifth-order models).

The fault has occurred abruptly in all the three phases, which is a balanced three-phased event. Therefore, the fundamental-frequency current transients must be present at this operation situation.

The fault has cleared at the phase-currents pass zero, which makes this event to be an unbalanced three-phased event. Therefore the fundamental-frequency current transients must be suppressed in this situation. The model of induction generators must recognise such events to predict an appropriate behaviour of the machine current.

When the user-written model implemented into the tool PSS/E is a higher-order transient model and does not recognise the difference between balanced and unbalanced three-phased events, there is a risk that this model would predict fundamental-frequency transients in the machine current at any kinds of events. This behaviour would be in contrast to physical behaviour of induction generators.

In the model presented in this work, such details have been implemented in the user-written fifth-order model of induction generators. This has resulted in accurate predictions, but complicated the generator model.

Appendix 6.A. Induction generator parameters vs. transient voltage stability

Electric parameters of grid-connected induction generators may influence short-term voltage stability of the power grid (Akhmatov et al, 2000(c)).

Fig. 6.9 shows that the critical speed, ω_{CR} , of an induction generator may be increased by simply increase of the rotor resistance. In this case, short-term voltage stability has been improved as well. In the following, the relation between electric parameters of the grid-connected induction generators and short-term voltage stability of the power grid is shown.

The simulations have been made with the induction generator data given in **Appendix 4.A**, in case of tiny generator rotors, $H_G = 0.5$ s. The power system, which is modelled in this investigation, is relatively strong. Its equivalent is shown in **Fig. 6.A.1**. The electric power network consists of an infinite source (bus 101), a line, and an induction generator (bus 102). The induction generator power rating is 0.5 MW and the short circuit capacity in the connection point is 4.0 MVA, i.e. an approximate ratio of 8. The induction generator is at rated operation at pre-faulted operation. The disturbance is a three-phase short-circuit fault applied to the induction generator terminals.

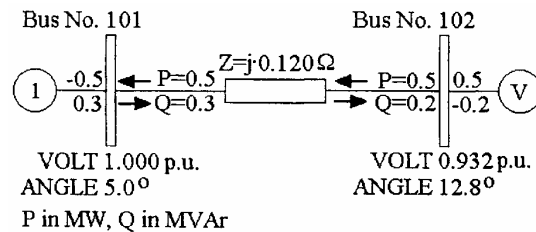


Fig. 6.A.1. Configuration of a simple (strong) network. Reported in (Akhmatov et al, 2000(c)).

The simulation results at different electric parameters of the induction generator are shown in **Fig. 6.A.2**.

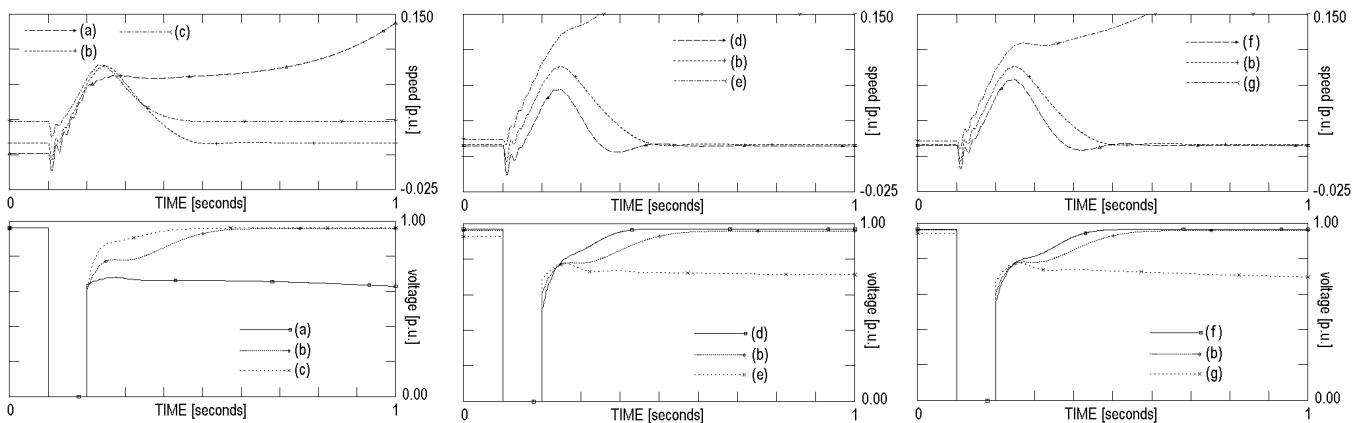


Fig. 6.A.2. Dynamic behaviour of speed and terminal voltage. Influence of generator parameters on dynamic stability: (a) $-R_R \cdot 1/2, X_R \cdot 1, X_S \cdot 1$, collapse, (b) $-R_R \cdot 1, X_R \cdot 1, X_S \cdot 1$, recovery, (c) $-R_R \cdot 2, X_R \cdot 1, X_S \cdot 1$, recovery, (d) $-R_R \cdot 1, X_R \cdot 1/2, X_S \cdot 1$, recovery, (e) $-R_R \cdot 1, X_R \cdot 2, X_S \cdot 1$, collapse, (f) $-R_R \cdot 1, X_R \cdot 1, X_S \cdot 1/2$, recovery, (g) $-R_R \cdot 1, X_R \cdot 1, X_S \cdot 2$, collapse. Reported in (Akhmatov et al, 2000(c)).

The value of magnetising reactance, X_M , influences maintaining of short-term voltage stability in a similar way as the values of X_S and X_R . Investigations on this are carried out, but without presentation of the simulated curves.

The value of stator resistance, R_S , has also influence on transient voltage stability of power grids with induction generators. This influence is, however, slight because the values of stator resistance are typically small compared with other impedance values in the induction generator. **Fig. 6.A.3** illustrates the influence of stator resistance on transient voltage stability. In this example, increase of the stator resistance does not lead to fatal consequences with respect to the dynamic stability. But it can be seen that larger values of the stator resistance result in worsening of dynamic stability.

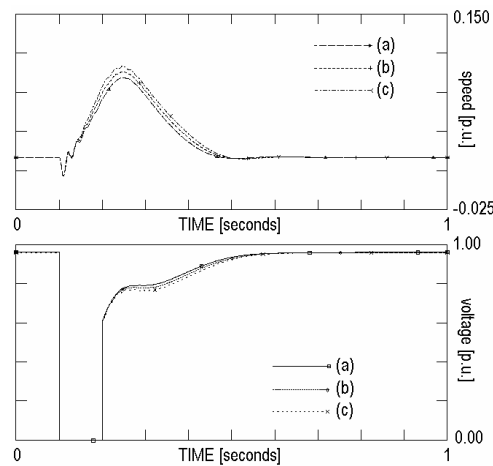


Fig. 6.A.3. Dynamic behaviour of speed and terminal voltage, influence of stator resistance on dynamic behaviours: (a) $-R_S/2$, (b) $-R_S/1$, (c) $-R_S/2$. Reported in (Akhmatov et al, 2000(c)).

Here, we may repeat our statement from **Section 6.10** that short-term voltage stability of the power system is improved when the induction generator parameters are:

- 3) The values of the stator resistance, R_S , the stator reactance, X_S , the magnetising reactance, X_M and the rotor reactance, X_R , are reduced.
- 4) The value of the rotor resistance, R_R , is increased.

A special issue⁵⁵: Application of high-temperature superconducting components with large wind farms

Dynamic models of a high-temperature superconducting cable (HTSC) and a superconducting fault current limiter (SFCL) are developed and implemented in the dynamic simulation tool PSS/E. The models of the HTS devices are applied in investigations of short-term voltage stability. Feasibility of such HTS components to be used together with large wind farms is investigated. A number of practical problems with relation to transient behaviour of the superconducting components are notified.

SI.1. Background

The idea to apply HTS components such as SFCL for current limiting at a short-circuit fault is described in many publications (Öhrström and Söder, 2003). This idea is based on the fact that the superconducting material goes from the superconducting state (zero dc-resistance) to the normal state (high resistance) when the current, $I(t)$, or the temperature, $T(t)$, of the HTS material exceed their respective critical values I_C and T_C (Sheahen, 1994). In such situations, the resistance of the HTS device, $R(t)$, may almost instantaneously change from zero to a finite high value. This reduces the fault current and may also improve the transient stability of the power system. When the short-circuit fault has been cleared, the HTS material should return to the superconducting state and normal operation of the power system will re-establish.

With this argumentation, application of HTS components would be attractive to improve short-term voltage stability of large wind farms. The superconducting current-limiting device could be placed at the wind farm connection point. Practically said, there are no delays in the transition process between the superconducting state and the normal state. This superconducting device would act immediately and prevent a significant voltage drop at the wind farm terminals. Ideally, the HTS device should replace dynamic reactive compensation to be commissioned with the large wind farm.

Notify that this idea should work in situations where the short-circuit current transients are significantly larger than the line current magnitude in normal operation.

SI.2. Wind farm model

The large wind farm consists of eighty 2 MW fixed-speed wind turbines equipped with induction generators. The wind farm supplies 150 MW to the 132 kV transmission network. The wind farm model has been described in **Section 6.7** and implemented in the simulation tool PSS/E.

⁵⁵ This special issue was not a part of the PhD thesis submitted to the supervisors and the censors to evaluate this work. The author has however chosen to include this issue into the final thesis to share the results with the readers of this thesis. This decision has been taken after the author saw the presentation at the Wind Power Workshop in Billund, Denmark, Oct. 2003, covering a similar topic (Öhrström and Söder, 2003). The work presented in this special issue is dated summer 2001, but has not been published before.

A short-circuit fault is subject to a 132 kV line in the transmission network on-land. The fault duration is 150 ms and the fault is cleared by tripping of the faulted line.

IS.3. Simplified model of superconducting fault-current limiter

In this case, the 20 km, 132 kV sea / underground cable connecting the large wind farm with the transmission power network. At the cable end in the connection point on-land, there is placed a SFCL.

Commonly, superconducting fault-current limiters are treated as switches with two levels of the electric resistance. When the HTS material is in the superconducting state, the resistance is zero or small. When the HTS material is in the normal state, the resistance is large.

There are a number of common assumptions applied to perform a simplified representation of such SFCL in short-term voltage stability investigations. The HTS material is in the superconducting state at normal operation of the power grid. When a short-circuit fault occurs, the SFCL has switched to the large-resistant, normal state. The transition time is a few ms. The SFCL is in the normal state so long as the short-circuit fault is applied and its large resistance in the normal state is kept constant (independently from the current going through the SFCL itself).

In the simulation example, it is assumed that the transition time of the SFCL from the superconducting state to the normal state is 5 ms. The transition begins immediately after the short-circuit fault has occurred. The resistance of the SFCL in the normal state is the parameter of the investigations and can be in the range of several ohms. This value is kept constant so long as the SFCL is in the normal state. The simulation results are shown in **Fig.IS.3.1**.

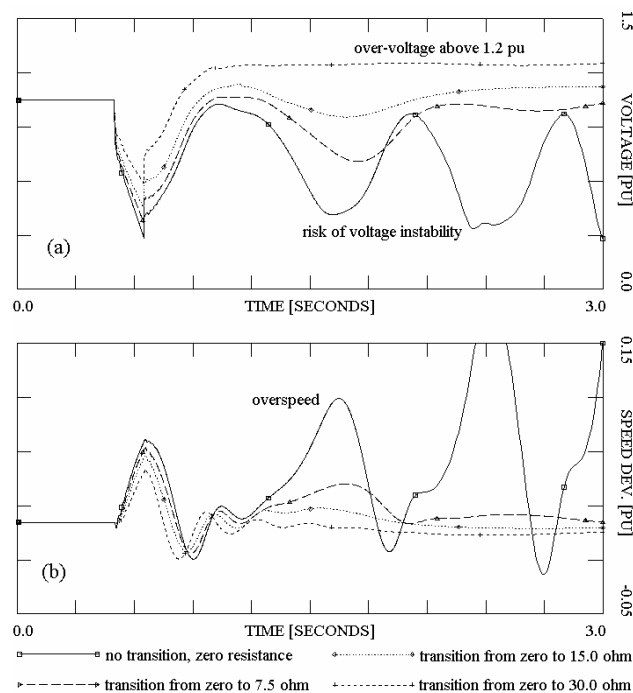


Fig.SI.3.1. Result of resistance increasing in SFCL at a short circuit fault. Terminal voltage – (a) and speed deviation – (b) in the windmill WT01 in the farm at different values of the resistance of SFCL in the normal state.

In other words, the simplified model of the SFCL is performed as a switch with a delay time of 5 ms between the two pre-defined resistance values. As seen from the simulations with use of the simplified SFCL model, increase of the SFCL resistance reduces the voltage drop and improves short-term voltage stability. When the resistance is excessively large, there can be a risk of over-voltage, which may follow to protective disconnection of the wind turbines (Eltra, 2000). Such a risk can be if the HTS material applied in the SFCL does not return to the superconducting state immediately after the voltage re-establishment.

The optimal values of the SFCL resistance in the normal state are in the range of 15 ohm, which is reached with the simplified model. Improvement of short-term voltage stability can be explained by the fact that the SFCL operates as a large power load absorbing the electric power from the wind turbines at the short-circuit fault. Therefore the wind turbines do not accelerate much during the fault. Application of such superconducting devices seems to prevent fatal over-speeding of the wind turbines and stabilise operation of the large wind farm.

However, these conclusions are reached with use of the simplified model of such superconducting devices. There is a risk that the simplified models disregard physics of such superconducting components, which is why they may produce inadequate results.

IS.4. Physical approach of HTS components

A simplified representation of a HTS device as a switch between the two resistance values is not always sufficient in investigations of short-term voltage stability. A physical approach of such HTS components with the current- and temperature- dependence of the line resistance should be taken into account. Furthermore, this physical approach should be applied in all the three phases of the HTS component been incorporated into the ac-grid. A suitable representation of the cooling mechanisms may also be required.

IS.4.1. Current- and temperature- dependence of line resistance

Generally, a superconducting material can be in one of the three states:

- 1) The superconducting state (zero dc-resistance),
- 2) The flux-flow state, and
- 3) The normal state (large resistance).

The flux-flow is the transition area between the superconducting and the normal states. Being in the superconducting state, the resistance in dc-mode is zero, but the ac-resistance of HTS material is finite and must be modelled as being in the flux-flow state (Jensen, 2003). In the flux-flow state, the resistivity of the HTS material is commonly given as the power-law.

$$\rho_{HTS} = \rho_C \cdot \left(\frac{I(t)}{I_C} \right)^{n-1} \cdot \left(\frac{T_C - T_0}{T_C - T(t)} \right)^n, \quad (\text{IS.4.1})$$

where ρ_C is the critical flux-flow resistivity, I_C is the critical current, T_C is the critical temperature of the superconducting material, T_0 is the initial operational temperature of the HTS component. The symbols $I(t)$ and $T(t)$ denote the current peak-magnitude and the temperature of the HTS material, respectively.

In the normal state, the resistivity of the HTS material is temperature-dependent as:

$$\rho_{HTS} = \alpha_{HTS} \cdot T(t) + \beta_{HTS}, \quad (\text{IS.4.2})$$

with the material temperature factors α_{HTS} and β_{HTS} .

Eqs. (IS.4.1) -(IS.4.2) are only valid in case of a bulk-HTS component. In the HTS tapes applied in the HTS cables, the HTS material is formed as filaments within a ductile matrix of silver or its alloys. When the HTS material is surrounded by a matrix material, the total resistivity of the HTS tapes will be (Jensen, 2003):

$$\rho_{TAPE} = \left(\frac{1}{1+r} \cdot \rho_{HTS}^{-1} + \frac{r}{1+r} \cdot \rho_{MATRIX}^{-1} \right)^{-1}, \quad (\text{IS.4.3})$$

where r is the matrix-material / HTS ratio of the tape cross-area.

A number of tapes can be applied in a single-phase HTS component to reach the desired current through the HTS component. When the number of such tapes is N , the resistance of the HTS component becomes

$$R(t) = \frac{l}{a \cdot N} \cdot \rho_{TAPE}(t), \quad (\text{IS.4.4})$$

where l is the length and a is the cross-area of a HTS tape.

IS.4.2. Temperature- and cooling model

To maintain operation in the superconducting state, the HTS tapes must be at the temperature below the critical temperature, T_C . For the majority of ceramic HTS materials, the critical temperatures are around 90 K, which is why they must operate at cooling by liquid nitrogen (at 77 K at an atmospheric pressure).

The common consideration is that the warm dielectric design will be preferred instead of the cold dielectric design. The warm dielectric design has a cryostat within each of the three-phase HTS cables. Here, only the HTS tapes are under low temperature whereas the dielectric and the shield are at room temperature. This implies that the three-phase cable will consist of three single-phase cables where each single-phase cable is with its individual thermal and electric insulation and individual shielding.

The cooling system may also influence the design of the three-phase HTS cable. The three-phase HTS cable is placed between the cooling and pumping stations. To maintain recirculation of the liquid nitrogen, the two phases must be operated as forward with respect to the liquid nitrogen flow between the two ends of the cable. The last single phase must be operated as return for the liquid nitrogen flow. The temperature of the HTS component is described as:

$$C_p \cdot \frac{dT(t)}{dt} = P(t) - h(\Delta T) \cdot A \cdot \Delta T(t), \quad (\text{IS.4.5})$$

where C_p is the heat capacity of the HTS component, $P(t)$ is the power losses in the HTS component, ΔT is the temperature difference between the HTS component surface and the coolant that is liquid nitrogen, h is the heat transfer coefficient that is dependent on the temperature difference ΔT (Incropera, 1996), and A is the surface area of the HTS component in contact with the coolant. Notice that $h(\Delta T)$ describes an irreversible process of the heat exchange between the HTS leader surface and liquid nitrogen (Incropera, 1996).

IS.4.3. Transient approach of line current

The model of the HTS components must be implemented into the simulation tool PSS/E. In this simulation tool, the standardised models of conventional cables are given by their well-known PI-equivalents (Kundur, 1994) in the positive-sequence system. The HTS component models must comply with the interface of the simulation tool PSS/E, which is absolutely necessary for reaching an appropriate operation of such models. This implies that the superconducting components must be initiated as positive-sequence PI-equivalents in load flow simulations. In post-following transient simulations, the HTS components need an adequate representation to comply with other positive-sequence models of conventional components such as cables and overhead lines, which are a part of the meshed power network and modelled with use of the tool PSS/E.

This introduces several restrictions on the transient representation of the HTS cables in the tool PSS/E, which is why we are talking about a transient approach. The model of the three-phase HTS cable is given by its positive-sequence PI-equivalent. The goal is to represent the response of the resistance of the superconducting tapes on the current transients and the temperature variations in each single-phase cable. These transients are excited in the modelled HTS cable according to the simplified representation:

$$L \cdot \frac{dI(t)}{dt} = -R(t) \cdot I(t) + \Delta V(t), \quad (\text{IS.4.6})$$

where the parameters appearing in the equation must be interpreted as: L is the effective inductance (including its self-inductance and the contributions from the cryostat and the shield) and $R(t)$ is the resistance of the single-phase HTS component given by **Eqs. (IS.4.1) -(IS.4.4)**, $I(t)$ is the line current going through the single-phase HTS component and $\Delta V(t)$ is the voltage drop between the two ends of the HTS component cables.

In this approach, the transients in the capacitive elements of the cable are disregarded because:

- 1) It is necessary to comply with the dynamic interface of the tool PSS/E and its standardised cable representation as positive-sequence PI-equivalents.
- 2) It is assumed that such transients will not influence the line current transients in the HTS tapes in any significant way.

The HTS components are sensitive with respect to the current transients in the HTS material and may therefore show strongly asymmetrical behaviour of the resistance values in each single phase. The single-phase resistance will be influenced both by the current transients and the energy dissipation, which is why the fundamental frequency and its higher harmonics will be present in the resistance behaviour. To interface the HTS component model to the dynamic simulation tool PSS/E, the positive-sequence component of the three-phase resistance is applied in the network solution in means of the resistance of the HTS component. The positive-sequence component will also contain the fundamental frequency and its higher harmonics, which is why accurate implementation of the HTS component model into the tool PSS/E must be reached to respect the dynamic interface of the tool PSS/E (it does not contain such fundamental frequency or its harmonics).

The positive-sequence current going through the three-phase HTS component is defined in agreement with the current of other conventional cables and overhead lines feeding into the common node of the power network. Changes in the current transients in the HTS material relate to the changes in the voltage at the ends of the HTS component. Again, the change in the HTS component resistance influences the voltage profile and the current flow in the power network around the HTS component. This performs a coupling between the HTS component model and the meshed power network model in the tool PSS/E.

IS.5. Formulation of practical problems on stability

Investigations of short-term voltage with application of HTS components have been carried out on two simulation examples.

- 1) The first example illustrates the case where a part of the 10 km long 136 kV underground cable connecting the large wind farm with the substation in the transmission power network is realised as the HTSC. This implies that the 136 kV underground cable consists of the 5 km HTS cable and the 5 km conventional cable.
- 2) The second example treats the case where the 10 km conventional underground cable has the SFCL at the end connected to the transmission power network.

In the both cases, a number of practical problems have been notified. These problems need a solution before the HTS components can be assumed as a realistic alternative to other arrangements applied to improve transient voltage stability.

IS.5.1. Case of HTS cables

The tapes of the HTS cable are formed as superconducting ceramic BSSCO filaments within the ductile silver matrix. The cross-section of one tape is 0.2 mm × 3.0 mm and there are 66 tapes in a single-phase HTS cable. The tapes operate at cooling in fluid nitrogen at 77 K and their stationary temperature is assumed to be 80 K. Such assumptions are very realistic (Jensen, 2003).

The whole three-phase HTS cable consists of three single-phase cables with warm dielectric design. The total length of the cable system is 5 km, but it consists of a number of sections with

their cooling and pumping stations in series. This is necessary to perform an efficient cooling through the cable length and avoid excessive temperature gradients through the total length of the cable system.

The power to be transmitted through the cable system is 150 MW at the rated voltage of 136 kV. Therefore the rated current of the cable is 650 A RMS in rated undisturbed operation. The expected short-circuit current in the connection point is around the ratio of 2 of the rated current. The HTS cable is therefore designed to the critical current of 1200 A peak. The power-factor $n = 5$.

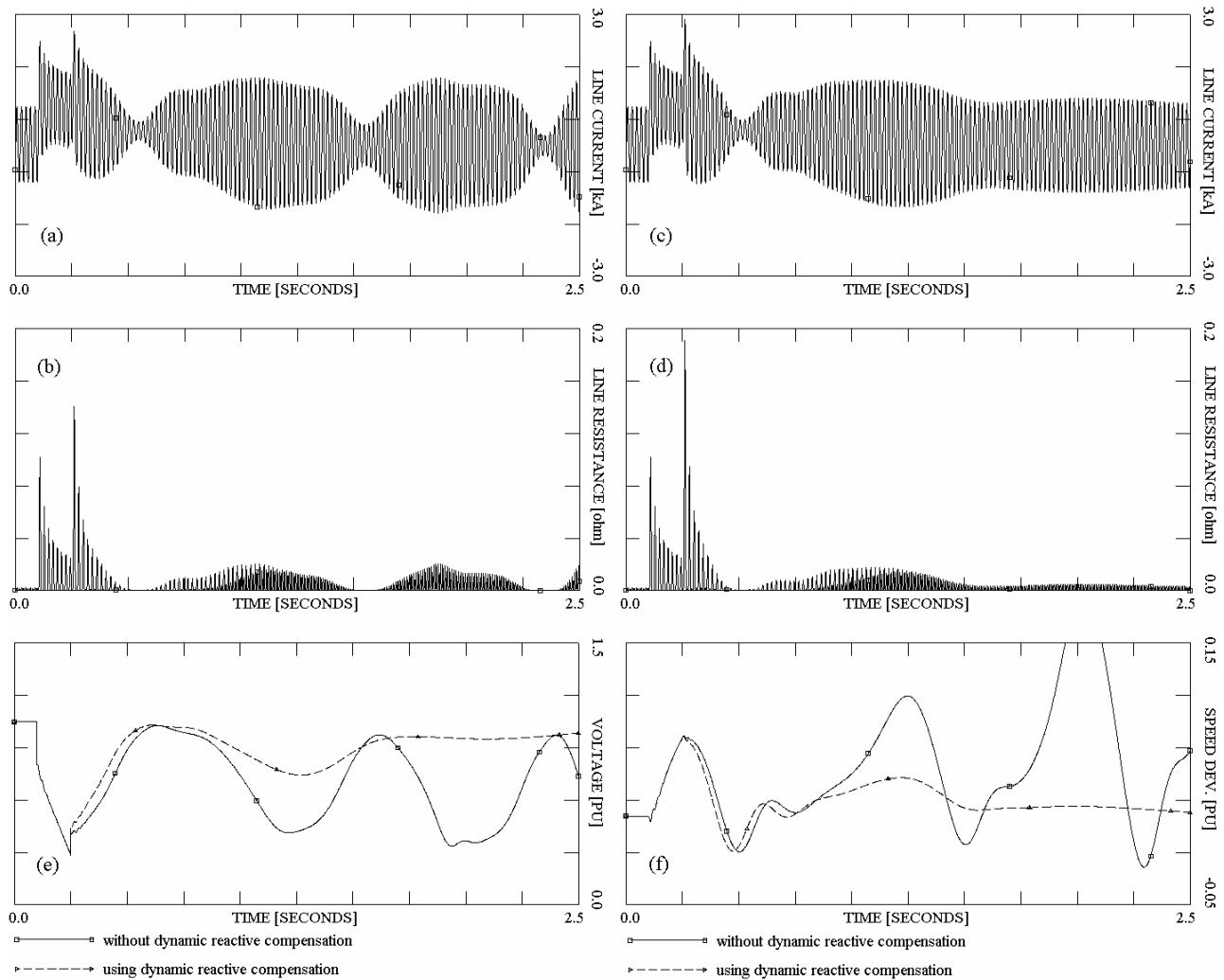


Fig.IS.5.1. Transient behaviour in the HTS cable at a short circuit fault – with and without dynamic reactive compensation of the large wind farm in the connection point. Line current in a single-phase HTSC without – (a) and with – (b) dynamic reactive compensation. Resistance of a single-phase HTSC without – (c) and with – (d) dynamic reactive compensation. Voltage of a selected wind turbine in the large wind farm in both cases – (e). Generator speed of a selected wind turbine in the wind farm in both cases – (f).

At a short circuit fault in the transmission power network, the voltage drops which initiates current transients in the HTS cable. The resistance of the HTS tapes increases as the result of the current transients, which is shown in **Fig. IS.5.1**. This resistance increase is relatively small and insufficient to improve short-term voltage stability without use of other arrangements. When

dynamic reactive compensation is not used, the voltage shows a tendency to uncontrollable decay. Therefore there is a risk of protective disconnection of the large wind farm. This solution will not comply with the Specifications of the Danish TSO (Eltra, 2000).

When the large wind farm trips, the voltage recovers and the HTS cable will be in no-load operation and the resistance of the HTS tapes decays to its low-level. Increase of the HTS tapes' resistance is small because the ratio between the short-circuit current and the current at normal operation is also small. It is only around 2. This value is common for the Danish power network, which is a relatively strong, meshed power network with relatively short distances between substations.

The temperature of the HTS material increases by around 1 K only. This is not enough to quench the HTS cable at the short-circuit fault. Notice that the power-factor of the HTS cable is 5 that is poor. This design parameter is set so to avoid a risk of necessary quenching of the cable.

When dynamic reactive compensation is applied, the voltage re-establishes after the fault has been cleared. The resistance of the HTS tapes decays to its original, undisturbed level. Notice that the resistance of each single-phase HTS cable contains the fundamental frequency and its higher harmonics.

IS.5.2. Application of SFCL

The SFCL is placed at the end of the conventional 10 km underground cable and simulated as the bulk-ceramic BSCCO coil with the critical current of 1300 A peak per 1 cm². The power-factor of this HTS component, n , may be in the range of 9 to 15. Therefore this component can be extremely sensitive to even small changes in the current magnitude. The SFCL is represented in the simulations as three single-phase coils.

There can be a number of practical problems dealing with interaction of such current limiters and the meshed transmission power system. The main problem found in this short investigation is performing of efficient cooling of the SFCL at quenching and avoiding a risk of over-heating of the superconducting material. Notify that the current which activates the quenching mechanism of the SFCL is only around the factor 2 of the rated current at normal operation. On the other hand, the resistance of the SFCL must reach around 10 to 15 ohms at the short-circuit fault to improve short-term voltage stability. When the short-circuit fault has been cleared, the cooling system must bring the superconducting material to the superconducting state.

The demand of sensitivity of the SCFL to the current - to recognise that a short-circuit fault has occurred in the grid - requires therefore that the critical current, I_C , must be low and the power-factor, n , must be large. In this investigation, a parameter study is made where the critical current, I_C , has been between 650 A peak and 1000 A peak, the power-factor, n , in the range of 9 to 15, and the effective length of the coil-formed superconducting wire between 10 m to 100 m.

This investigation has shown that:

- 1) When the critical current, I_C , is relatively large or/and the power-factor, n , is relatively small, then quenching of the SFCL does not occur. In this case, the resistance of the SFCL shows a fluctuating behaviour like "spikes" coming with the fundamental frequency and its higher

harmonics. The same picture has been seen in simulations of the HTS cable. Since the SFCL does not quench and its resistance is not kept around 10 to 15 ohms, the voltage shows a tendency to an uncontrollable decay. This lead to protective disconnection of the large wind farm and the solution does not comply with the Specifications of the Danish TSO (Eltra, 2000).

- 2) When the SFCL quenches, the thermal run-over of the SFCL has been seen. This thermal run-over occurs because of inefficient cooling of the superconducting material when this is in the normal state (high resistance). Furthermore, it is extremely difficult to control the temperature of the superconducting material at quenching. When the resistance increases, then the temperature also increases and so on. This introduces a positive coupling between the resistance and the temperature of the superconducting material.

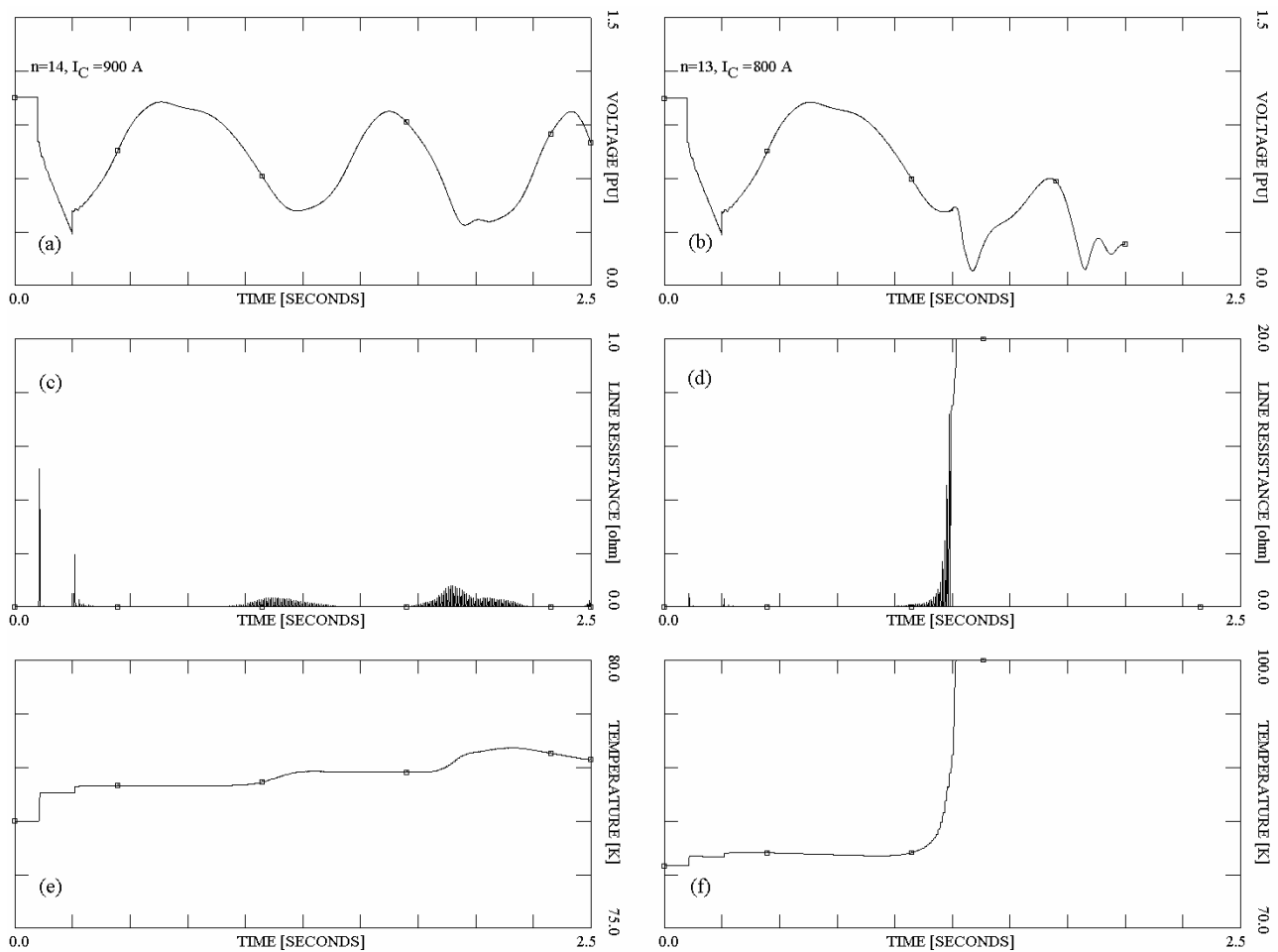


Fig.IS.5.2. Simulation results with use of the SFCL: voltage of a selected wind turbine in the large wind farm in a case of no quenching – (a) and quenching and thermal run-over – (b). Line resistance of the SFCL at no quenching – (c) and quenching and thermal run-over – (d). Temperature of the SFCL coil at no quenching – (e) and quenching and thermal run-over – (f).

This behaviour is illustrated in **Fig. IS.5.2**. The thermal run-over in the superconducting material of the SFCL will not only destabilise operation of the SFCL itself, but also in a risk of voltage instability and disconnection of the large wind farm. Notice that the combination of (i) a

relatively small ratio between the short-circuit current in the meshed power network and the rated current at normal operation in the SFCL and (ii) a risk of the thermal run-over will make it extremely difficult to optimise the design of the SFCL.

IS.6. Resume

Simulations are made with application of a simplified and a physical-approach model of the HTS components to be incorporated into the ac-grid to stabilise operation of large wind farms. In terms of the simplified model, which are built-up *on assumptions* that (i) the HTS components operate as switches with two resistance levels and (ii) quenching occurs when the short-circuit fault has occurred and removes when the fault has been cleared, such HTS components will contribute to improvement of short-term voltage stability.

When the physical-approach model is applied, the investigation has exposed a number of practical problems, which must be solved for successful application of such HTS components to stabilise the wind farm operation at grid faults. It is required that the HTS component has quenched at a short circuit fault, e.i. the superconducting material goes over to the normal state (high resistance). When the current sensitivity of the HTS component is insufficient, then such quenching will not occur. The superconducting material sustains in the flux-flow state, which is characterised by the "spike-wise" behaviour of the resistance with the fundamental frequency and its higher harmonics. However, this is not enough to reduce the voltage drop or to stabilise the voltage after the fault has been cleared.

When the current sensitivity is sufficient to quench the HTS component at the grid fault, then the superconducting material is in the normal state and the return to the superconducting state seems to be a problem because the thermal run-over may develop. The return to the superconducting state must be by the cooling of the HTS component. There will be a number of practical problems to deal with.

- 1) The ratio between the short-circuit current in the given meshed power network and the current in the HTS component at normal operation is around 2. The energy dissipation is the current squared. When the short-circuit fault has been cleared and the HTS material is still in the normal state, the energy dissipation in the quenched HTS component does not reduce sufficiently, but only by the ratio of 4. It seems to be insufficient to perform acceptable cooling to return the superconducting material to the superconducting state.
- 2) The cooling process in the liquid nitrogen is an irreversible process (Incropera, 1996). The cooling is efficient within a narrow range of the temperature differences between the HTS material and the coolant. When this range is exceeded once, the cooling becomes less efficient.
- 3) When the cooling is insufficient, there is an enforced positive coupling between the temperature increase and the increase of the HTS material resistance.

Notify that experiments with successful applications of SFCL are made at conditions where the ratio between the short-circuit current (the first transient peak) and the current at normal operation

is around 4 or larger. Such conditions are not reached in the simulation cases described in this issue.

This issue does not interpret the HTS technology as inapplicable in meshed power networks to improve short-term voltage stability. It focuses rather on the necessity of (i) adequate representation of such HTS components in the dynamic simulation tools to avoid misleading results and (ii) accuracy of the simulations and interpretation of the results.

The main target of this investigation has been to clarify whether the HTS components could replace the conventional arrangements, such as dynamic reactive compensation, to improve short-term voltage stability. The negative result reached in this investigation is the result as well. This investigation shows that the main problem could be connected with insufficient cooling of such HTS components.

On the other hand, this investigation shows that the short-circuit current level in the given power network is relatively low which is why the HTS components that have the large critical current, I_C , may be incorporated into the power network and operate without a risk of quenching.

IS.7. Acknowledgements and credits

The transient model of the HTS components applied in this investigation is developed in (Jensen, 2003). The author of this thesis has only performed implementation of this model into the simulation tool PSS/E as a user-written model. The data applied in this investigation have been kindly offered by Dr. K. H. Jensen, who is the author of (Jensen, 2003).

About author



Photo: At the Nøjsomheds Odde wind farm, Denmark, Autumn 2001.

Vladislav Akhmatov is born in Moscow, Russia, in 1969. He received the degree of engineer-physicist from the Institute of Electron-technique of Moscow in Russia, and the degrees of M.Sc. and the Ph.D. from Technical University of Denmark in 1999, respectively, 2003. He has been with the Consulting Dept. of the power distribution company NES A/S, Copenhagen, Denmark, from 1998 till 2003. In 2003 he has joined ELTRA A.m.b.a. that is the transmission system operator in western Denmark. His primary work is modelling and analysis of electric power grids with large penetration of wind power and distributed generation. Vladislav Akhmatov has published around twenty articles on this subject in last five years.

ISBN Softbound: 87-91184-18-5
ISBN CD-ROM: 87-91184-19-3